Canadian Technical Report of
Hydrography and Ocean Sciences 188

1997

Moored Acoustic Doppler Current Profiler Measurements on the Labrador Shelf, 1993-1994

by

B.J.W. Greenan, S.J. Prinsenberg, and A. van der Baaren

Ocean Sciences Division
Maritimes Region
Fisheries and Oceans Canada

Bedford Institute of Oceanography
P.O. Box 1006
Dartmouth, Nova Scotia
Canada, B2Y 4A2

Cat. No. Fs 97-18/188E ISSN 0711-6764

Correct Citation for this publication:

Greenan, B.J.W., S.J. Prinsenberg, and A. van der Baaren. 1997. Moored acoustic Doppler profiler measurements on the Labrador Shelf, 1993-1994. Can. Tech. Rep. Hydrogr. Ocean Sci. 188:vii + 149 pp.

TABLE OF CONTENTS

ABSTRACT

Greenan, B.J.W., S.J. Prinsenberg and A. van der Baaren. 1996. Moored Acoustic Doppler Current Profiler Measurements on the Labrador Shelf, 1993-1994. Can. Tech. Rep. Hydrogr. Ocean Sci. 188: vii+149 pp.

An acoustic Doppler current profiler was moored on the ocean bottom of the Labrador Shelf for the period of November 1993 to July 1994. This instrument provided hourly data throughout this period in ten bins ranging from 0 to 73 m depth. During the period of sea ice coverage at this location from January through May, the 0 m bin monitored pack-ice movement. The magnitude of monthly-averaged current reached a maximum in November for all depth bins and steadily decreased to a minimum in March. The currents for the period of April to July increased only slightly above the minimum. A comparison with 2 m winds measured with an anemometer on an ice beacon at the ADCP location during the period March 5-13, 1994 demonstrated that the winds accounted for 51% of the variance in the ice motion.

RÉSUMÉ

Greenan, B.J.W., S.J. Prinsenberg and A. van der Baaren. 1996. Moored Acoustic Doppler Current Profiler Measurements on the Labrador Shelf, 1993-1994. Can. Tech. Rep. Hydrogr. Ocean Sci. 188: vii+149 pp.

Un courantomètre acoustique Doppler a été ancré sur le fond océanique de la plate-forme continentale du Labrador entre novembre 1993 et juillet 1994. Cet instrument a enregistré les valeurs horaires pendant toute cette période dans dix casiers allant de 0 à 73 m de profondeur. Durant la période au cours de laquelle la mer est recouverte de glace de mer, soit de janvier à mai, les enregistrements dans le casier de 0 m ont permis de suivre le mouvement de la banquise. Le courant moyen mensuel a atteint une valeur maximale en novembre dans tous les casiers de profondeur et a diminué progressivement jusqu'à une valeur minimale en mars. La vitesse des courants pendant la période d'avril à juillet n'a que légèrement augmenté au-dessus de la valeur minimale. En comparant les mesures du vent de 2 m faites au moyen d'un anémomètre monté sur une balise de glace à l'emplacement du courantomètre Doppler durant la période allant du 5 au 13 mars 1994, il ressort que les vents sont à l'origine de 51 % de la variance du déplacement de la glace.

Table Captions

Table 1: Monthly mean u (easterly), v (northerly), and w (upward) components of ADCP current measurements along with magnitude and direction.

Table 2: Results of complex regression analysis for the ocean current vectors with the 2m winds of beacon 8668 as the independent variable for the period of March 5-13, 1994. The subscripts on U represent the depths relative to the ice/ocean interface. *A* represents the response factor, θ is the turning angle relative to the 2 m wind, and r^2 is the coefficient of determination. The statistics are compiled from 216 observations.

Table 3: Results of complex regression analysis for the ocean current vectors with CMC 0-Hour forecast as the independent variable for the period of March 5-13, 1994. The subscripts on U represent the depths relative to the ice/ocean interface. *A* represents the response factor, θ is the turning angle relative to the 2 m wind, and r^2 is the coefficient of determination. The statistics are compiled from 17 observations.

Table 4: Results of complex correlation analysis for the ocean current vectors and the CMC gridded wind interpolated to the site of the ADCP. Analysis is for the total sampling period, for period of ice cover, and period of no ice cover at all depths relative to the ice/ocean interface. *A* is the response factor, r is the correlation coefficient, θ is the turning angle relative to the CMC wind, *t* is Student's t statistic, and n is the number of observations used in the computation. ADCP α and CMC α are the vector mean directions for the designated time periods.

Figure Captions

Figure 1: Deployment location of bottom-mounted acoustic Doppler current profiler for period of November 1993-July 1994

Figure 2: Monthly-mean horizontal velocity vectors for the water column above the ADCP location.

Figure 3: Monthly means of the u (easterly), v (northerly) and w (upward) components of velocity and magnitude for 0.0 m. Error bars represent one standard deviation for the monthly mean. The dashed line shows the mean current computed over 15 days.

Figure 4: Monthly means of the u (easterly), v (northerly) and w (upward) components of velocity and magnitude for 3.5 m. Error bars represent one standard deviation for the monthly mean. The dashed line shows the mean current computed over 15 days.

Figure 5: Monthly means of the u (easterly), v (northerly) and w (upward) components of velocity and magnitude for 12.2 m. Error bars represent one standard deviation for the monthly mean. The dashed line shows the mean current computed over 15 days.

Figure 6: Monthly means of the u (easterly), v (northerly) and w (upward) components of velocity and magnitude for 20.9 m. Error bars represent one standard deviation for the monthly mean. The dashed line shows the mean current computed over 15 days.

Figure 7: Monthly means of the u (easterly), v (northerly) and w (upward) components of velocity and magnitude for 29.6 m. Error bars represent one standard deviation for the monthly mean. The dashed line shows the mean current computed over 15 days.

Figure 8: Monthly means of the u (easterly), v (northerly) and w (upward) components of velocity and magnitude for 38.3 m. Error bars represent one standard deviation for the monthly mean. The dashed line shows the mean current computed over 15 days.

Figure 9: Monthly means of the u (easterly), v (northerly) and w (upward) components of velocity and magnitude for 46.9 m. Error bars represent one standard deviation for the monthly mean. The dashed line shows the mean current computed over 15 days.

Figure 10: Monthly means of the u (easterly), v (northerly) and w (upward) components of velocity and magnitude for 55.6 m. Error bars represent one standard deviation for the monthly mean. The dashed line shows the mean current computed over 15 days.

Figure 11: Monthly means of the u (easterly), v (northerly) and w (upward) components of velocity and magnitude for 64.3 m. Error bars represent one standard deviation for the monthly mean. The dashed line shows the mean current computed over 15 days.

1.0 INTRODUCTION

The continental shelf region east of Newfoundland and Labrador is covered by a marginal ice zone (MIZ) from January to June. Most of this ice is formed on the Labrador shelf during the winter months, but some enters from Baffin Bay bringing with it the annual flux of icebergs. The combined pack ice moves southward due to wind forcing and advection of the inshore and offshore branches of the Labrador current.

The field component of the Newfoundland and Labrador sea ice program at the Bedford Institute of Oceanography has involved deploying location and anemometer beacons and ice pressure systems in the marginal ice zone off the coast of southern Labrador. These in-situ measurements are being compared with satellite imagery as well as observed and forecast winds. To complement these atmospheric and sea ice measurements, the 1994 Newfoundland Shelf Sea Ice Program (Peterson et al, 1995) also included the deployment of a bottom-mounted Acoustic Doppler Current Profiler (ADCP). This instrument provides a source of oceanographic information which has not been monitored before in this field program. Measurements of the vertical structure of the ocean currents on the Labrador Shelf are sparse, especially under sea ice, and provide a necessary data source for studying the physical interaction of the atmosphere, ice cover, and ocean that is incorporated into numerical ice-ocean forecast models.

2.0 INSTRUMENT

An RDI ADCP acoustic Doppler current profiler (ADCP) was deployed in October 1993 on the ocean bottom in a trawl-resistant package (Dessureault et al., 1991) which prevents damage from bottom trawling. The profiler was located in a depth of 80 m of water between Hamilton Bank and the Labrador coast (53.85°N, 56.05°W), as indicated in Figure 1. Data were collected over the period of November 1, 1993 to July 14, 1994. The data point interval was one hour with the 350 pings in a data ensemble. The ADCP provided data in 10 bins centered 0.0, 3.5, 12.2, 20.9, 29.6, 38.3, 46.9, 55.6, 64.3, and 73.0 m relative to the ocean surface. The ADCP transducer frequency was 150 kHz with a head angle of 20°. The four-beam configuration of the ADCP enables resolution of three velocity components in each depth bin along with a fourth component referred to as the error velocity which is the difference between the vertical velocity as measured by any two opposite beams. The percentage of pings used in a bin average is logged in addition to the echo intensity of each beam. In such a configuration the reliability of data collected in the 0 and 3.5 m bins is substantially reduced when ice is not present on the surface.

For shipboard use the ADCP obtains ship velocity by measuring the Doppler shift of an acoustic pulse reflected off the ocean bottom. As in Belliveau et al. (1990), this bottom tracking mode of the profiler was used to monitor the motion of the sea ice on the ocean surface. The reasonably continuous ice coverage along the southern Labrador coast

for the first four months of the year makes this type of deployment feasible. In the area of the deployment the sea ice consisted mainly of floes of first year ice which were typically less than a meter in thickness.

3.0 OCEAN CURRENTS

Vector plots (Figure 2) of the monthly mean horizontal flow at the various depth bins above the ADCP demonstrate a variation in vertical structure for different months of the year. In November, the magnitudes at all levels are at a maximum and, except for the two top bins, there appears to be an almost constant shear throughout the layer. In subsequent months the magnitude decreases at all levels reaching a minimum in March and then increasing slightly to the end of the record in July. A linear vertical shear remains present in December, however, there is almost no shear in the 12.2-73.0 m layer for the month of January. The structure of the vertical shear in this water column does not display a clear trend in the February-July period. Due to the limitations of the ADCP in the ocean bottom-mounted configuration, the monthly mean data in the 0 and 3.5 m bins must be interpreted carefully since the instrument provides useable data only when ice cover is present.

Monthly mean components of velocity for each depth bin as measured by the ADCP are presented in Figures 3 to 12 and summarized in Table 1. The means computed over 15 days are depicted as dashed lines in the same figures. Positive u, v, and w components represent the eastward, northward, and upward directions, respectively. The w-component of velocity is at least one order of magnitude smaller than the u and v components. The 0 and 3.5 m bins indicate a decreasing trend in magnitude from the start of the recording period in November until a minimum is reached in March. The annual variation in the baroclinic component of the Labrador Current is similar to this trend and is determined primarily by the density-driven outflow from Baffin Bay (Lazier and Wright, 1993). Lazier and Wright found that the baroclinic component of the Labrador Current has a maximum in September-October and a minimum in March-April, whereas the wind-forcing over the shelf has a maximum in December and a minimum in May-June (Narayanan et al., 1996). In November and December the u-component monthly mean is significantly larger than the v-component in both the 0 and 3.5 m bins. There is little westward flow in this area and it appears that the North-South fluctuations tend to cancel. As expected, the variance in the currents reaches minimum in February/March because these are months in which ice cover is almost continuous and this is when the ADCP provides useable data.

The depth bins from 12.2 to 73.0 m all demonstrate a decreasing trend in velocity magnitude throughout the period from November to March with only a slight increase by July. In general, the change in magnitude decreases with depth. At 12.2 m the magnitude decreases from 17.19 in November to 1.33 cm s^{-1} in March, while at 73.0 m the change is only from 7.88 to 1.87 cm s^{-1}. As well, the variance remains relatively constant at these lower levels throughout the period of deployment. One unusual result of the monthly

analysis is that, except for the month of March, the direction of the currents in the 0 and 3.5 m depth bins tends to be shifted abruptly to the left of the 12.2 m bin. This discrepancy is less noticeable in months of almost continuous ice coverage and is completely absent in March.

On March 4, ice beacon 8668 was deployed on a large composite flow made up of pancake ice near the location of the ADCP. Due to prevailing winds and pack-ice conditions during the week after deployment the beacon did not move significantly from its deployment site until the March 13. Beacon 8668 was equipped with a R.M. Young anemometer mounted on a 2 m mast and the data were transmitted through the Argos satellite system. The anemometer beacon computes a ten minute vector average of wind speed and direction once per hour and transmits these averages for each of the previous six hours along with the barometric pressure and air temperature. The anemometer has an accuracy (precision) of 1.0 m s^{-1} (0.5 m s^{-1}) for wind speeds < 10 m s^{-1}, 10% (10%) for wind speeds > 10 m s^{-1}, and 5° (1°) for wind direction. All beacon data and observed ice and ocean profile data collected during the 1994 field survey are presented in more detail in Peterson et al. (1995).

The results of a complex regression, for the period of March 5-13, of the ice drift and ocean currents relative to the 2 m wind (beacon 8668) show that the hourly 2 m winds can account for 51% of the variance in the ice motion (labeled $U_{0.0}$, Table 2). The ice responds at 2.4% of the 2 m wind, moving downwind with a small turning angle of 0.63° to the left. Peterson and Symonds (1988) found response factors of ~5% and turning angles ranging from 3 to 40° for 6-hourly data. The coastal landfast ice impedes the ice drift of the inshore pack ice in this area and causes the ice to drift parallel to the coast which is to the left of the predominant wind direction. This eliminates the expected ice drift angle to the right of the wind. Ocean currents measured by the ADCP reveal that below the pack ice the turning angle increases from 0.3° at 3.5 m depth to 50° (to the right) at 73 m (Table 2). The response factor, *A*, relative to the 2m wind decreases from 2.2% at 3.5 m to ~0.9% at 20.9 m then remains constant throughout the remainder of the water column. The speed does not decrease with depth possibly due to channeling of the flow between Hamilton Bank and the mainland. The correlation coefficient decreases from 0.57 at 3.5 m to ~0.26 at 29.6 m and below. These results are consistent with the CTD measurements which showed a well-mixed water column throughout the entire depth.

In addition, a complex correlation analysis was performed with the ADCP horizontal flow field and gridded wind data obtained from the Canadian Meteorological Centre (CMC) Regional Finite Element Model. The prognostic wind data at the $\sigma = 1$ level (~10m above surface) for the 0-hour forecast were interpolated bilinearly to coincide with the ADCP site on the Labrador Shelf. The gridpoints used in the interpolation were the four gridpoints adjacent to the ADCP site. Since the wind data were recorded every twelve hours, the hourly ADCP data were interpolated linearly to coincide with the 12-hourly wind observations. Appendix B contains stick plots of the 12 hourly ADCP velocity time series and CMC wind time series used in the correlation

analysis. Analysis was done for the period of March 5-13 (ice beacon located above ADCP), for the total sampling period (November 1993 to July 1994), for the period when there was ice cover (December 1993 to June 1994), and for the period when there was no ice cover (November 1993, and June to July 1994), The results for the first time period are summarized in Table 3 while the remaining three are summarized in Table 4.

Complex correlation coefficients were computed for the two vector quantities, water velocity and wind velocity, using this formulation found in Barber (1961):

$$\rho = \mathbf{g}^*(t)\mathbf{k}^*(t)/\sigma_g\sigma_k = re^{i\theta} \tag{1}$$

where * indicates the complex conjugate, **g** and **k** are vector quantities written as complex numbers (eg. $\mathbf{g} = g_x + ig_y = Ue^{i\alpha}$), and σ is the mean square modulus (magnitude) of the vector. g_x and g_y are the horizontal vector components and U and α are the magnitude and direction of the vector. The complex correlation coefficient is itself a complex number in which the modulus, $|\rho| = r$, represents the similarities in fluctuations between the two vectors and ranges between 0 and 1. The argument, θ, is the average angle that the second vector, **k** (current), bears to the first, **g** (wind). Note that Barber's formulation includes the mean in the computation of the complex correlation coefficient. In this report, the complex correlation coefficients were computed to compare wind and water velocity vectors *whose means were removed.* The magnitude and argument (turning angle) of the correlation coefficients were computed between the water's velocity at all depths and the wind data. Qualitatively, retention of the mean vectors in the computation does not change the results. The response factor, *A*, is the slope of the best fit line of regression. It is the magnitude of the regression coefficient for a complex regression performed between the wind and water velocities with the wind as the independent variable.

Student's *t* statistic was computed (Table 4) to test the null hypothesis that a correlation does not exist between the variables:

$$H_0:\ \rho = 0.\ \ t = |\rho|/s_{|\rho|} \tag{2}$$

where $s_{|\rho|}^2 = (1-|\rho|^2)/(n-2)$. n is the number of observations used in the computation. Significant values for Student's *t* are $t_{0.05(2),200} = 1.972$, $t_{0.05(2),300} = 1.968$, and $t_{0.05(2),500} = 1.965$. In all cases, the correlations appear to be significant with 95% confidence.

The results summarized in Table 3 reinforce the comparison of anemometer beacon winds with ADCP currents given in Table 2. The response factor using the CMC forecast winds was approximately 50% of that using the 2 m anemometer winds; 30% of the difference can be explained by differences in height of the winds (10 m vs. 2 m) with the remainder due to overestimation of the wind speed by the CMC model (Greenan and Prinsenberg, 1997). As expected, the angle between the CMC and the ADCP is offset by about 9° to the left as compared to the anemometer vs. ADCP. Due to the limited number

of observations for the CMC data set, θ does not vary as smoothly as in Table 2. The correlation coefficient is very similar for both the CMC and anemometer results.

Results in Table 4 show that correlation was best during times of ice cover keeping in mind that reliability of the ADCP was greater at that time for the top two bins. The average angle that the ocean current bore in relation to the wind increases dramatically at 12 m. Where the two quantities had been similarly directed for the upper two bins they were more than 20° apart on average at 12 m. Figure 13 has three-dimensional representations of the computed correlation coefficients which shows the difference in the correlation of the wind with the top two bins to that of the wind with the bins at depth. Also, from the stick plots in Appendix B, it is seen that the current vectors and wind are closely matched for 0 m and 3.5 m, but below this the water seemingly flowed independently of the local wind.

4.0 SUMMARY

An acoustic Doppler current profiler provided hourly data from November 1993 to July 1994 in ten depth bins ranging from 0 to 73 m. During the period of sea ice coverage at this location from January through May, the 0 m bin monitored pack ice movement. Relative to free-ice drift values, the inshore pack ice at this location was impeded by the coastal land-fast ice and was forced to move parallel to the coastline directly downwind instead of to the right of the wind. The magnitude of monthly-averaged current reached a maximum in November for all depth bins and steadily decreased to a minimum in March. The currents for the period of April to July increased only slightly above the minimum. Caution must be used in interpreting monthly-averaged results in the 0 and 3.5 m depth bins due to the limitations of the ADCP in a ocean bottom-mounted configuration when sea ice is not present at the ocean surface. One unusual result of the monthly analysis is that, except for the month of March, the 0 and 3.5 m depth bins tend to be shifted abruptly to the left of the 12.2 m bin. This discrepancy is less noticeable in months of almost continuous ice coverage and is completely absent in March.

A comparison with 2 m winds measured with an anemometer on an ice beacon at the ADCP location during the period March 5-13, 1994 demonstrated that the winds accounted for 51% of the variance in the ice motion. The ice responds at 2.4% of the 2 m wind, moving downwind with a small turning angle of 0.63° to the left. These results were reinforced by a comparison of CMC forecast winds with the ADCP data.

ACKNOWLEDGMENTS

This research was supported by the Panel of Energy Research and Development. The authors wish to thank the crew of the CSS Hudson, chief scientists C. Ross and J. Lazier, and the support staff from Ocean Science Division for their adept work in the deployment and recovery of the ADCP. We also wish to thank M. Scotney for processing the data and I. Peterson and D. Belliveau for their reading of the manuscript.

REFERENCES

Barber, N.F., 1961. Experimental Correlograms and Fourier Transforms, Pergamon, N.Y., 124-125.

Belliveau, D.J., G.L. Bugden, B.M. Eid, and C.J. Calnan, 1990. Sea ice velocity measurements by upward-looking Doppler current profilers. *J. Atmos. Oceanic Technol.*, **7**, 596-602.

Dessureault, J.-G., D.J. Belliveau and S.W. Young. 1991. Design and tests of a trawl-resistant package for an acoustic Doppler current profiler. *IEEE J. Ocean. Engineering*, **16**, 397-401.

Greenan, B. J W., and S. J. Prinsenberg, 1997: A comparison of forecast winds with observations in the Labrador Shelf marginal ice zone. (in preparation)

Lazier, J.R.N., and D.G. Wright. 1993. Annual velocity variations in the Labrador Current. *J. Phys. Oceanogr.*, **23**, 659-678.

Narayanan, S., S. J. Prinsenberg, and P. C. Smith, 1996. Current meter observations from the Labrador and Newfoundland Shelves and comparisons with barotropic model predictions and IPP surface currents. *Atmos.-Ocean*, 34(1), 227-255.

Peterson, I.K., and G. Symonds, 1988. Ice floe trajectories off Labrador and Newfoundland: 1985-1987. *Can. Tech. Rep. Hydrogr. Ocean Sci.*, **104**, Bedford Institute of Oceanography, Dartmouth, Nova Scotia, 101 pp.

Peterson, I.K., S.J. Prinsenberg, and G.A. Fowler, 1995. Newfoundland Shelf Sea Ice Program, 1993 and 1994. *Can. Tech. Rep. Hydrogr. Ocean Sci.*, **167**, Bedford Institute of Oceanography, Dartmouth, Nova Scotia, 129 pp.

TABLES

Table 1: Monthly mean u (easterly), v (northerly), and w (upward) components of ADCP current measurements along with magnitude and direction.

MONTH	u (cm s^{-1})	v (cm s^{-1})	w (cm s^{-1})	MAGNITUDE of u and v vector (cm s^{-1})	DIRECTION of u and v vector (°T)
November 1993					
0.0 m	66.79	-9.87	-1.01	67.51	98
3.5 m	44.96	-7.61	-0.67	45.60	100
12.2 m	13.01	-11.24	-0.32	17.19	131
20.9 m	11.19	-11.48	-0.18	16.03	136
29.6 m	9.48	-10.30	0.02	14.00	137
38.3 m	8.40	-9.13	0.04	12.41	137
46.9 m	7.78	-7.91	0.04	11.09	135
55.6 m	7.37	-6.81	-0.02	10.03	133
64.3 m	7.00	-5.79	-0.01	9.08	130
73.0 m	6.72	-4.12	-0.08	7.88	121
December 1993					
0.0 m	30.17	-15.37	-0.50	33.86	117
3.5 m	23.30	-10.56	-0.30	25.58	114
12.2 m	3.42	-6.59	0.67	7.43	153
20.9 m	3.52	-5.32	0.03	6.38	147
29.6 m	3.25	-4.45	0.01	5.51	144
38.3 m	3.18	-3.78	-0.03	4.94	140
46.9 m	3.38	-3.25	-0.06	4.69	134
55.6 m	3.44	-2.83	-0.09	4.45	129
64.3 m	3.58	-2.31	-0.07	4.26	123
73.0 m	3.31	-1.51	-0.13	3.64	115
January 1994					
0.0 m	16.35	-10.84	-0.11	19.62	124
3.5 m	15.64	-9.07	-0.34	18.08	120
12.2 m	6.38	-6.96	0.71	9.44	137
20.9 m	6.74	-6.95	0.03	9.68	136
29.6 m	6.13	-6.26	-0.00	8.77	136
38.3 m	6.00	-5.73	-0.04	8.30	134
46.9 m	6.07	-5.33	-0.05	8.07	131
55.6 m	6.25	-5.03	-0.03	8.02	129
64.3 m	6.42	-4.69	-0.01	7.94	126
73.0 m	6.16	-3.93	-0.01	7.31	123

MONTH	u (cm s^{-1})	v (cm s^{-1})	w (cm s^{-1})	MAGNITUDE of u and v vector (cm s^{-1})	DIRECTION of u and v vector (°T)
February 1994					
0.0 m	11.94	-6.97	-0.05	13.82	120
3.5 m	10.87	-5.92	-0.41	12.37	119
12.2 m	3.21	-3.32	0.73	4.62	136
20.9 m	3.29	-3.26	-0.05	4.63	135
29.6 m	3.22	-2.73	-0.08	4.23	130
38.3 m	3.53	-2.55	-0.06	4.36	126
46.9 m	4.17	-2.66	-0.08	4.95	123
55.6 m	4.96	-3.03	-0.07	5.82	121
64.3 m	5.38	-2.92	-0.00	6.12	119
73.0 m	5.53	-2.13	-0.10	5.92	111
March 1994					
0.0 m	1.62	-2.21	-0.22	2.74	144
3.5 m	1.49	-1.61	-0.53	2.20	137
12.2 m	1.10	-0.75	0.51	1.33	124
20.9 m	0.31	-0.82	-0.10	0.88	159
29.6 m	0.45	-0.43	-0.19	0.62	134
38.3 m	0.64	-0.29	-0.21	0.71	114
46.9 m	1.00	-0.25	-0.21	1.03	104
55.6 m	1.42	-0.31	-0.15	1.46	102
64.3 m	1.87	-0.38	-0.14	1.91	101
73.0 m	1.78	-0.57	0.01	1.87	108
April 1994					
0.0 m	-1.22	1.66	-0.73	2.06	-36
3.5 m	-0.50	1.28	-0.74	1.37	-21
12.2 m	3.57	-2.15	0.43	4.16	121
20.9 m	3.64	-2.66	-0.09	4.51	126
29.6 m	3.40	-2.15	-0.14	4.03	122
38.3 m	3.11	-1.57	-0.13	3.48	117
46.9 m	2.97	-1.27	-0.10	3.23	113
55.6 m	2.95	-1.02	-0.05	3.12	109
64.3 m	3.04	-0.70	-0.01	3.12	103
73.0 m	2.74	-0.42	0.04	2.77	99

MONTH	u (cm s^{-1})	v (cm s^{-1})	w (cm s^{-1})	MAGNITUDE of u and v vector (cm s^{-1})	DIRECTION of u and v vector (°T)
May 1994					
0.0 m	1.51	-0.87	-0.32	1.74	120
3.5 m	1.41	-0.70	-0.46	1.57	117
12.2 m	2.12	-1.30	0.54	2.48	121
20.9 m	2.41	-1.11	0.05	2.66	115
29.6 m	2.04	-0.38	0.12	2.07	101
38.3 m	1.48	-0.10	0.22	1.48	94
46.9 m	1.53	-0.06	0.32	1.53	92
55.6 m	1.51	-0.00	0.40	1.51	90
64.3 m	1.52	0.08	0.43	1.52	87
73.0 m	1.19	0.50	0.21	1.29	67
June 1994					
0.0 m	9.57	-2.75	-0.86	9.95	106
3.5 m	8.01	-1.95	-0.58	8.25	104
12.2 m	1.89	-2.40	0.78	3.05	142
20.9 m	1.21	-0.64	0.03	1.37	118
29.6 m	1.39	-0.48	0.04	1.47	109
38.3 m	1.71	-0.83	0.09	1.90	116
46.9 m	1.88	-0.83	0.17	2.05	114
55.6 m	1.81	-0.68	0.23	1.94	111
64.3 m	1.87	-0.47	0.31	1.92	104
73.0 m	1.85	0.00	0.26	1.85	90
July 1994					
0.0 m	8.43	7.20	-0.84	11.08	50
3.5 m	6.61	5.95	-0.41	8.89	48
12.2 m	2.15	-3.02	0.75	3.70	145
20.9 m	1.22	-0.84	0.09	1.48	125
29.6 m	1.21	-1.20	0.05	1.71	135
38.3 m	1.96	-1.73	0.01	2.61	131
46.9 m	2.31	-1.95	0.01	3.02	130
55.6 m	2.56	-1.89	0.03	3.18	126
64.3 m	2.87	-1.85	0.03	3.41	123
73.0 m	2.94	-1.58	0.01	3.34	118

Table 2: Results of complex regression analysis for the ocean current vectors with the 2m winds of beacon 8668 as the independent variable for the period of March 5-13, 1994. The subscripts on U represent the depths relative to the ice/ocean interface. *A* represents the response factor, θ is the turning angle relative to the 2 m wind, and r^2 is the coefficient of determination. The statistics are compiled from 216 observations.

	A	θ	r^2
$U_{0.0}$ ADCP	0.024	-0.63	0.51
$U_{-3.5}$ ADCP	0.022	0.33	0.57
$U_{-12.2}$ ADCP	0.011	5.1	0.45
$U_{-20.9}$ ADCP	0.009	15	0.31
$U_{-29.6}$ ADCP	0.0083	24	0.26
$U_{-38.3}$ ADCP	0.0084	31	0.25
$U_{-46.9}$ ADCP	0.0083	35	0.24
$U_{-55.6}$ ADCP	0.0087	39	0.26
$U_{-64.3}$ ADCP	0.0091	43	0.27
$U_{-73.0}$ ADCP	0.0087	50	0.27

Table 3: Results of complex regression analysis for the ocean current vectors with CMC 0-Hour forecast as the independent variable for the period of March 5-13, 1994. The subscripts on U represent the depths relative to the ice/ocean interface. *A* represents the response factor, θ is the turning angle relative to the 2 m wind, and r^2 is the coefficient of determination. The statistics are compiled from 17 observations.

	A	θ	r^2
$U_{0.0}$ ADCP	0.012	-9.2	0.53
$U_{-3.5}$ ADCP	0.011	-3.6	0.52
$U_{-12.2}$ ADCP	0.0061	-2.7	0.44
$U_{-20.9}$ ADCP	0.0046	-3.7	0.28
$U_{-29.6}$ ADCP	0.0045	10.3	0.25
$U_{-38.3}$ ADCP	0.0043	14.7	0.25
$U_{-46.9}$ ADCP	0.0041	22.6	0.23
$U_{-55.6}$ ADCP	0.0045	29.2	0.27
$U_{-64.3}$ ADCP	0.0044	29.3	0.25
$U_{-73.0}$ ADCP	0.0044	40.5	0.26

Table 4: Results of complex correlation analysis for the ocean current vectors and the CMC gridded wind interpolated to the site of the ADCP. Analysis is for the total sampling period, for period of ice cover, and period of no ice cover at all depths relative to the ice/ocean interface. *A* is the response factor, r is the correlation coefficient, θ is the turning angle relative to the CMC wind, *t* is Student's t statistic, and n is the number of observations used in the computation. ADCP α and CMC α are the vector mean directions for the designated time periods.

	0.0 m	3.5 m	12.2 m	20.9 m	29.6 m	38.3 m	46.9 m	55.6 m	64.3 m	73.0 m
Total										
A	0.04	0.03	0.01	0.01	0.01	0.01	0.01	0.01	0.01	0.01
r	0.63	0.65	0.52	0.46	0.44	0.43	0.44	0.45	0.47	0.47
θ	-1.51	-2.56	-18.99	-15.77	-9.26	-2.94	4.68	9.21	12.04	16.01
t	18.31	19.06	13.84	11.55	10.91	10.70	11.01	11.35	12.14	11.97
n	511									
ADCP α	-16.57	-15.80	-42.62	-40.71	-38.57	-35.04	-31.63	-29.30	-26.32	-23.75
CMC α	-8.73									
Ice										
A	0.02	0.02	0.01	0.01	0.01	0.01	0.01	0.01	0.01	0.01
r	0.76	0.75	0.57	0.49	0.46	0.45	0.45	0.46	0.48	0.48
θ	-7.11	-7.26	-17.49	-17.86	-11.56	-6.42	1.41	5.99	10.19	15.25
t	17.17	16.81	10.35	8.46	7.69	7.52	7.55	7.69	8.14	8.07
n	224									
ADCP α	-37.22	-32.71	-45.00	-42.46	-38.36	-34.70	-30.77	-29.30	-27.18	-25.76
CMC α	-19.99									
No ice										
A	0.06	0.04	0.01	0.01	0.01	0.01	0.01	0.01	0.01	0.01
r	0.72	0.70	0.50	0.43	0.42	0.42	0.43	0.44	0.46	0.45
θ	2.50	1.33	-19.11	-12.95	-7.05	0.21	7.26	11.88	13.33	16.47
t	17.28	16.35	9.87	8.06	7.90	7.71	8.01	8.22	8.72	8.43
n	287									
ADCP α	-7.91	-6.52	-41.07	-39.38	-38.73	-35.32	-32.41	-29.30	-25.38	-21.37
CMC α	4.56									

FIGURES

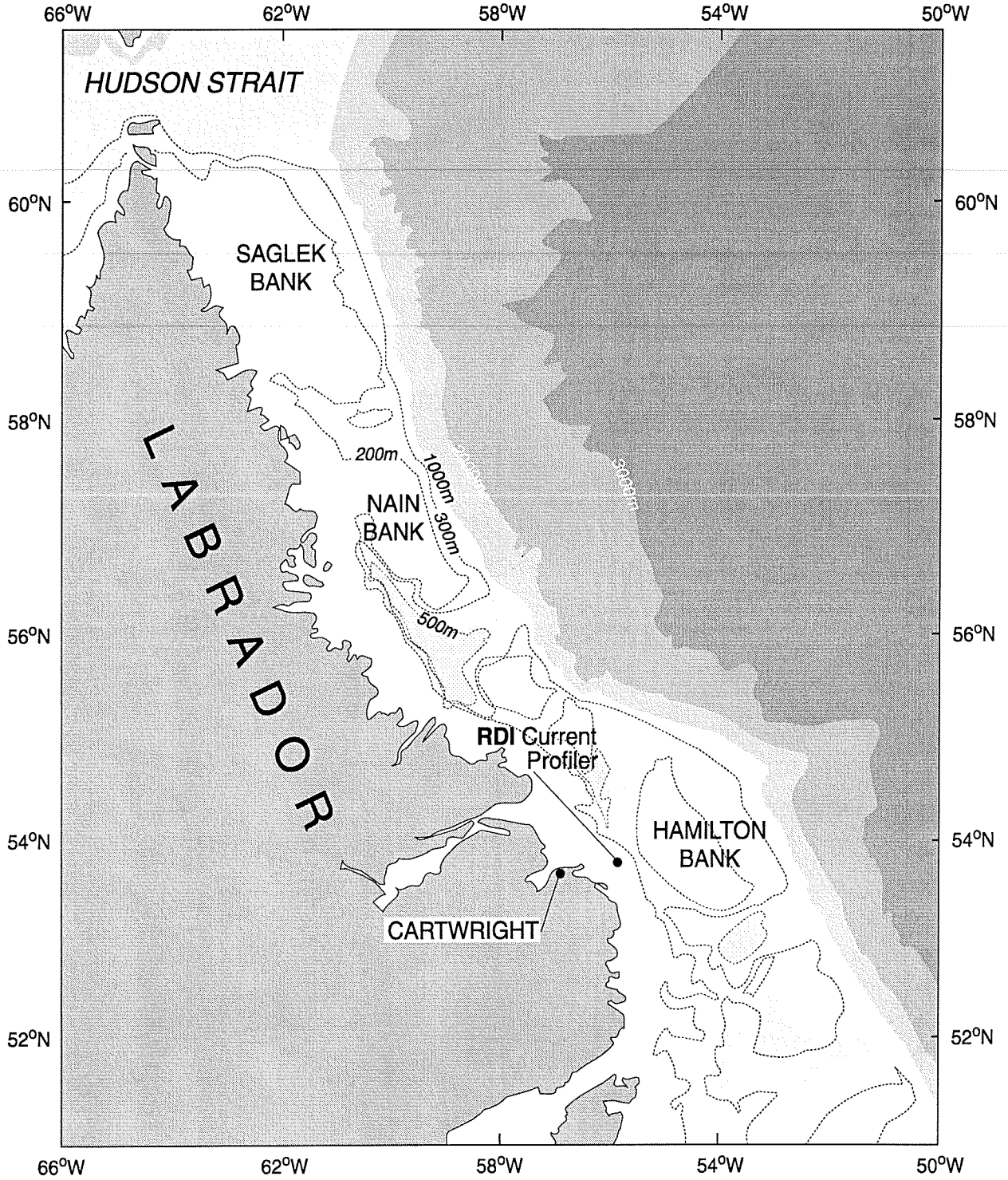

Figure 1: Deployment location of bottom-mounted acoustic Doppler current profiler for period of November 1993-July 1994

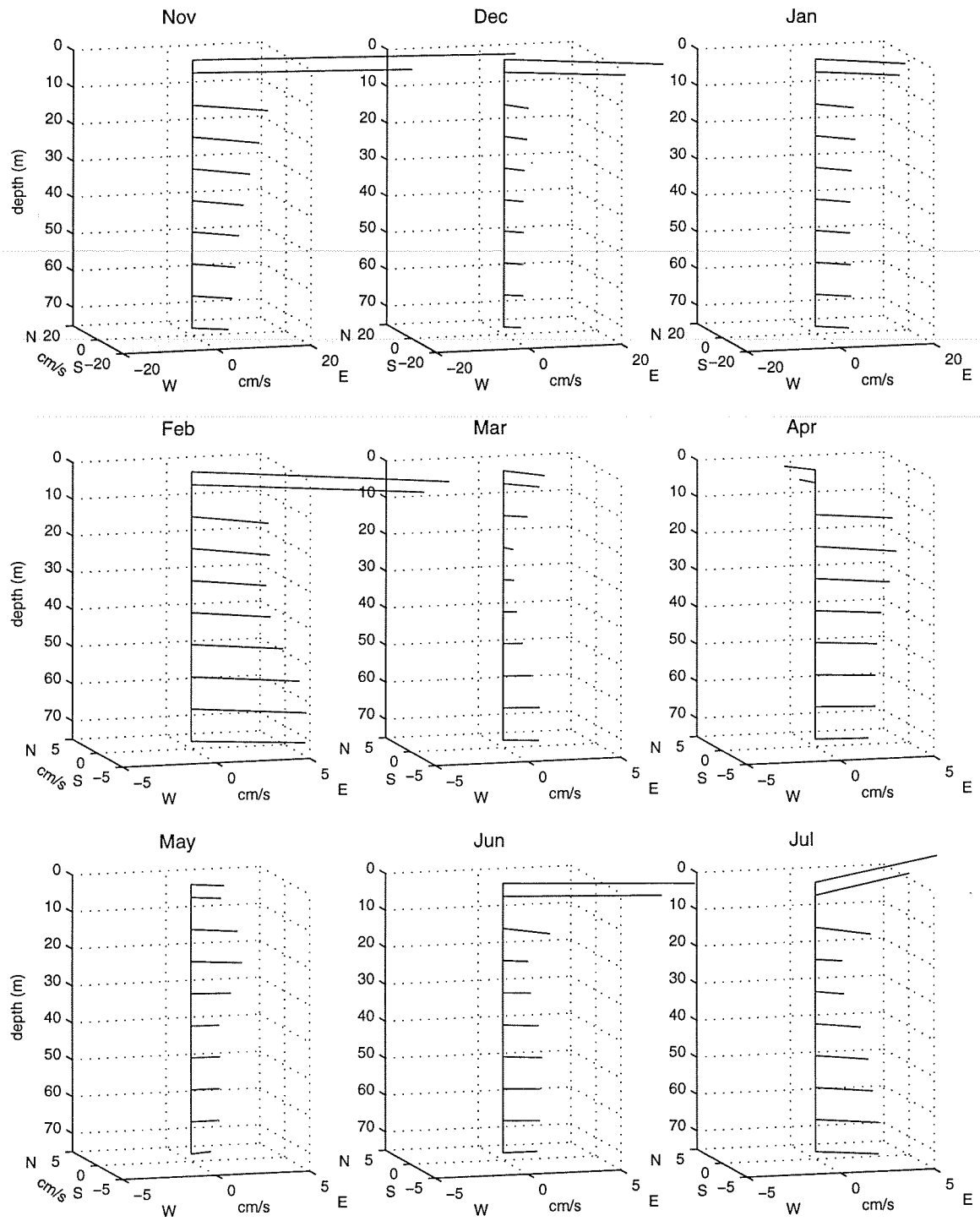

Figure 2: Monthly-mean horizontal velocity vectors for the water column above the ADCP location.

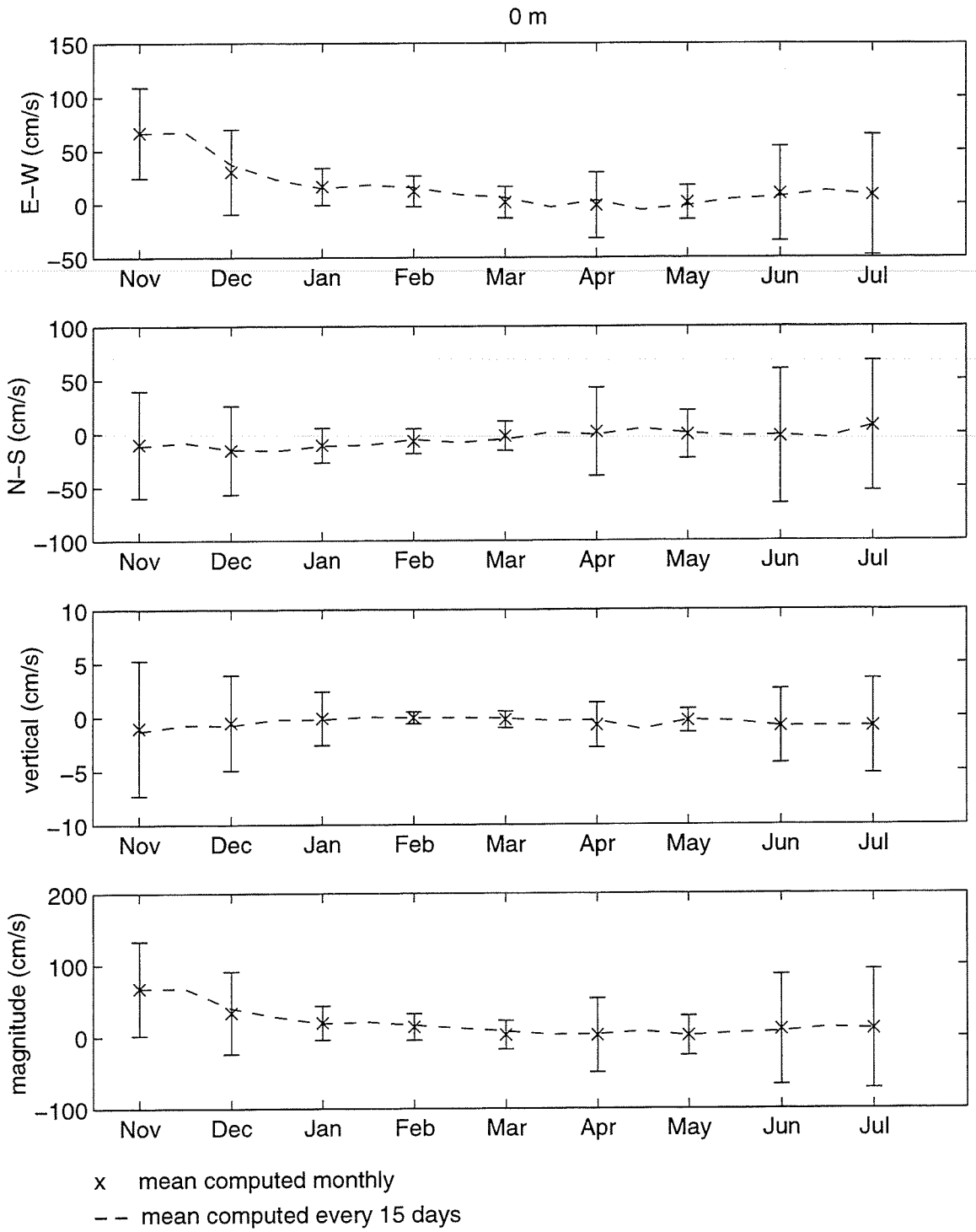

Figure 3: Monthly means of the u (easterly), v (northerly) and w (upward) components of velocity and magnitude for 0.0 m. Error bars represent one standard deviation for the monthly mean. The dashed line shows the mean current computed over 15 days.

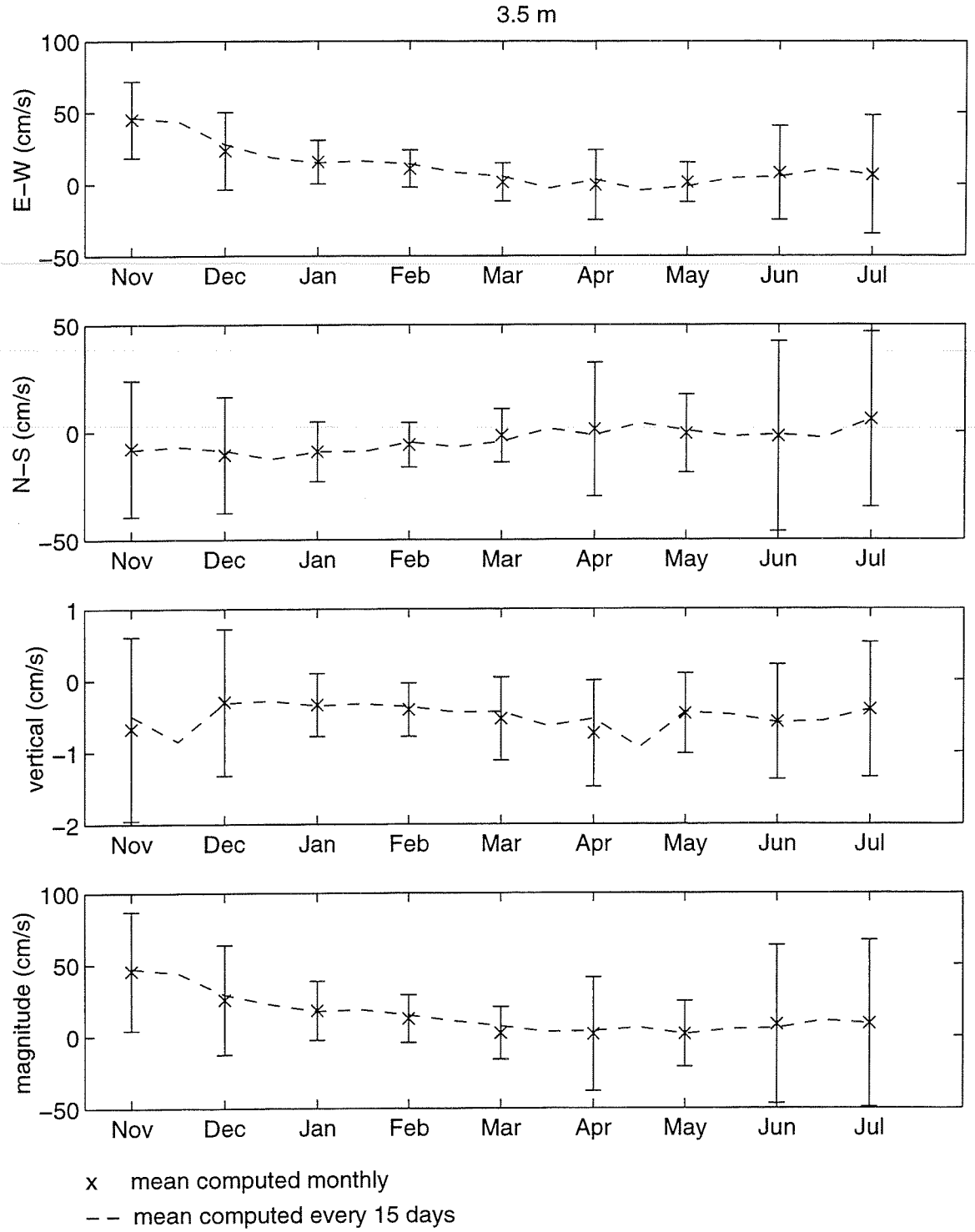

Figure 4: Monthly means of the u (easterly), v (northerly) and w (upward) components of velocity and magnitude for 3.5 m. Error bars represent one standard deviation for the monthly mean. The dashed line shows the mean current computed over 15 days.

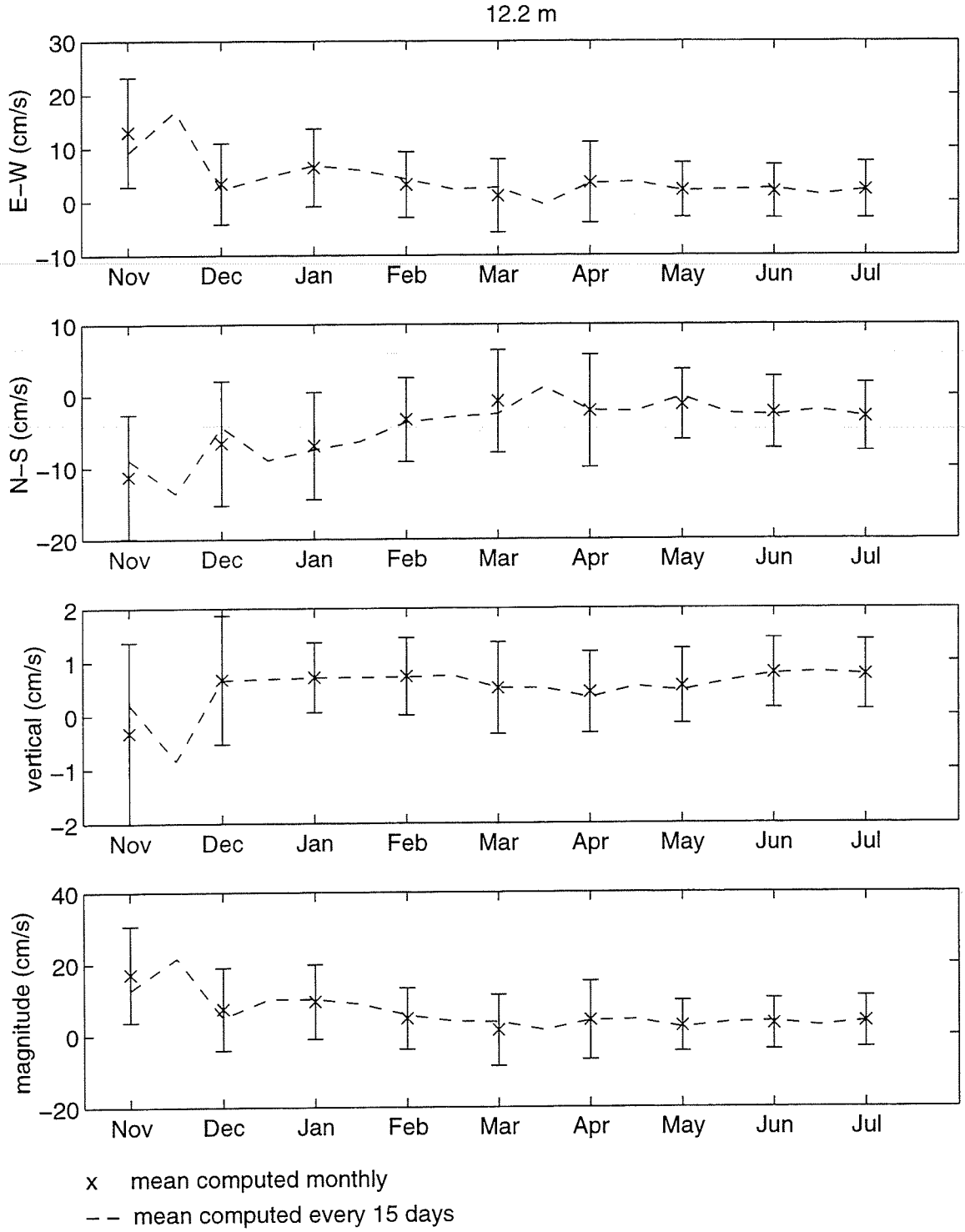

Figure 5: Monthly means of the u (easterly), v (northerly) and w (upward) components of velocity and magnitude for 12.2 m. Error bars represent one standard deviation for the monthly mean. The dashed line shows the mean current computed over 15 days.

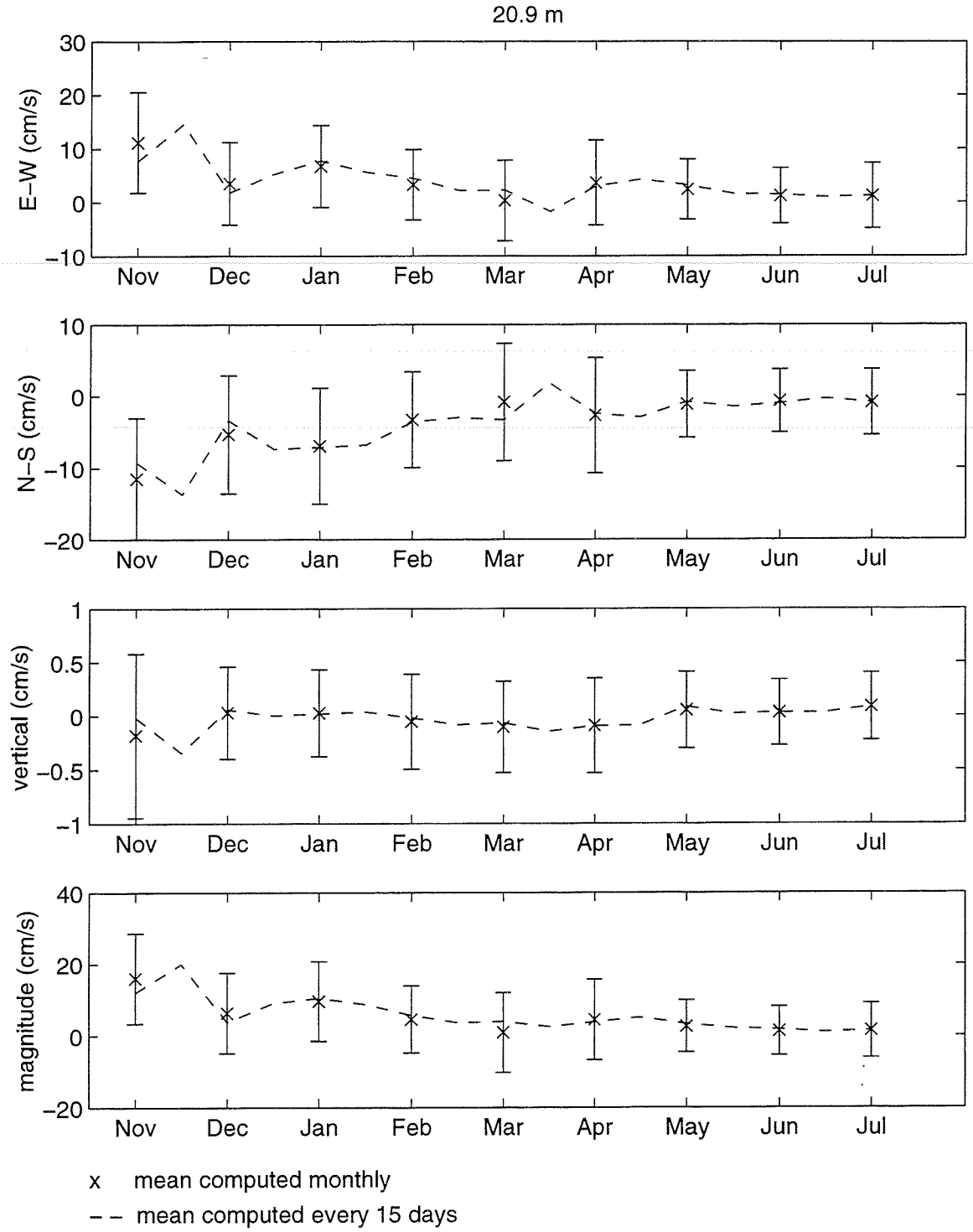

Figure 6: Monthly means of the u (easterly), v (northerly) and w (upward) components of velocity and magnitude for 20.9 m. Error bars represent one standard deviation for the monthly mean. The dashed line shows the mean current computed over 15 days.

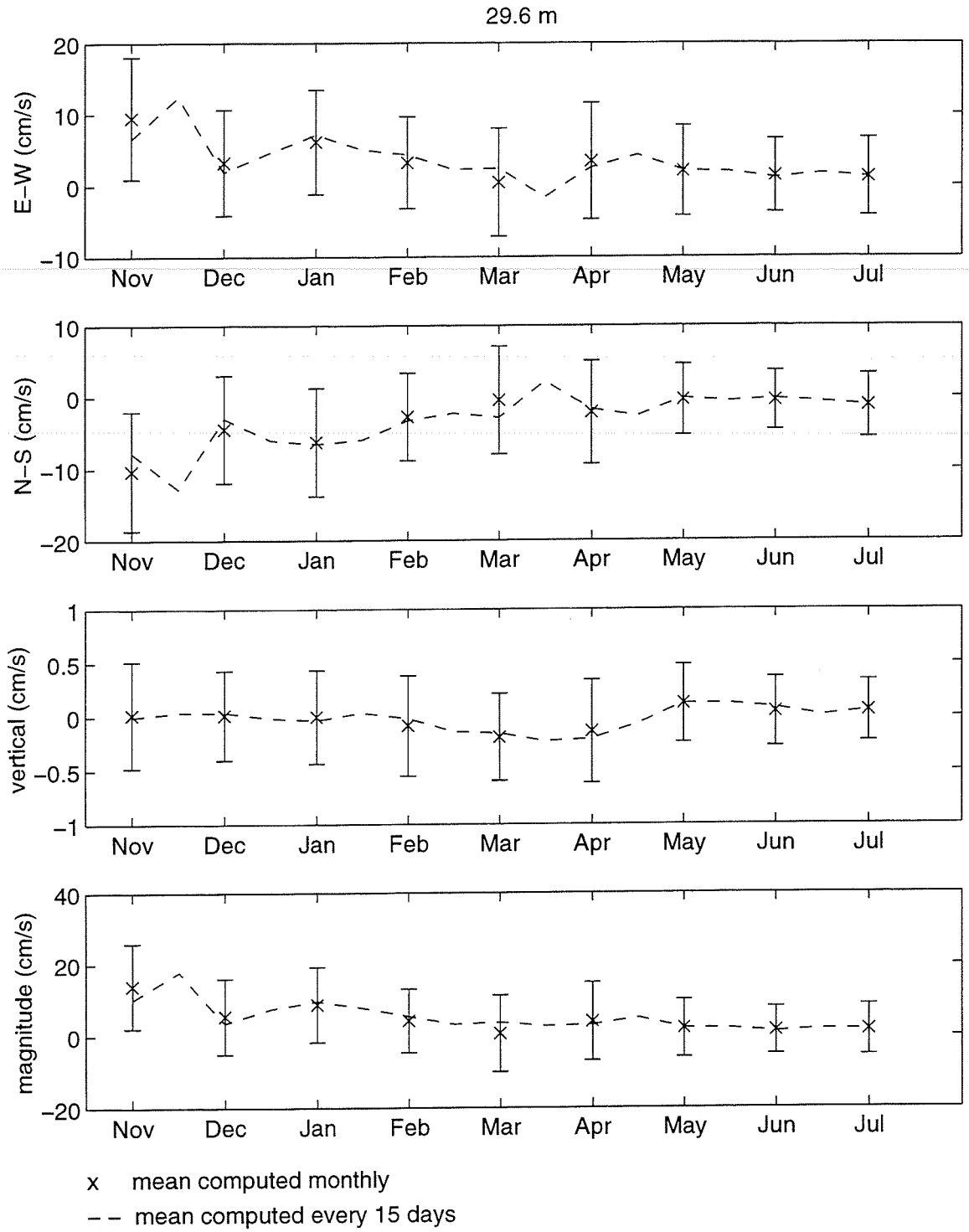

Figure 7: Monthly means of the u (easterly), v (northerly) and w (upward) components of velocity and magnitude for 29.6 m. Error bars represent one standard deviation for the monthly mean. The dashed line shows the mean current computed over 15 days.

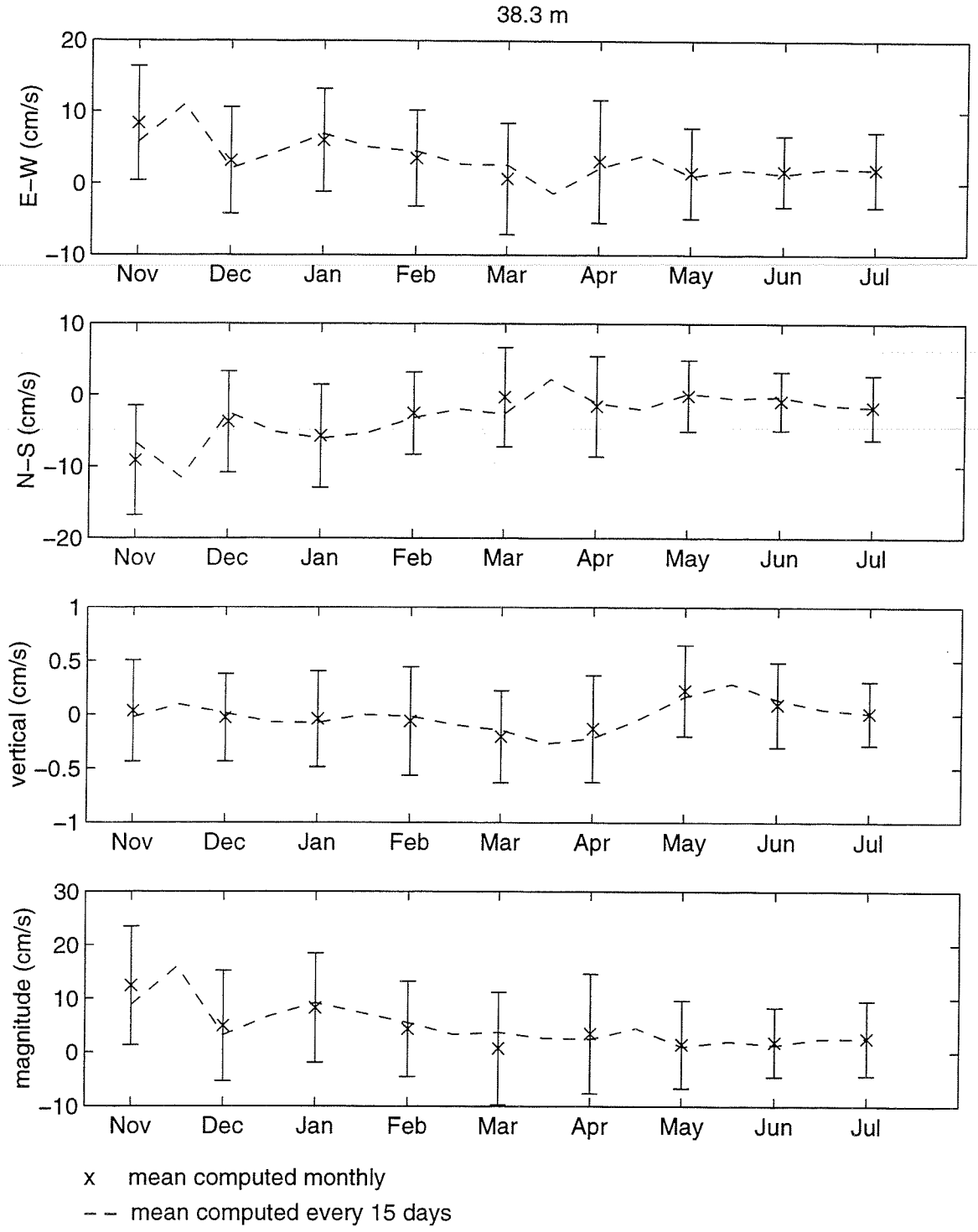

Figure 8: Monthly means of the u (easterly), v (northerly) and w (upward) components of velocity and magnitude for 38.3 m. Error bars represent one standard deviation for the monthly mean. The dashed line shows the mean current computed over 15 days.

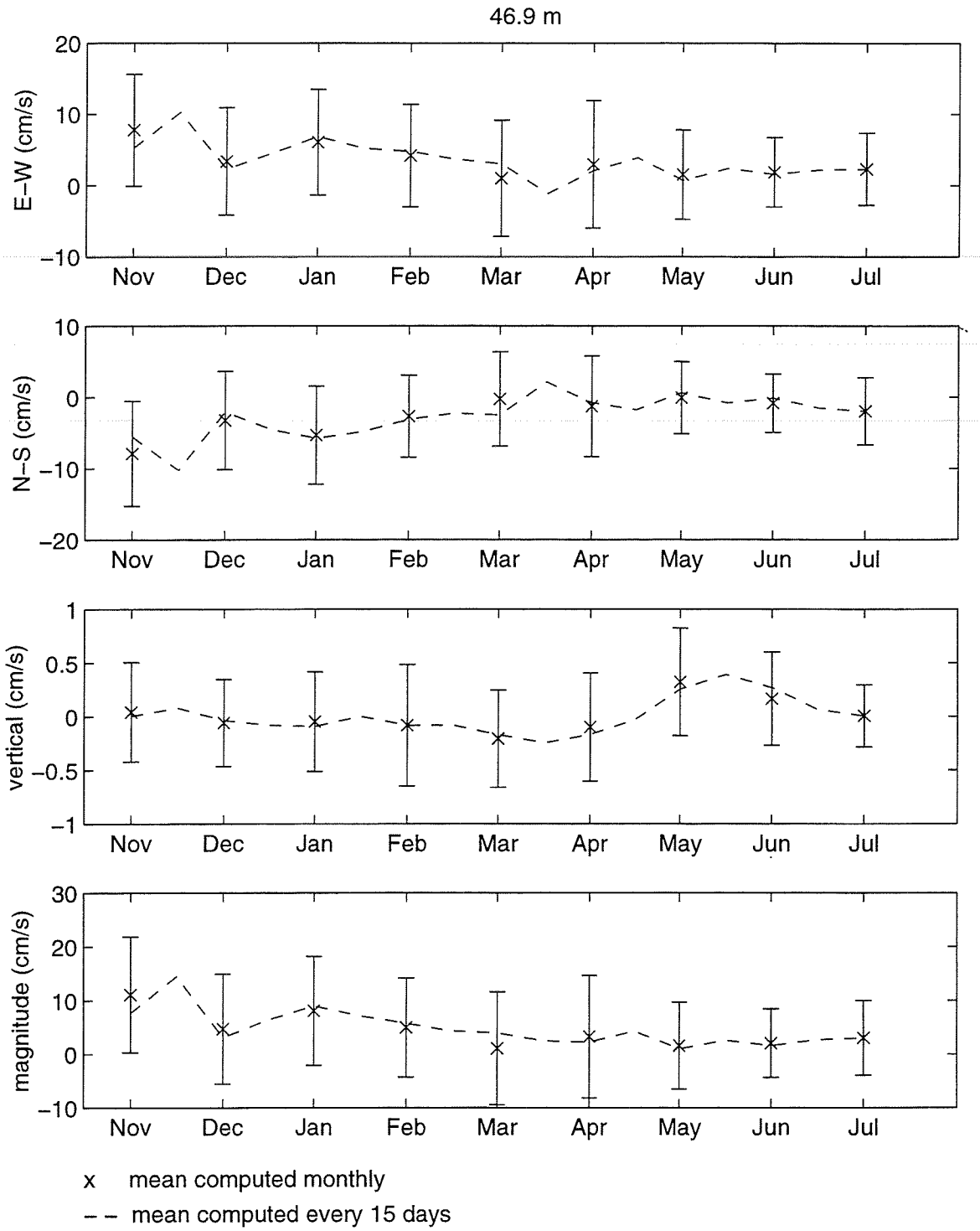

Figure 9: Monthly means of the u (easterly), v (northerly) and w (upward) components of velocity and magnitude for 46.9 m. Error bars represent one standard deviation for the monthly mean. The dashed line shows the mean current computed over 15 days.

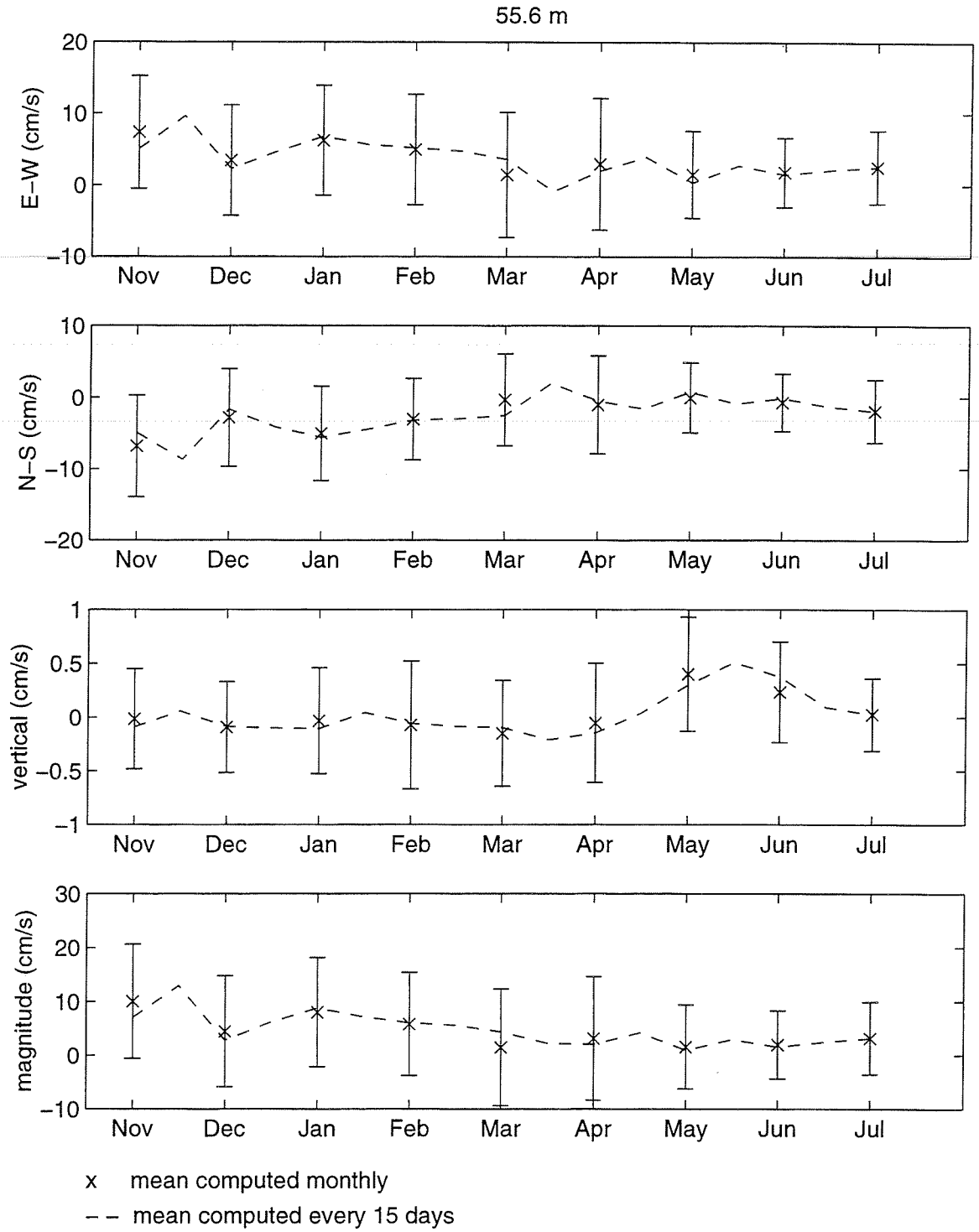

Figure 10: Monthly means of the u (easterly), v (northerly) and w (upward) components of velocity and magnitude for 55.6 m. Error bars represent one standard deviation for the monthly mean. The dashed line shows the mean current computed over 15 days.

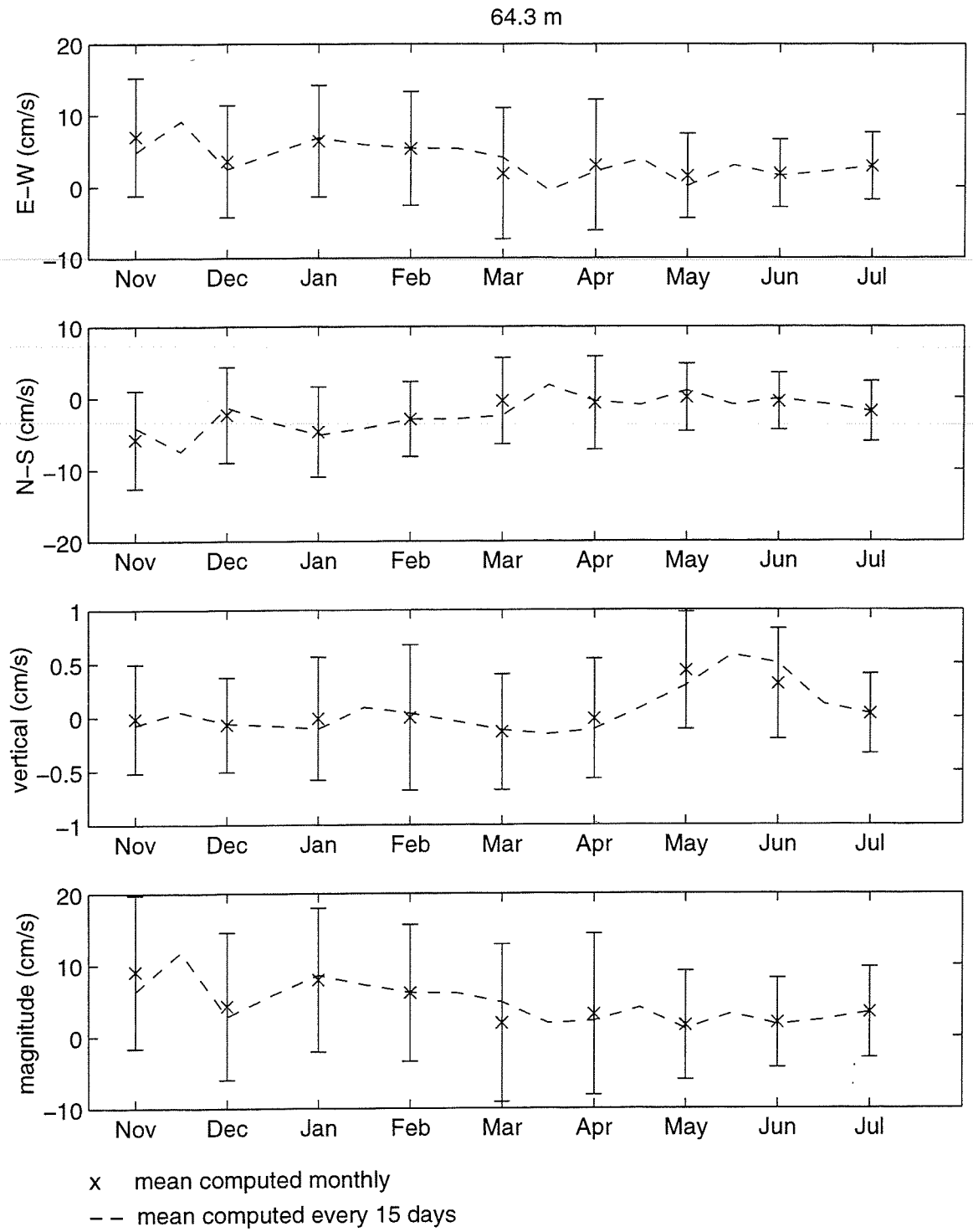

Figure 11: Monthly means of the u (easterly), v (northerly) and w (upward) components of velocity and magnitude for 64.3 m. Error bars represent one standard deviation for the monthly mean. The dashed line shows the mean current computed over 15 days.

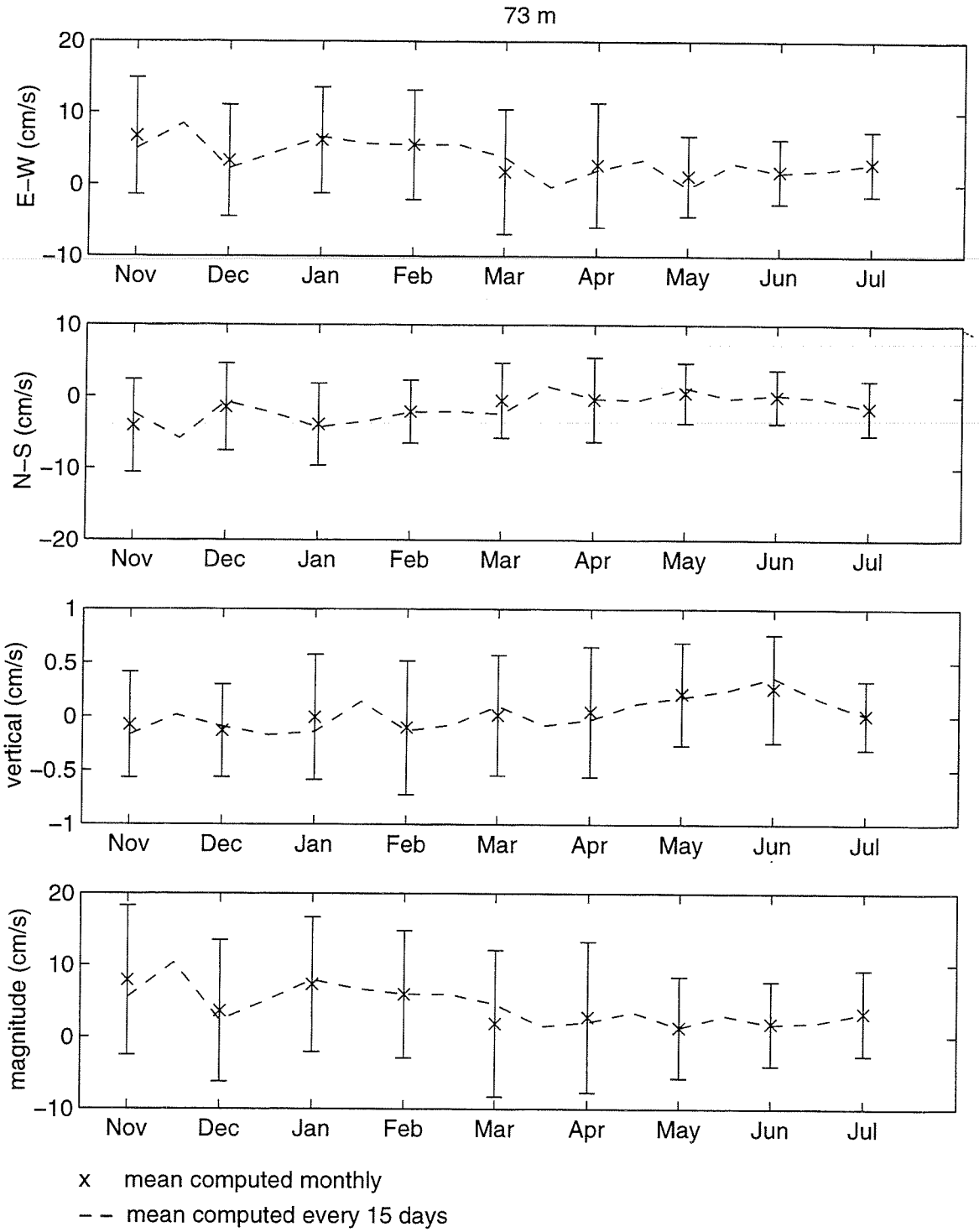

Figure 12: Monthly means of the u (easterly), v (northerly) and w (upward) components of velocity and magnitude for 73.0 m. Error bars represent one standard deviation for the monthly mean. The dashed line shows the mean current computed over 15 days.

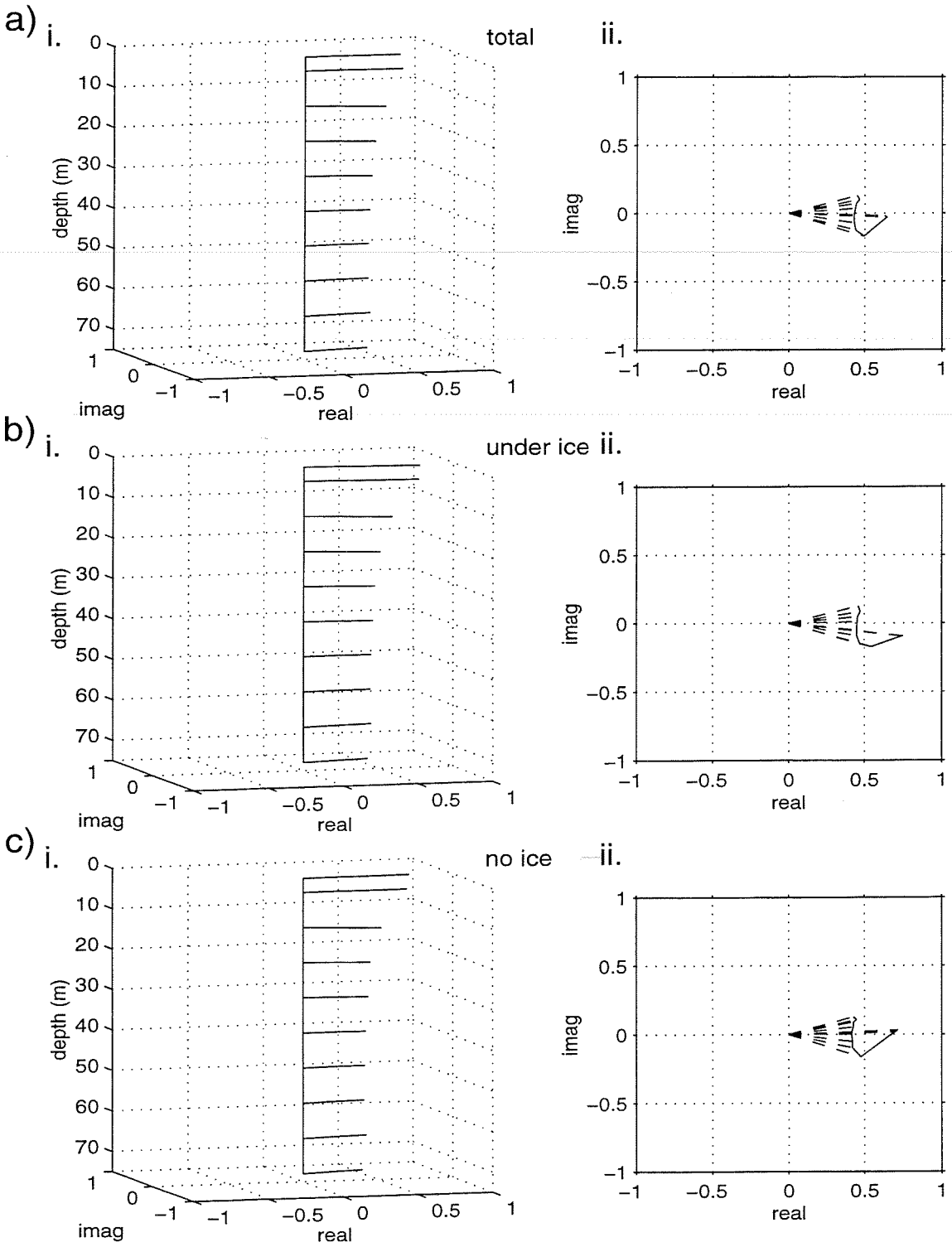

Figure 13: Complex correlation coefficients for correlation analysis between CMC gridded wind velocity and ADCP horizontal current for a) total time period, b) period of ice cover, and c) period of no ice cover; i) three dimensional view and ii) plan view.

APPENDIX A: RAW DATA

- ADCP data in 10 bins centered at 0.0, 3.5, 12.2, 20.9, 29.6, 38.3, 46.9, 55.6, 64.3, and 73.0 m relative to the ocean surface
- transducer frequency was 150 kHz with a head angle of 20°
- time series plots of hourly data presented monthly for each of the 10 bins

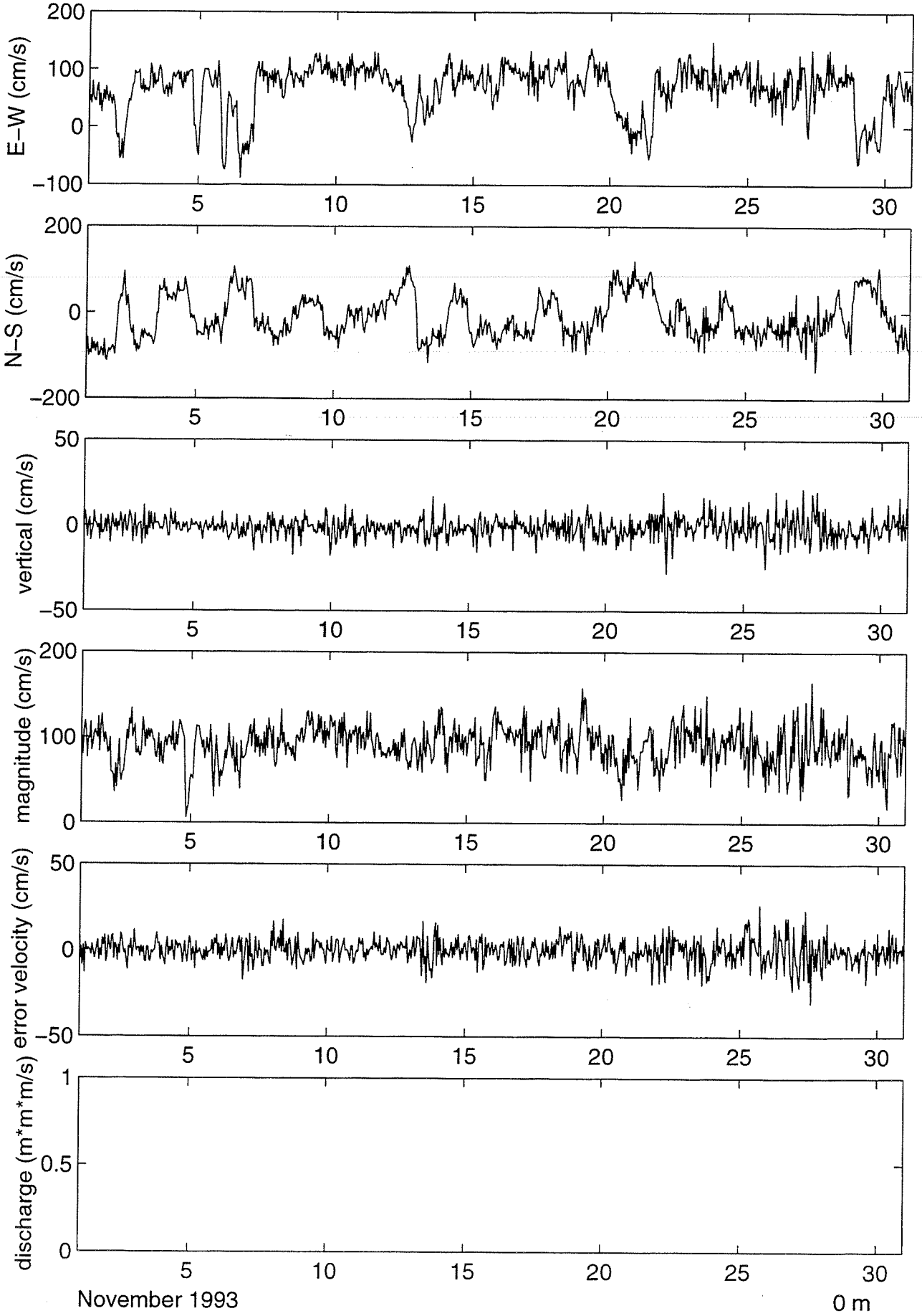
E–W (cm/s)
200
100
0
–100
N–S (cm/s)
200
0
–200
vertical (cm/s)
50
0
–50
magnitude (cm/s)
200
100
0
error velocity (cm/s)
50
0
–50
discharge (m*m*m/s)
1
0.5
0
5
10
15
20
25
30
November 1993
0 m

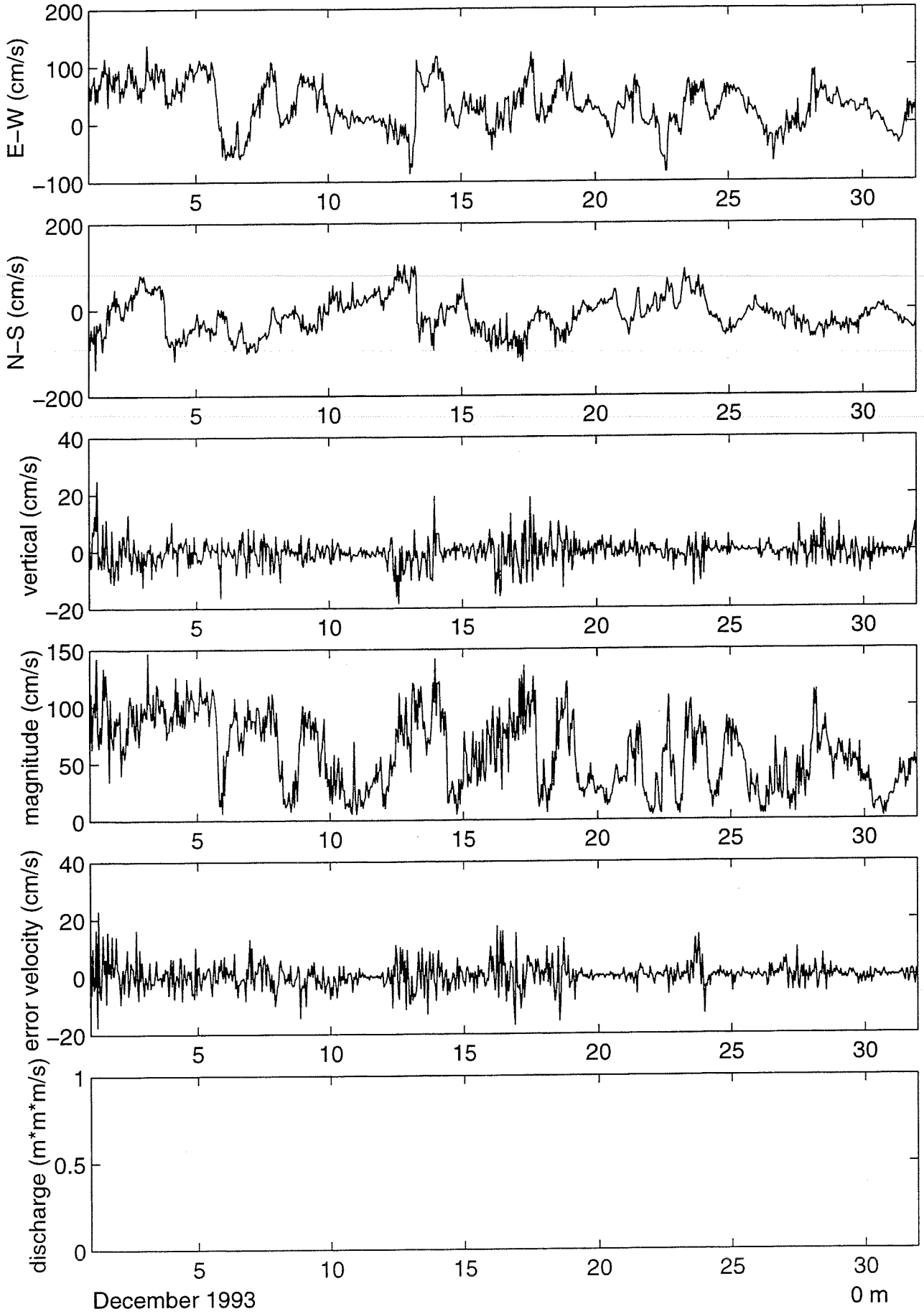
E–W (cm/s)
N–S (cm/s)
vertical (cm/s)
magnitude (cm/s)
error velocity (cm/s)
discharge (m*m*m/s)
December 1993
0 m

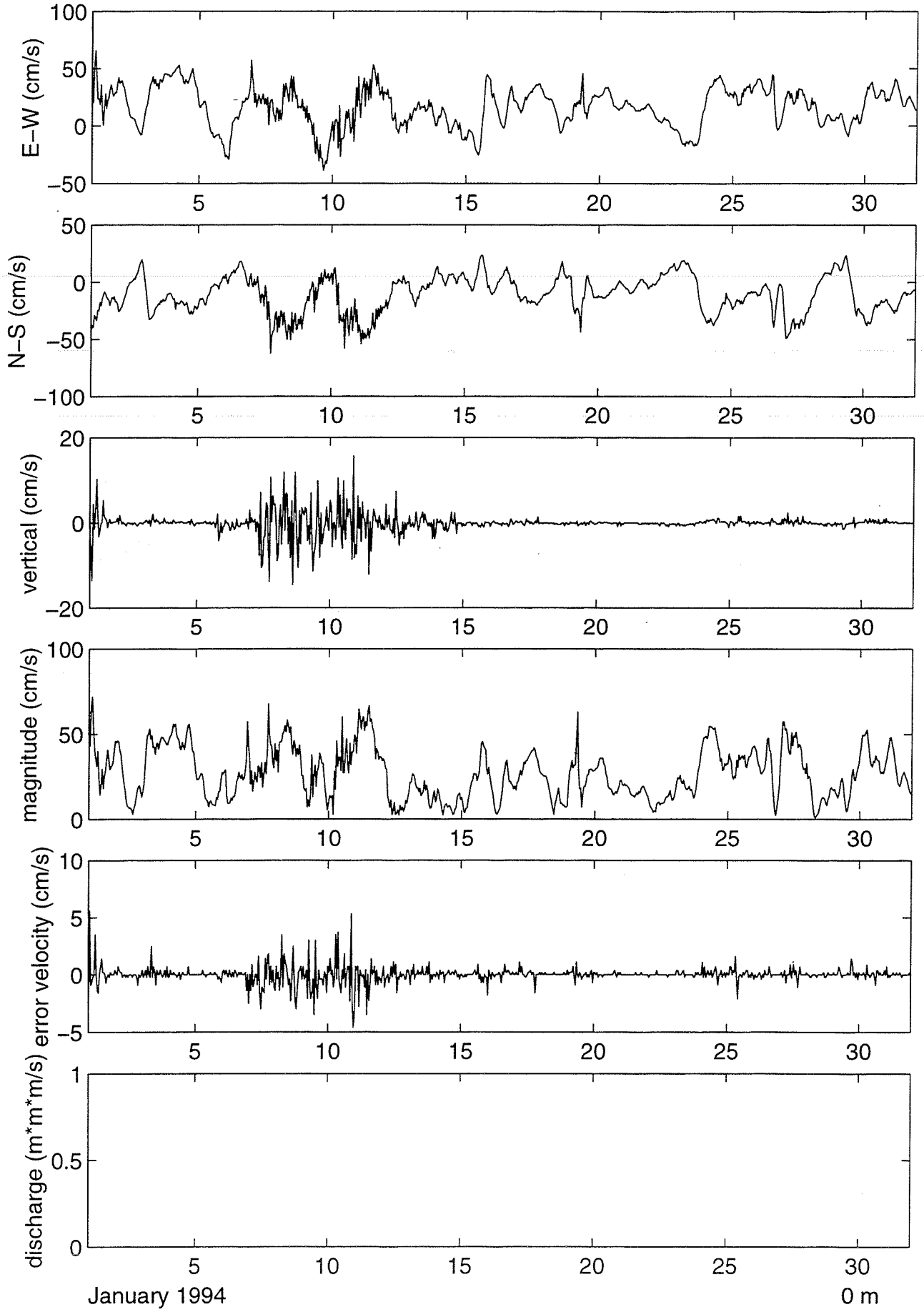
E–W (cm/s)
N–S (cm/s)
vertical (cm/s)
magnitude (cm/s)
error velocity (cm/s)
discharge (m*m*m/s)
January 1994
0 m

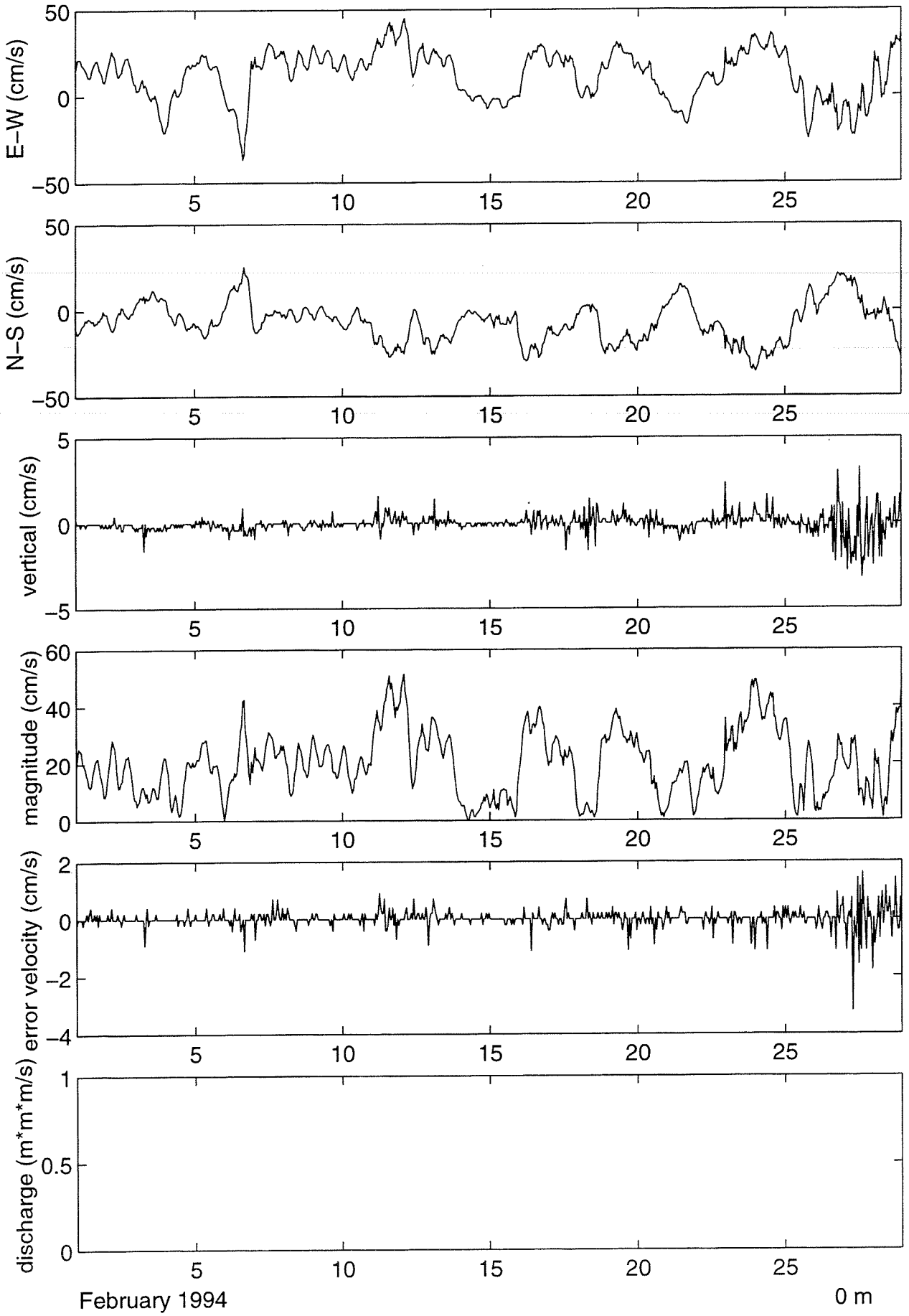
E–W (cm/s)
N–S (cm/s)
vertical (cm/s)
magnitude (cm/s)
error velocity (cm/s)
discharge (m*m*m/s)
February 1994
0 m

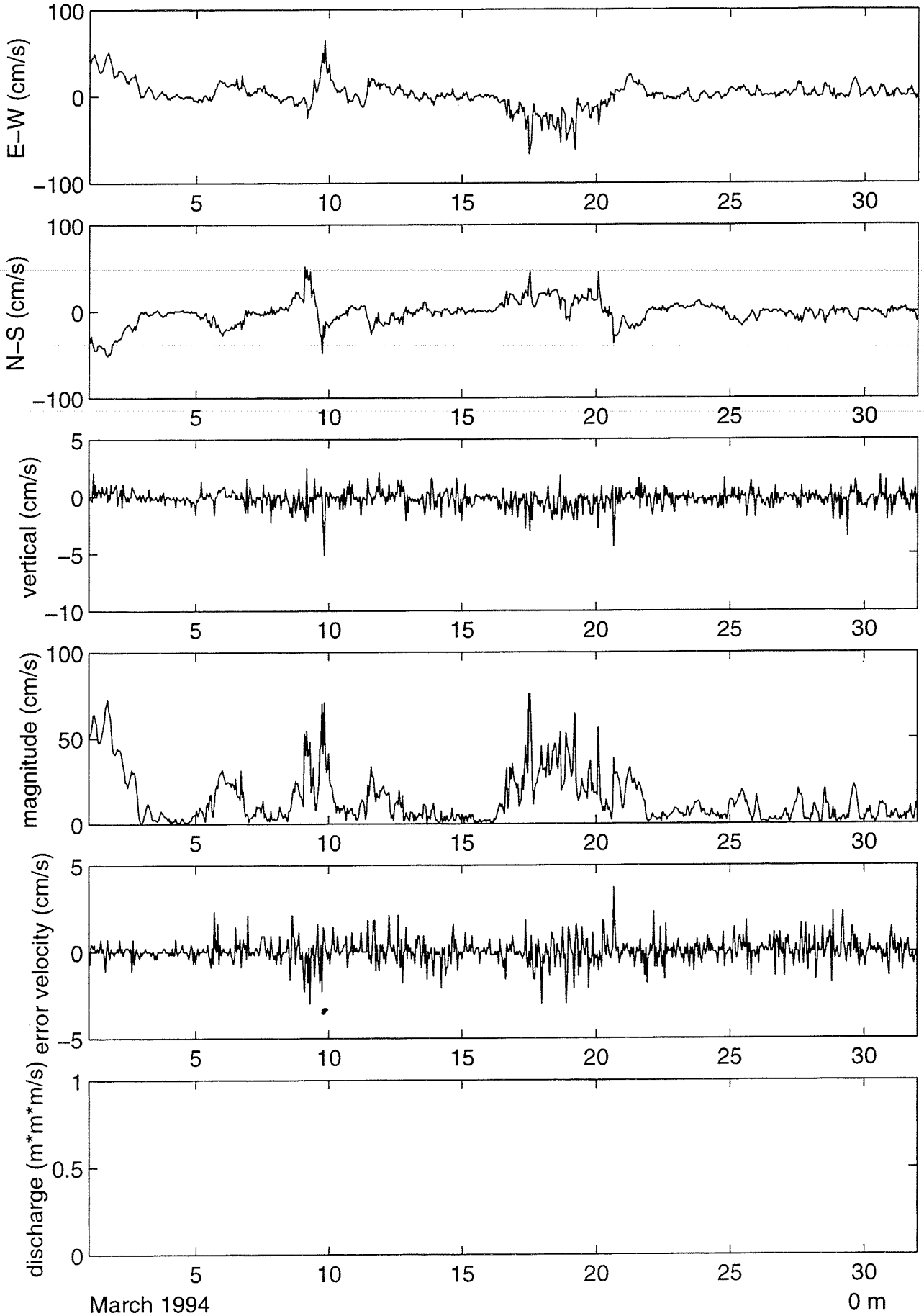
E–W (cm/s)
N–S (cm/s)
vertical (cm/s)
magnitude (cm/s)
error velocity (cm/s)
discharge (m*m*m/s)
March 1994
0 m

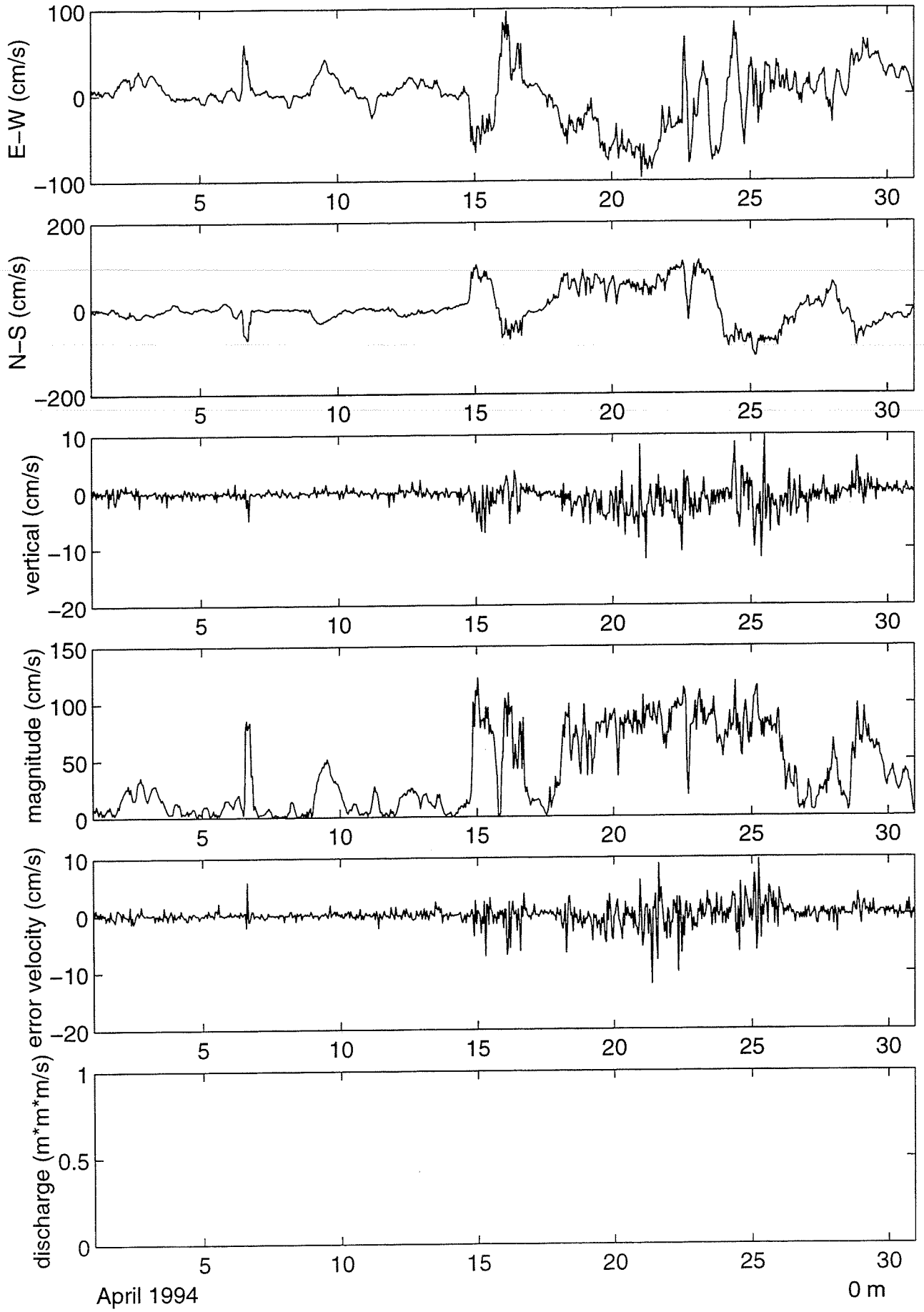
E–W (cm/s)
100
0
–100
N–S (cm/s)
200
0
–200
vertical (cm/s)
10
0
–10
–20
magnitude (cm/s)
150
100
50
0
error velocity (cm/s)
10
0
–10
–20
discharge (m*m*m/s)
1
0.5
0
5
10
15
20
25
30
April 1994
0 m

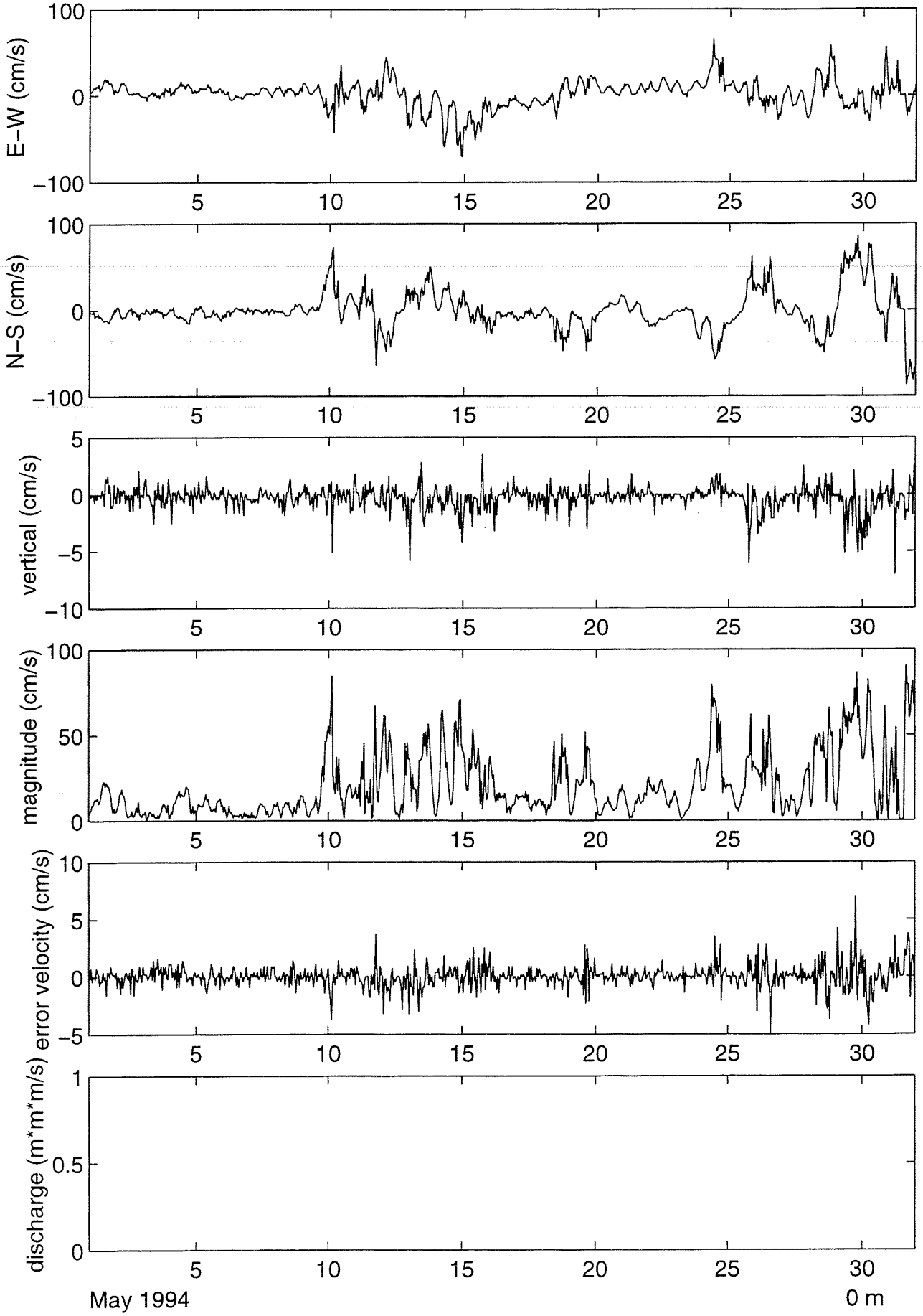
E–W (cm/s)
N–S (cm/s)
vertical (cm/s)
magnitude (cm/s)
error velocity (cm/s)
discharge (m*m*m/s)
May 1994
0 m

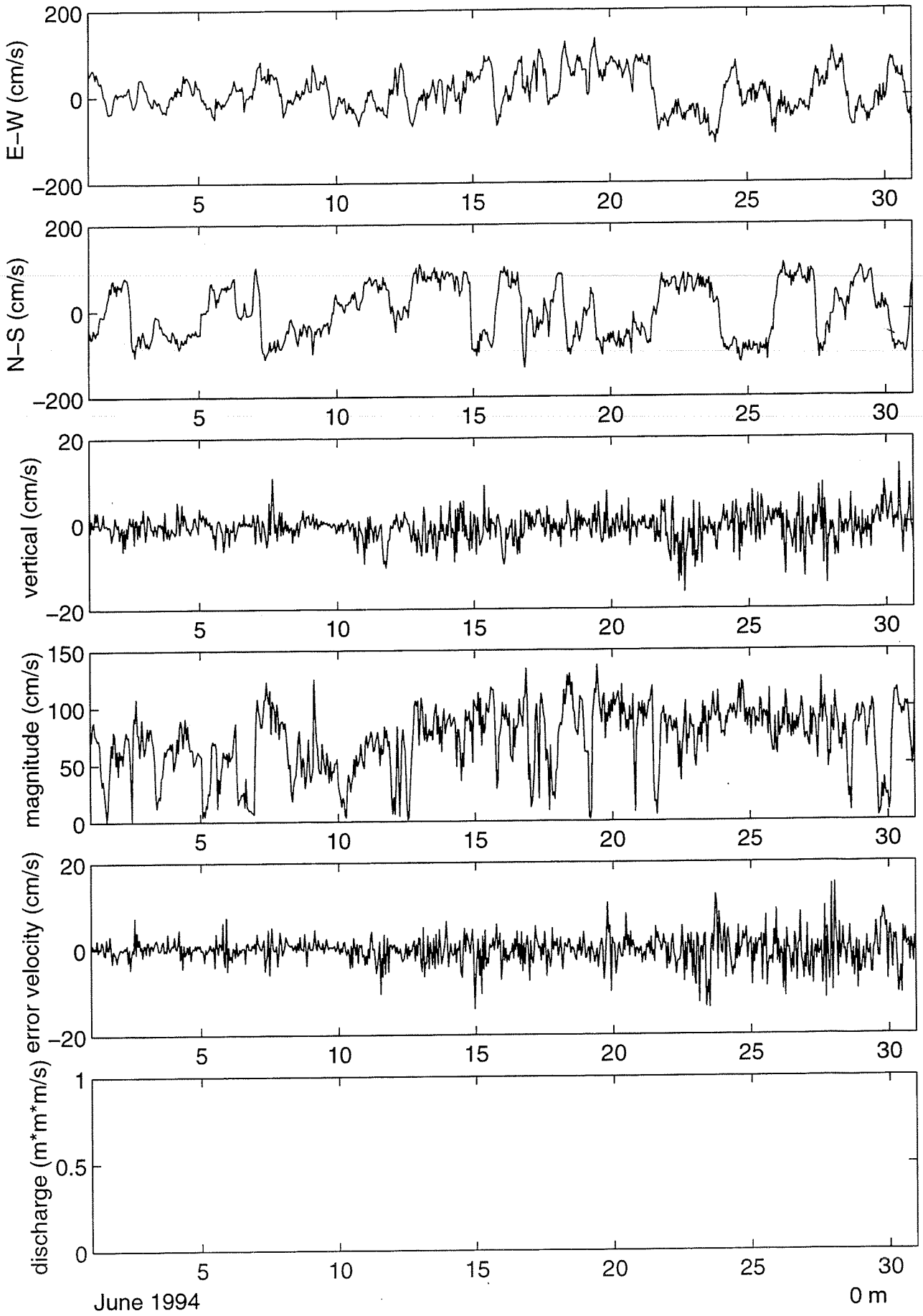
E–W (cm/s)
200
0
–200
N–S (cm/s)
200
0
–200
vertical (cm/s)
20
0
–20
magnitude (cm/s)
150
100
50
0
error velocity (cm/s)
20
0
–20
discharge (m*m*m/s)
1
0.5
0
5
10
15
20
25
30
June 1994
0 m

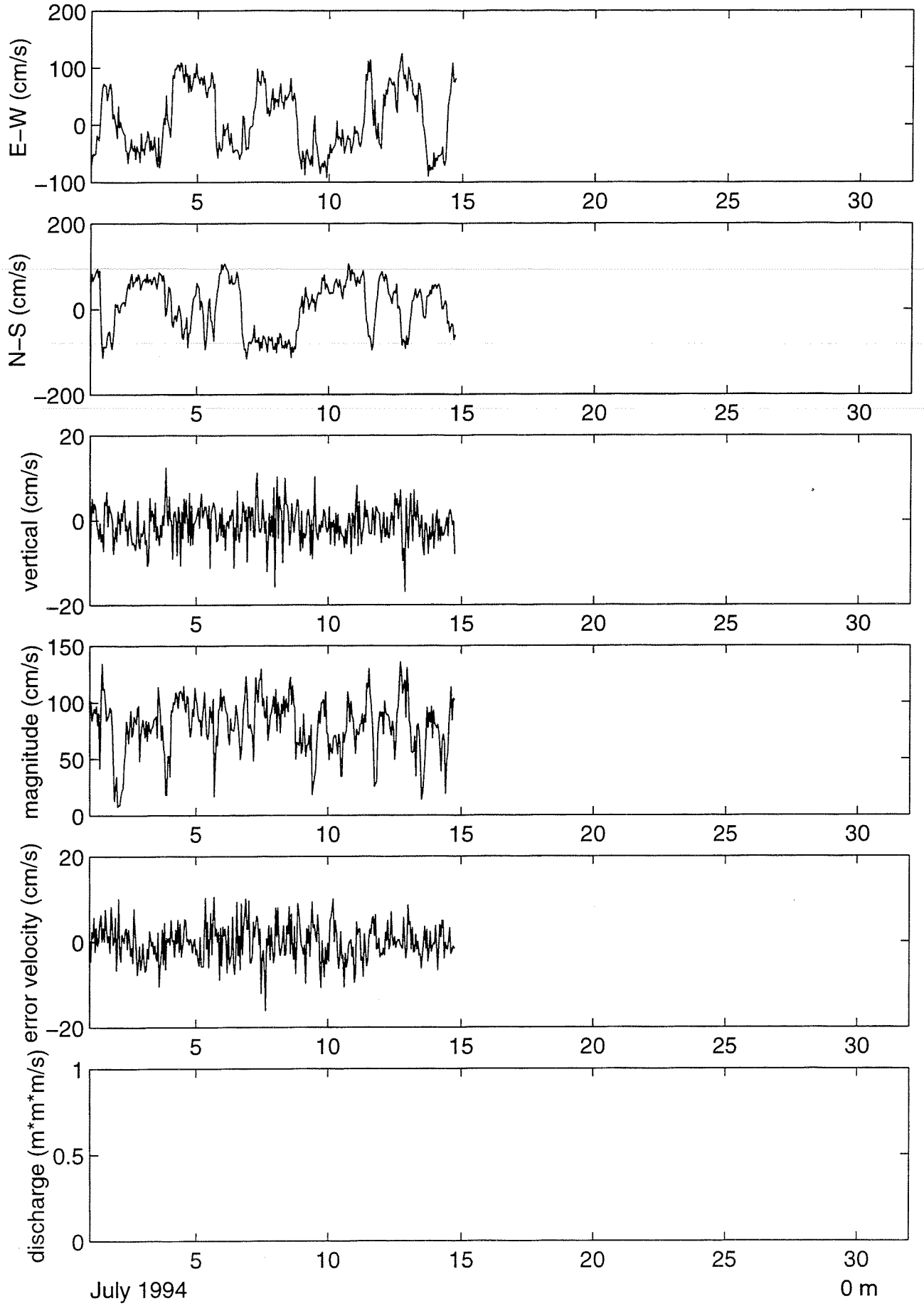
E–W (cm/s)
200
100
0
–100
N–S (cm/s)
200
0
–200
vertical (cm/s)
20
0
–20
magnitude (cm/s)
150
100
50
0
error velocity (cm/s)
20
0
–20
discharge (m*m*m/s)
1
0.5
0
5
10
15
20
25
30
July 1994
0 m

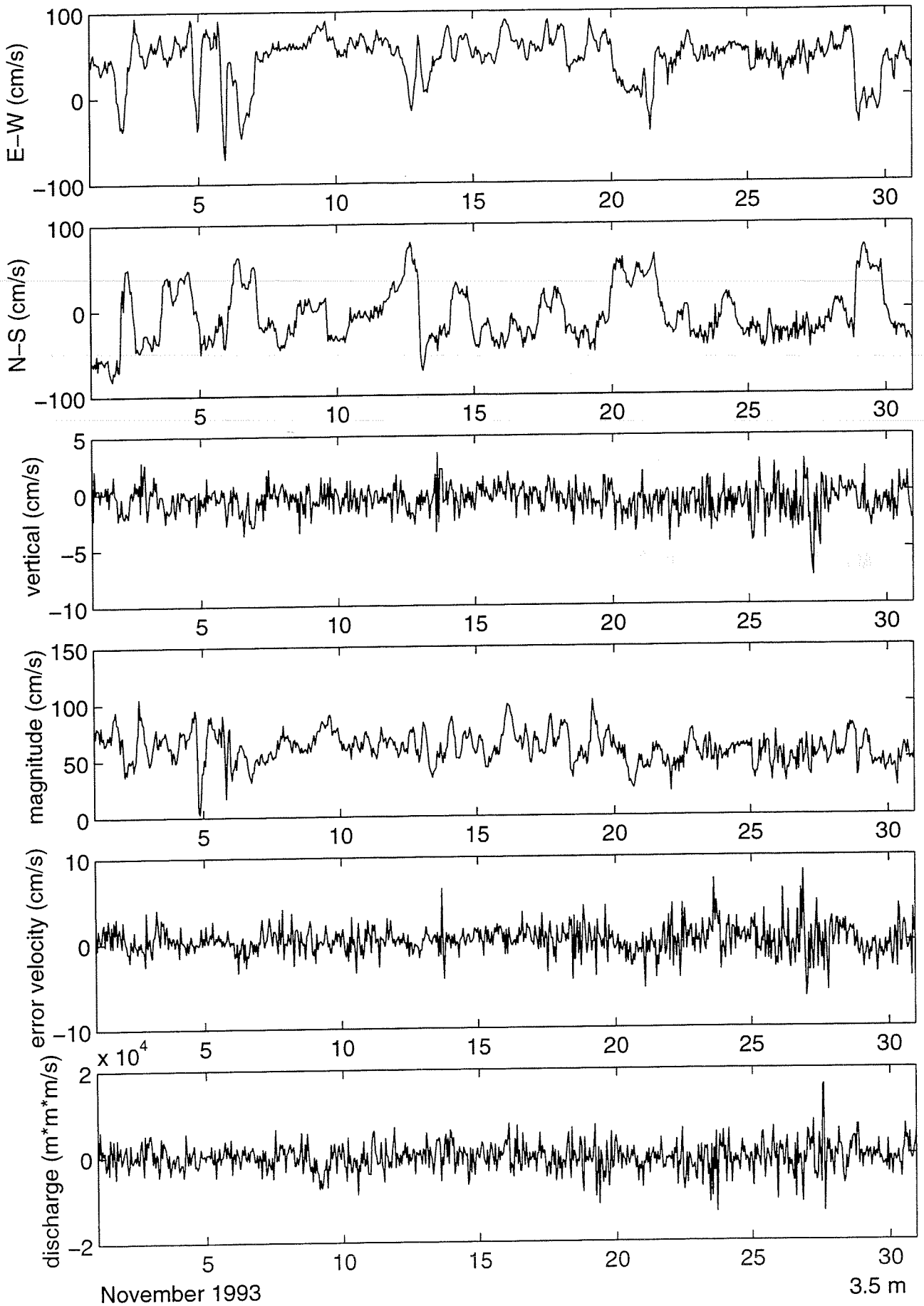
E–W (cm/s)
N–S (cm/s)
vertical (cm/s)
magnitude (cm/s)
error velocity (cm/s)
x 10^4
discharge (m*m*m/s)
November 1993
3.5 m

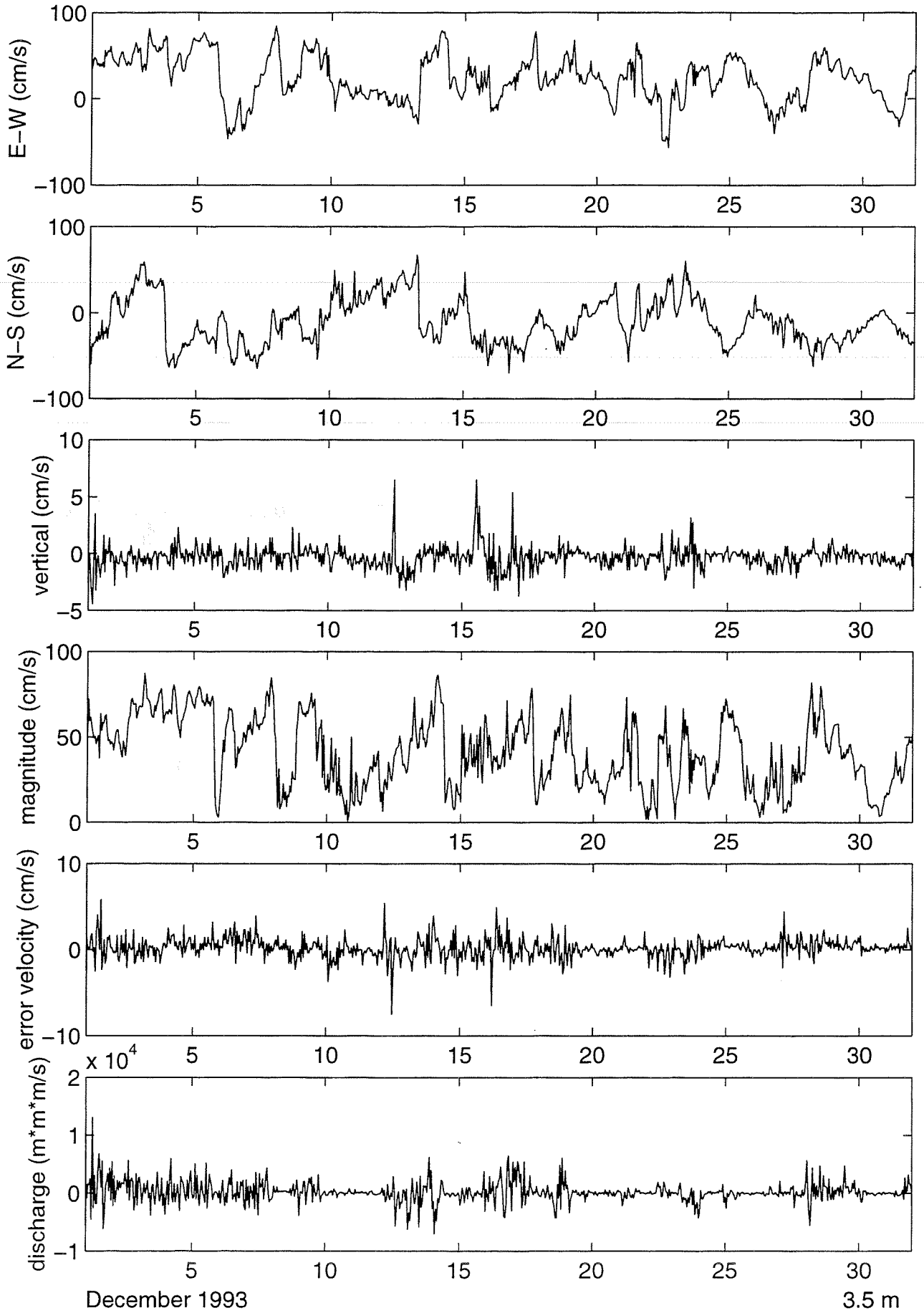
E–W (cm/s)
N–S (cm/s)
vertical (cm/s)
magnitude (cm/s)
error velocity (cm/s)
discharge (m*m*m/s)
x 10^4
December 1993
3.5 m

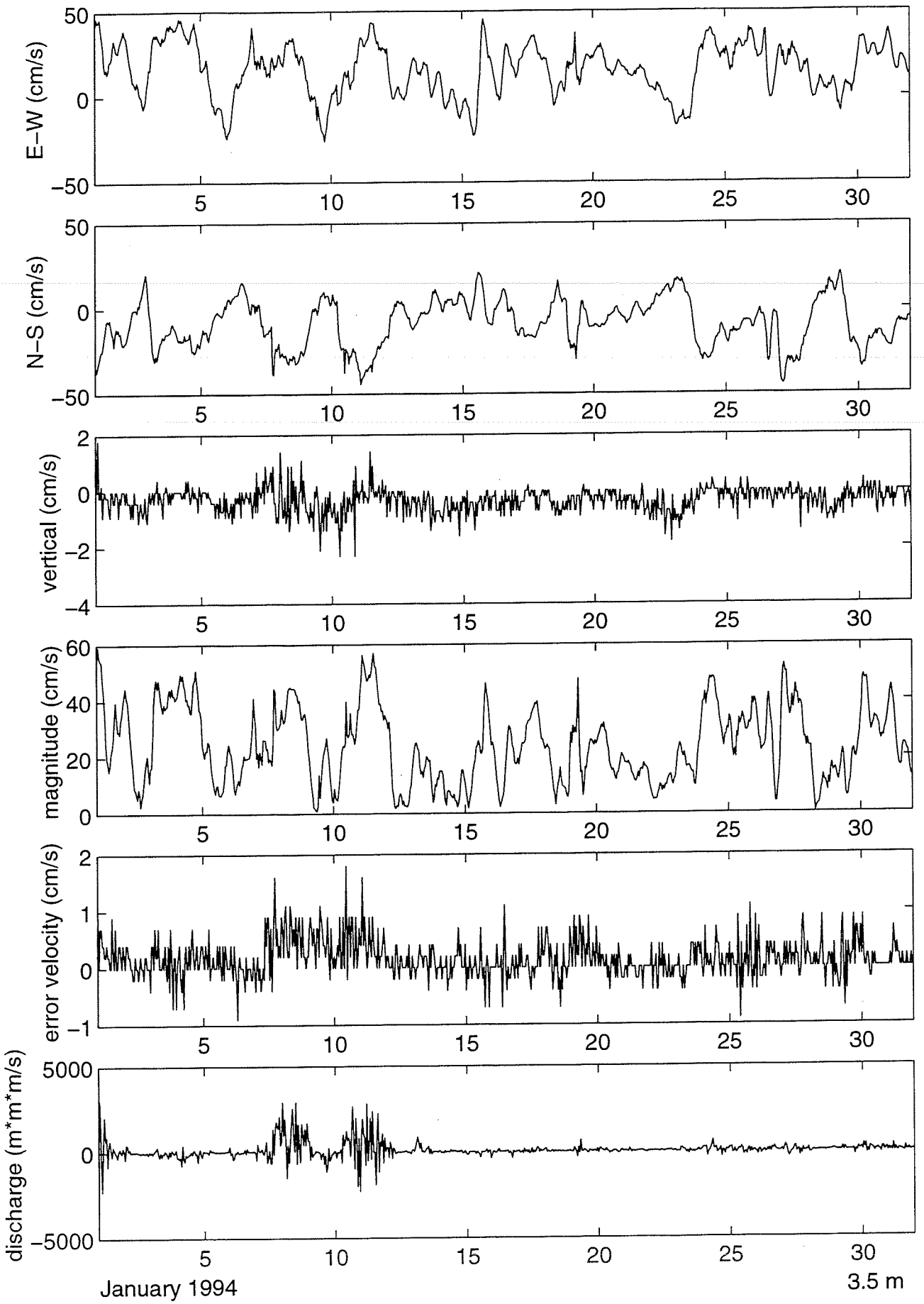
E–W (cm/s)
N–S (cm/s)
vertical (cm/s)
magnitude (cm/s)
error velocity (cm/s)
discharge (m*m*m/s)
January 1994
3.5 m

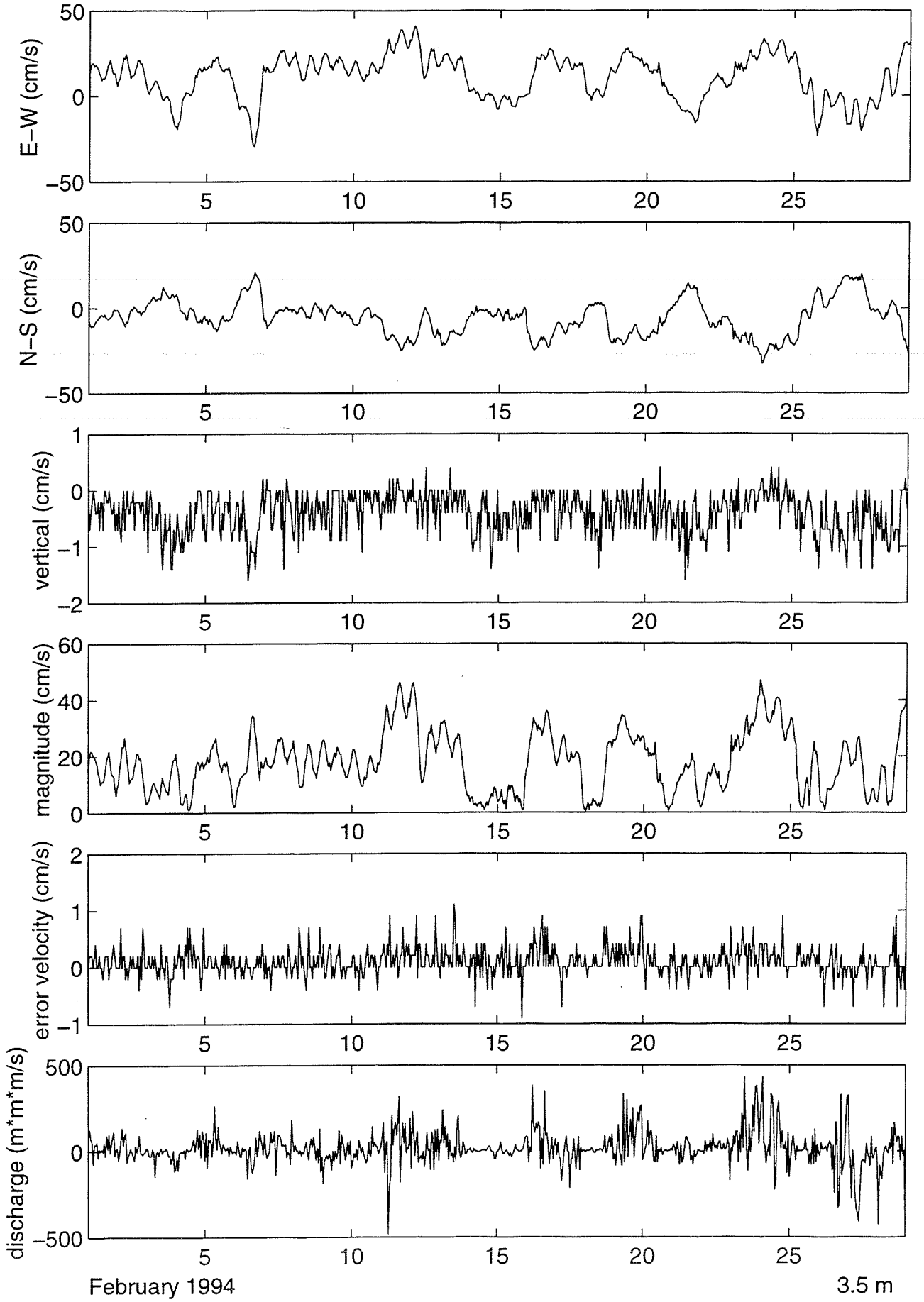
E–W (cm/s)
N–S (cm/s)
vertical (cm/s)
magnitude (cm/s)
error velocity (cm/s)
discharge (m*m*m/s)
February 1994
3.5 m

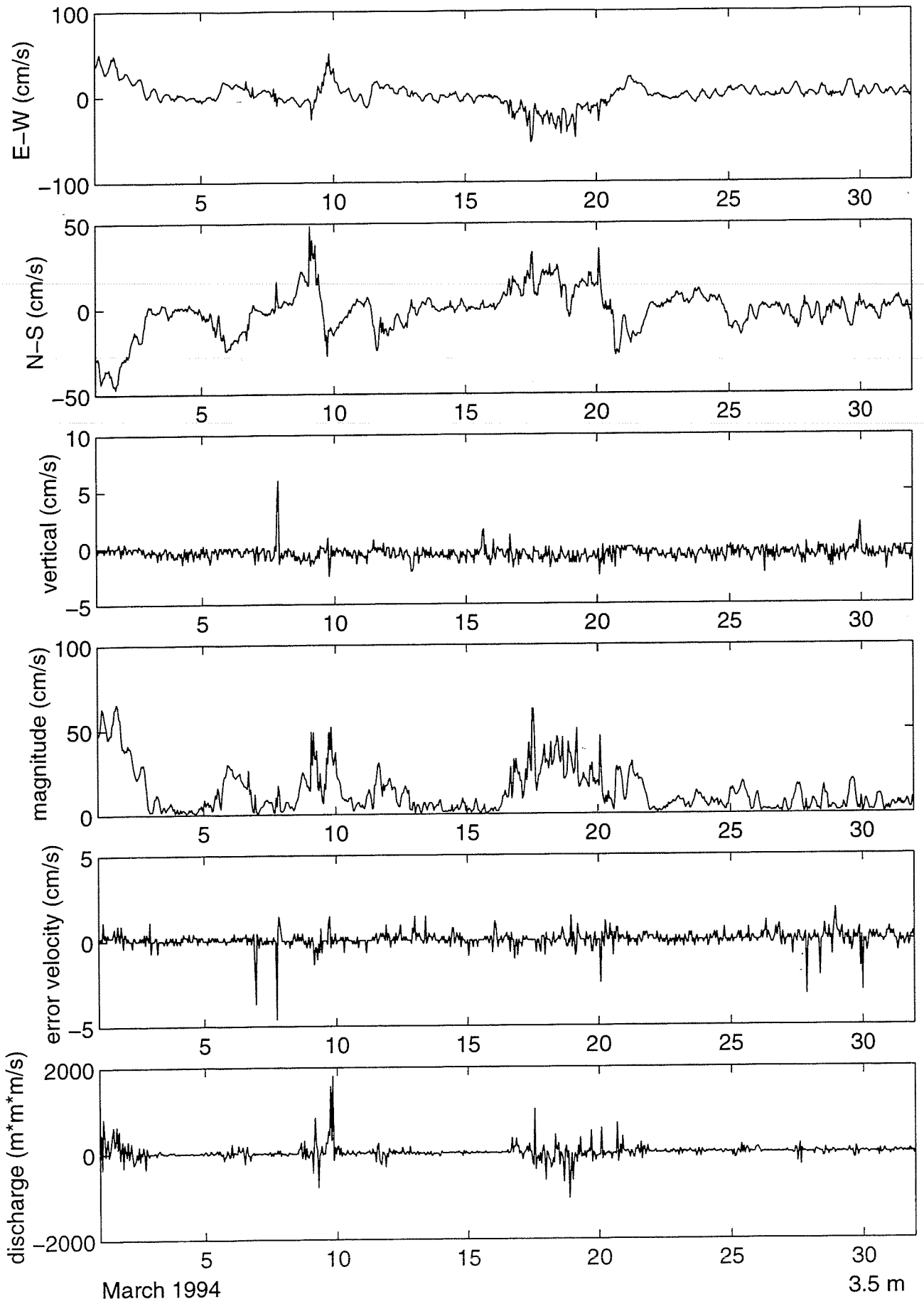
E–W (cm/s)
100
0
–100
N–S (cm/s)
50
0
–50
vertical (cm/s)
10
5
0
–5
magnitude (cm/s)
100
50
0
error velocity (cm/s)
5
0
–5
discharge (m*m*m/s)
2000
0
–2000
5
10
15
20
25
30
March 1994
3.5 m

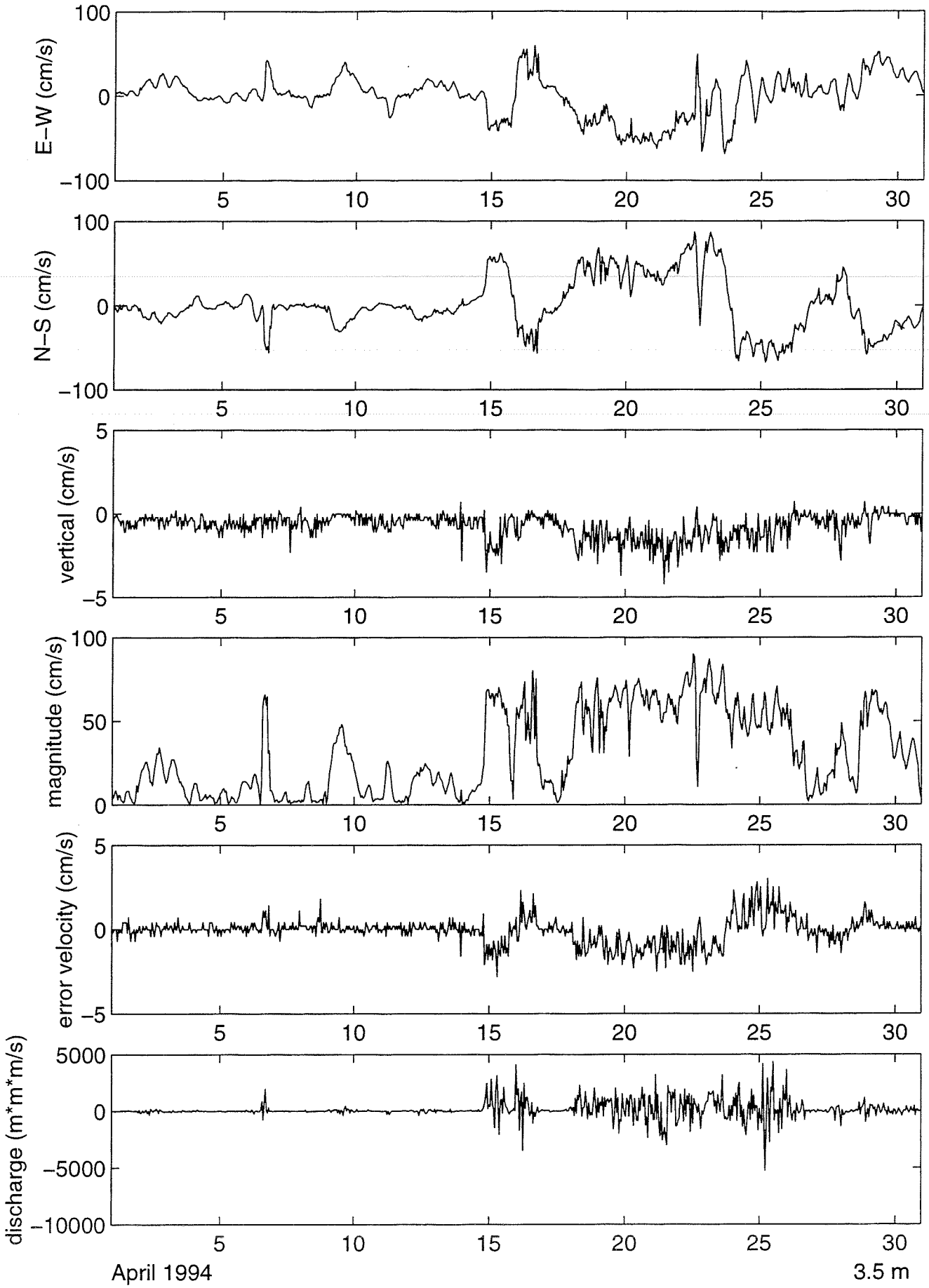
E–W (cm/s)
N–S (cm/s)
vertical (cm/s)
magnitude (cm/s)
error velocity (cm/s)
discharge (m*m*m/s)
100
0
–100
5
–5
50
5000
–5000
–10000
5
10
15
20
25
30
April 1994
3.5 m

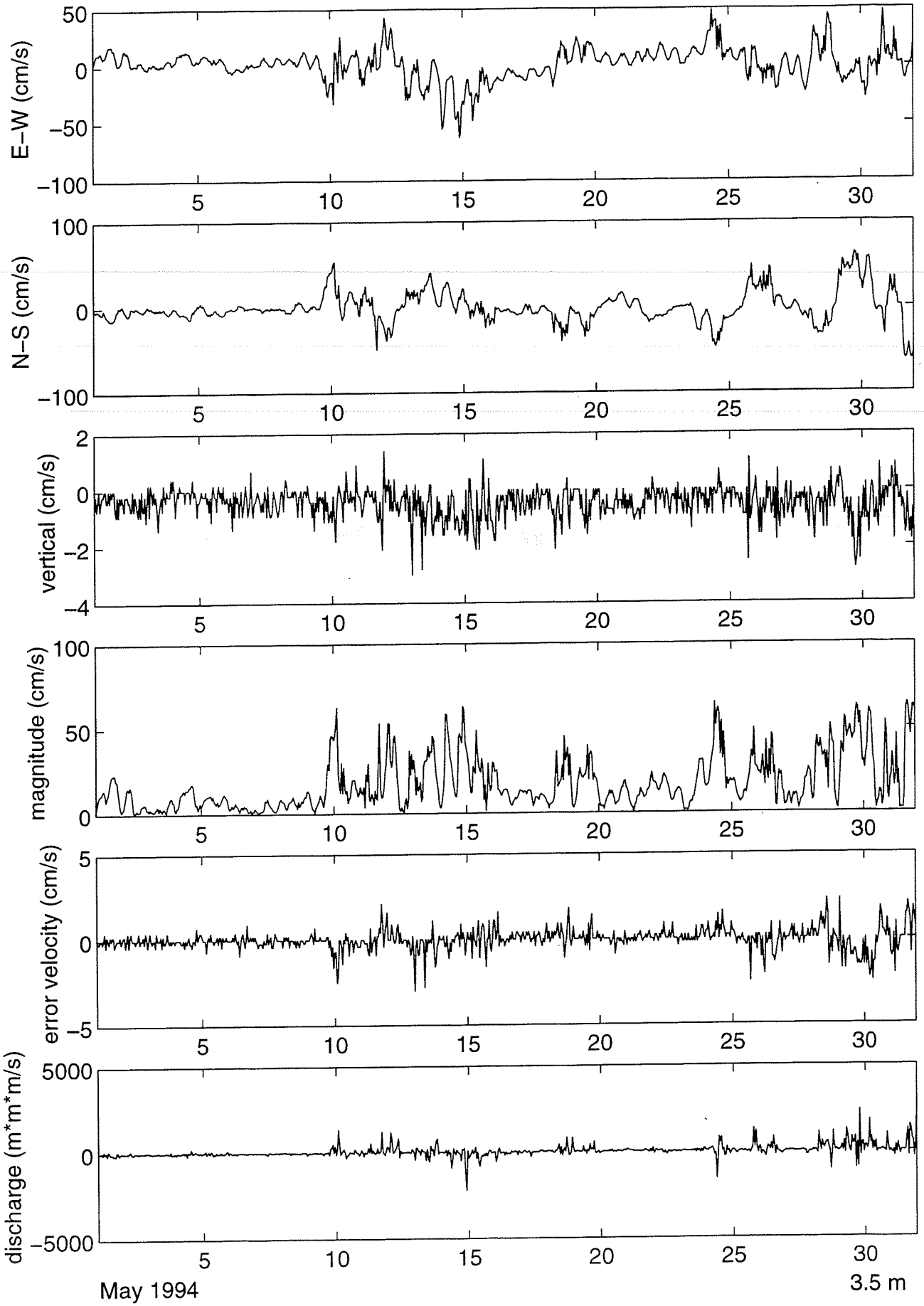
E–W (cm/s)
50
0
−50
−100
5
10
15
20
25
30
N–S (cm/s)
100
0
−100
vertical (cm/s)
2
0
−2
−4
magnitude (cm/s)
100
50
0
error velocity (cm/s)
5
0
−5
discharge (m*m*m/s)
5000
0
−5000
May 1994
3.5 m

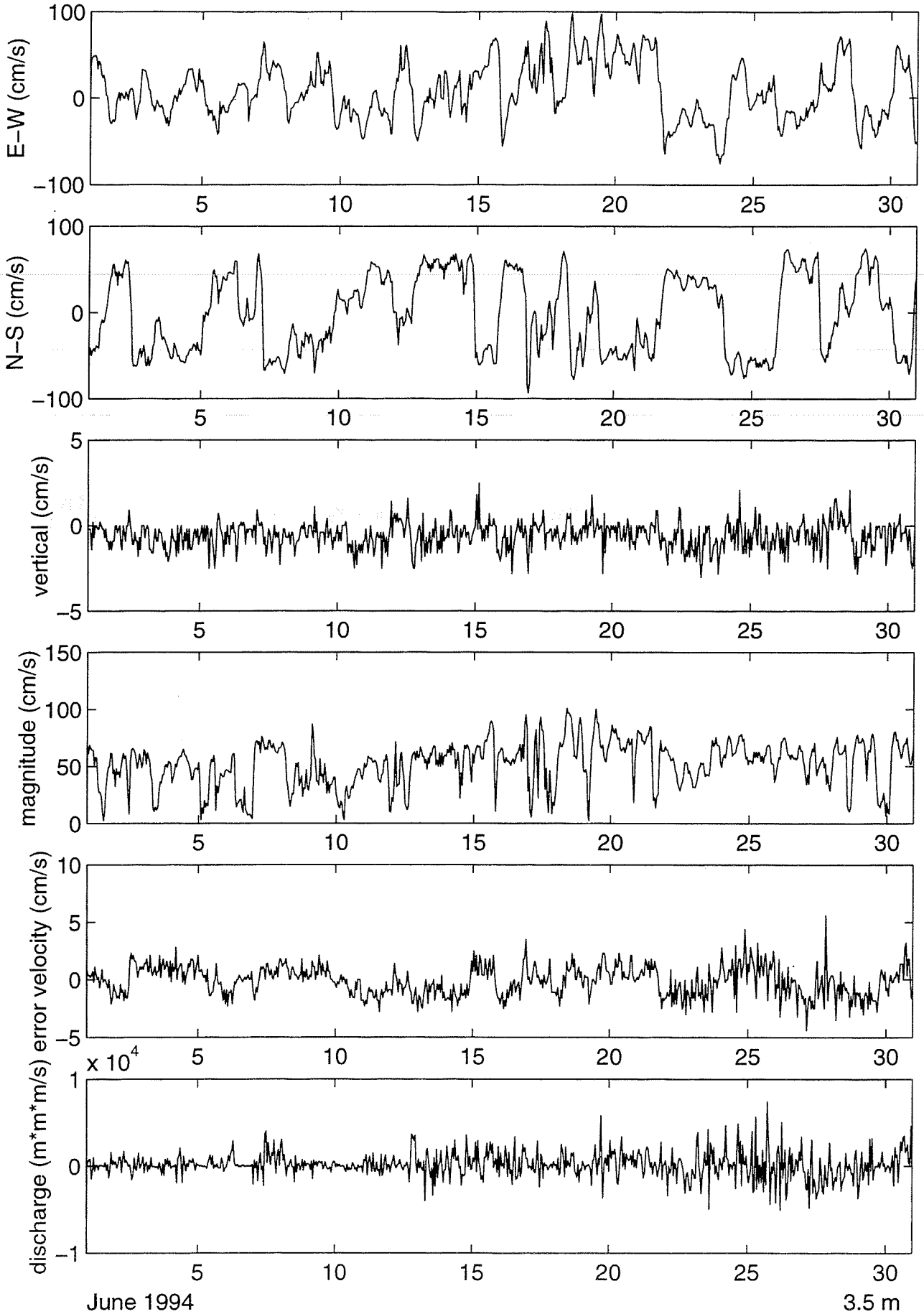
E–W (cm/s)
N–S (cm/s)
vertical (cm/s)
magnitude (cm/s)
error velocity (cm/s)
discharge (m*m*m/s)
x 10^4
June 1994
3.5 m

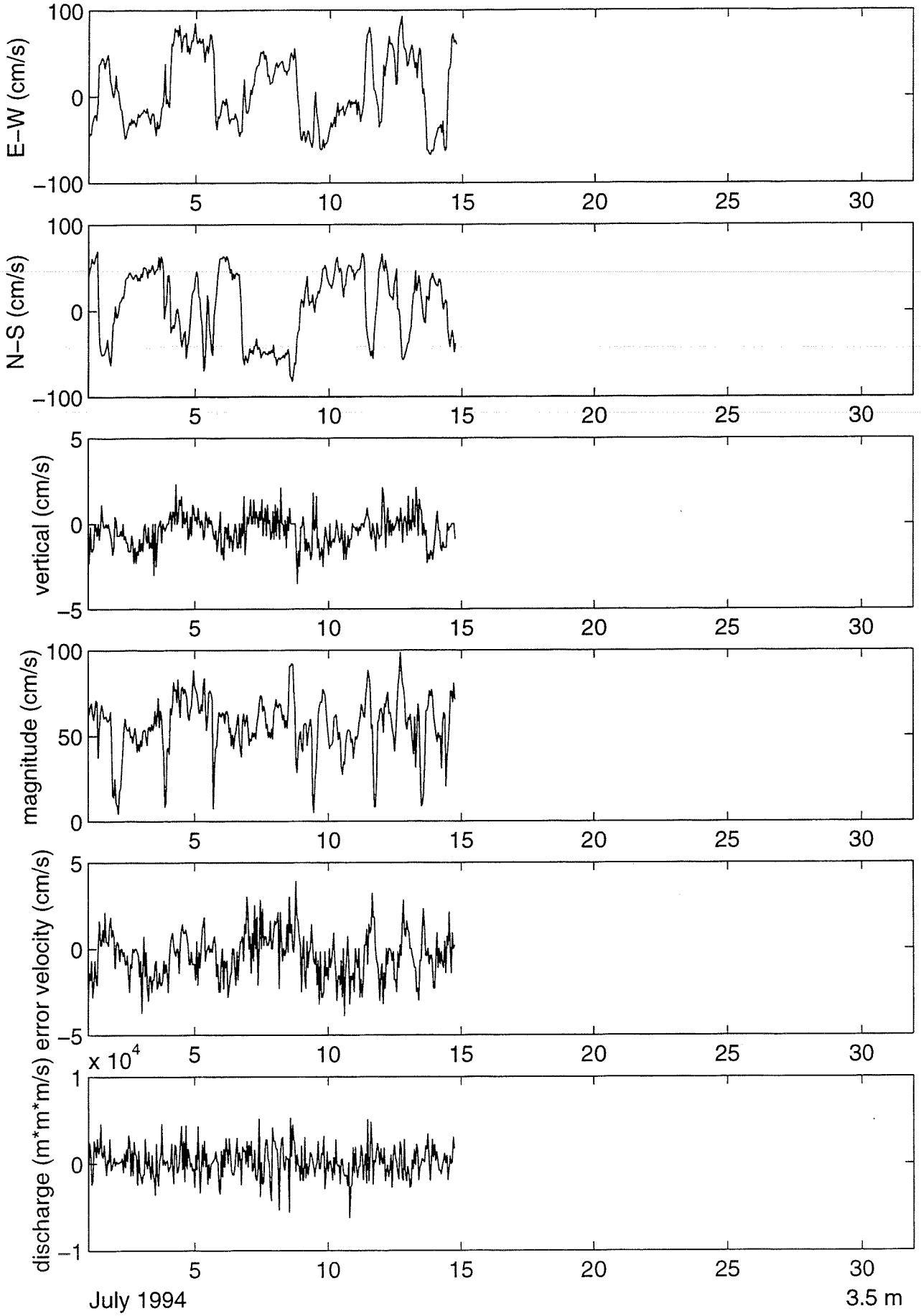
E–W (cm/s)
N–S (cm/s)
vertical (cm/s)
magnitude (cm/s)
error velocity (cm/s)
discharge (m*m*m/s)
x 10^4
July 1994
3.5 m

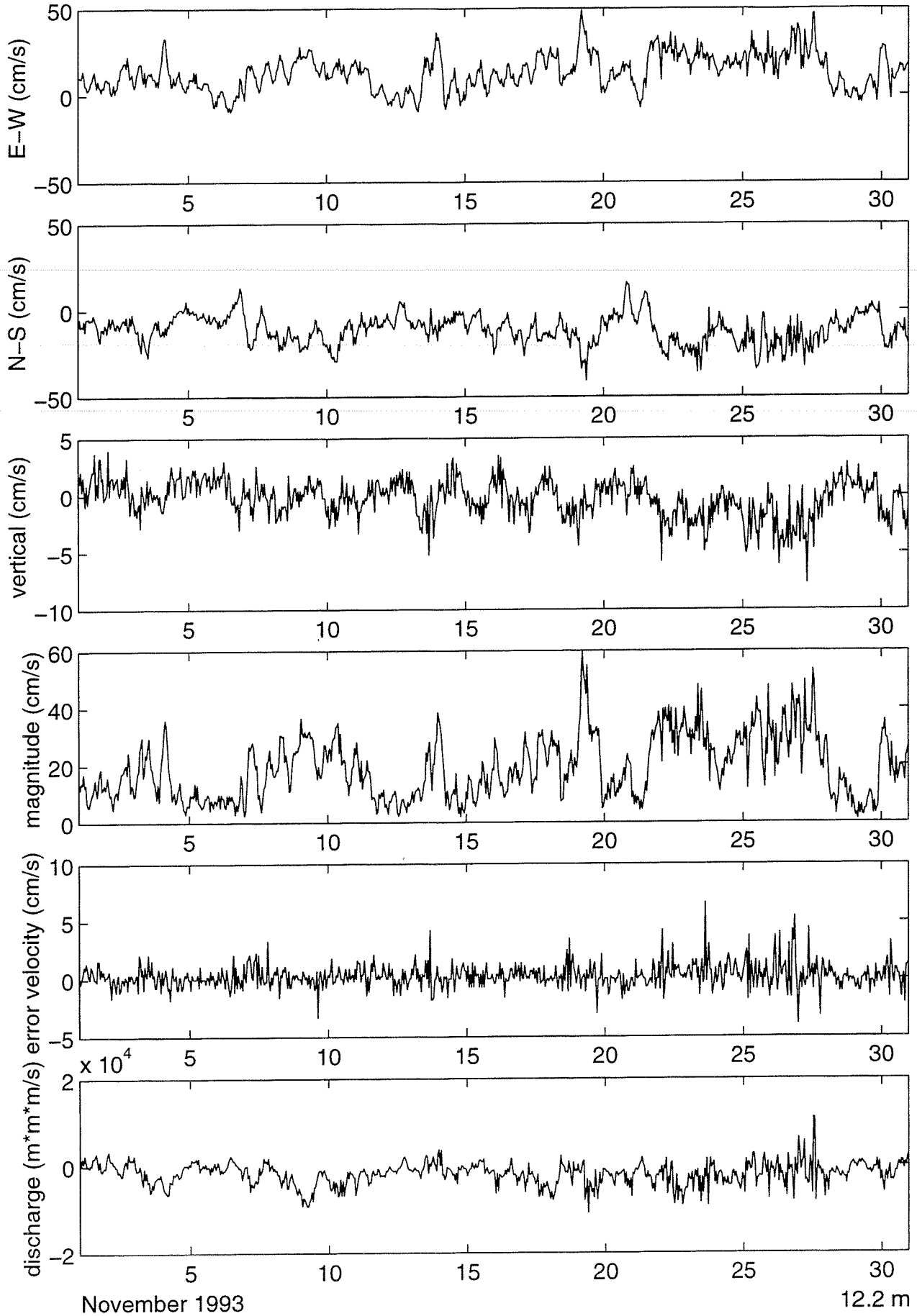
E–W (cm/s)
N–S (cm/s)
vertical (cm/s)
magnitude (cm/s)
error velocity (cm/s)
discharge (m*m*m/s)
x 10^4
November 1993
12.2 m

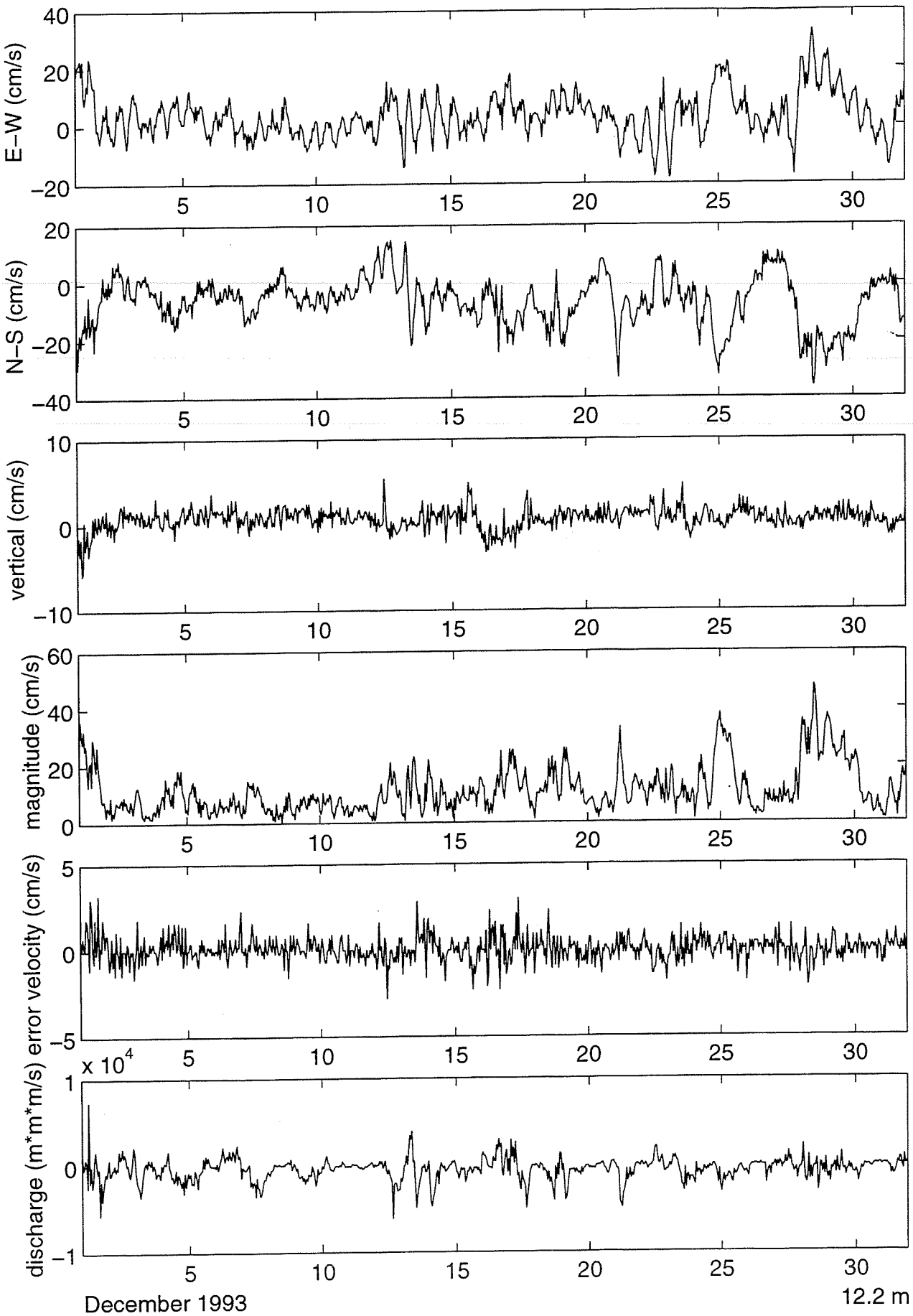
E–W (cm/s)
N–S (cm/s)
vertical (cm/s)
magnitude (cm/s)
error velocity (cm/s)
x 10^4
discharge (m*m*m/s)
December 1993
12.2 m

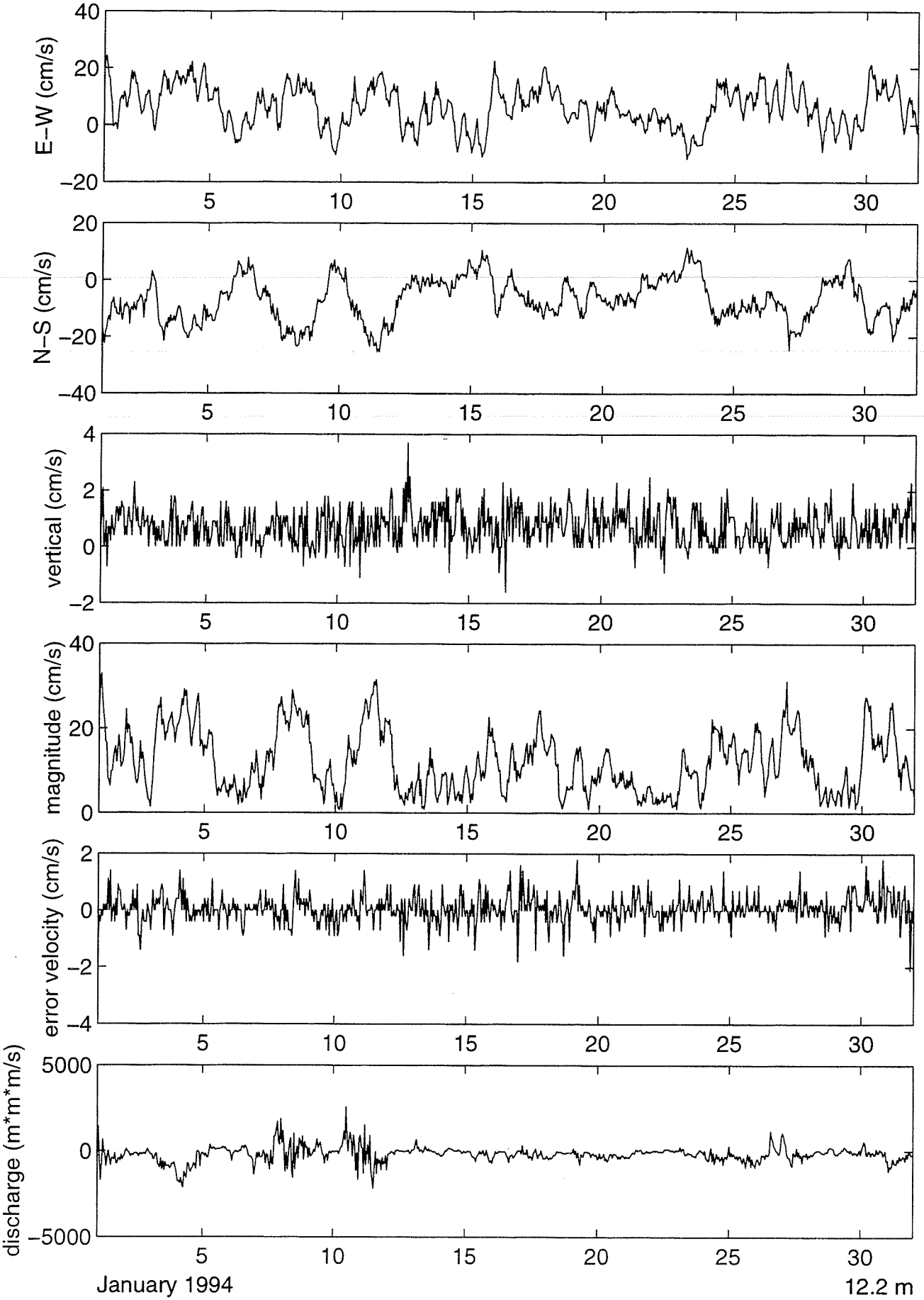
E–W (cm/s)
N–S (cm/s)
vertical (cm/s)
magnitude (cm/s)
error velocity (cm/s)
discharge (m*m*m/s)
January 1994
12.2 m

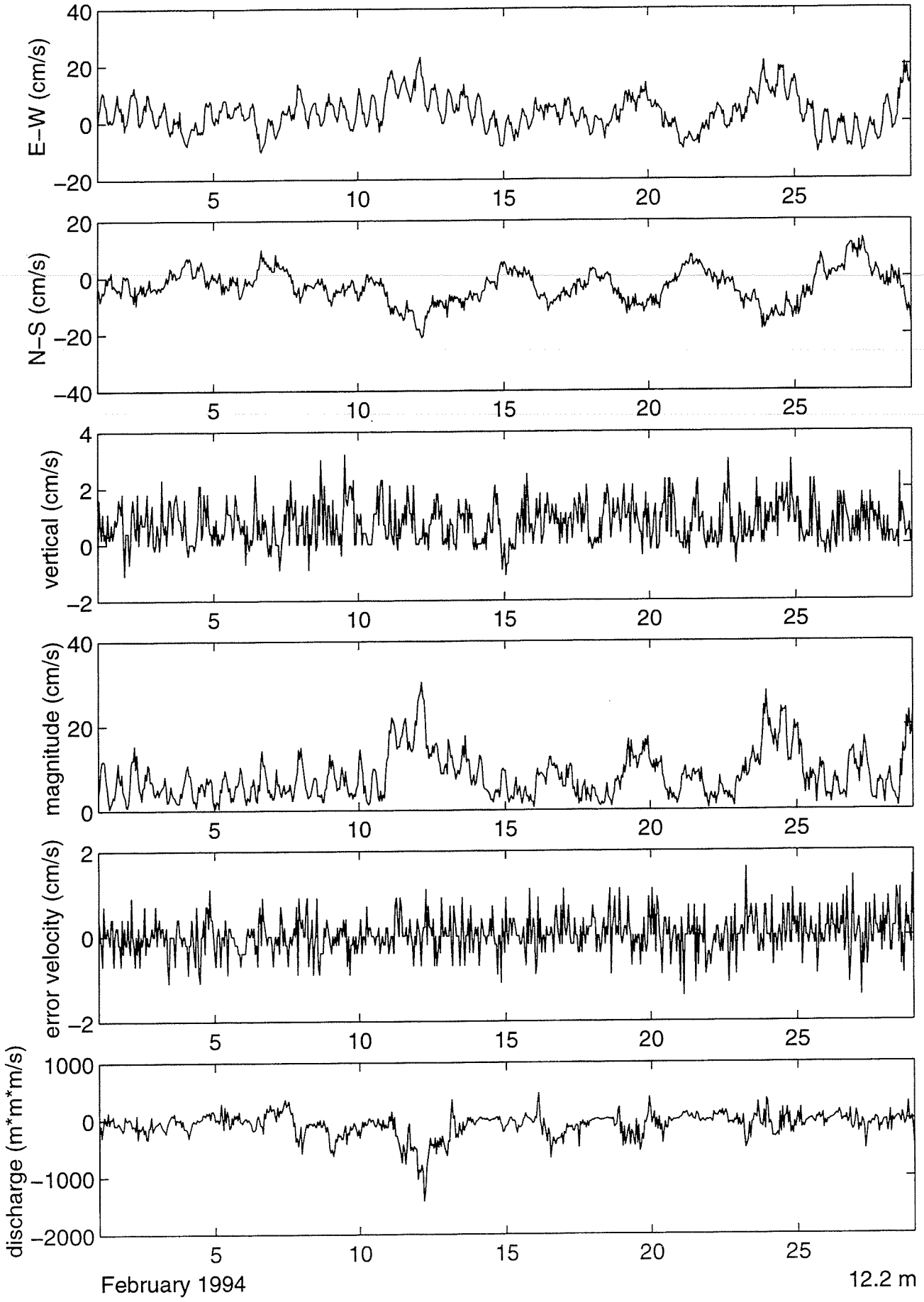
E–W (cm/s)
N–S (cm/s)
vertical (cm/s)
magnitude (cm/s)
error velocity (cm/s)
discharge (m*m*m/s)
February 1994
12.2 m

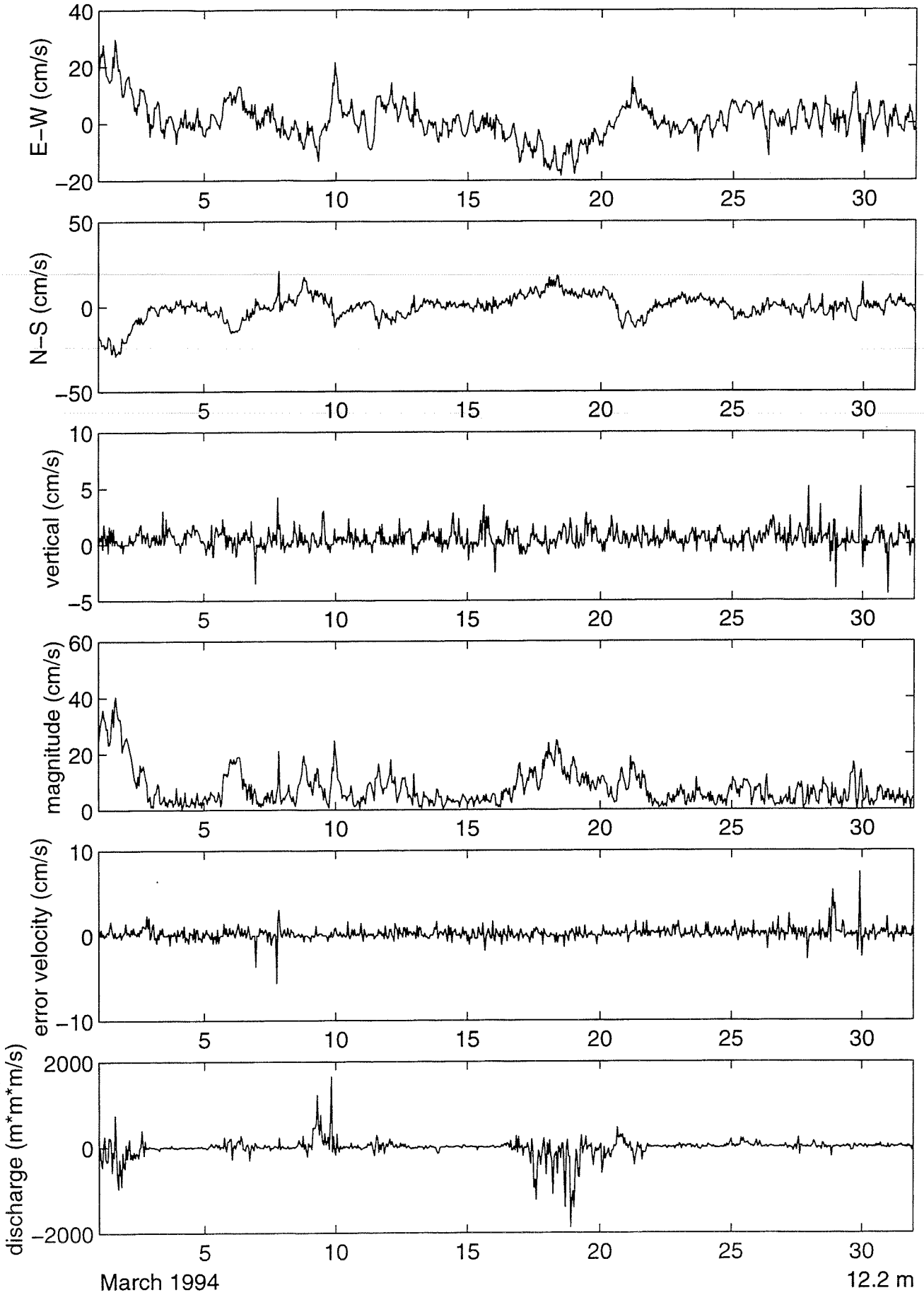
E–W (cm/s)
N–S (cm/s)
vertical (cm/s)
magnitude (cm/s)
error velocity (cm/s)
discharge (m*m*m/s)
March 1994
12.2 m

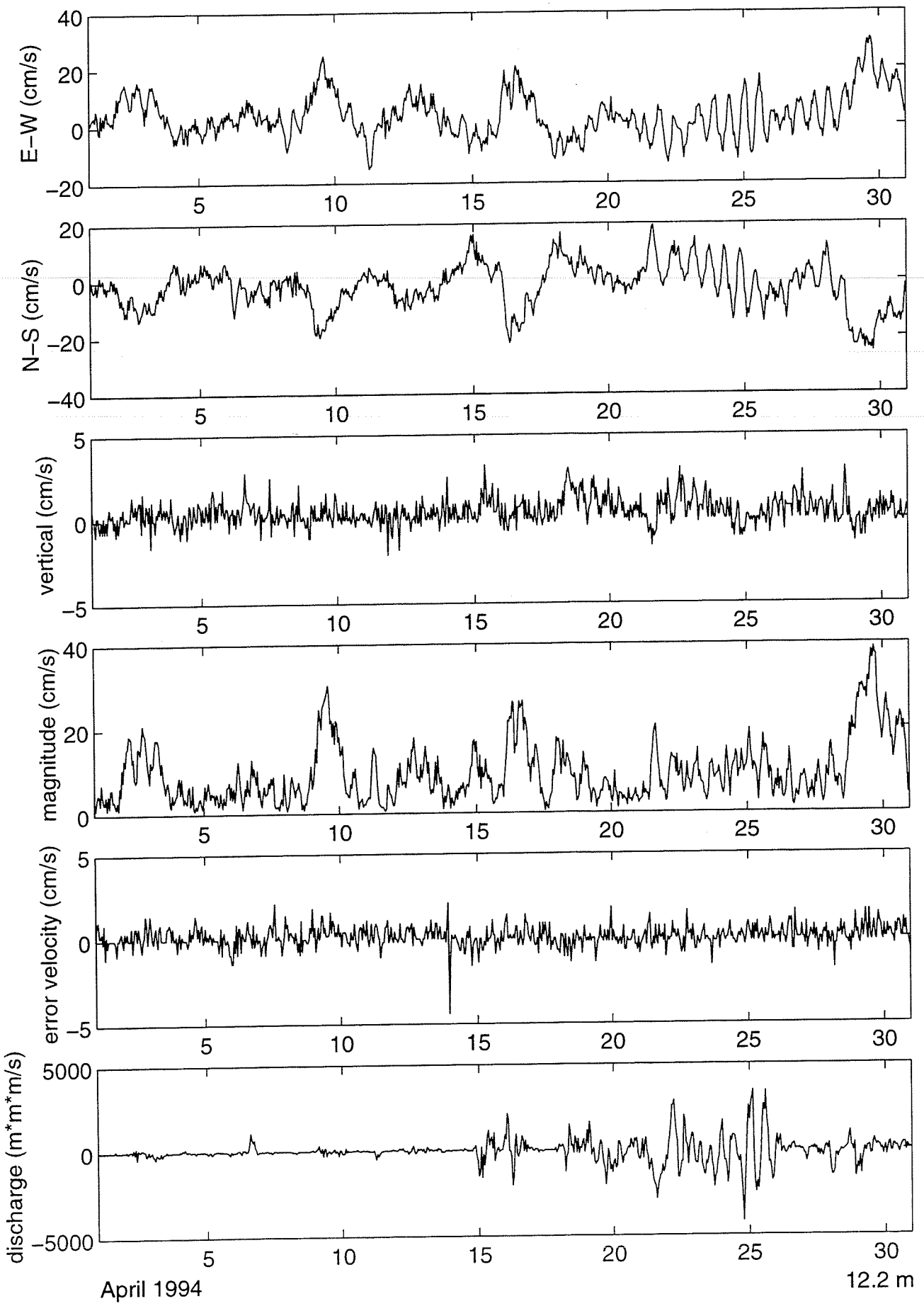
E–W (cm/s)
N–S (cm/s)
vertical (cm/s)
magnitude (cm/s)
error velocity (cm/s)
discharge (m*m*m/s)
April 1994
12.2 m

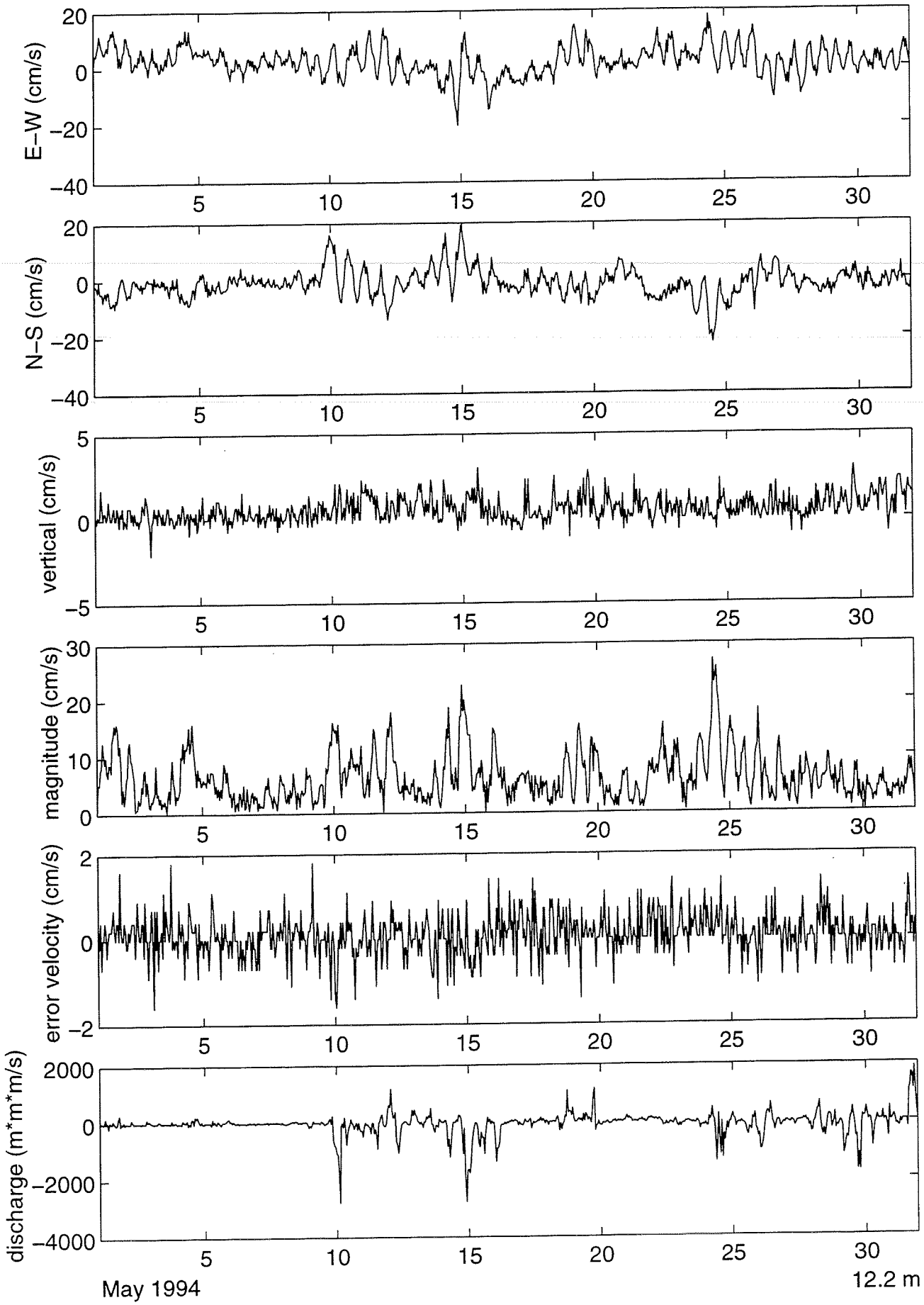
E–W (cm/s)
N–S (cm/s)
vertical (cm/s)
magnitude (cm/s)
error velocity (cm/s)
discharge (m*m*m/s)
May 1994
12.2 m

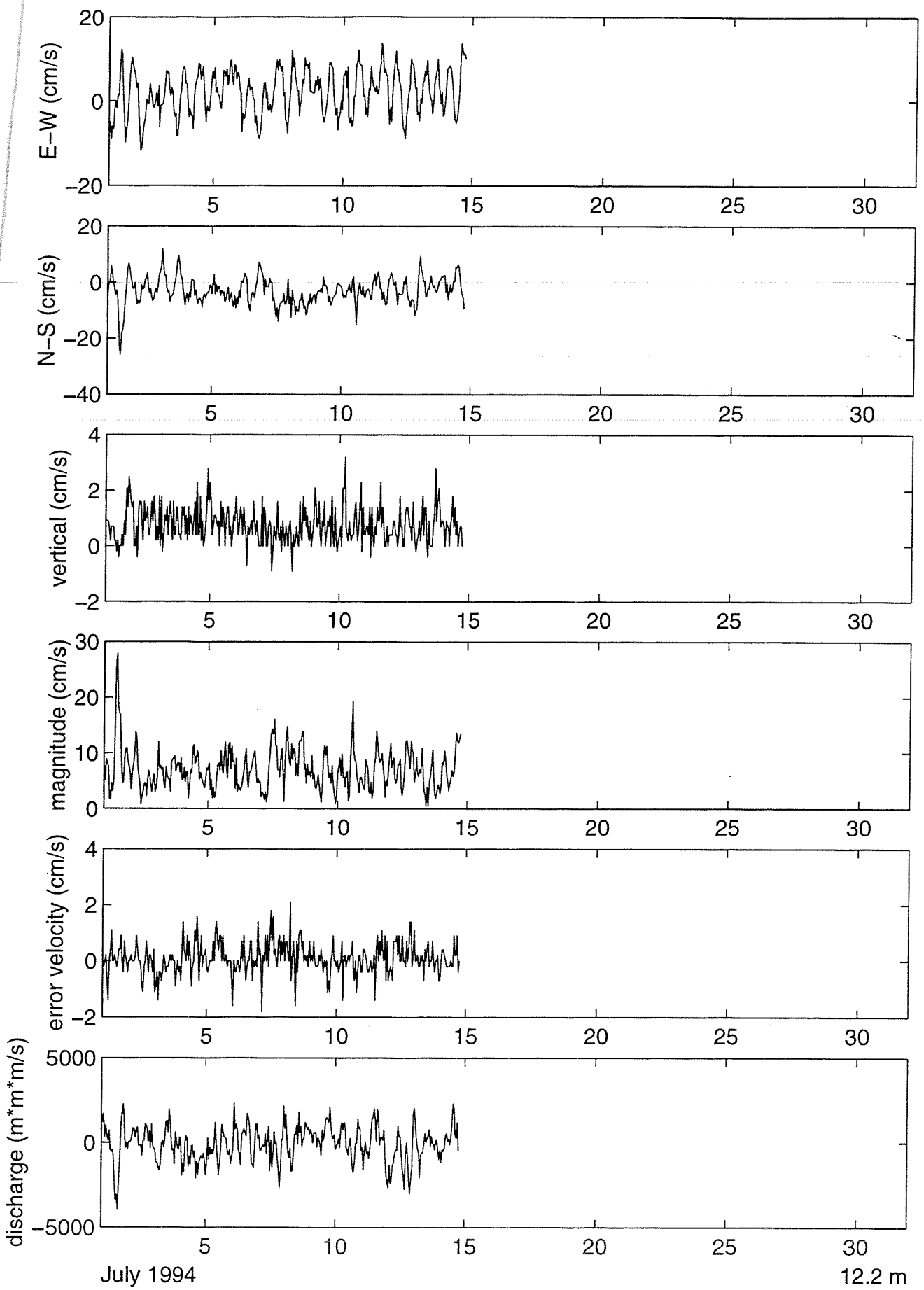
E–W (cm/s)
N–S (cm/s)
vertical (cm/s)
magnitude (cm/s)
error velocity (cm/s)
discharge (m*m*m/s)
July 1994
12.2 m

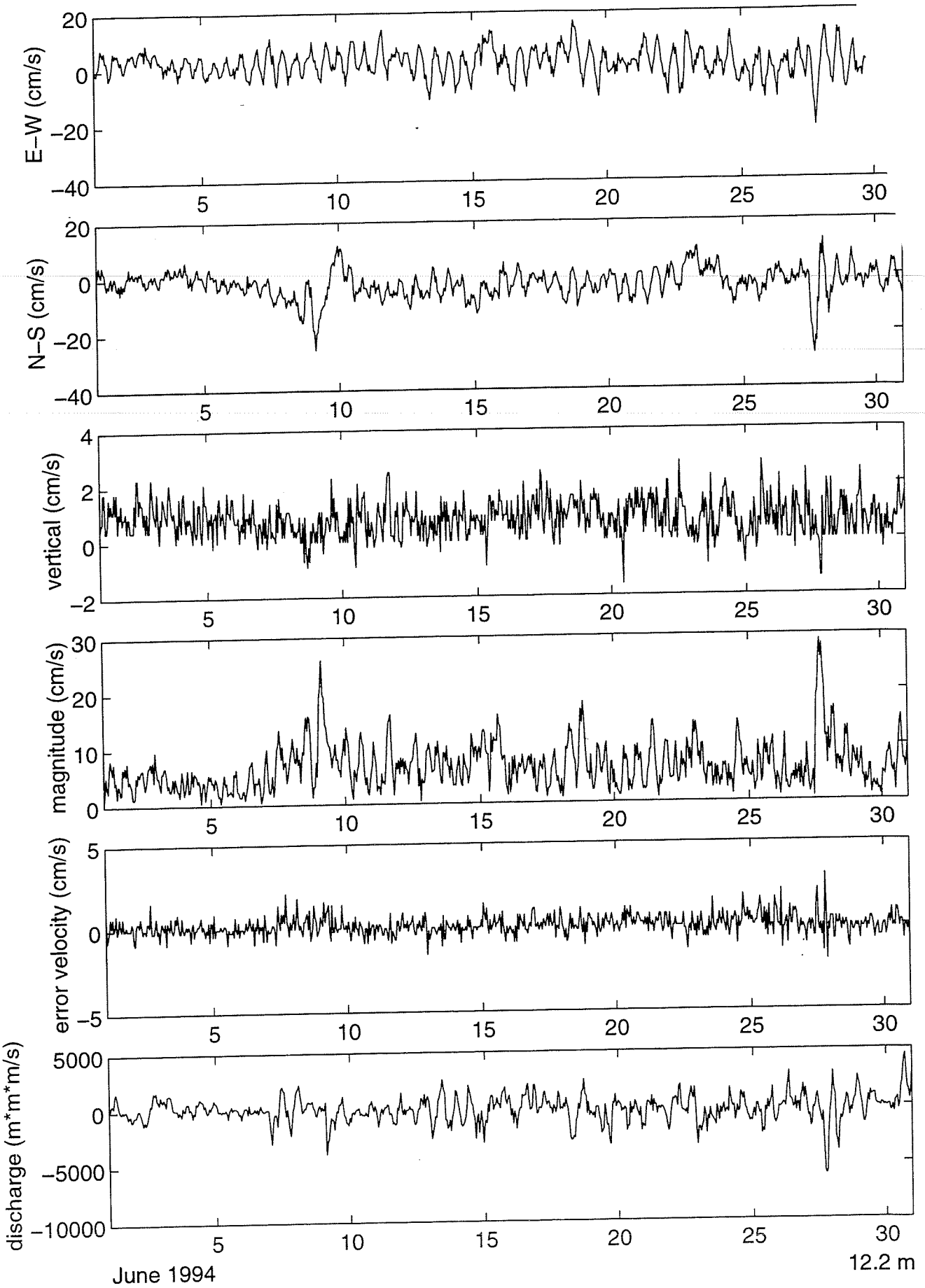
E–W (cm/s)
N–S (cm/s)
vertical (cm/s)
magnitude (cm/s)
error velocity (cm/s)
discharge (m*m*m/s)
June 1994
12.2 m

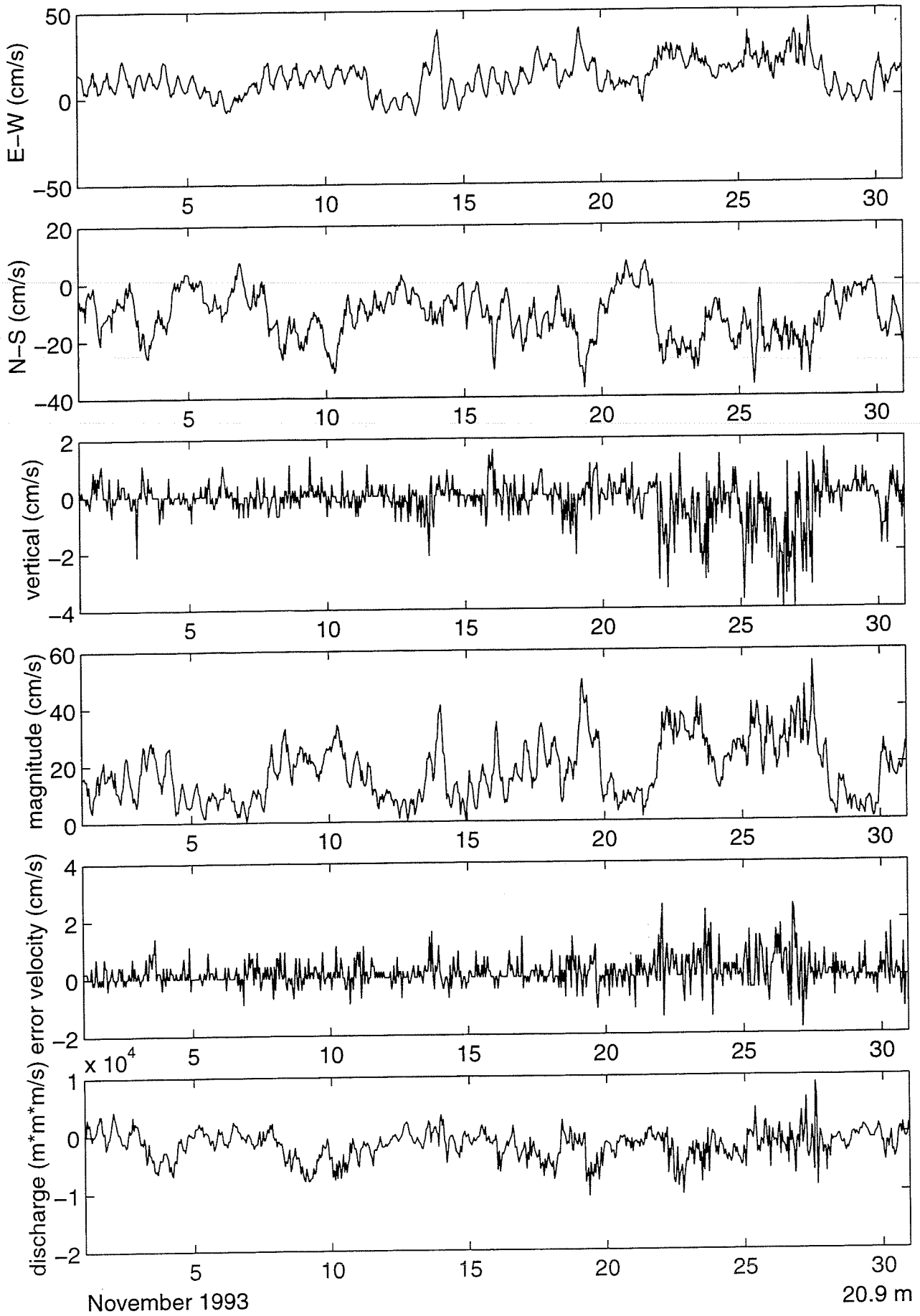
E–W (cm/s)
N–S (cm/s)
vertical (cm/s)
magnitude (cm/s)
error velocity (cm/s)
x 10^4
discharge (m*m*m/s)
November 1993
20.9 m

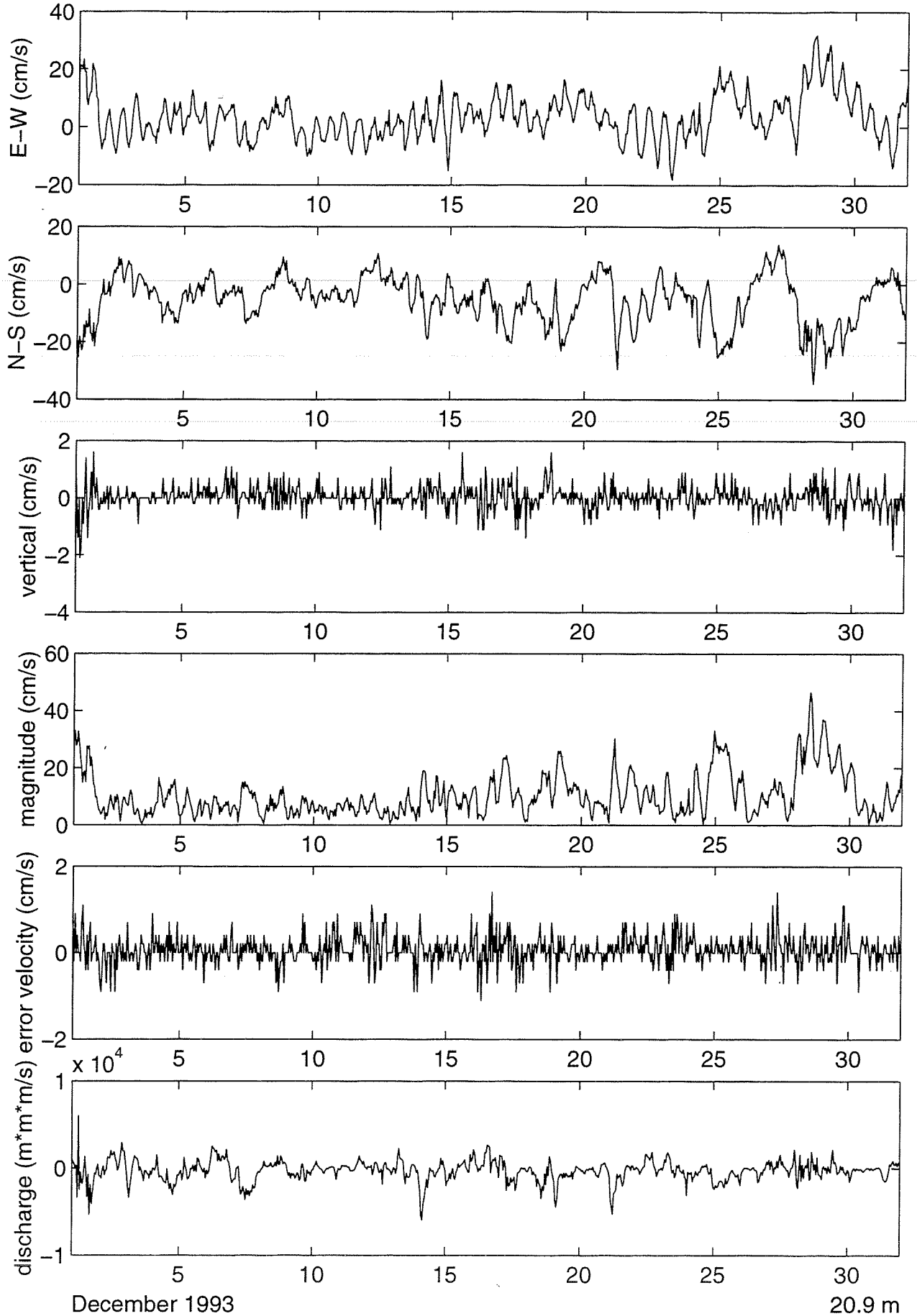
E–W (cm/s)
N–S (cm/s)
vertical (cm/s)
magnitude (cm/s)
error velocity (cm/s)
discharge (m*m*m/s)
x 10^4
December 1993
20.9 m

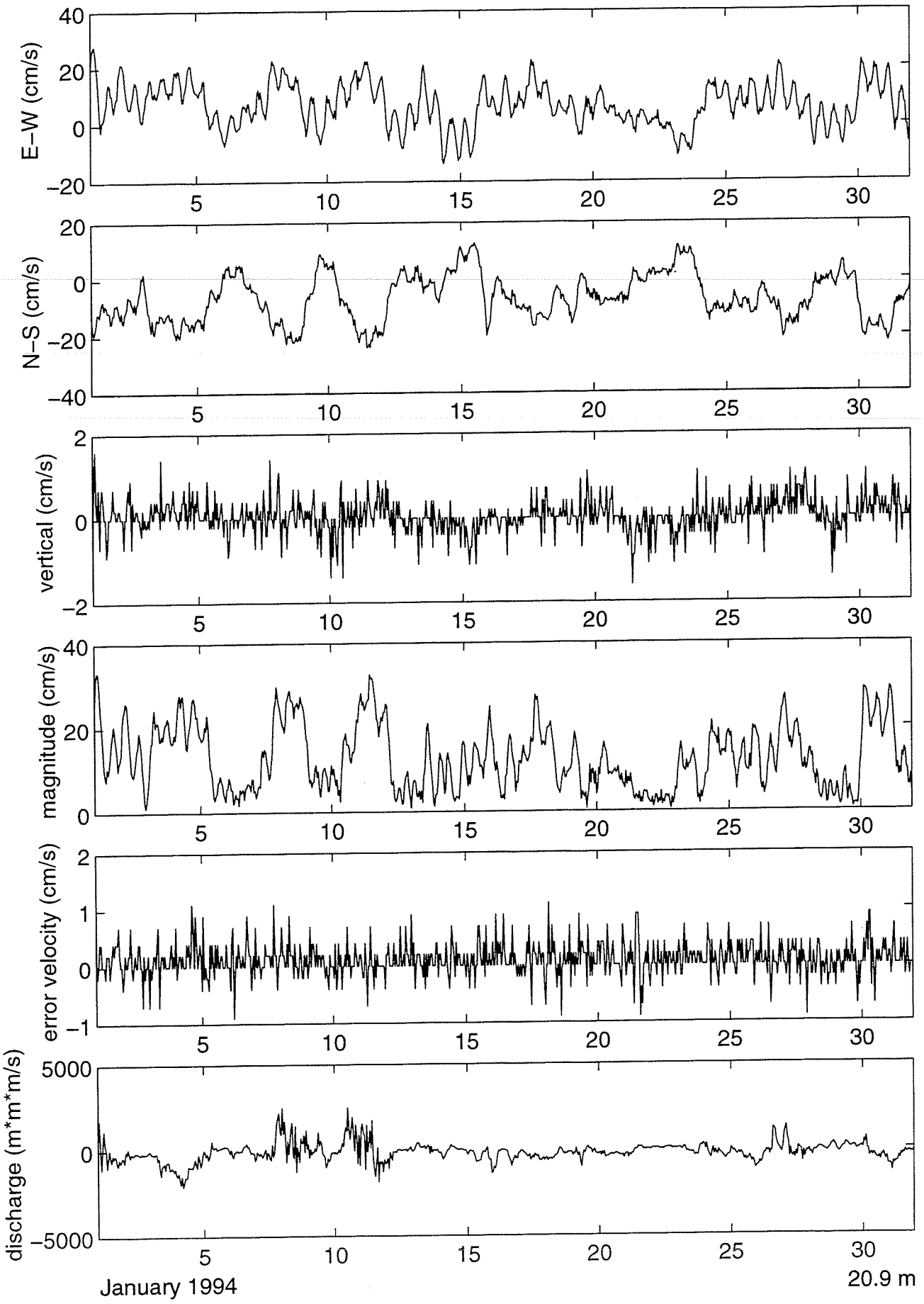
E–W (cm/s)
N–S (cm/s)
vertical (cm/s)
magnitude (cm/s)
error velocity (cm/s)
discharge (m*m*m/s)
January 1994
20.9 m

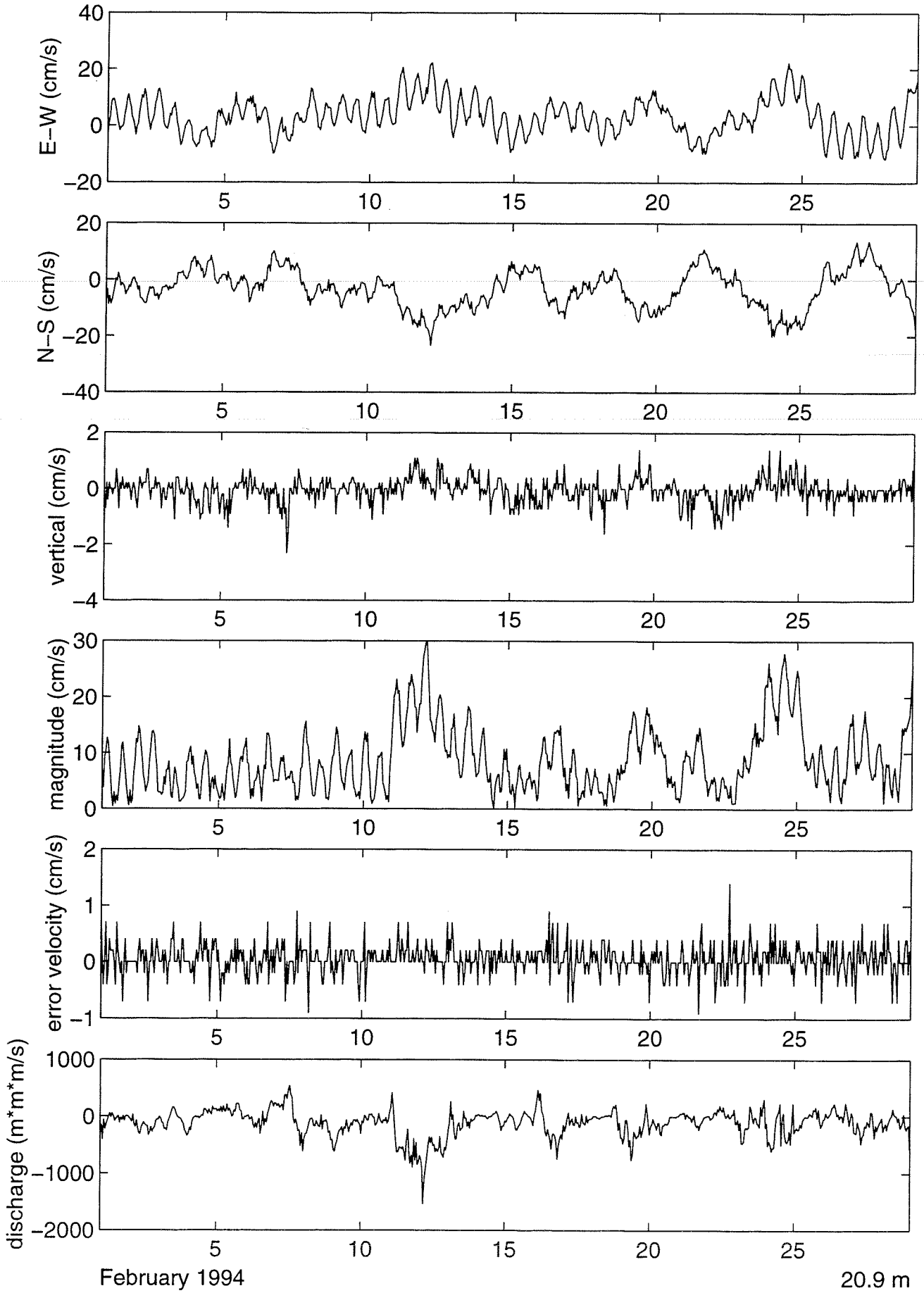
E–W (cm/s)
N–S (cm/s)
vertical (cm/s)
magnitude (cm/s)
error velocity (cm/s)
discharge (m*m*m/s)
February 1994
20.9 m

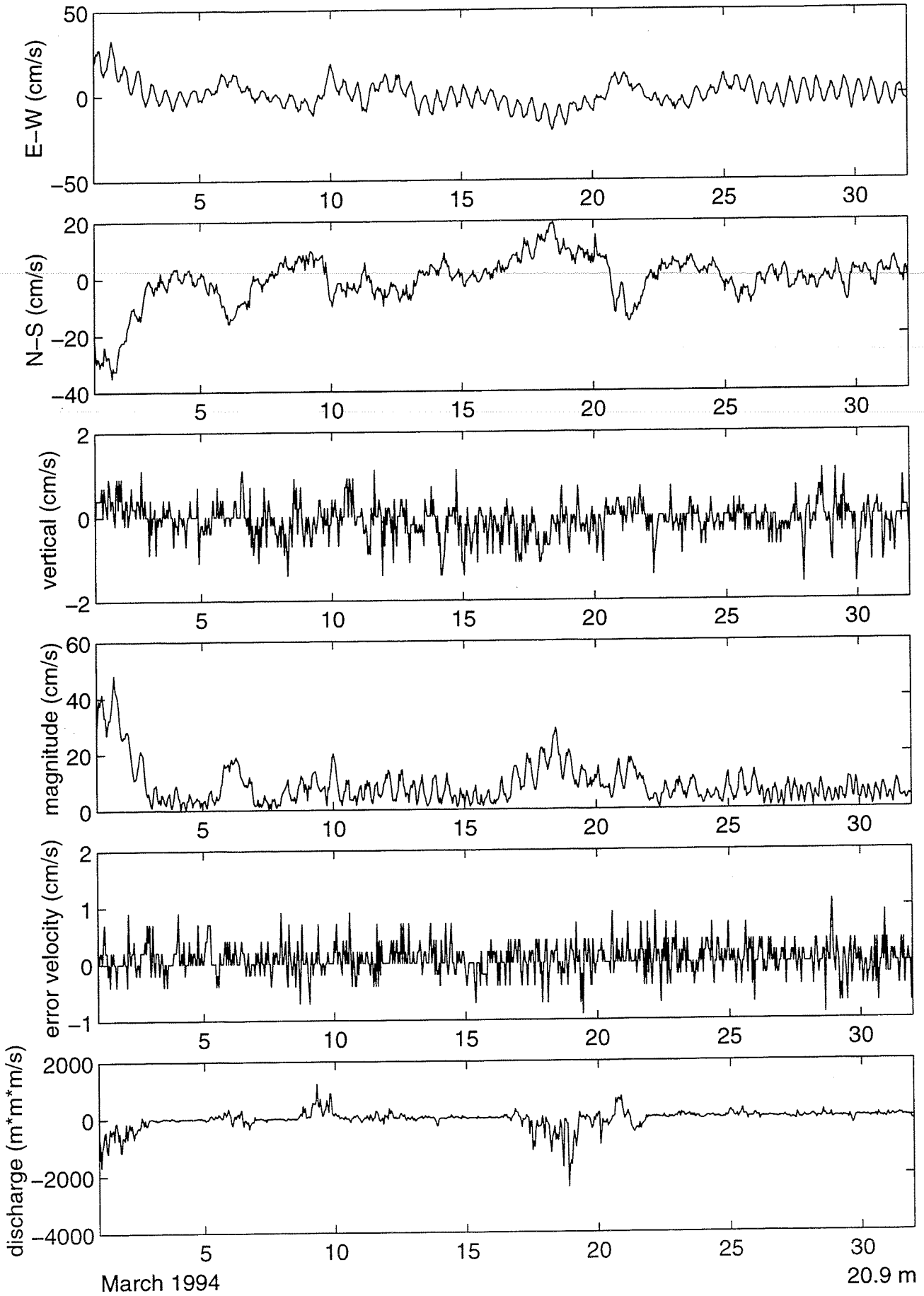
E–W (cm/s)
50
0
–50
N–S (cm/s)
20
0
–20
–40
vertical (cm/s)
2
0
–2
magnitude (cm/s)
60
40
20
0
error velocity (cm/s)
2
1
0
–1
discharge (m*m*m/s)
2000
0
–2000
–4000
5
10
15
20
25
30
March 1994
20.9 m

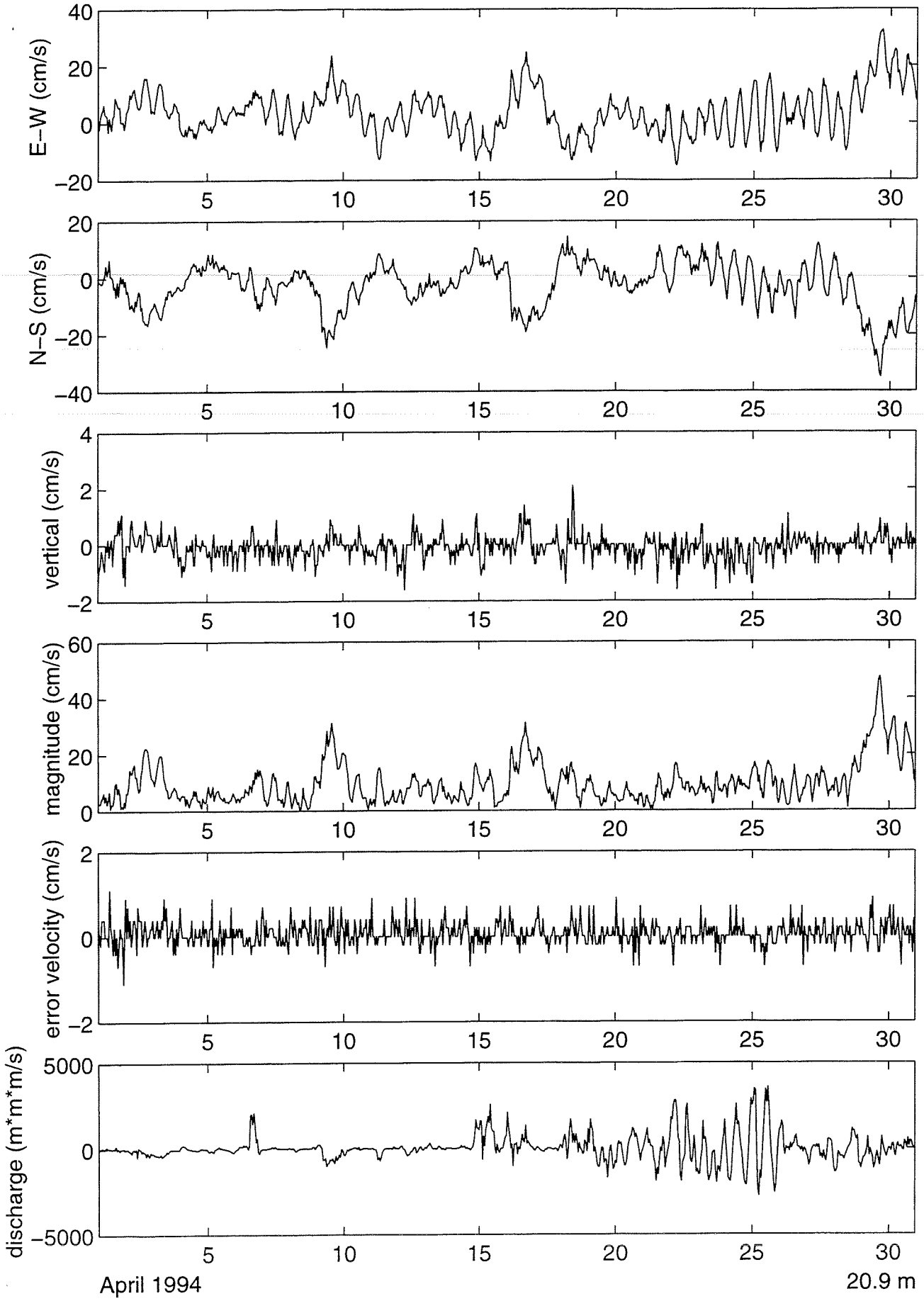
E–W (cm/s)
N–S (cm/s)
vertical (cm/s)
magnitude (cm/s)
error velocity (cm/s)
discharge (m*m*m/s)
April 1994
20.9 m

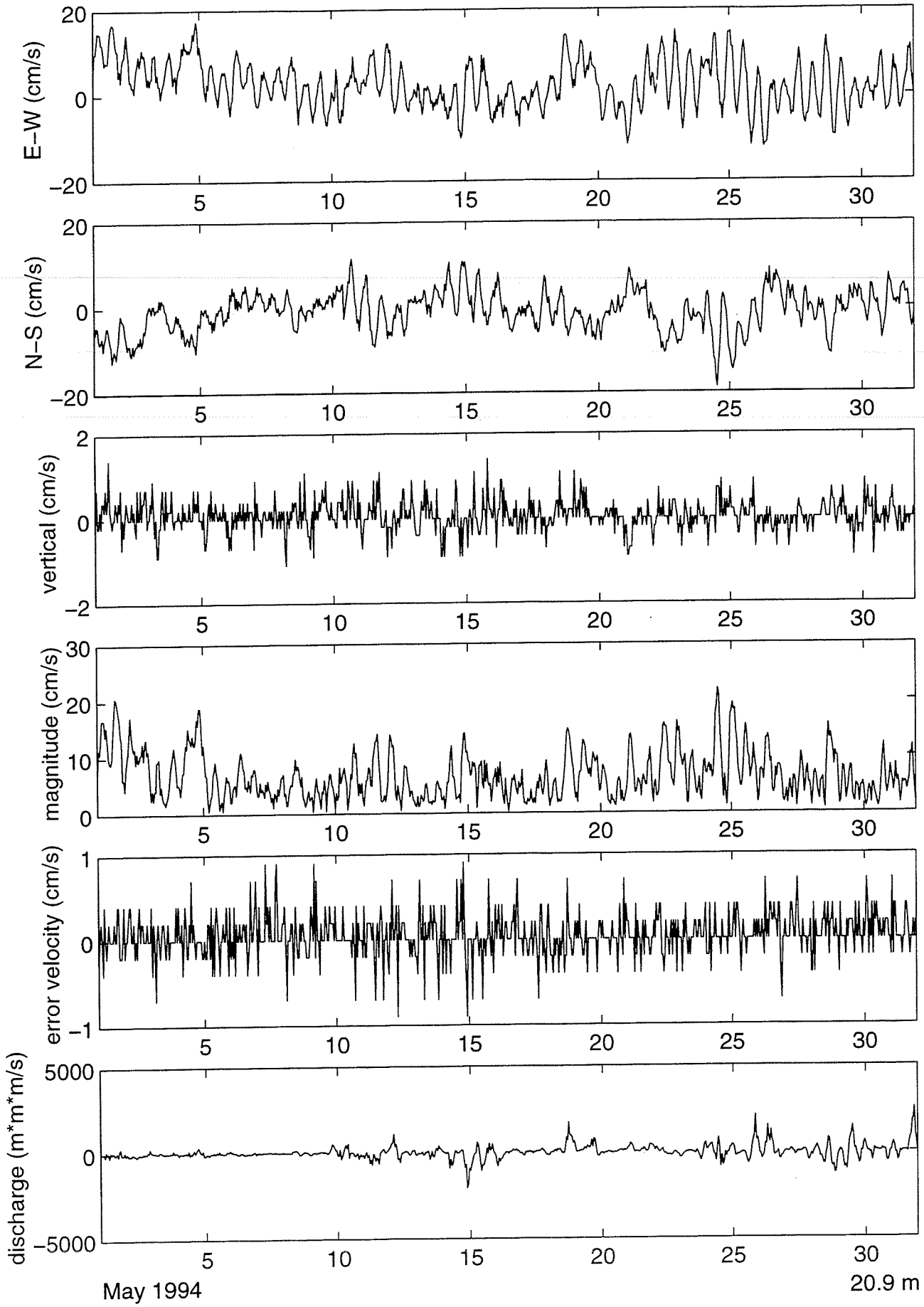
E–W (cm/s)
N–S (cm/s)
vertical (cm/s)
magnitude (cm/s)
error velocity (cm/s)
discharge (m*m*m/s)
May 1994
20.9 m

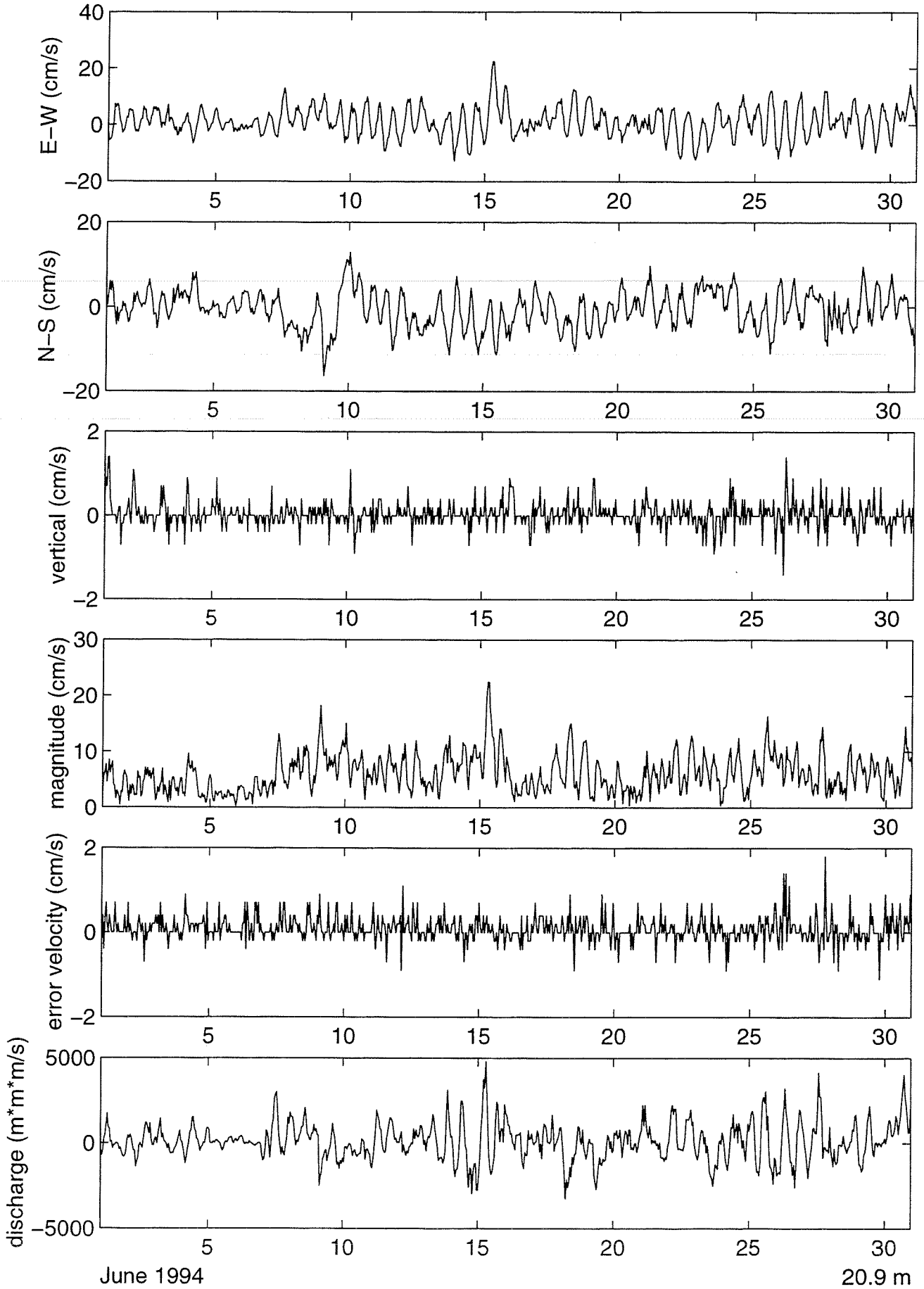
E–W (cm/s)
N–S (cm/s)
vertical (cm/s)
magnitude (cm/s)
error velocity (cm/s)
discharge (m*m*m/s)
June 1994
20.9 m

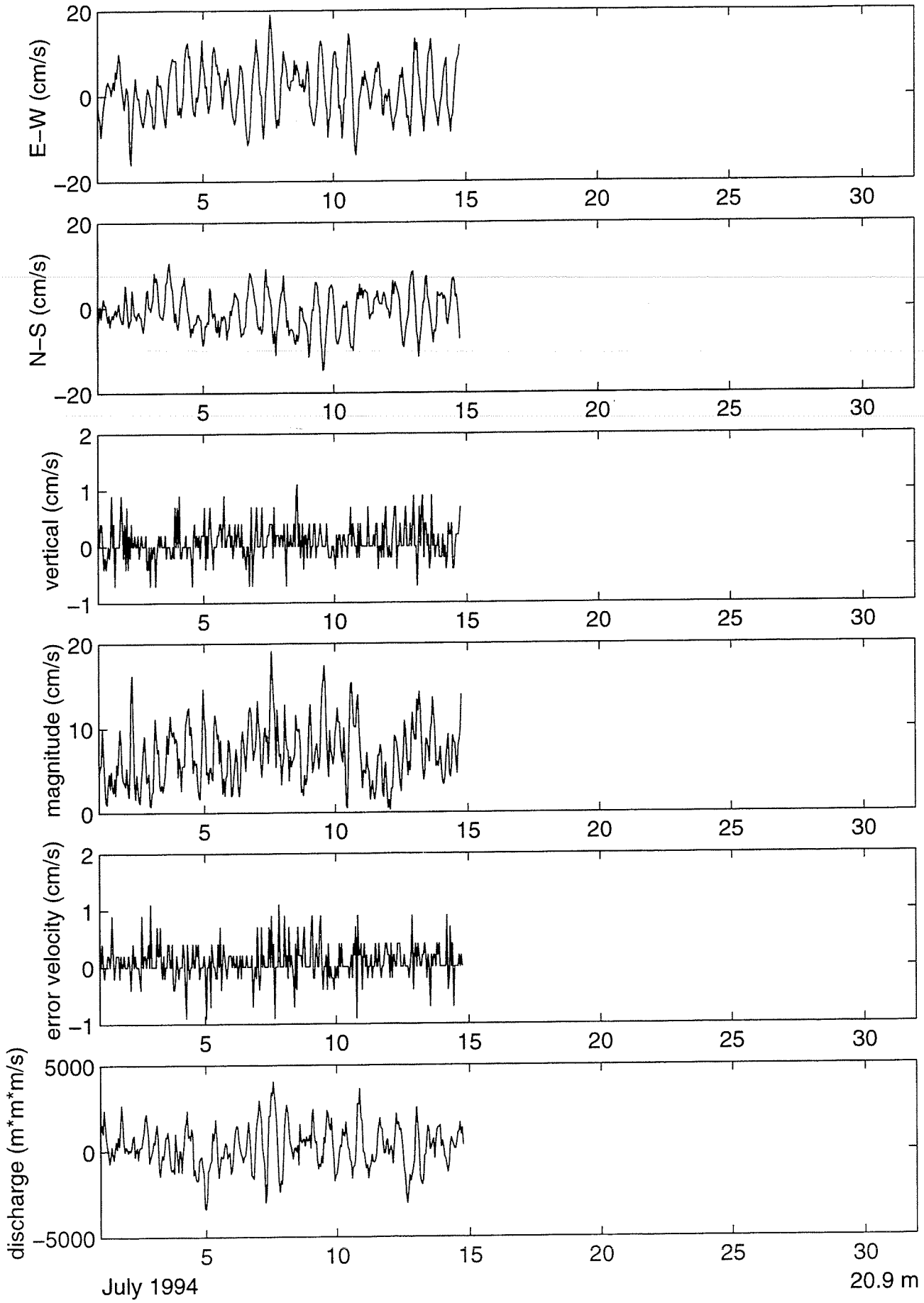
E–W (cm/s)
N–S (cm/s)
vertical (cm/s)
magnitude (cm/s)
error velocity (cm/s)
discharge (m*m*m/s)
July 1994
20.9 m

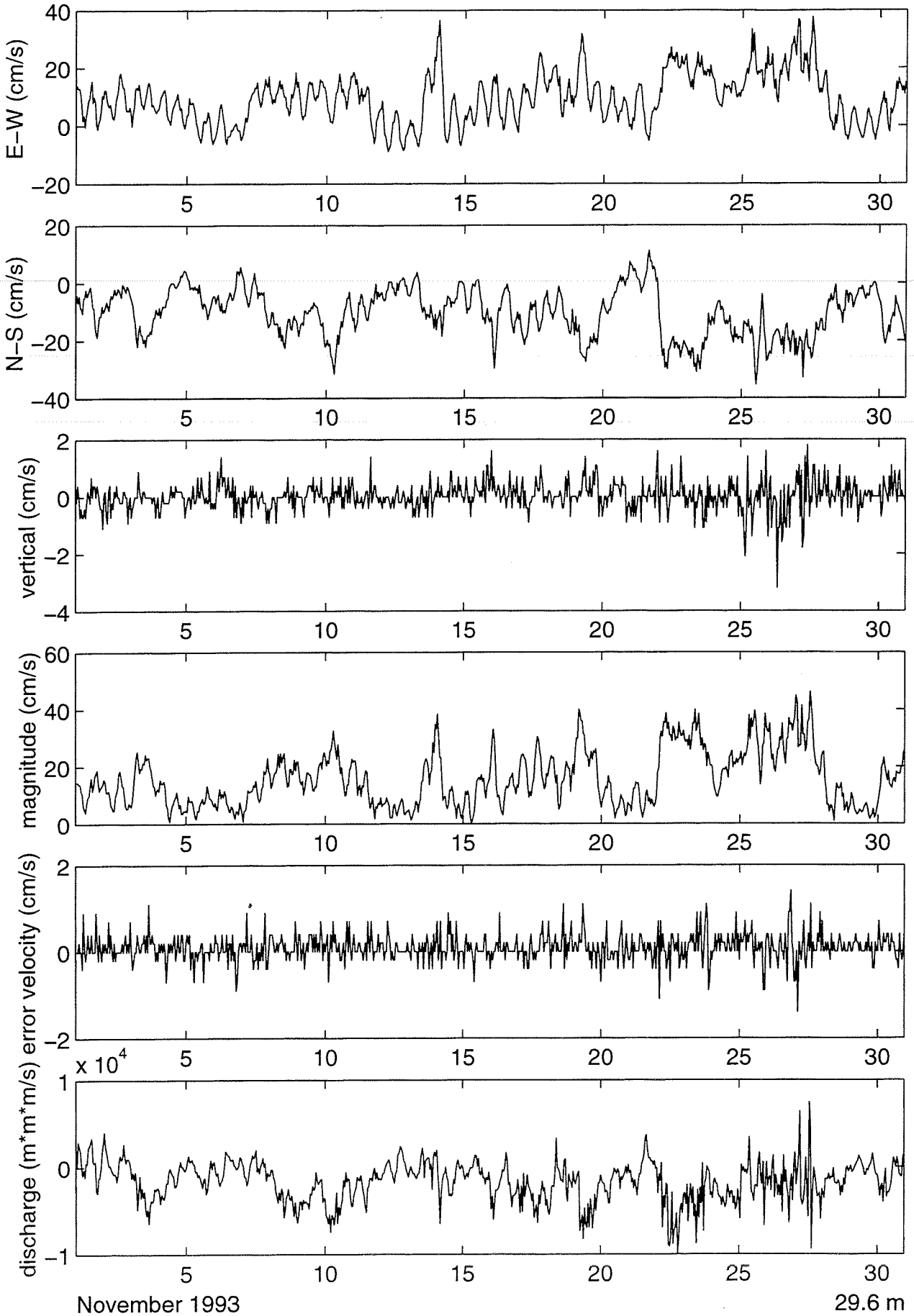
E–W (cm/s)
N–S (cm/s)
vertical (cm/s)
magnitude (cm/s)
error velocity (cm/s)
discharge (m*m*m/s)
x 10^4
November 1993
29.6 m

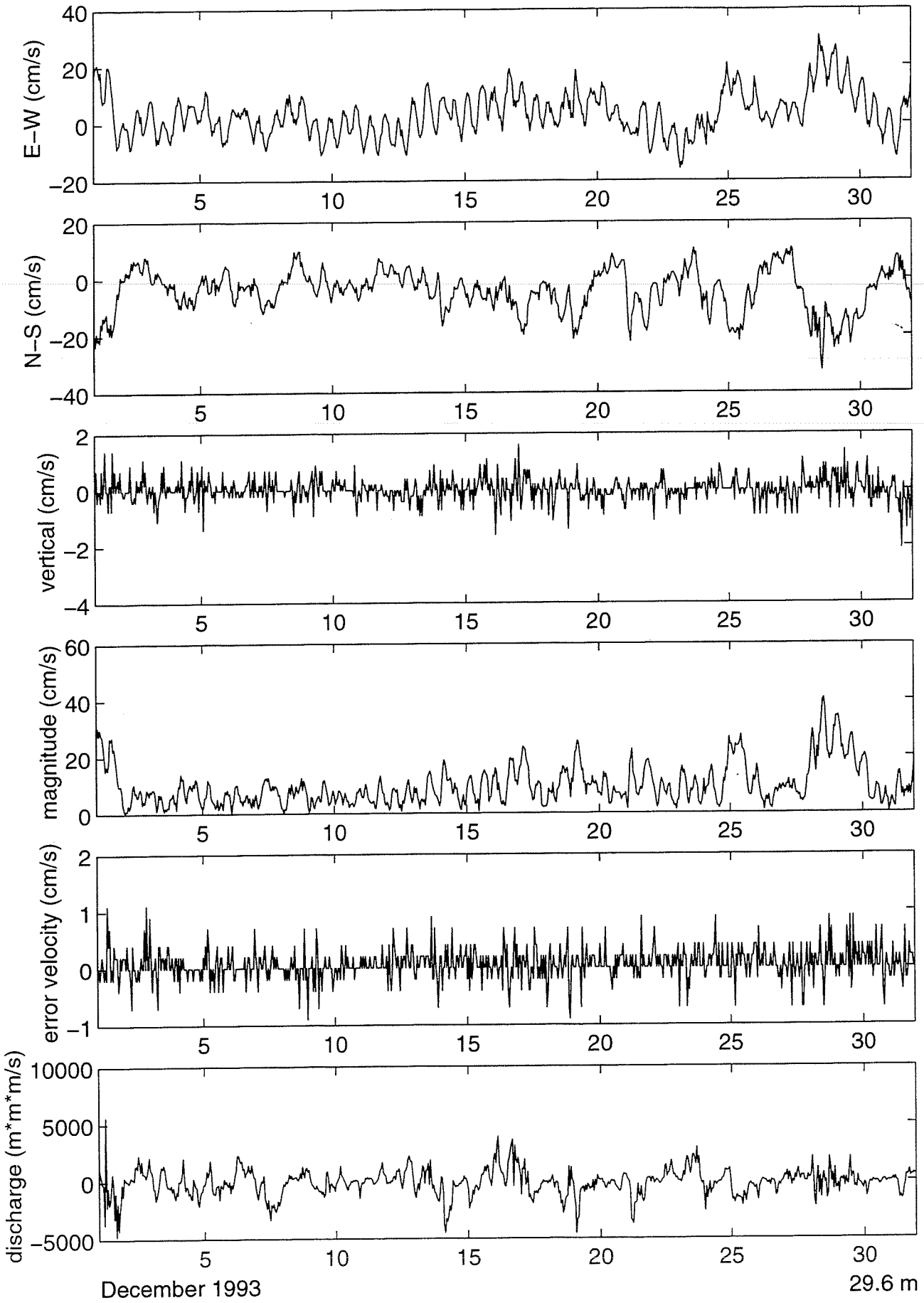
E–W (cm/s)
N–S (cm/s)
vertical (cm/s)
magnitude (cm/s)
error velocity (cm/s)
discharge (m*m*m/s)
December 1993
29.6 m

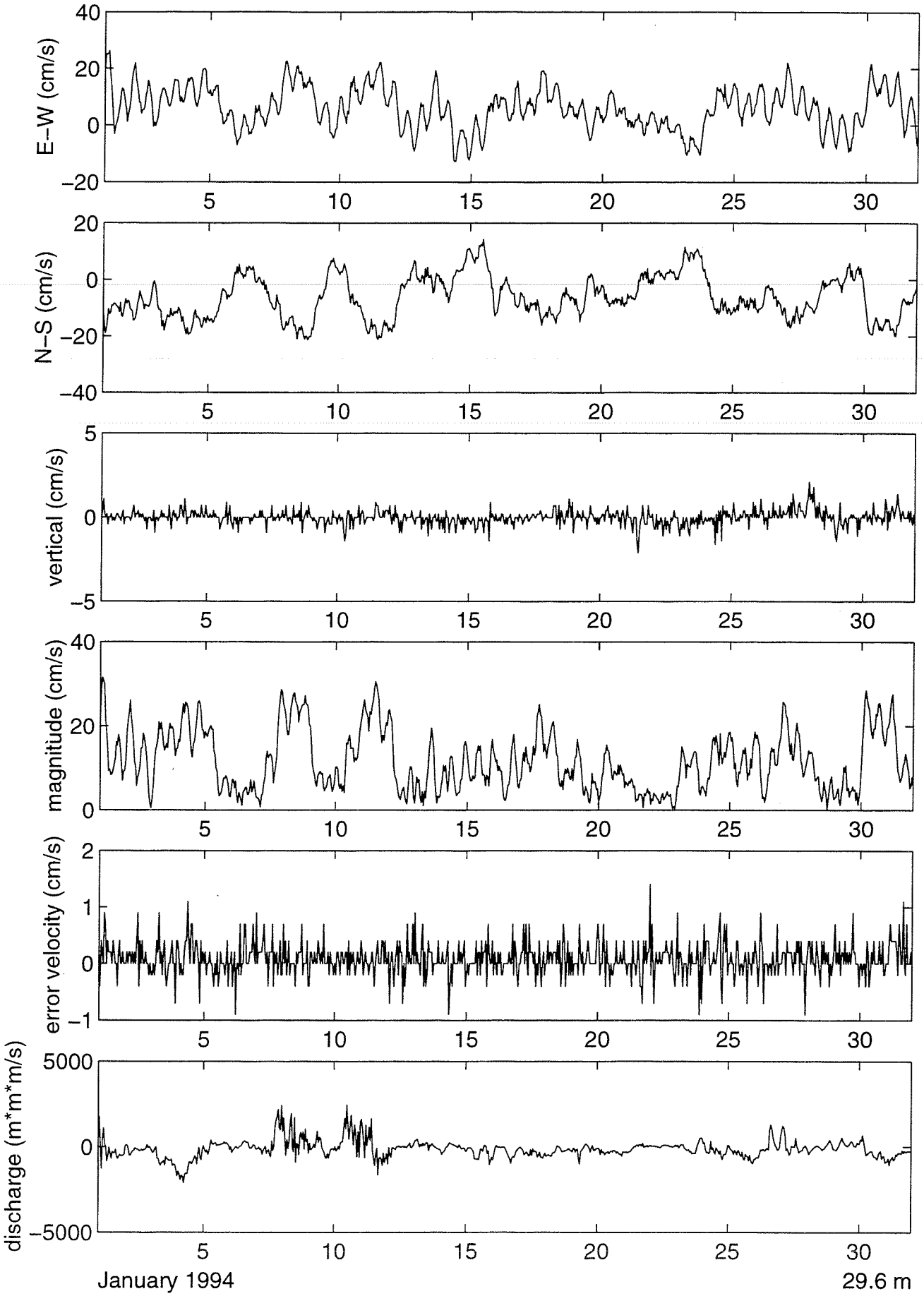
E–W (cm/s)
N–S (cm/s)
vertical (cm/s)
magnitude (cm/s)
error velocity (cm/s)
discharge (m*m*m/s)
January 1994
29.6 m

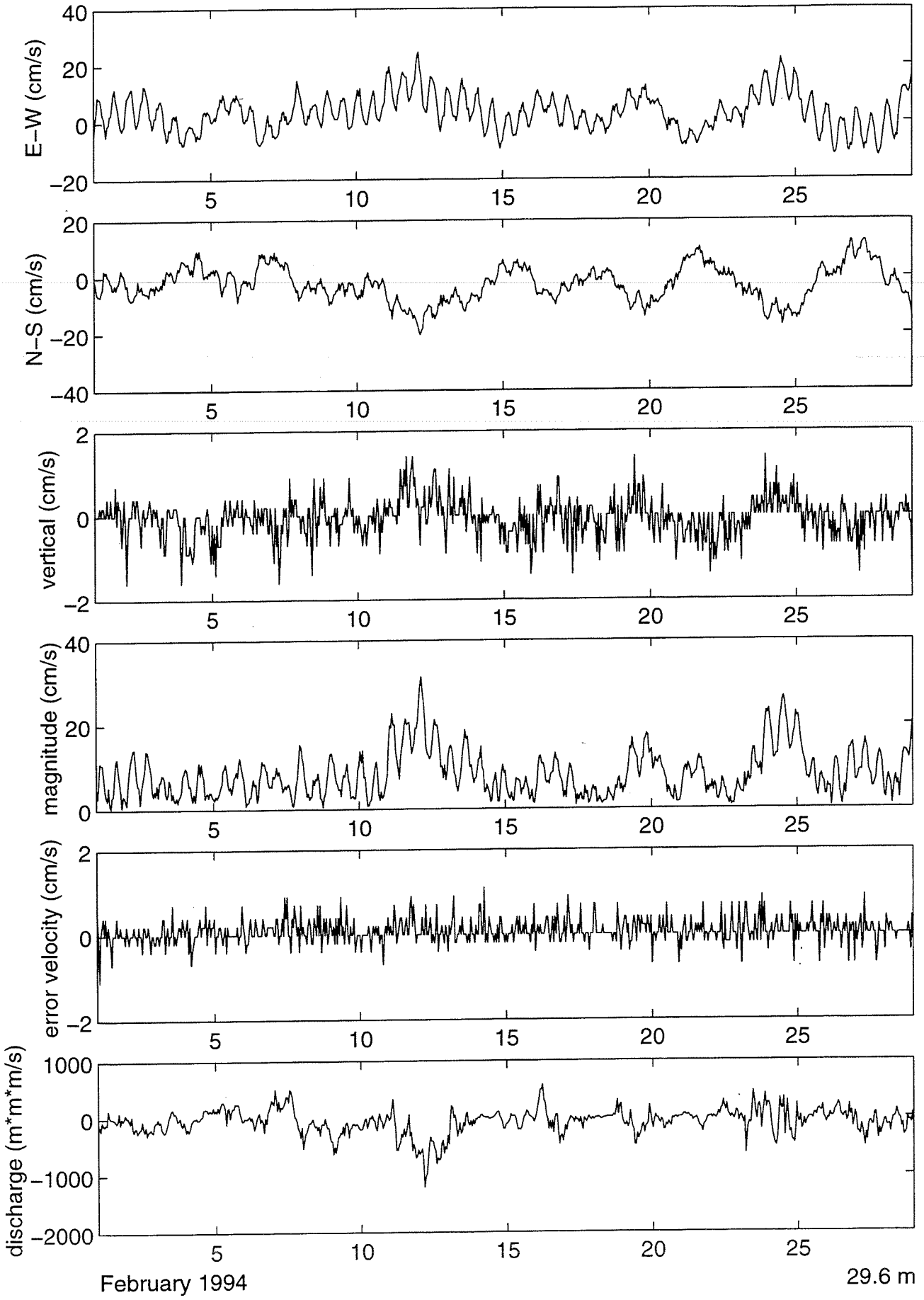
E–W (cm/s)
N–S (cm/s)
vertical (cm/s)
magnitude (cm/s)
error velocity (cm/s)
discharge (m*m*m/s)
February 1994
29.6 m

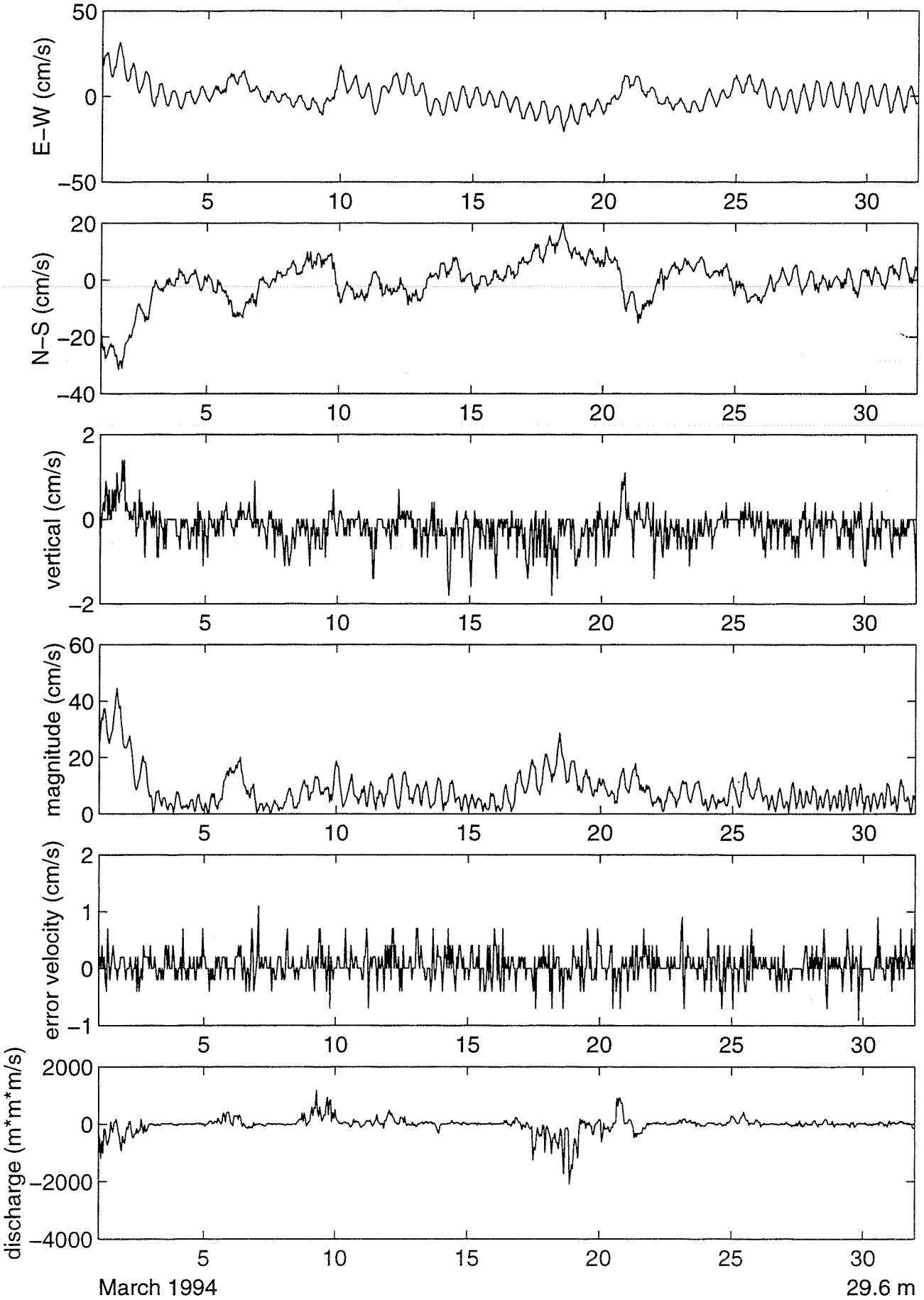
E–W (cm/s)
50
0
–50
N–S (cm/s)
20
0
–20
–40
vertical (cm/s)
2
0
–2
magnitude (cm/s)
60
40
20
0
error velocity (cm/s)
2
1
0
–1
discharge (m*m*m/s)
2000
0
–2000
–4000
5
10
15
20
25
30
March 1994
29.6 m

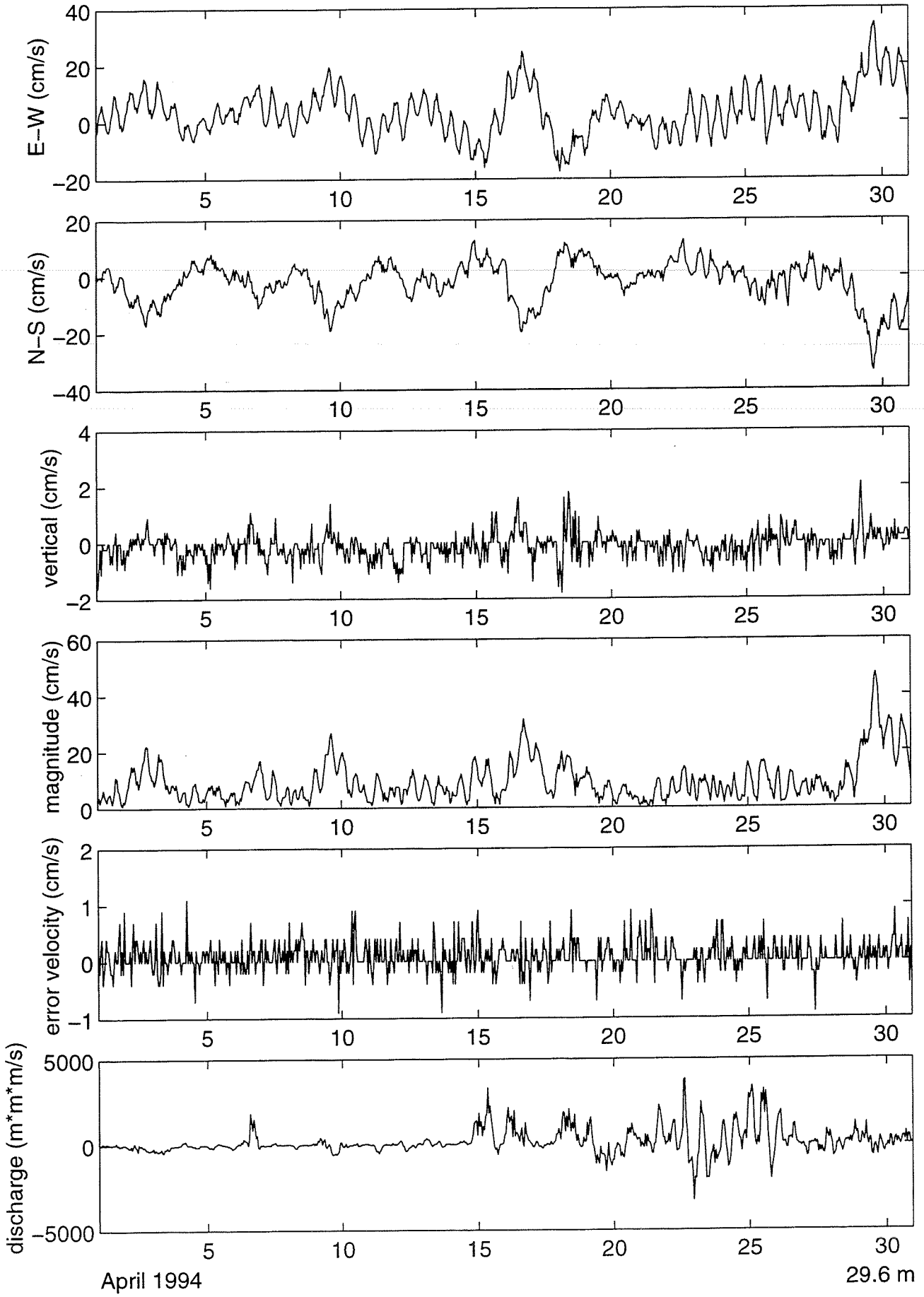
E–W (cm/s)
N–S (cm/s)
vertical (cm/s)
magnitude (cm/s)
error velocity (cm/s)
discharge (m*m*m/s)
April 1994
29.6 m

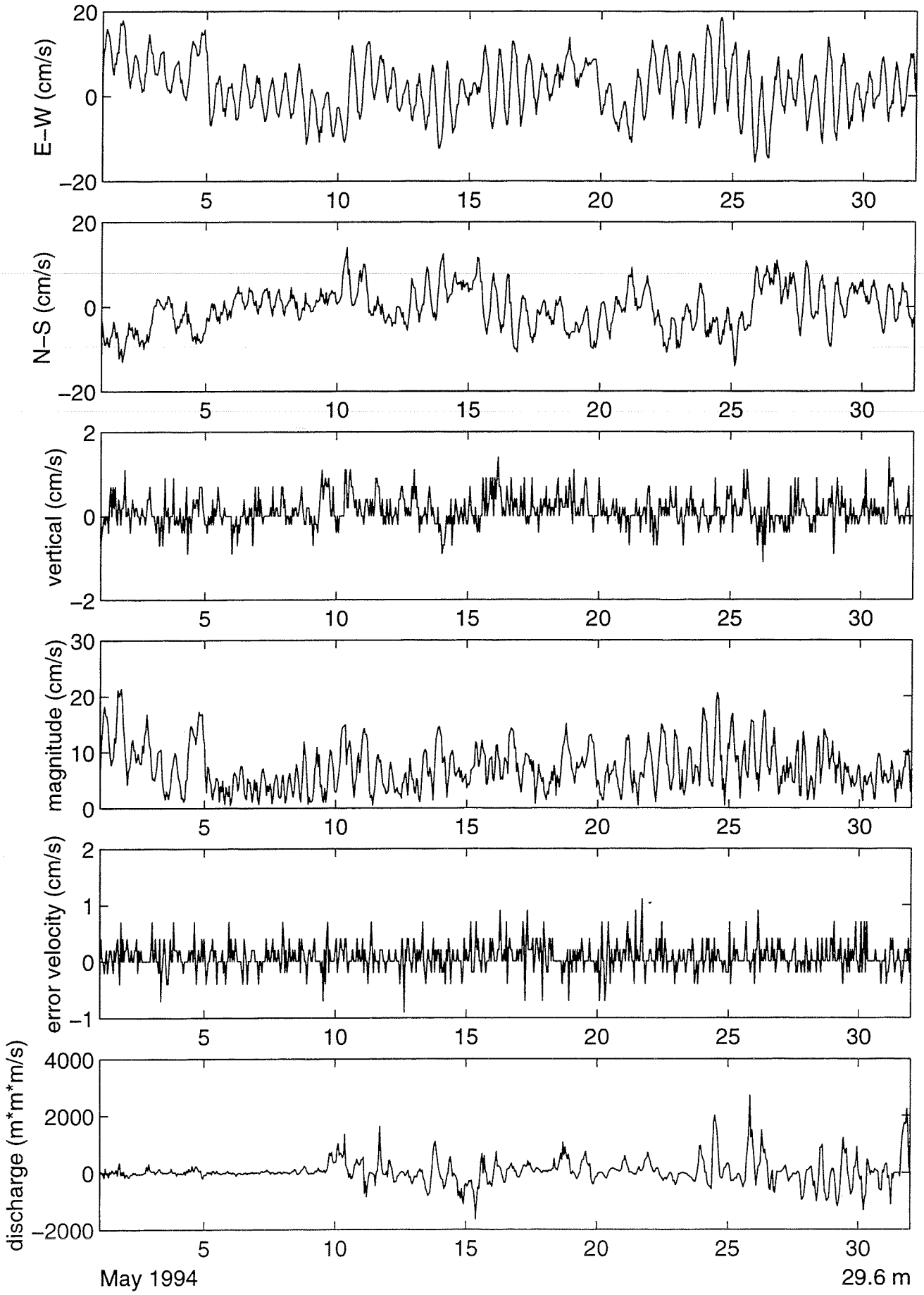
E–W (cm/s)
N–S (cm/s)
vertical (cm/s)
magnitude (cm/s)
error velocity (cm/s)
discharge (m*m*m/s)
May 1994
29.6 m

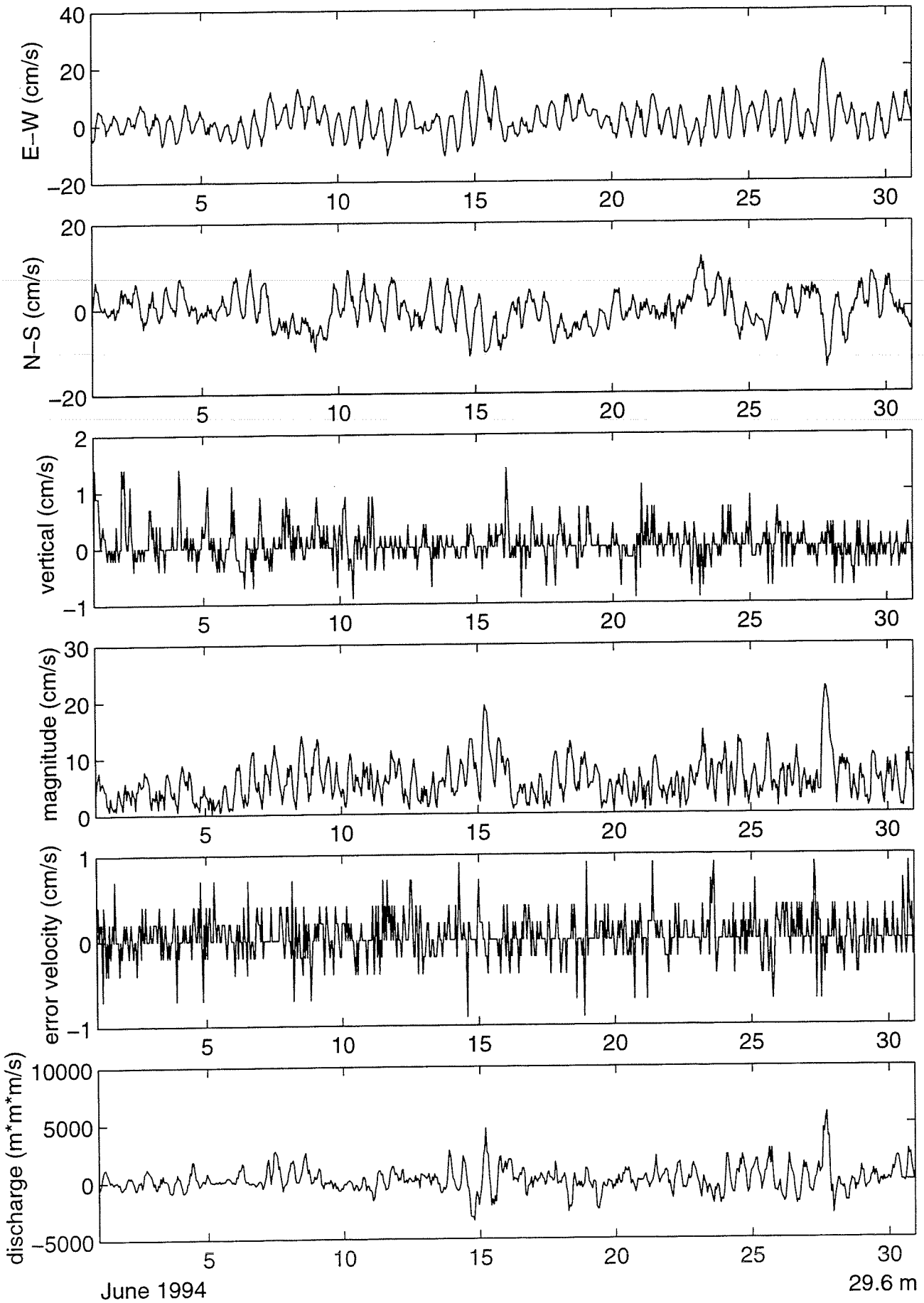
E–W (cm/s)
N–S (cm/s)
vertical (cm/s)
magnitude (cm/s)
error velocity (cm/s)
discharge (m*m*m/s)
June 1994
29.6 m

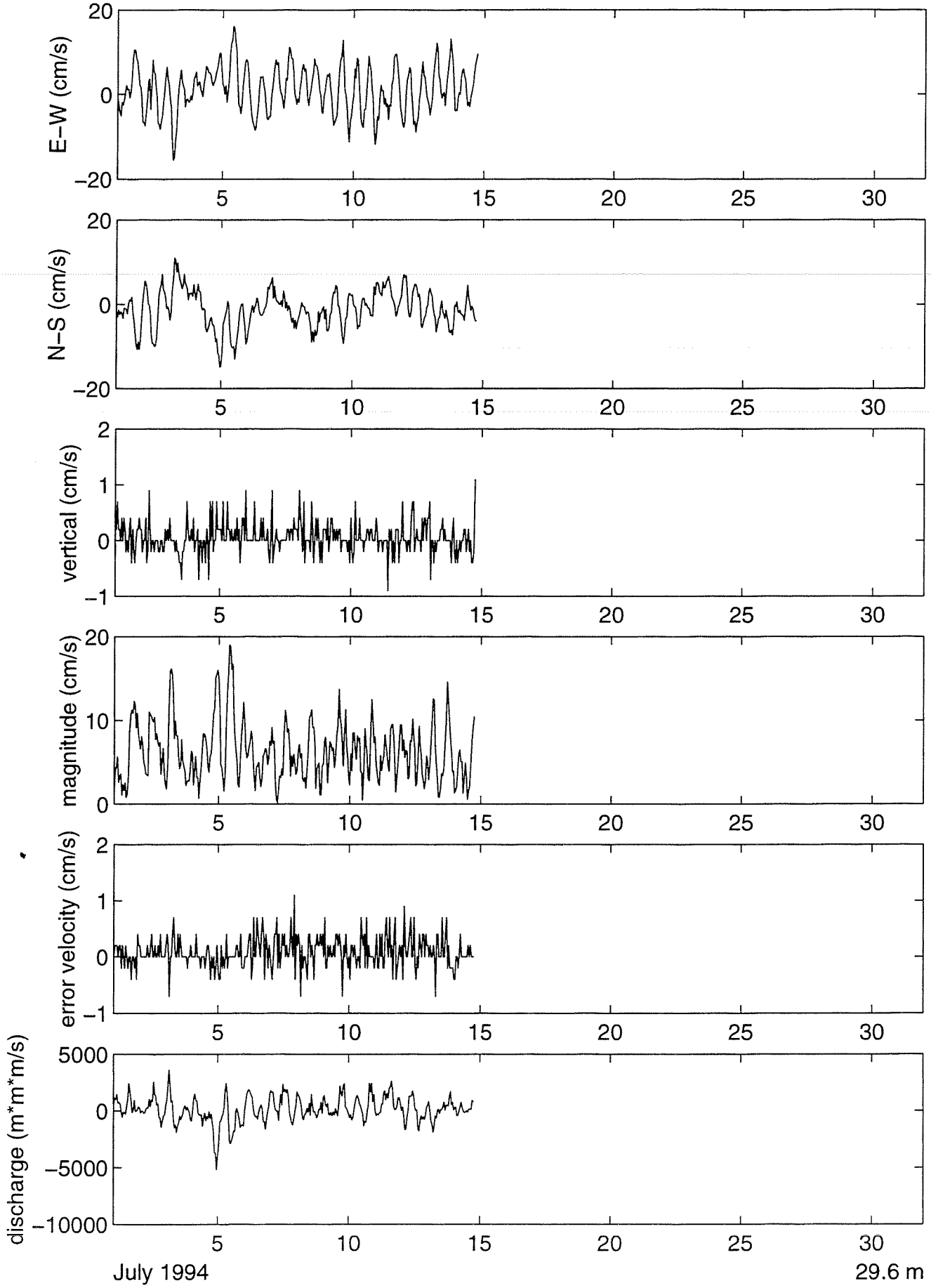
E–W (cm/s)
N–S (cm/s)
vertical (cm/s)
magnitude (cm/s)
error velocity (cm/s)
discharge (m*m*m/s)
July 1994
29.6 m

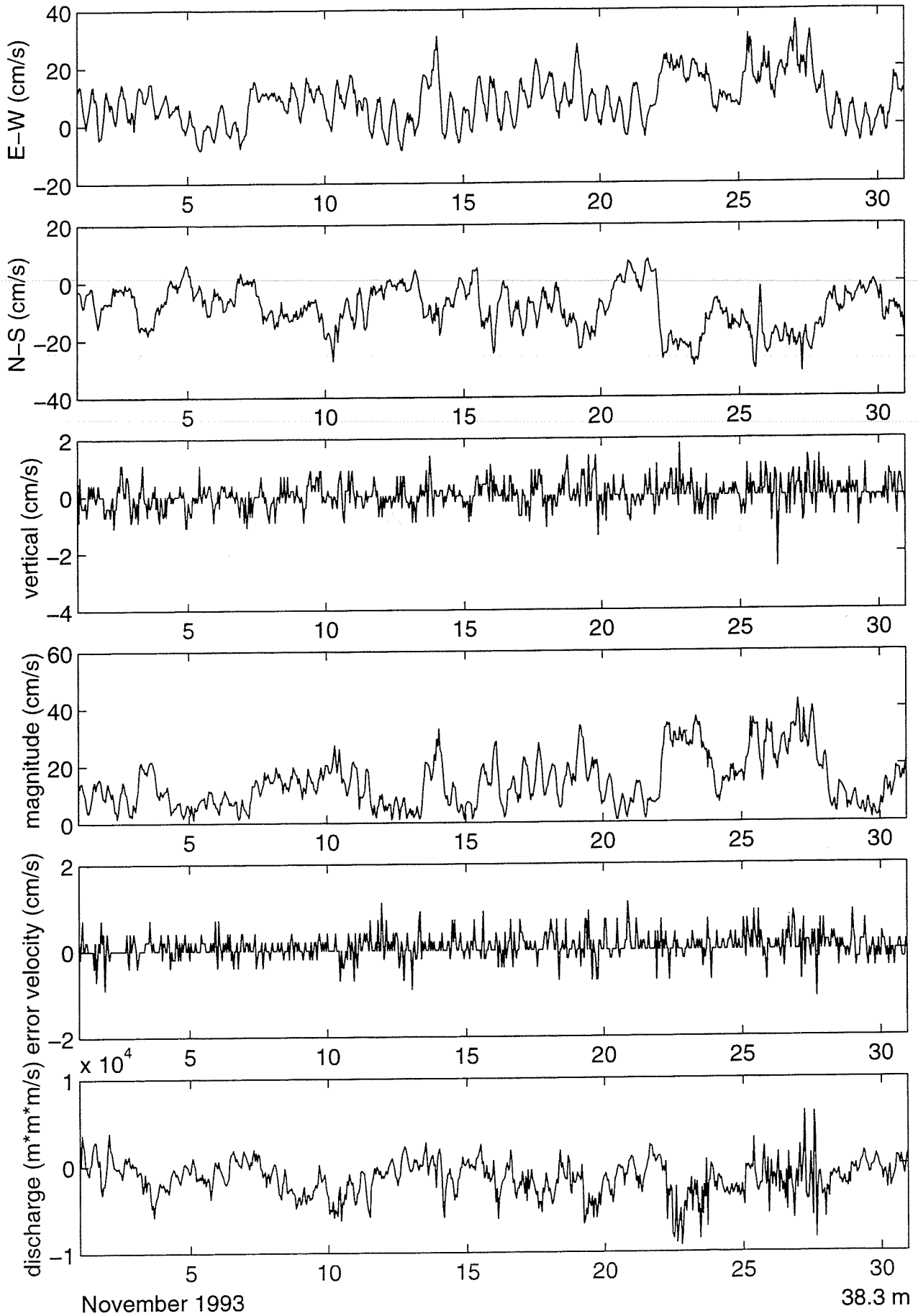
E–W (cm/s)
N–S (cm/s)
vertical (cm/s)
magnitude (cm/s)
error velocity (cm/s)
discharge (m*m*m/s)
x 10^4
November 1993
38.3 m

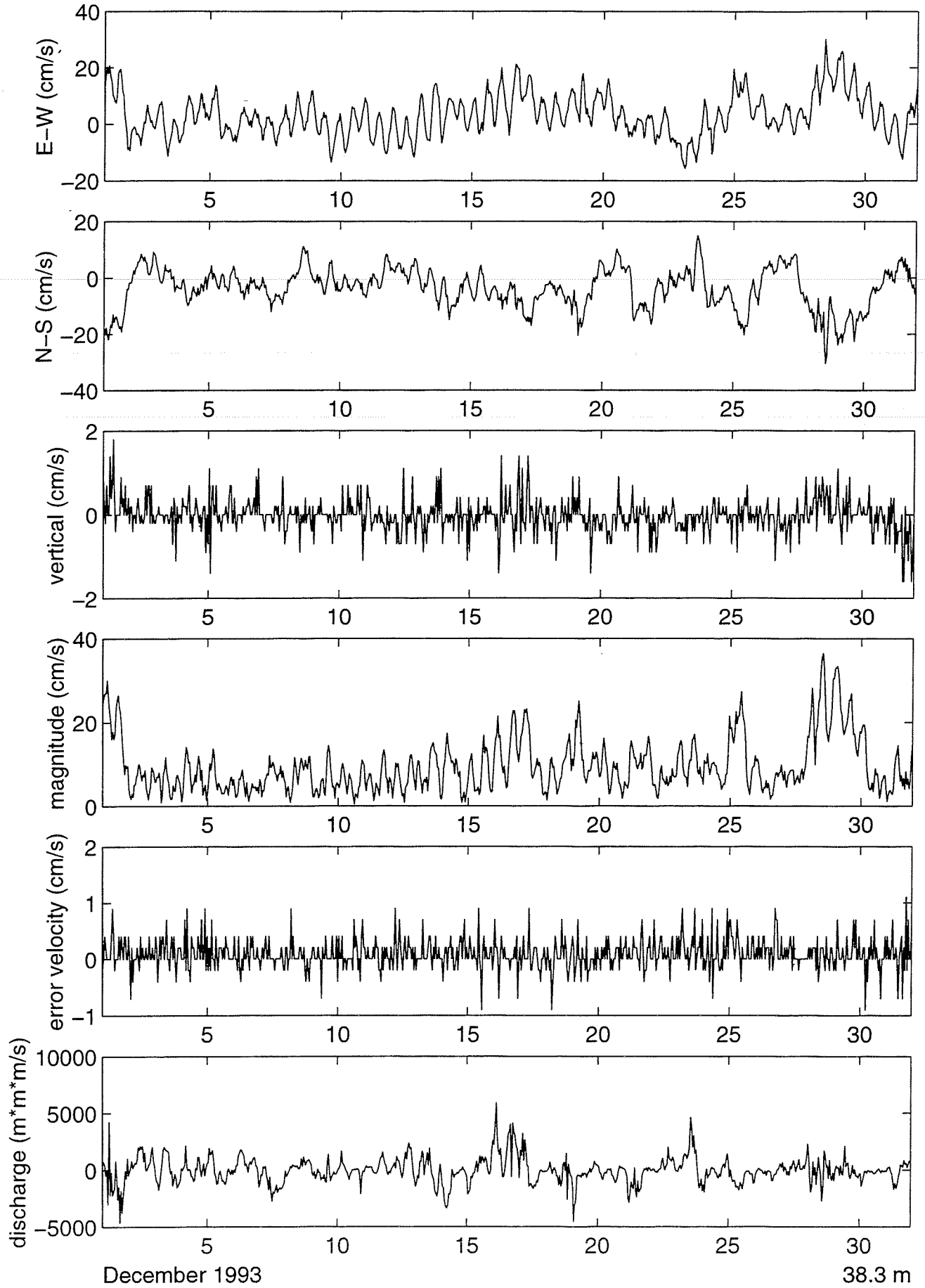
E–W (cm/s)
N–S (cm/s)
vertical (cm/s)
magnitude (cm/s)
error velocity (cm/s)
discharge (m*m*m/s)
December 1993
38.3 m

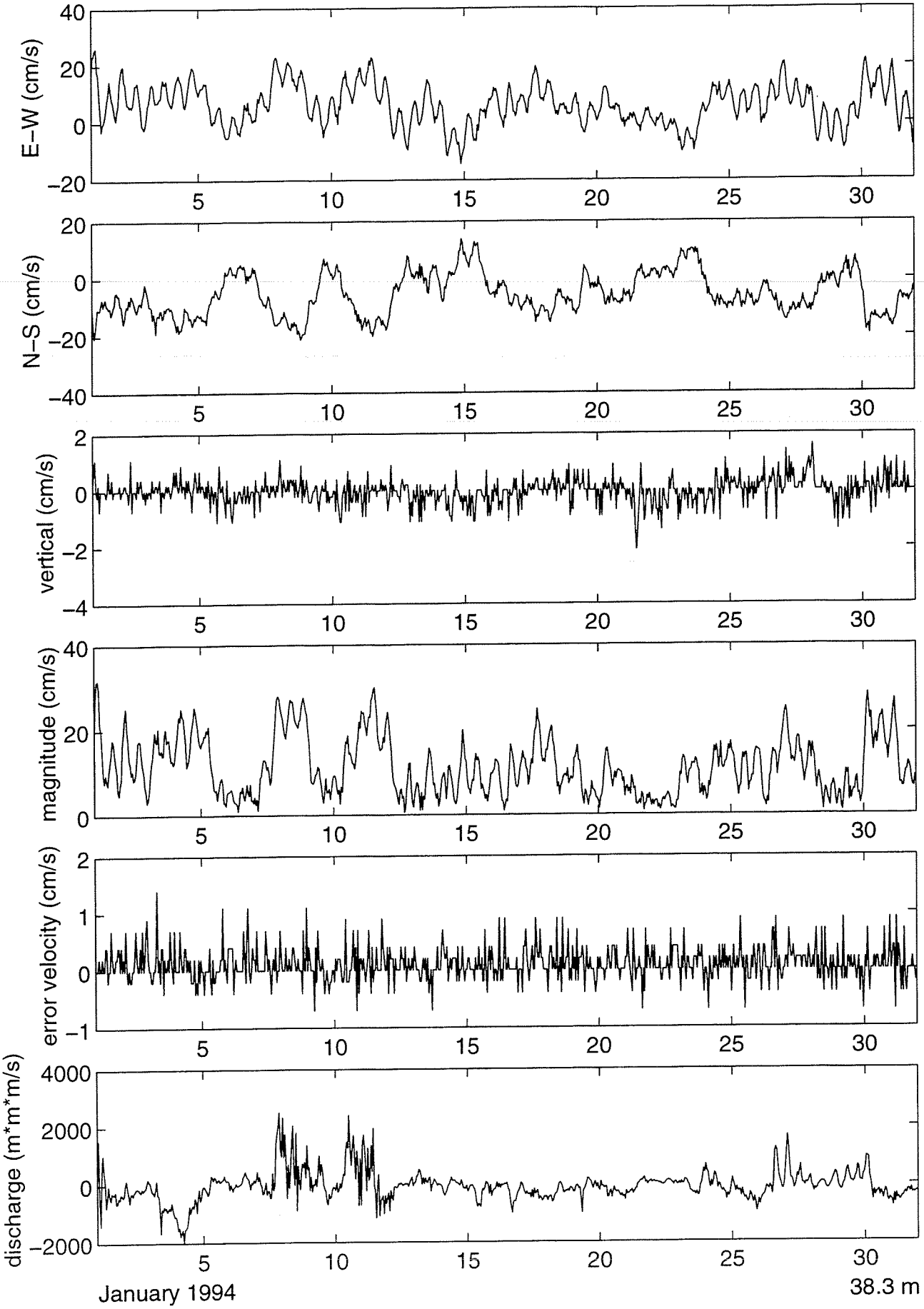
E–W (cm/s)
N–S (cm/s)
vertical (cm/s)
magnitude (cm/s)
error velocity (cm/s)
discharge (m*m*m/s)
January 1994
38.3 m

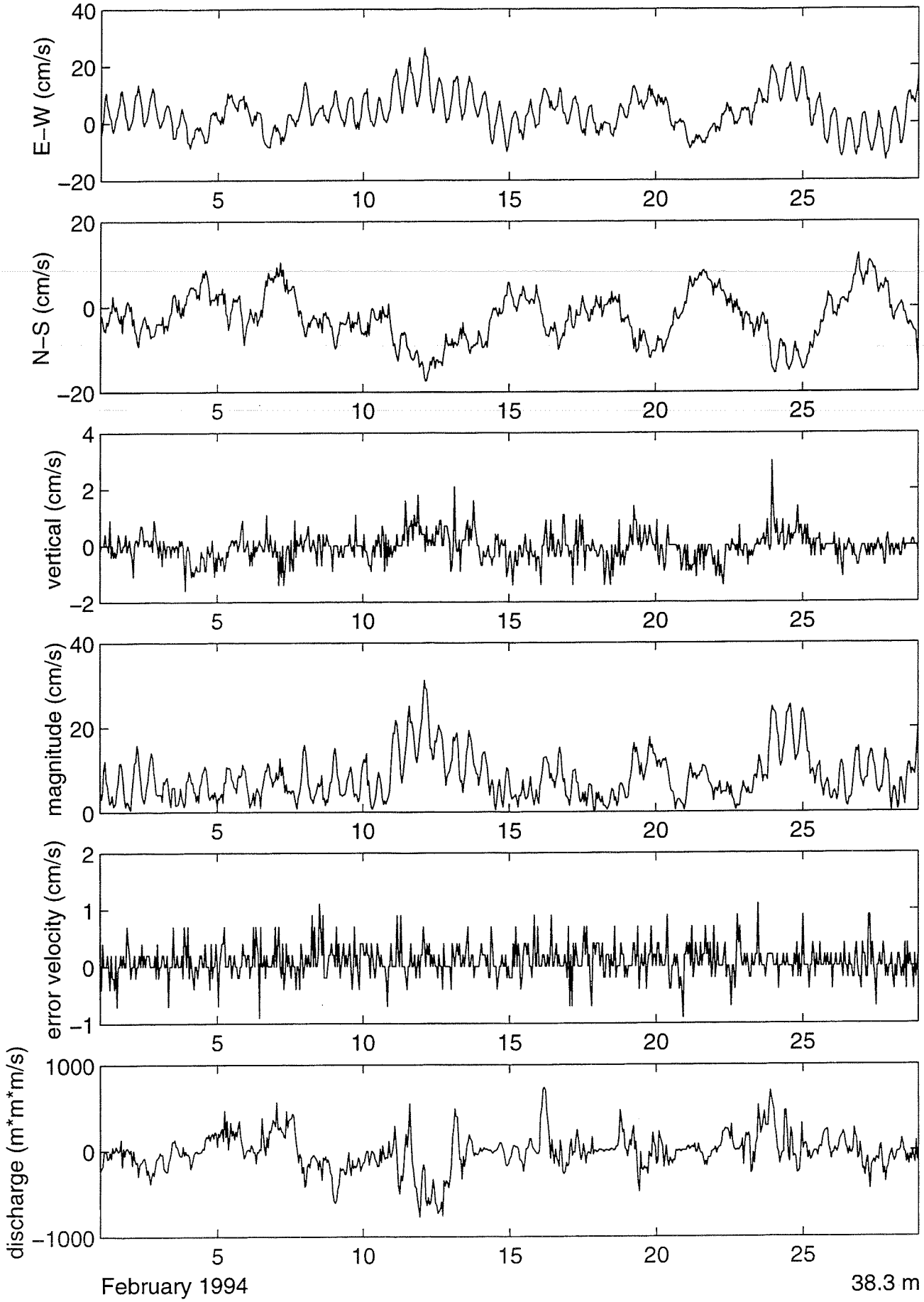
E–W (cm/s)
N–S (cm/s)
vertical (cm/s)
magnitude (cm/s)
error velocity (cm/s)
discharge (m*m*m/s)
February 1994
38.3 m

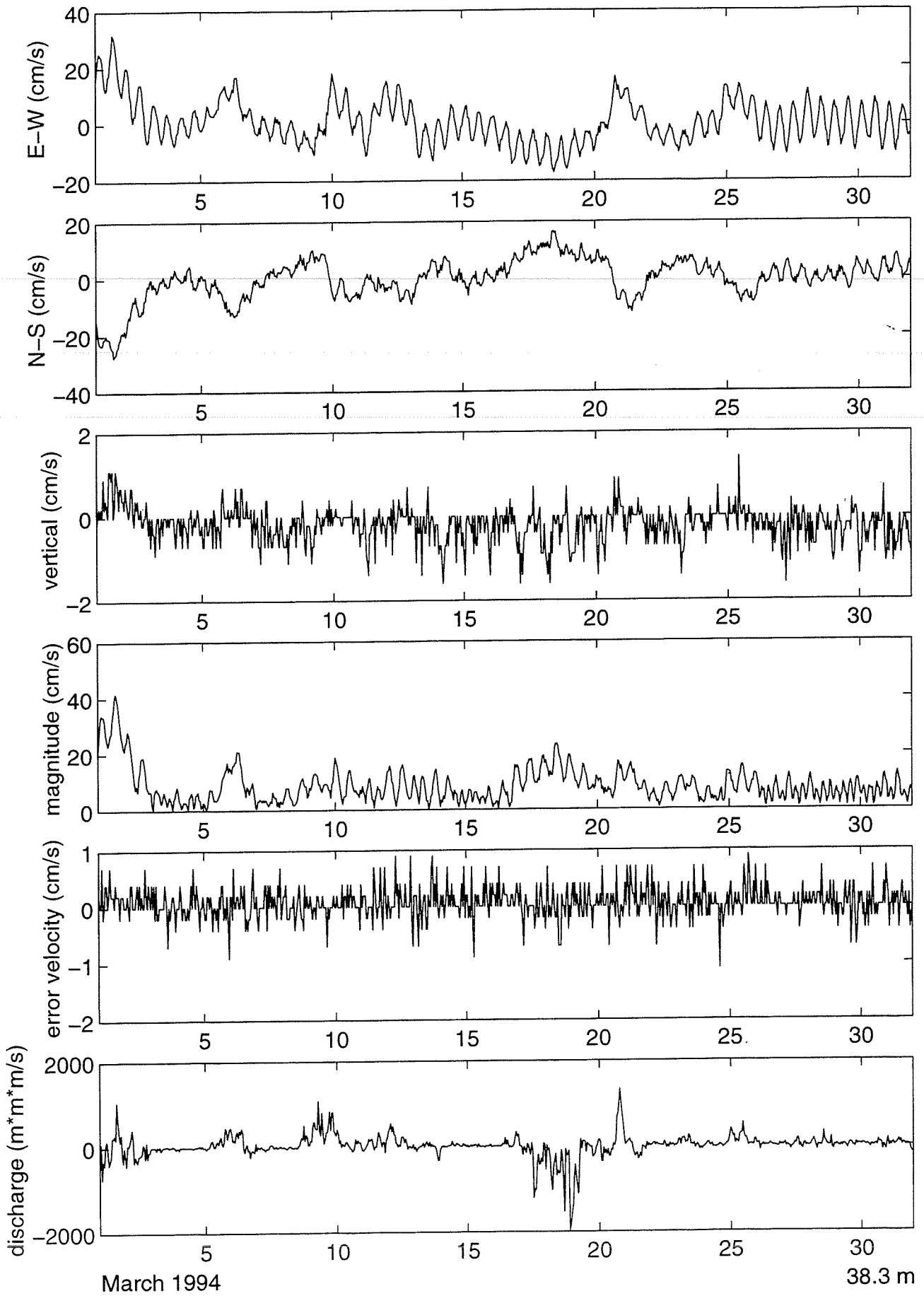
E–W (cm/s)
N–S (cm/s)
vertical (cm/s)
magnitude (cm/s)
error velocity (cm/s)
discharge (m*m*m/s)
March 1994
38.3 m

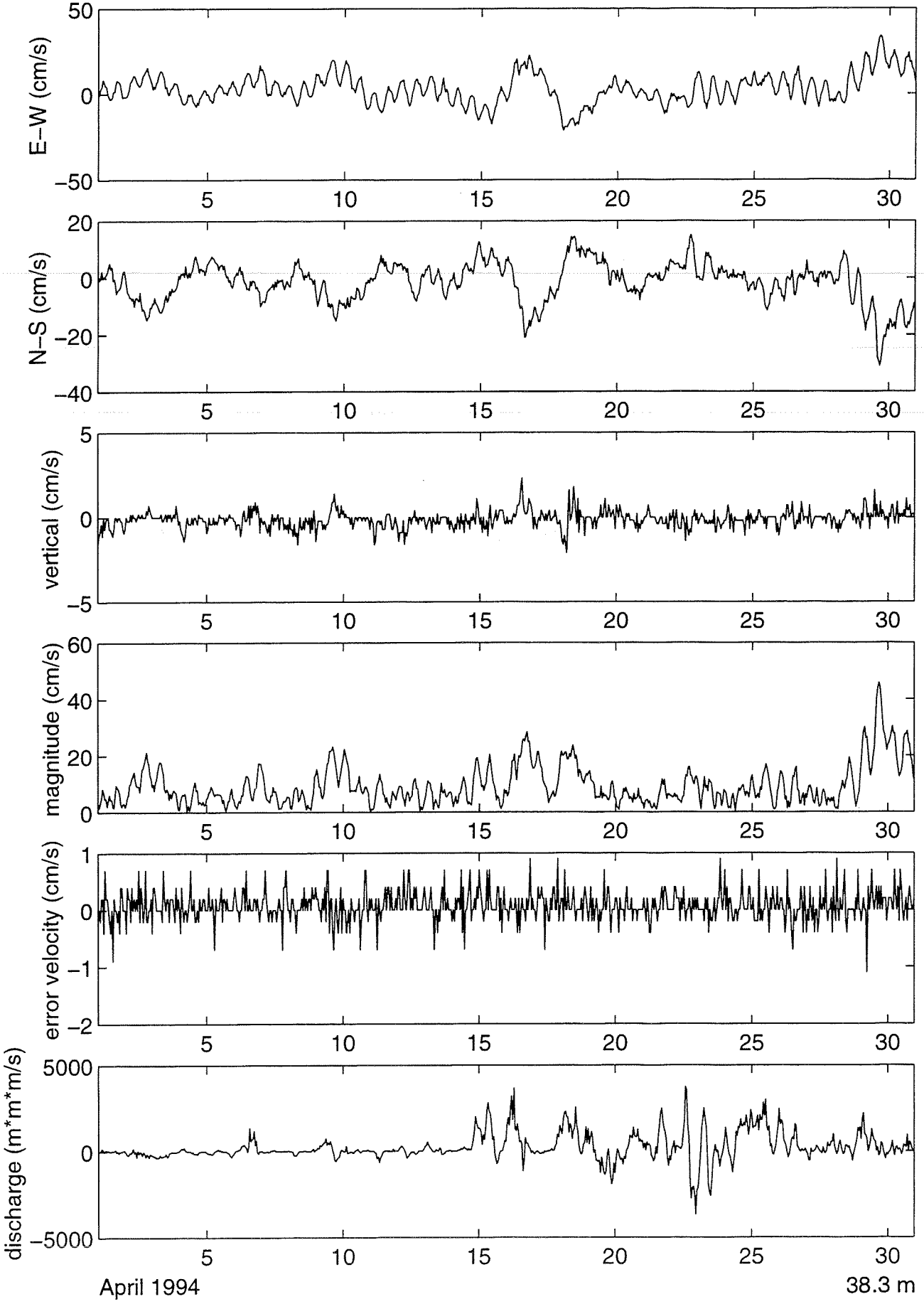
E–W (cm/s)
50
0
–50
N–S (cm/s)
20
0
–20
–40
vertical (cm/s)
5
0
–5
magnitude (cm/s)
60
40
20
0
error velocity (cm/s)
1
0
–1
–2
discharge (m*m*m/s)
5000
0
–5000
5
10
15
20
25
30
April 1994
38.3 m

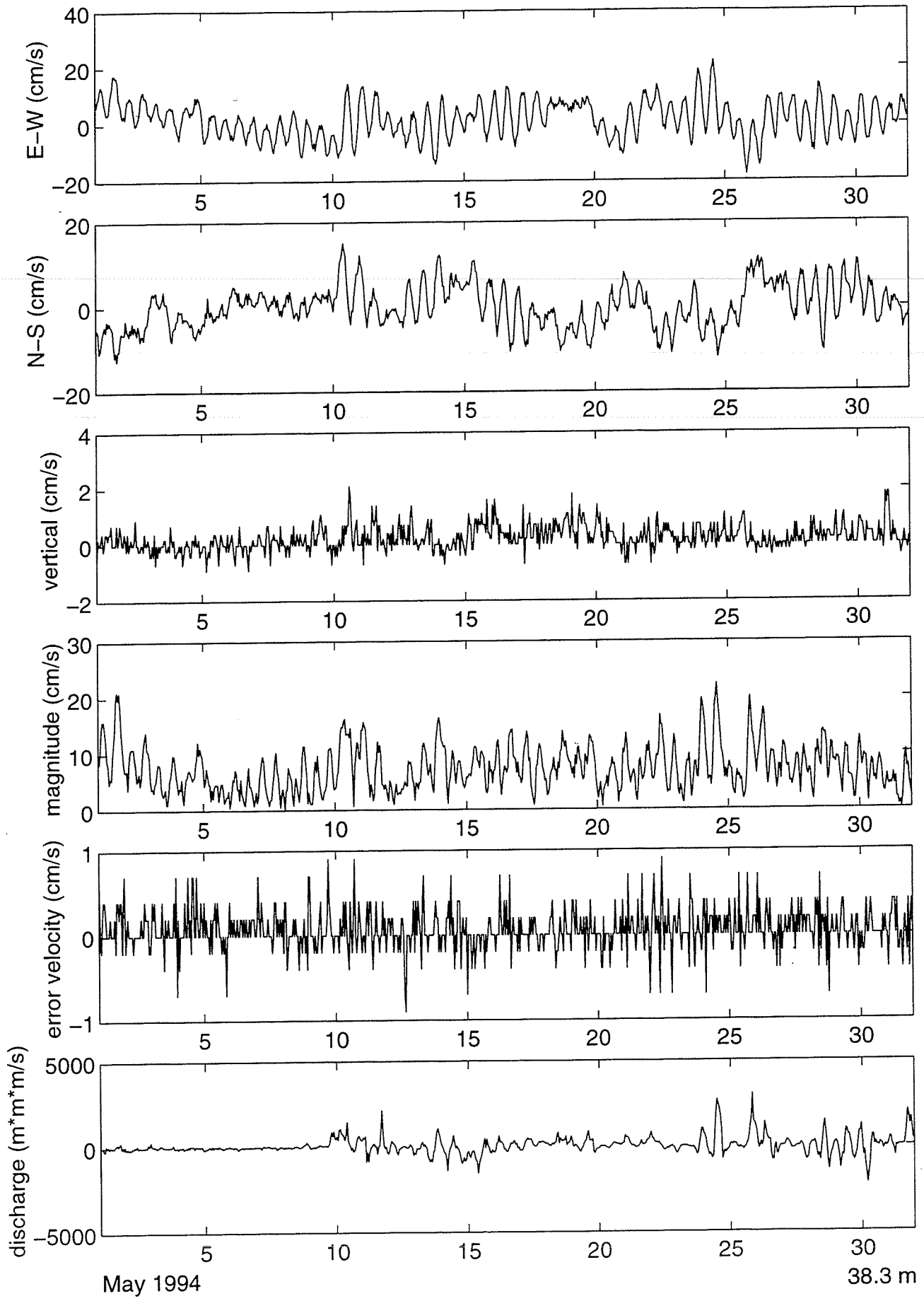
E–W (cm/s)
N–S (cm/s)
vertical (cm/s)
magnitude (cm/s)
error velocity (cm/s)
discharge (m*m*m/s)
May 1994
38.3 m

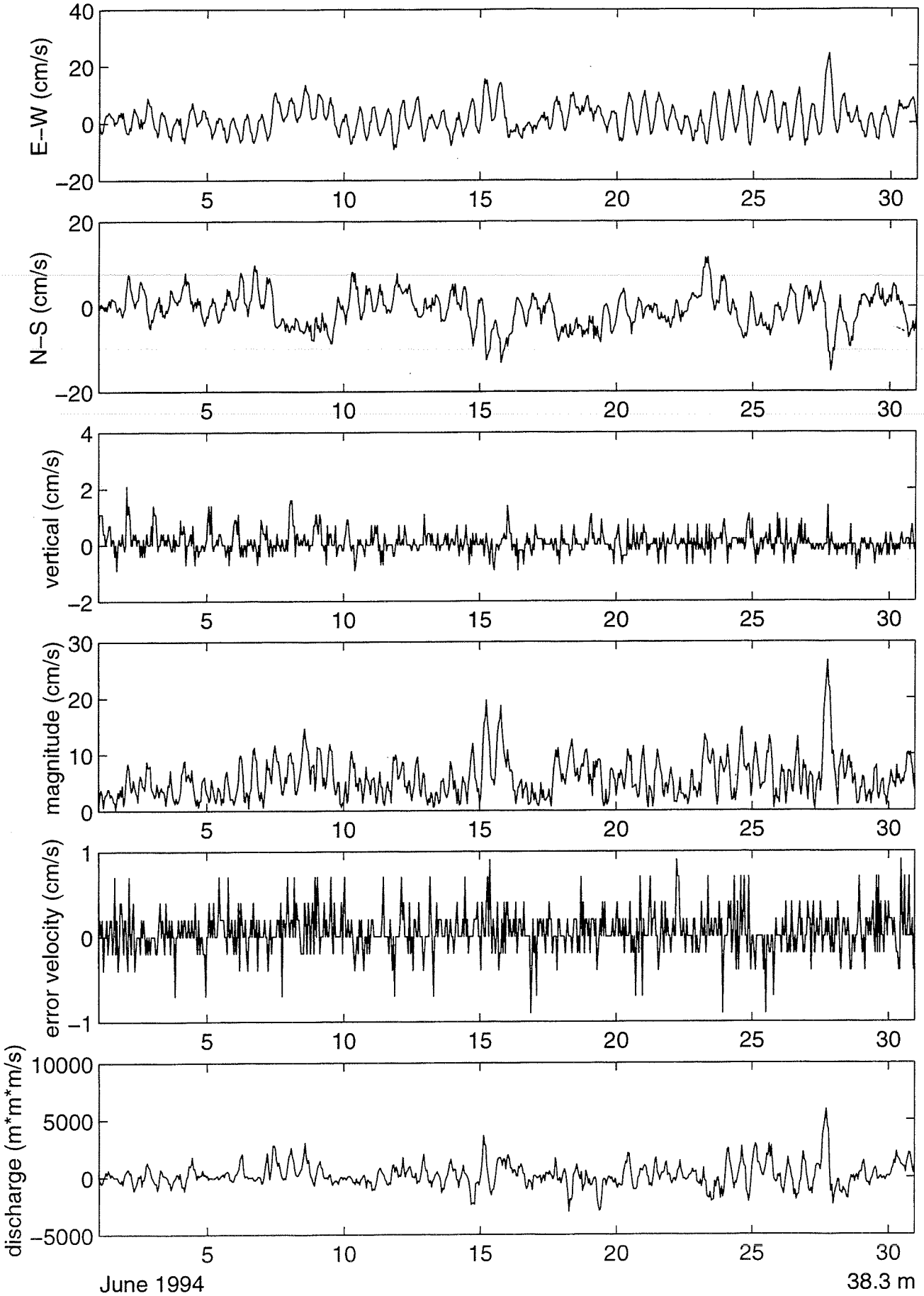
E–W (cm/s)
N–S (cm/s)
vertical (cm/s)
magnitude (cm/s)
error velocity (cm/s)
discharge (m*m*m/s)
June 1994
38.3 m

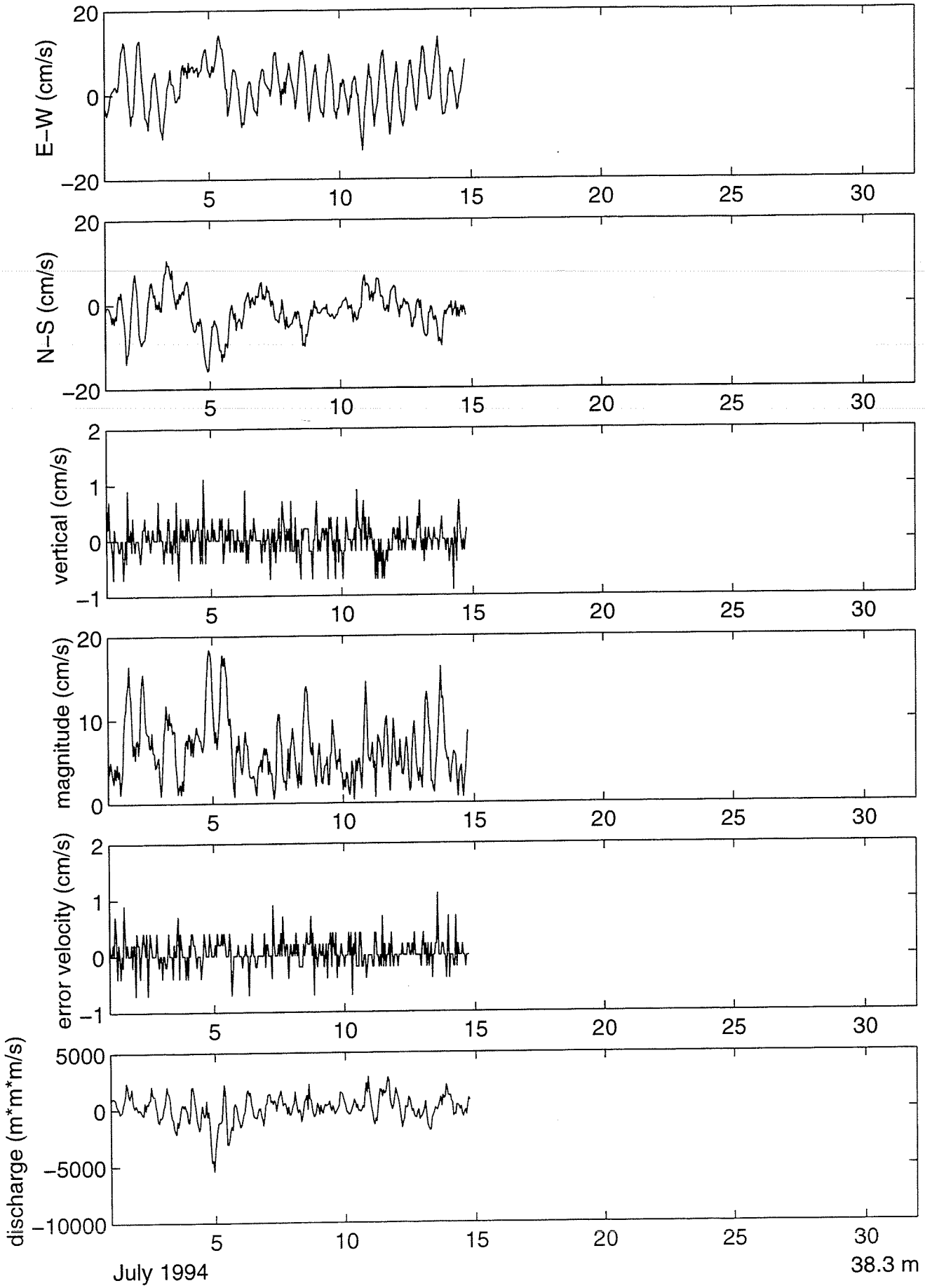
E–W (cm/s)
N–S (cm/s)
vertical (cm/s)
magnitude (cm/s)
error velocity (cm/s)
discharge (m*m*m/s)
July 1994
38.3 m

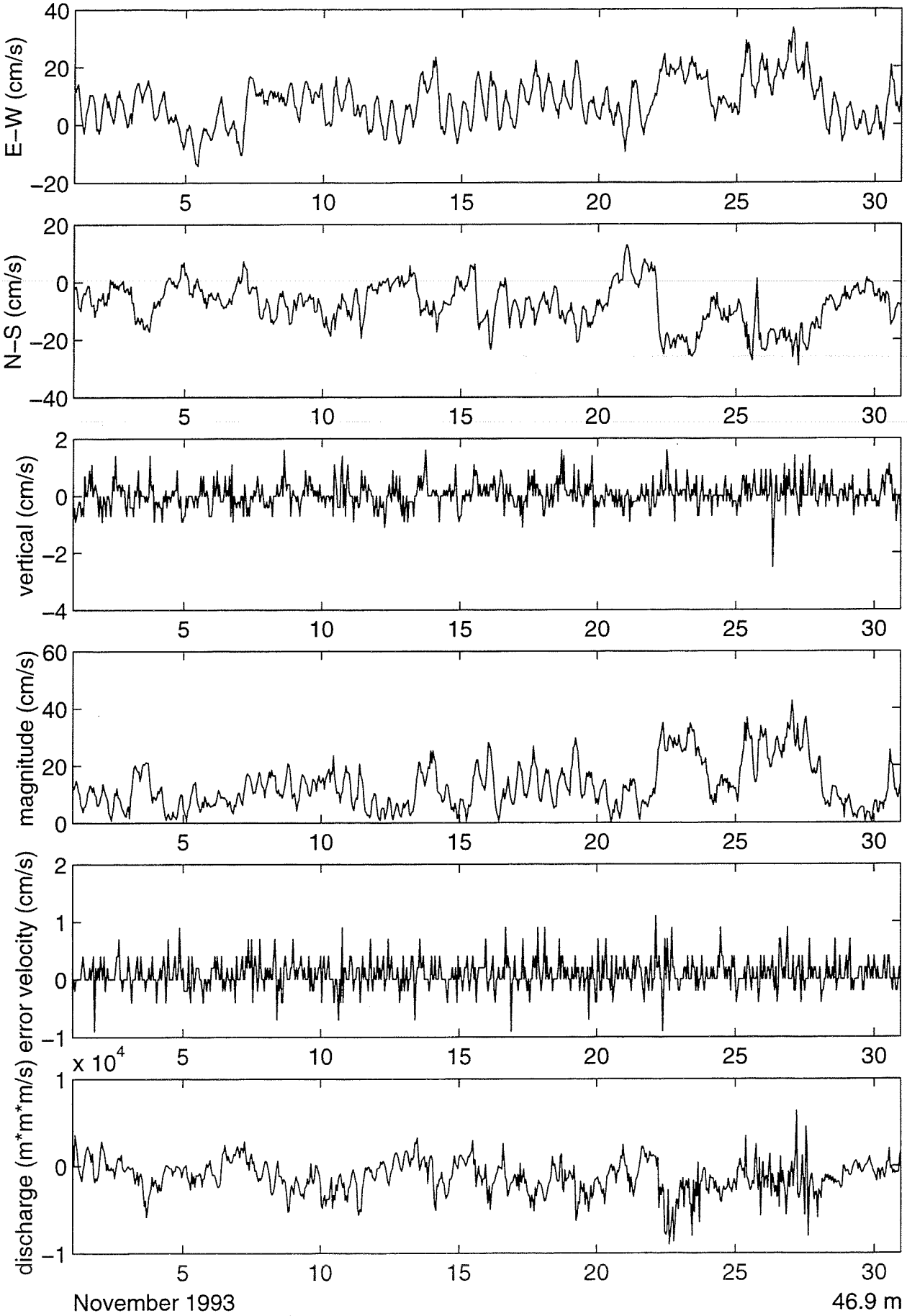
E–W (cm/s)
N–S (cm/s)
vertical (cm/s)
magnitude (cm/s)
error velocity (cm/s)
discharge (m*m*m/s)
x 10^4
November 1993
46.9 m

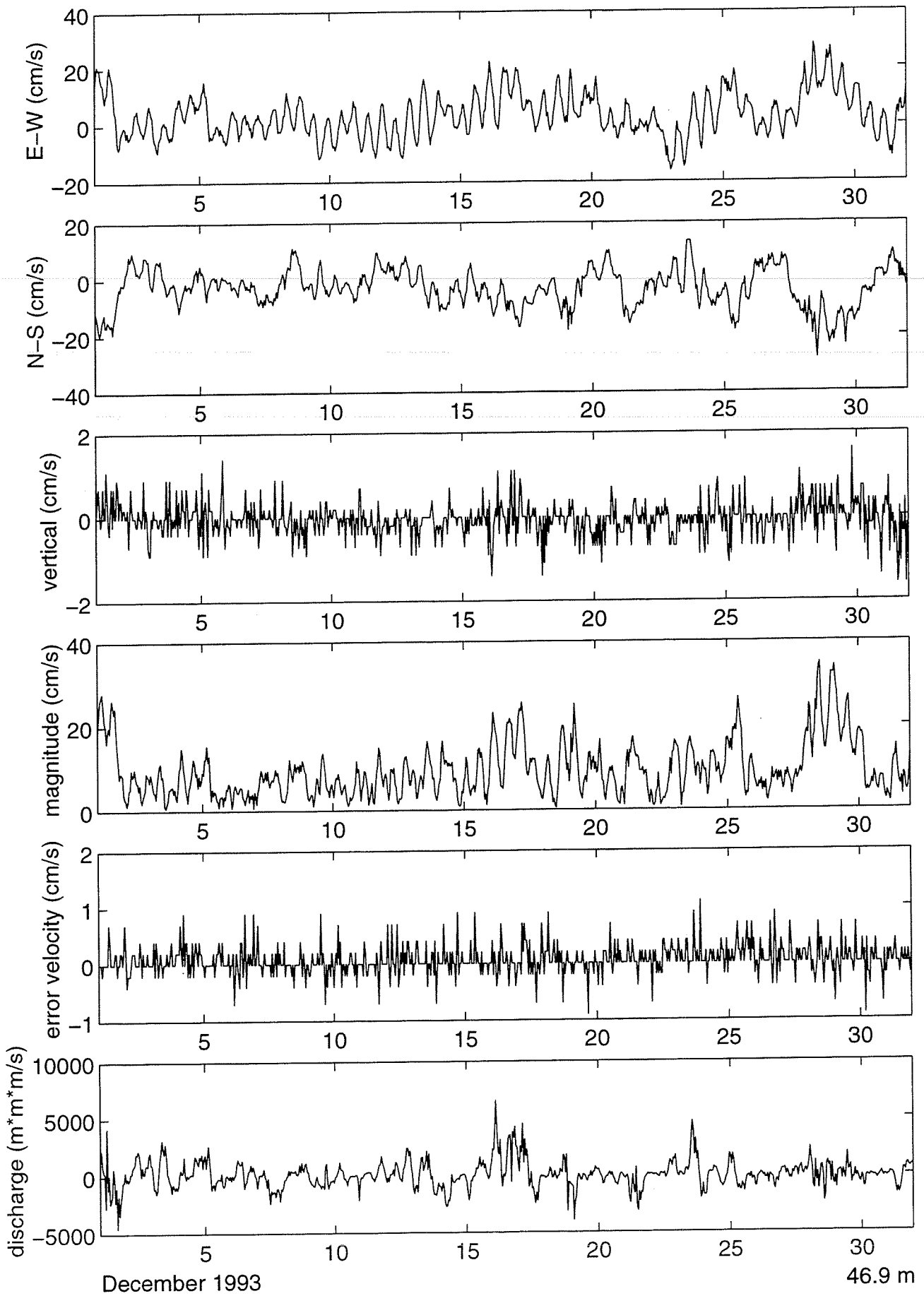
E–W (cm/s)
N–S (cm/s)
vertical (cm/s)
magnitude (cm/s)
error velocity (cm/s)
discharge (m*m*m/s)
December 1993
46.9 m

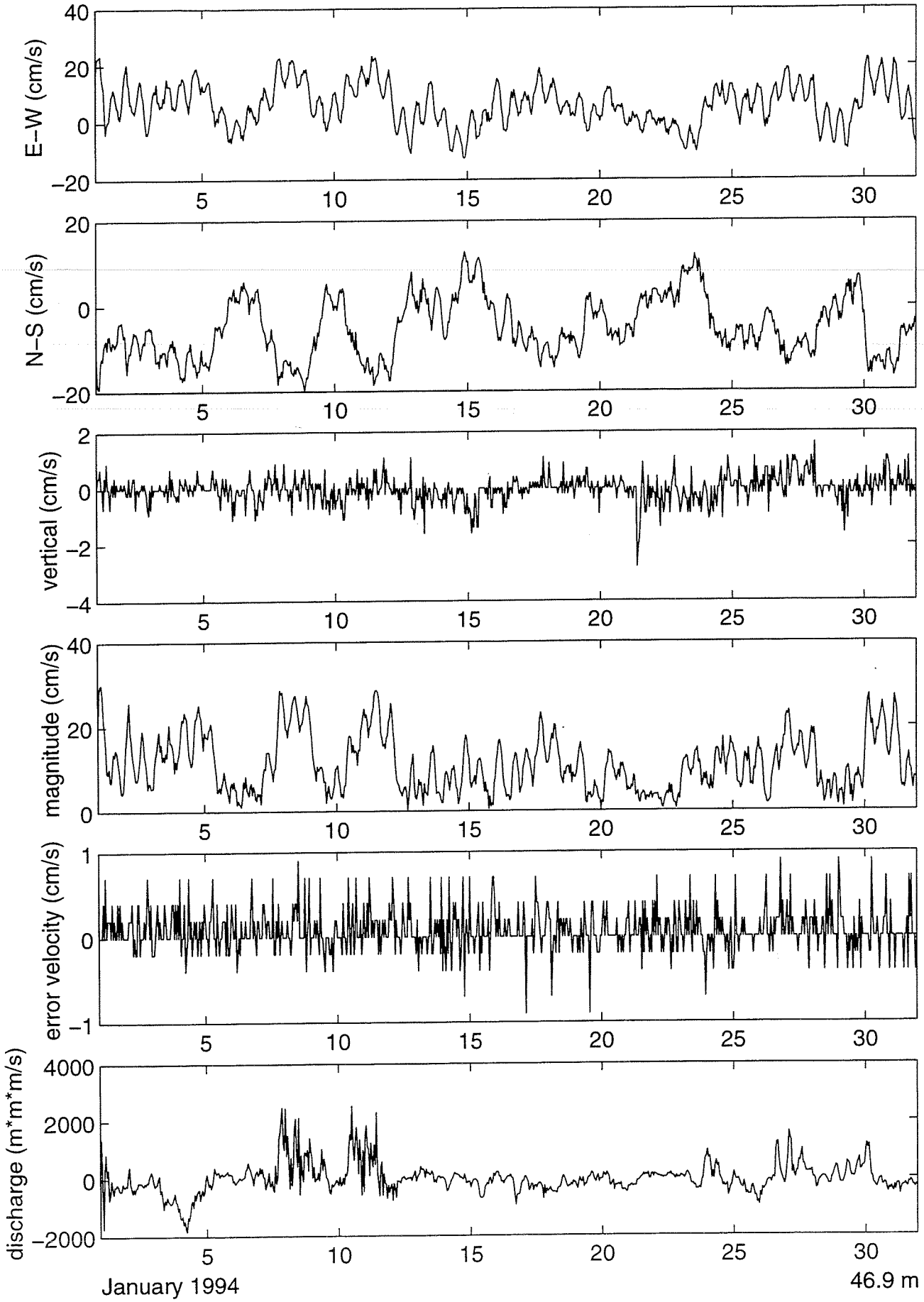
E–W (cm/s)
N–S (cm/s)
vertical (cm/s)
magnitude (cm/s)
error velocity (cm/s)
discharge (m*m*m/s)
January 1994
46.9 m

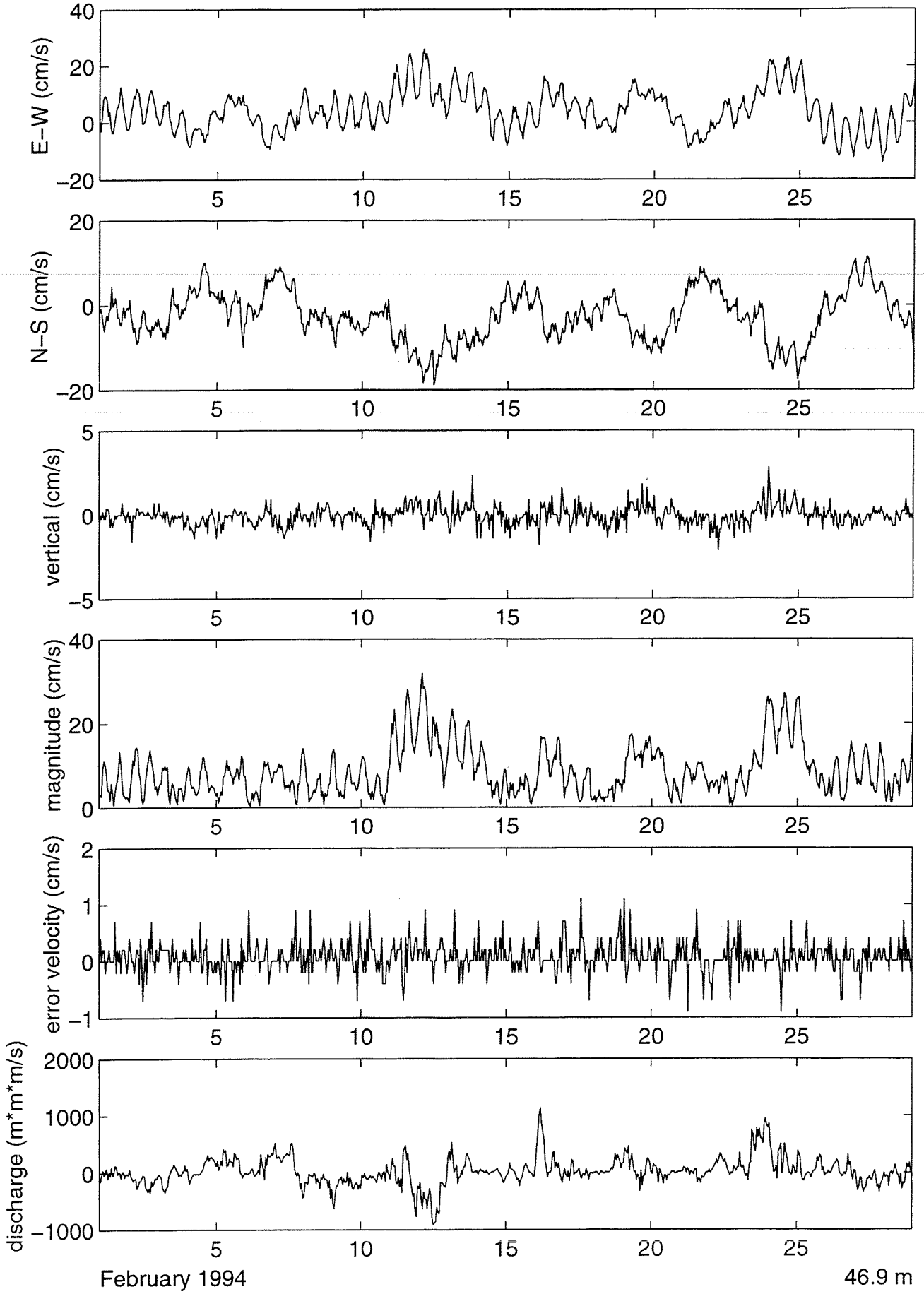
E–W (cm/s)
N–S (cm/s)
vertical (cm/s)
magnitude (cm/s)
error velocity (cm/s)
discharge (m*m*m/s)
February 1994
46.9 m

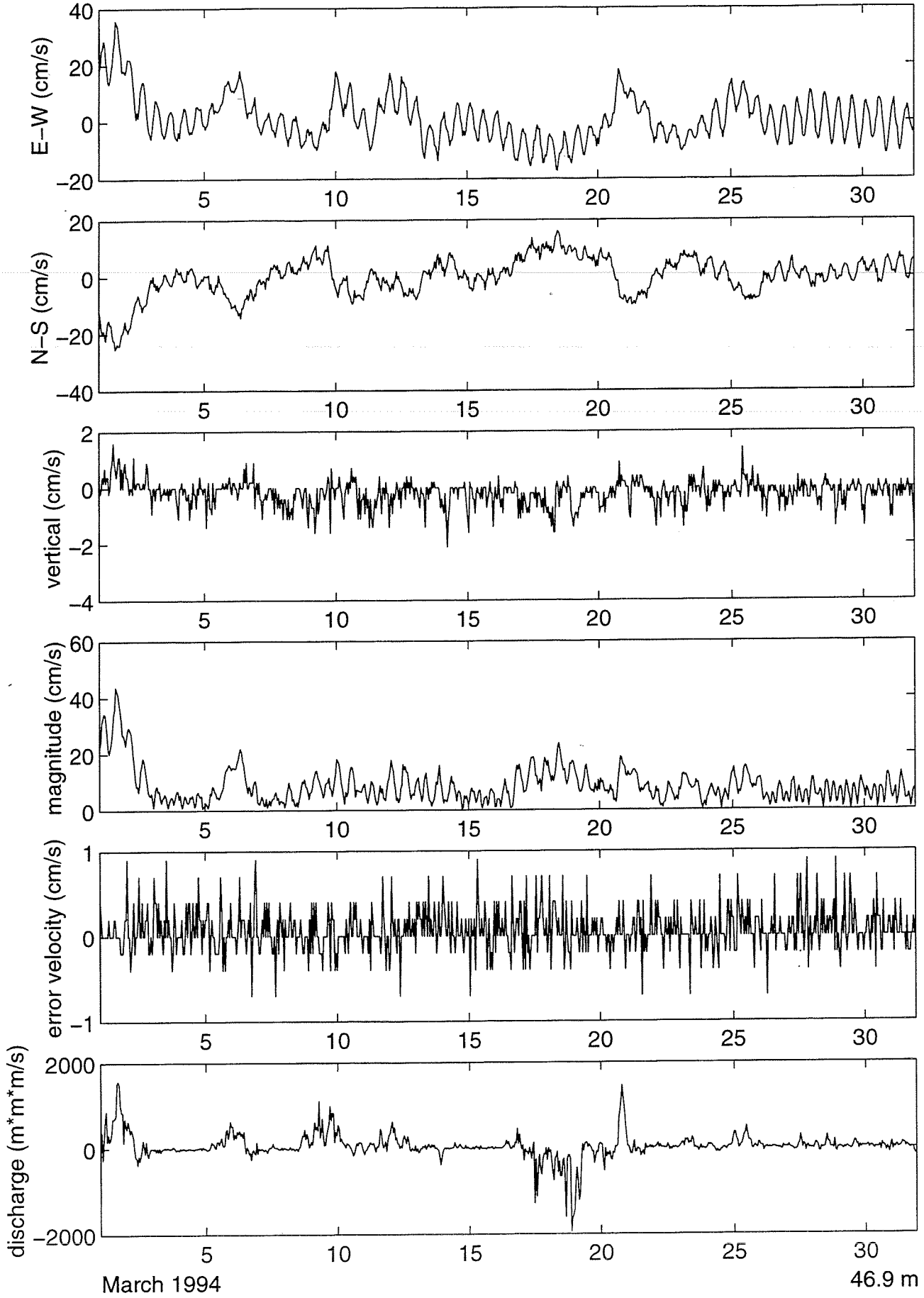
E–W (cm/s)
N–S (cm/s)
vertical (cm/s)
magnitude (cm/s)
error velocity (cm/s)
discharge (m*m*m/s)
March 1994
46.9 m

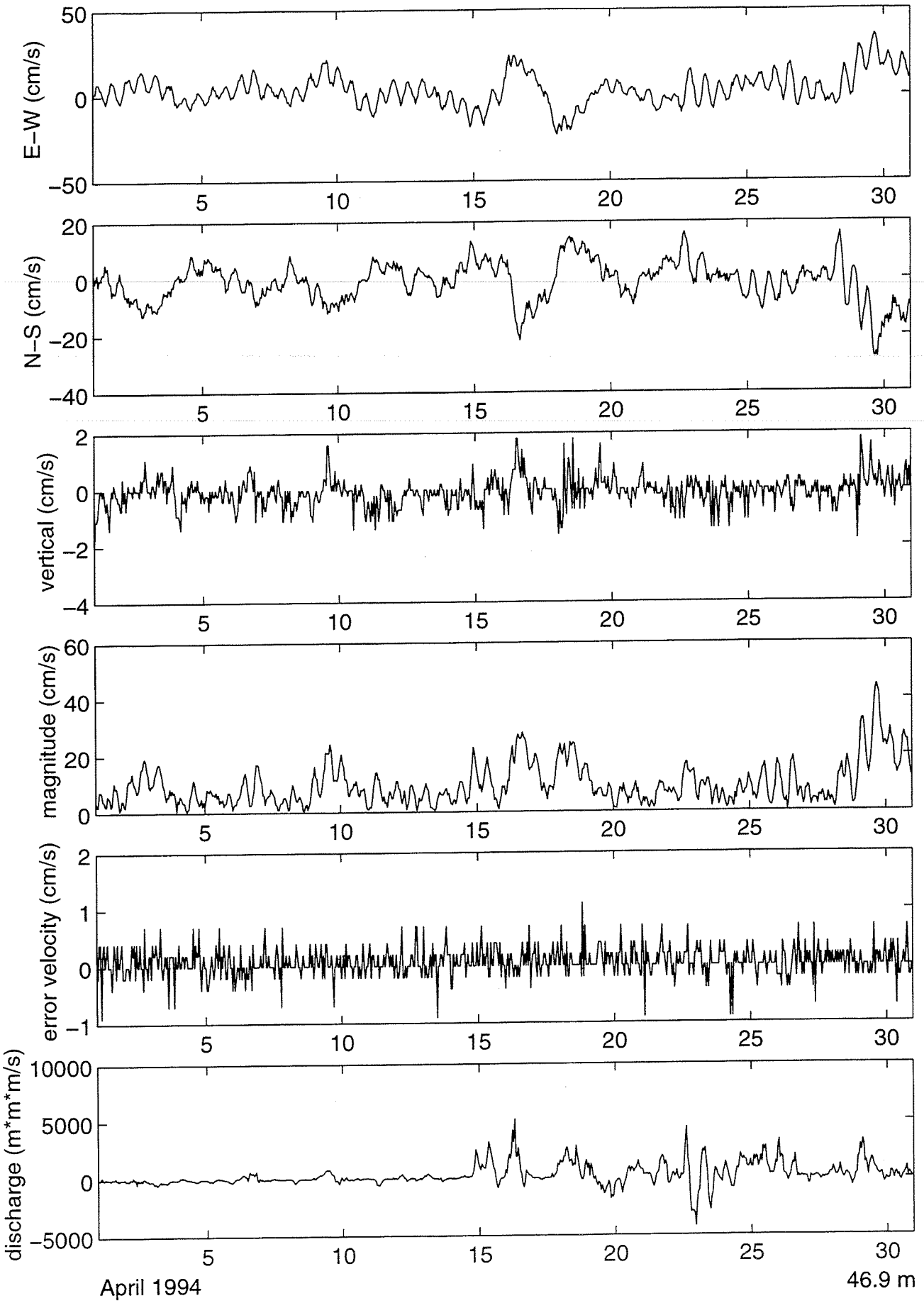
E–W (cm/s)
50
0
–50
N–S (cm/s)
20
0
–20
–40
vertical (cm/s)
2
0
–2
–4
magnitude (cm/s)
60
40
20
0
error velocity (cm/s)
2
1
0
–1
discharge (m*m*m/s)
10000
5000
0
–5000
5
10
15
20
25
30
April 1994
46.9 m

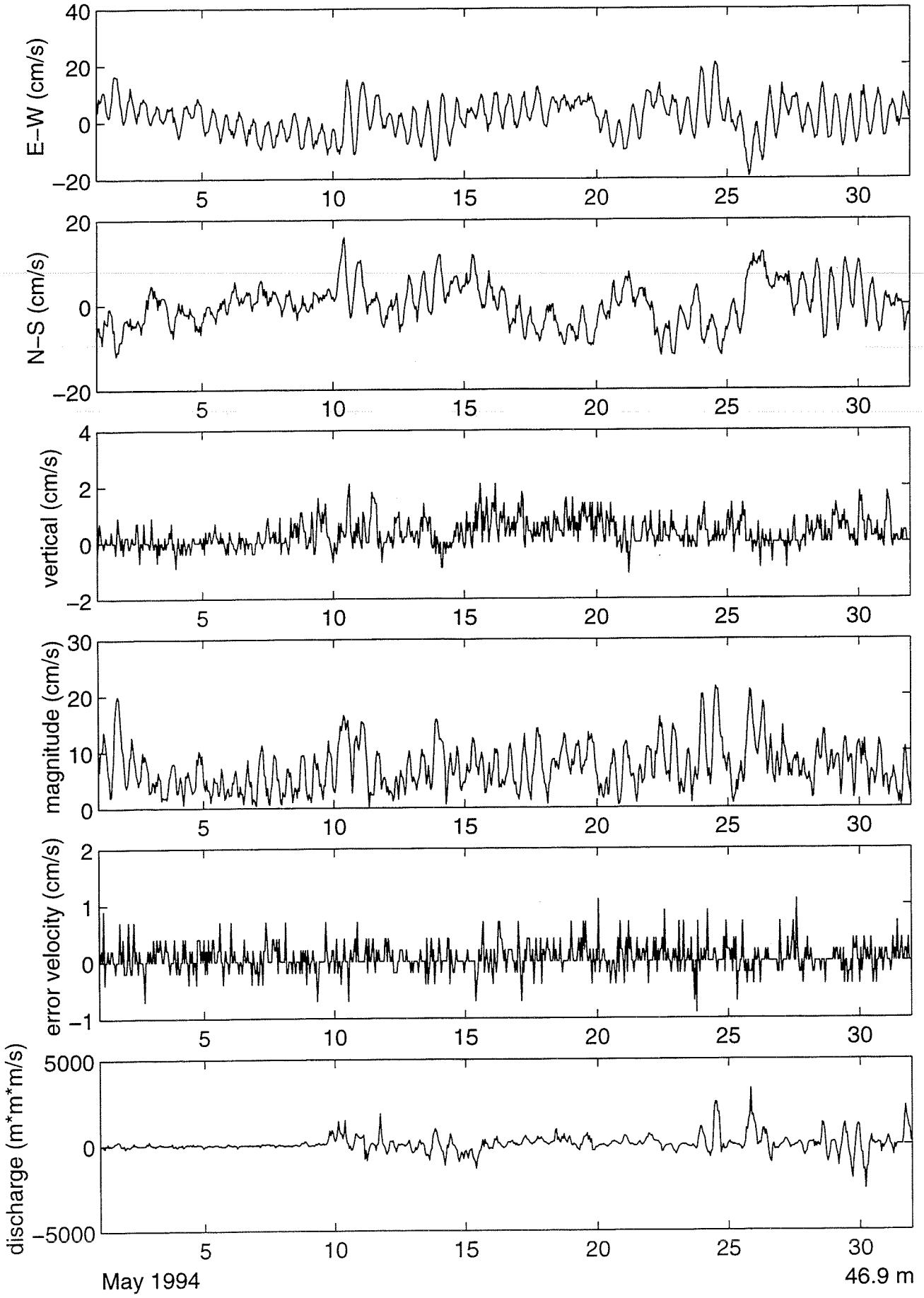
E–W (cm/s)
N–S (cm/s)
vertical (cm/s)
magnitude (cm/s)
error velocity (cm/s)
discharge (m*m*m/s)
May 1994
46.9 m

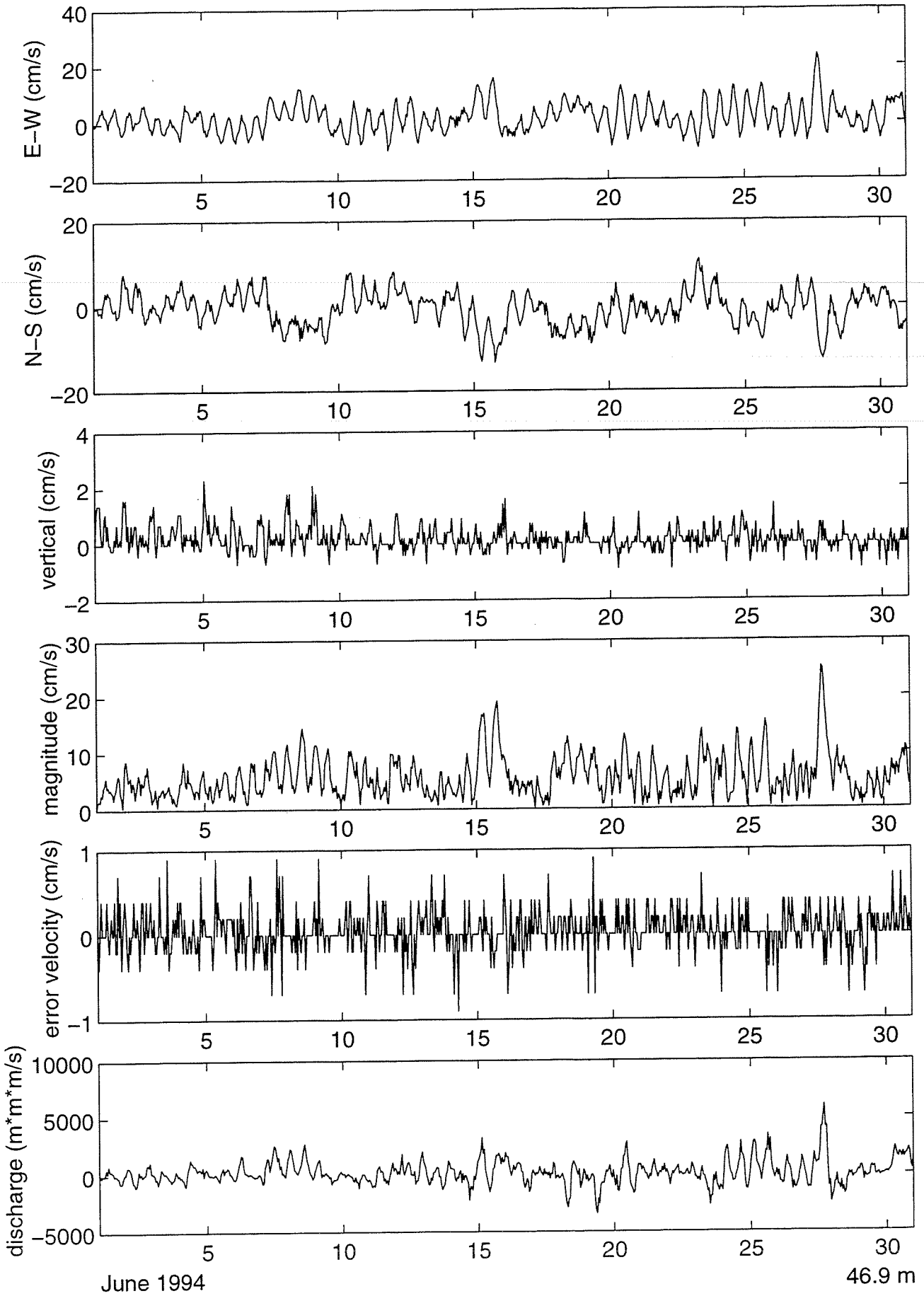
E–W (cm/s)
N–S (cm/s)
vertical (cm/s)
magnitude (cm/s)
error velocity (cm/s)
discharge (m*m*m/s)
June 1994
46.9 m

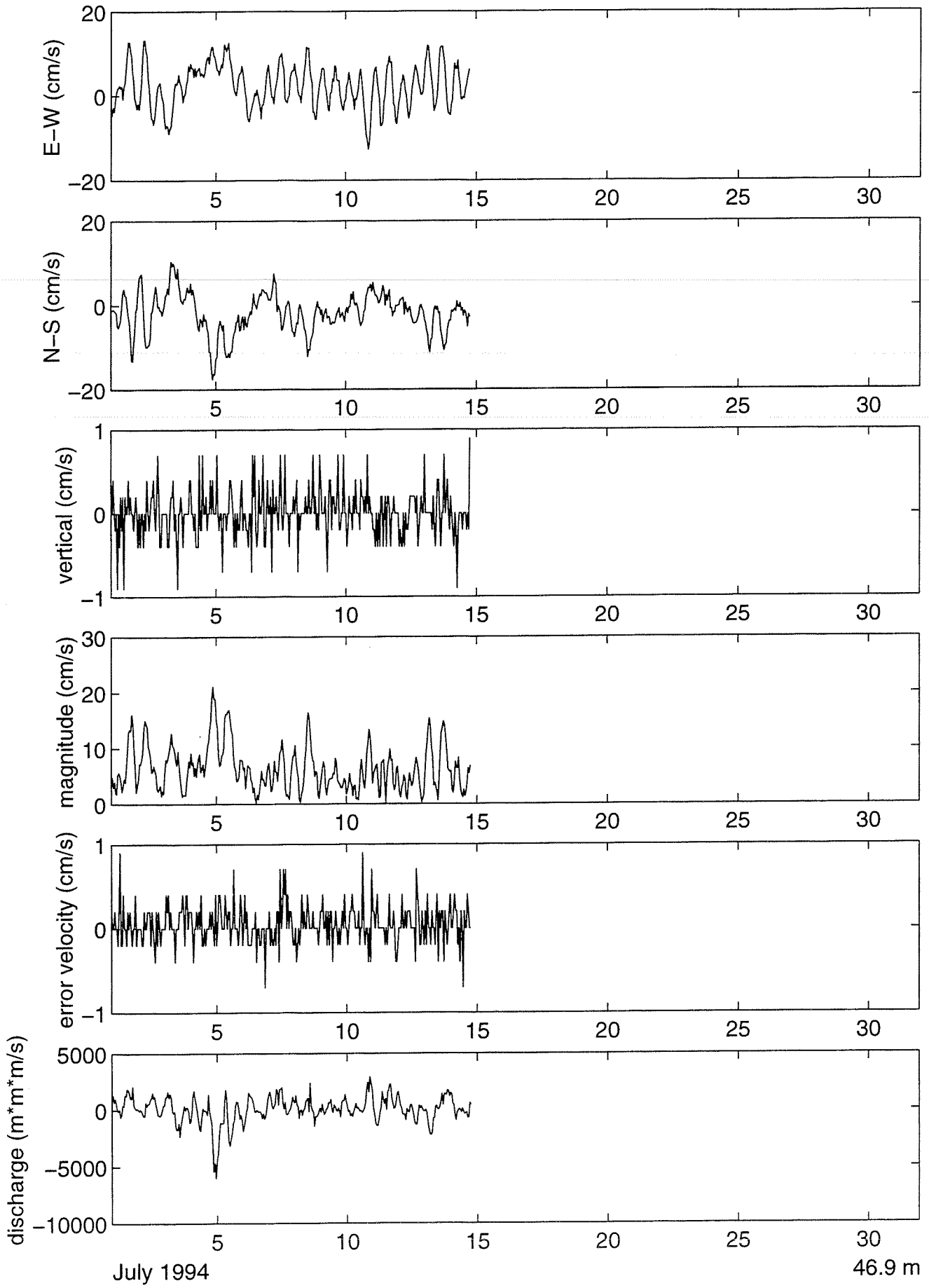
E–W (cm/s)
N–S (cm/s)
vertical (cm/s)
magnitude (cm/s)
error velocity (cm/s)
discharge (m*m*m/s)
July 1994
46.9 m

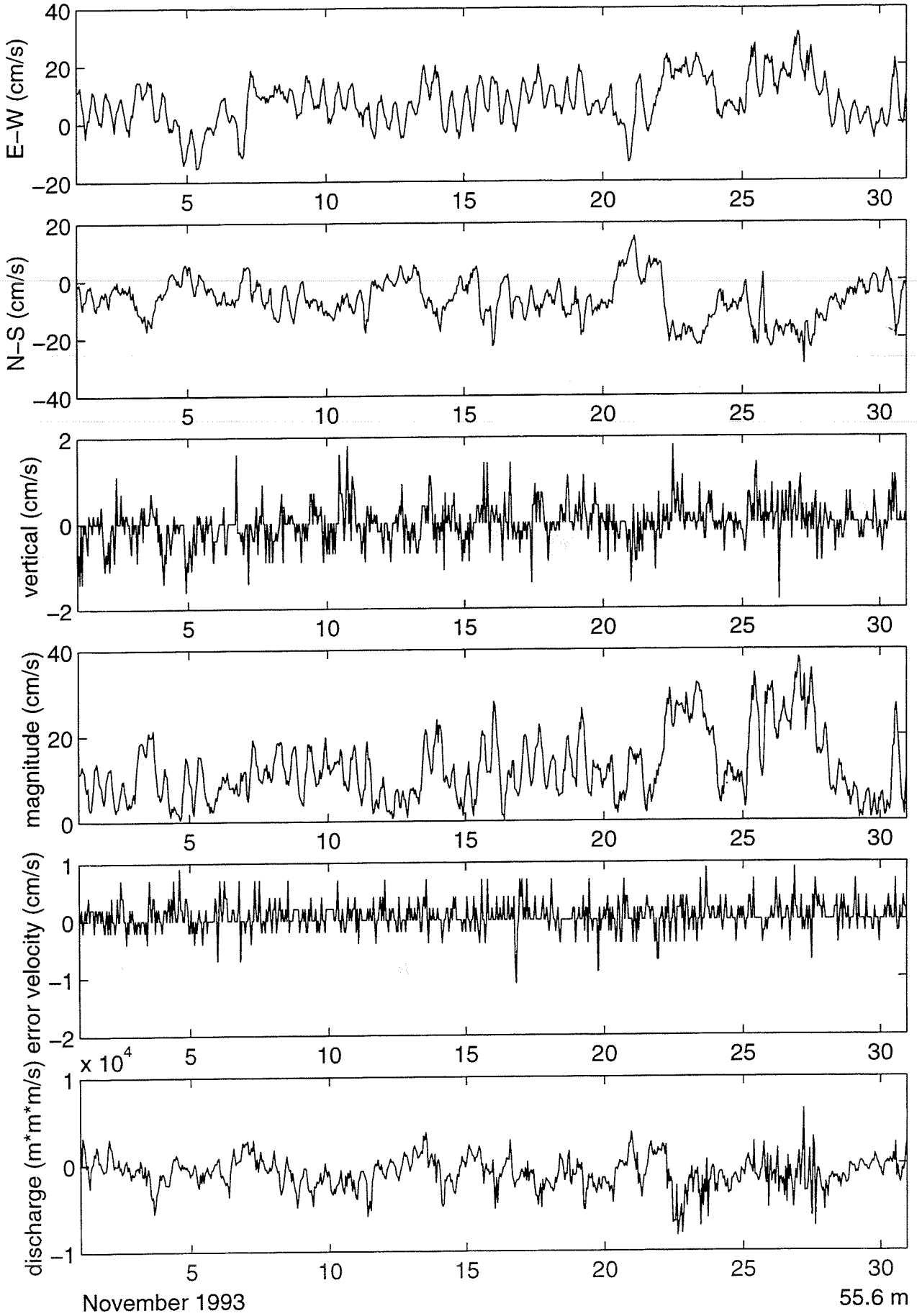
E–W (cm/s)
N–S (cm/s)
vertical (cm/s)
magnitude (cm/s)
error velocity (cm/s)
discharge (m*m*m/s)
x 10^4
November 1993
55.6 m

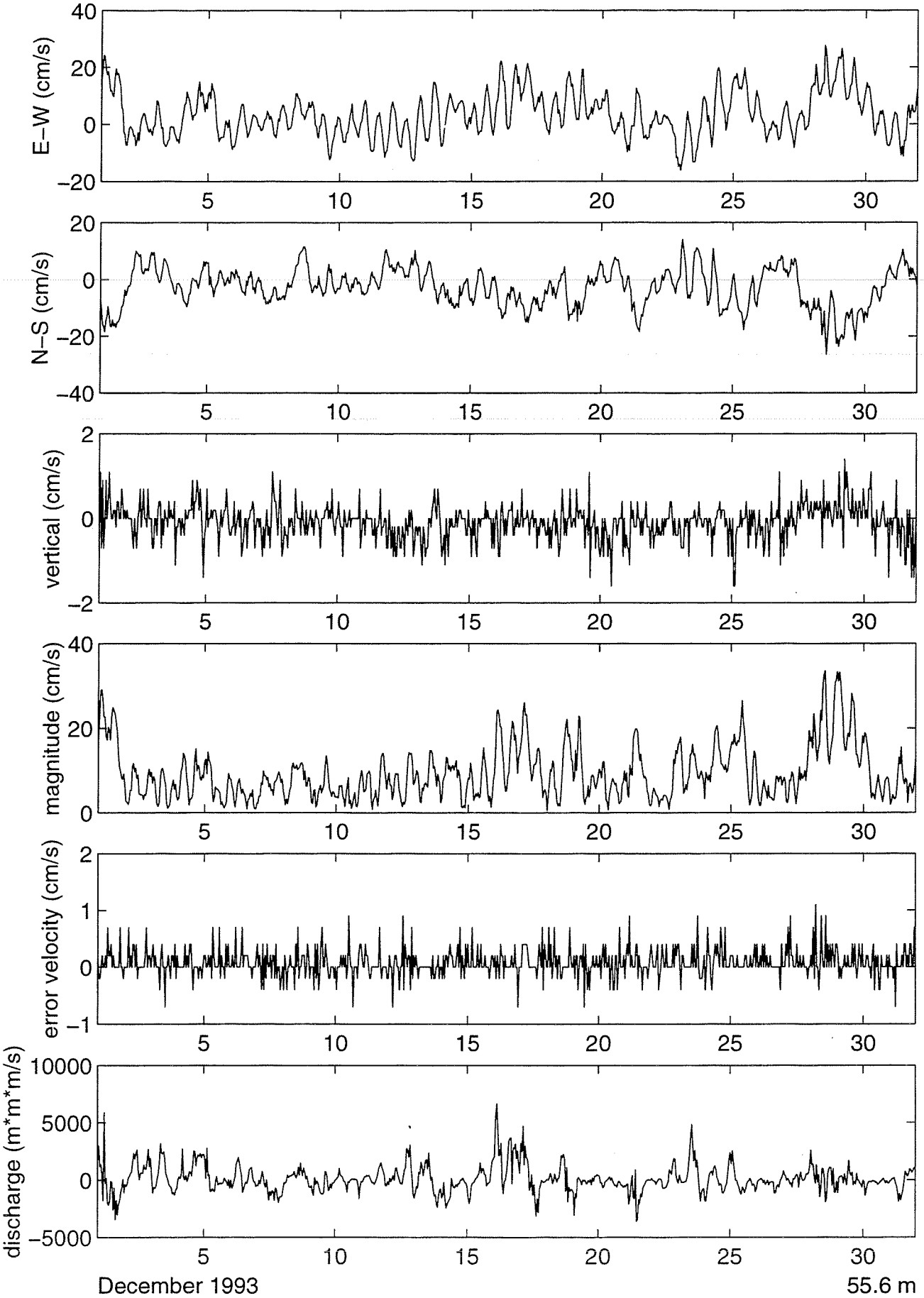
E–W (cm/s)
N–S (cm/s)
vertical (cm/s)
magnitude (cm/s)
error velocity (cm/s)
discharge (m*m*m/s)
December 1993
55.6 m

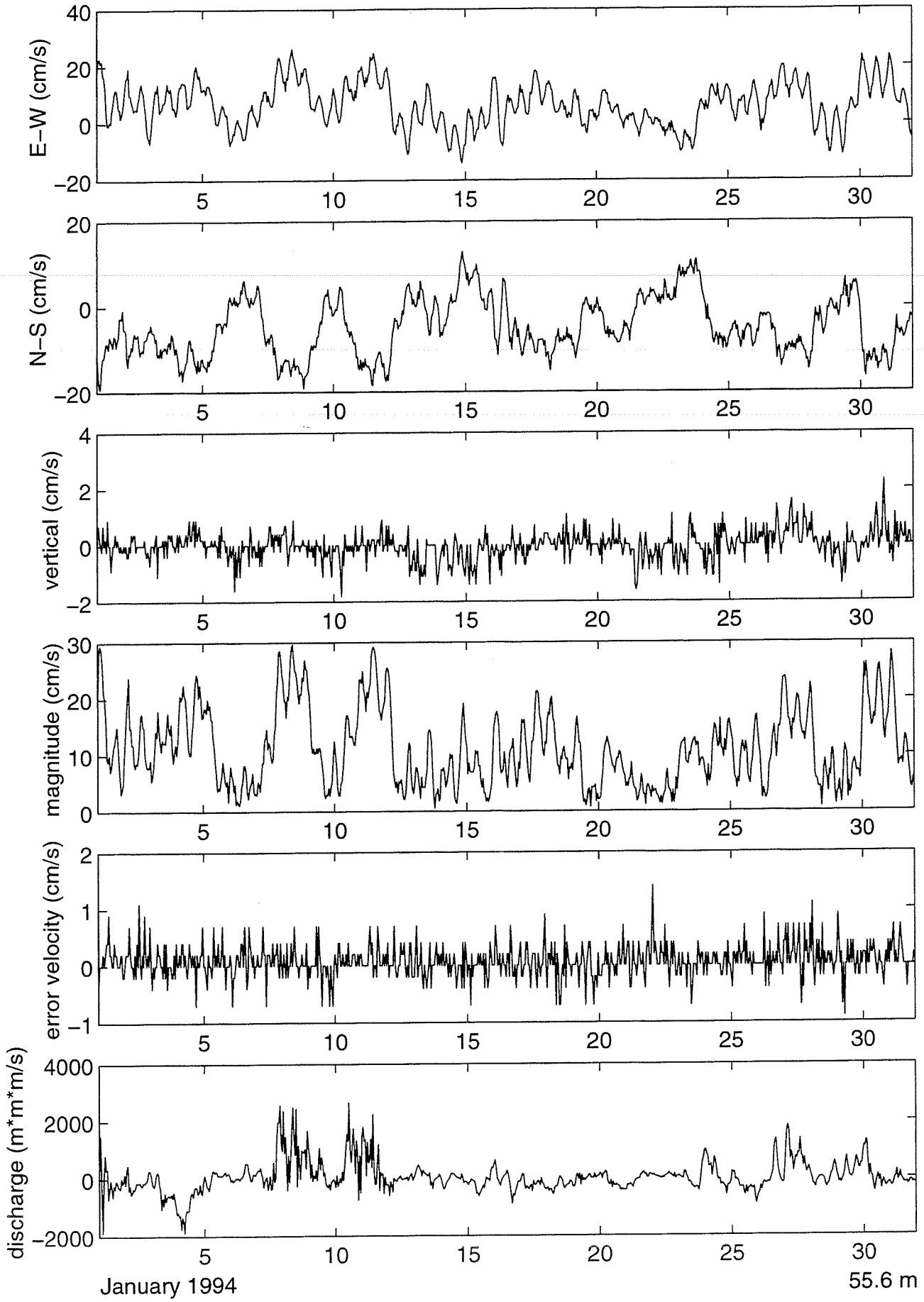
E–W (cm/s)
N–S (cm/s)
vertical (cm/s)
magnitude (cm/s)
error velocity (cm/s)
discharge (m*m*m/s)
January 1994
55.6 m

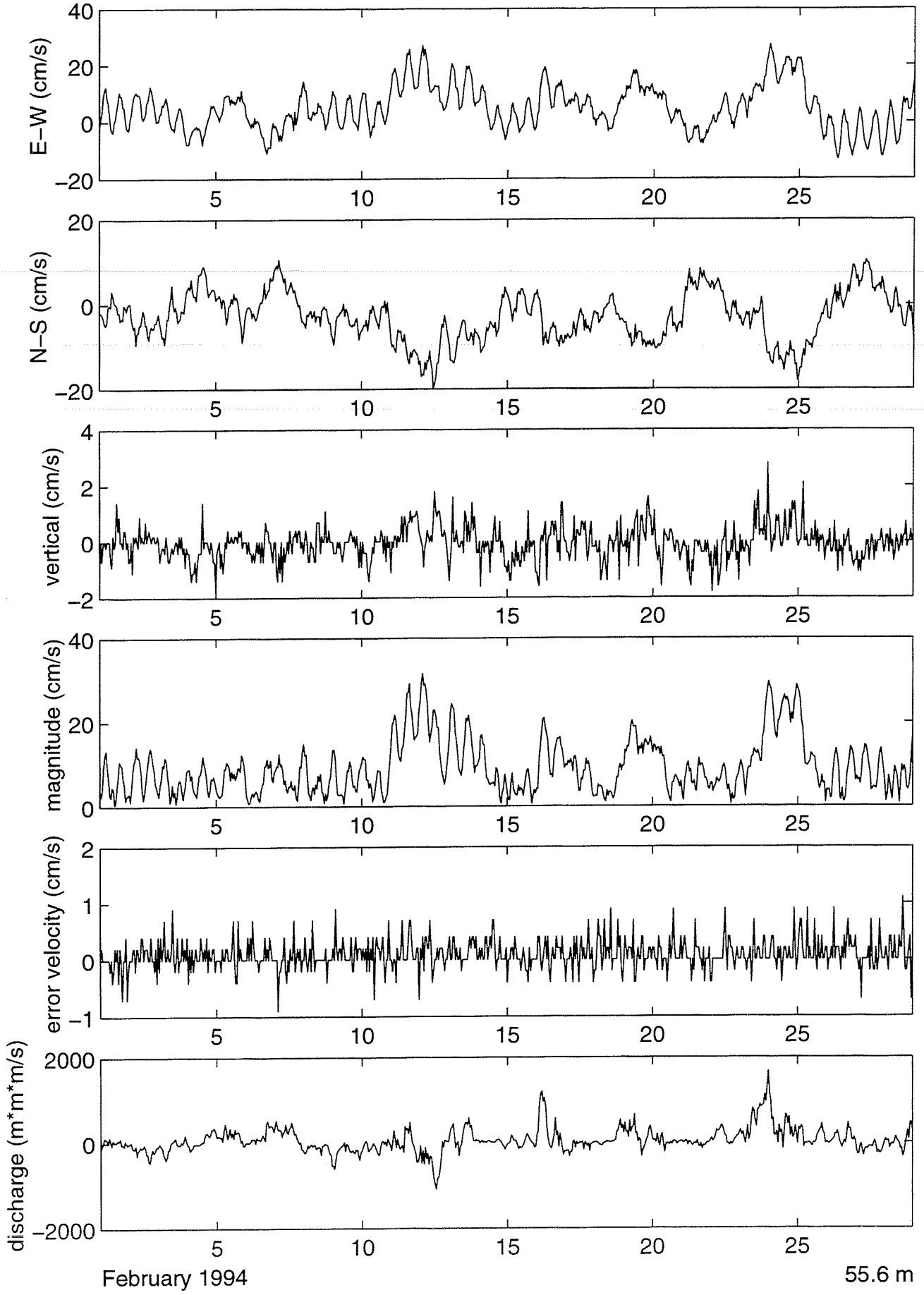
E–W (cm/s)
N–S (cm/s)
vertical (cm/s)
magnitude (cm/s)
error velocity (cm/s)
discharge (m*m*m/s)
February 1994
55.6 m

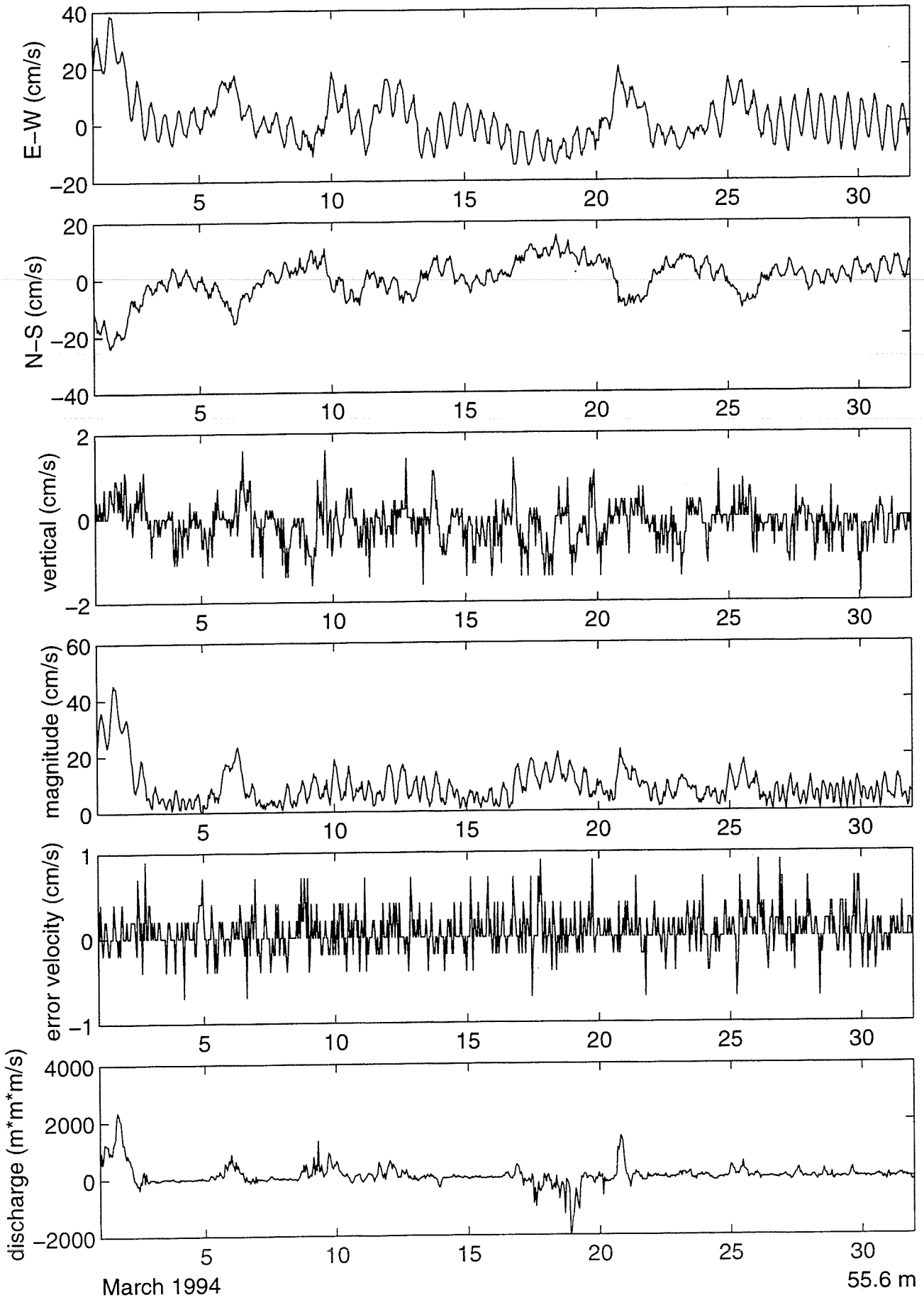
E–W (cm/s)
N–S (cm/s)
vertical (cm/s)
magnitude (cm/s)
error velocity (cm/s)
discharge (m*m*m/s)
March 1994
55.6 m

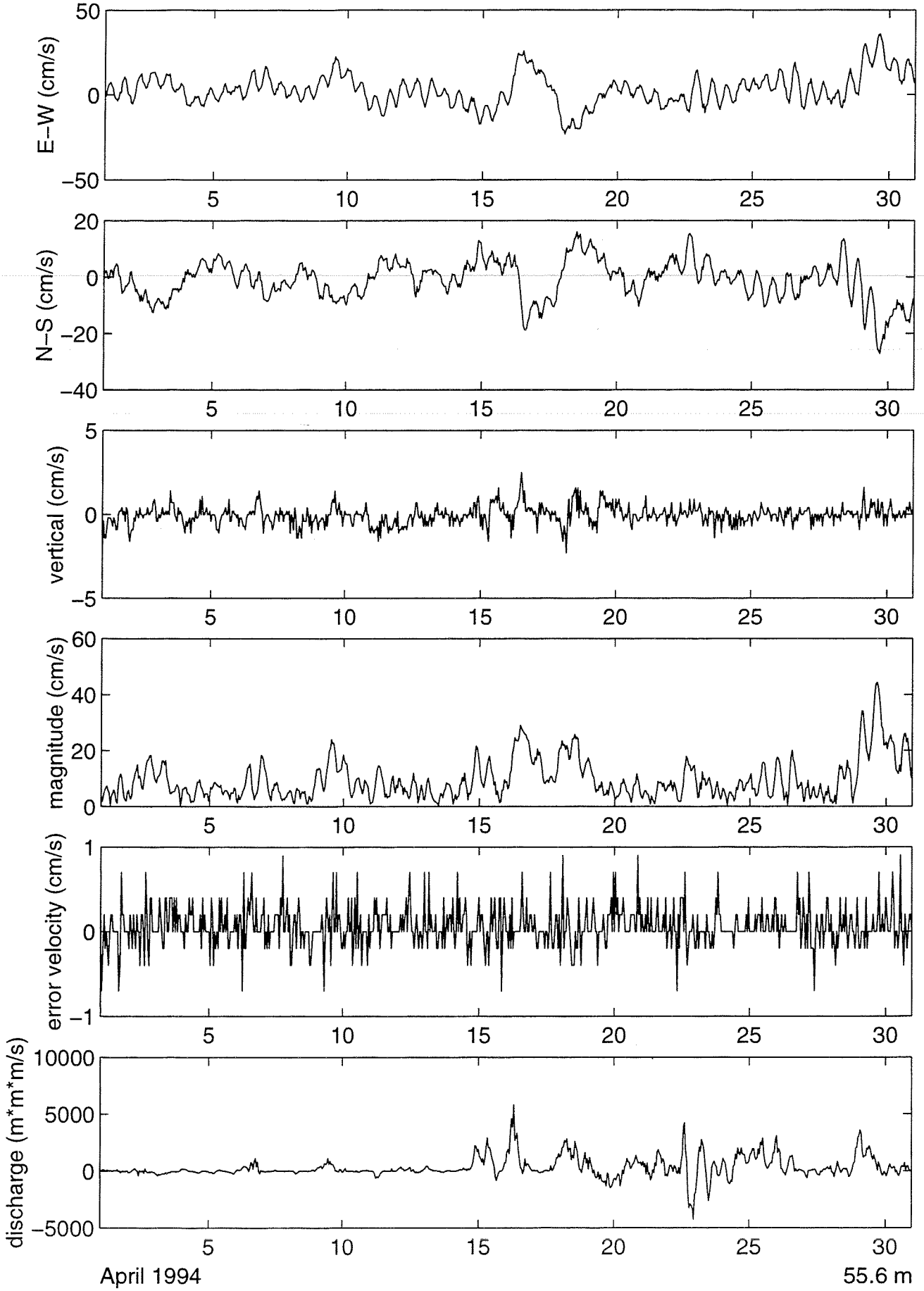
E–W (cm/s)
N–S (cm/s)
vertical (cm/s)
magnitude (cm/s)
error velocity (cm/s)
discharge (m*m*m/s)
April 1994
55.6 m

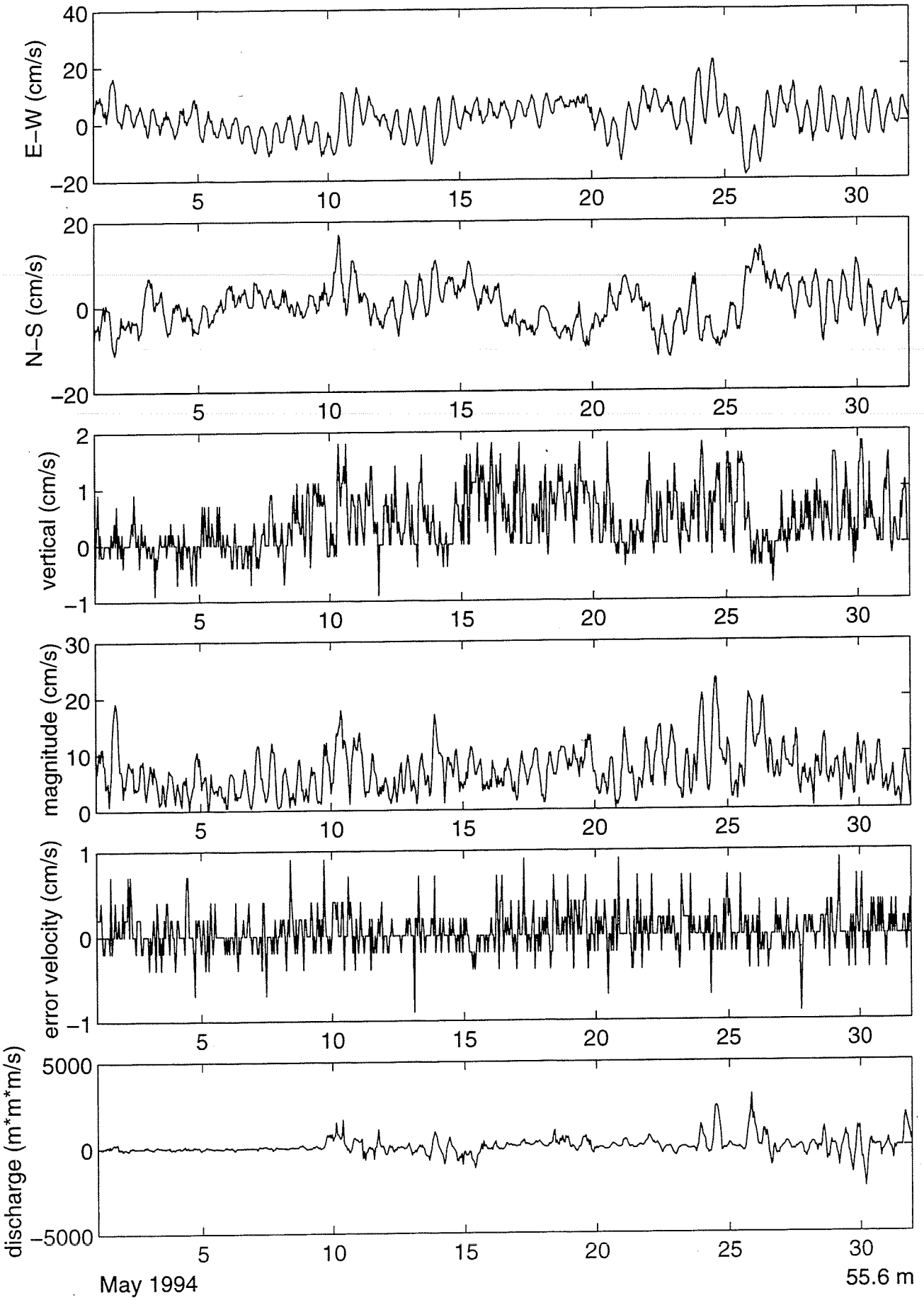
E–W (cm/s)
N–S (cm/s)
vertical (cm/s)
magnitude (cm/s)
error velocity (cm/s)
discharge (m*m*m/s)
May 1994
55.6 m

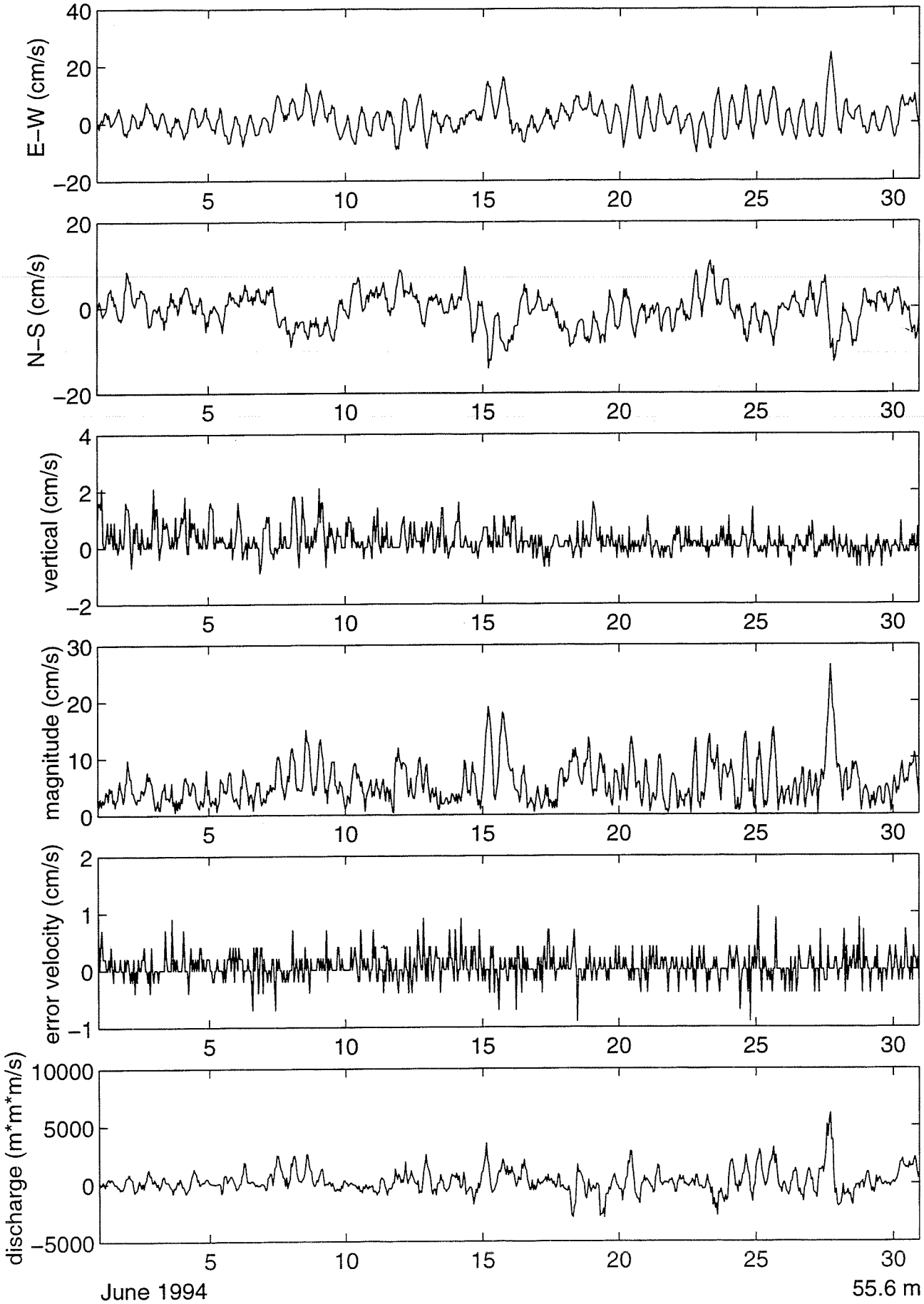
E–W (cm/s)
N–S (cm/s)
vertical (cm/s)
magnitude (cm/s)
error velocity (cm/s)
discharge (m*m*m/s)
June 1994
55.6 m

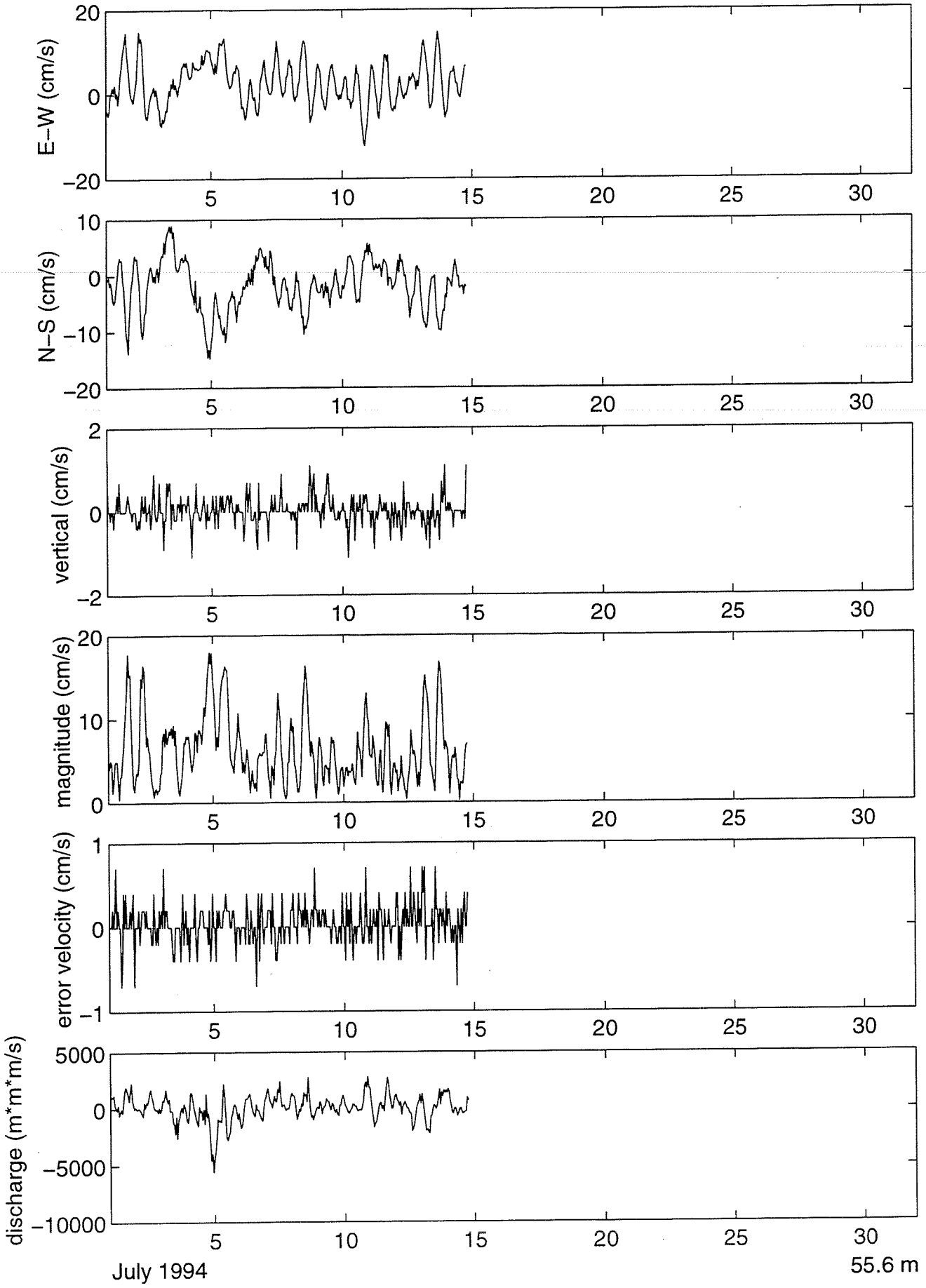
E–W (cm/s)
N–S (cm/s)
vertical (cm/s)
magnitude (cm/s)
error velocity (cm/s)
discharge (m*m*m/s)
July 1994
55.6 m

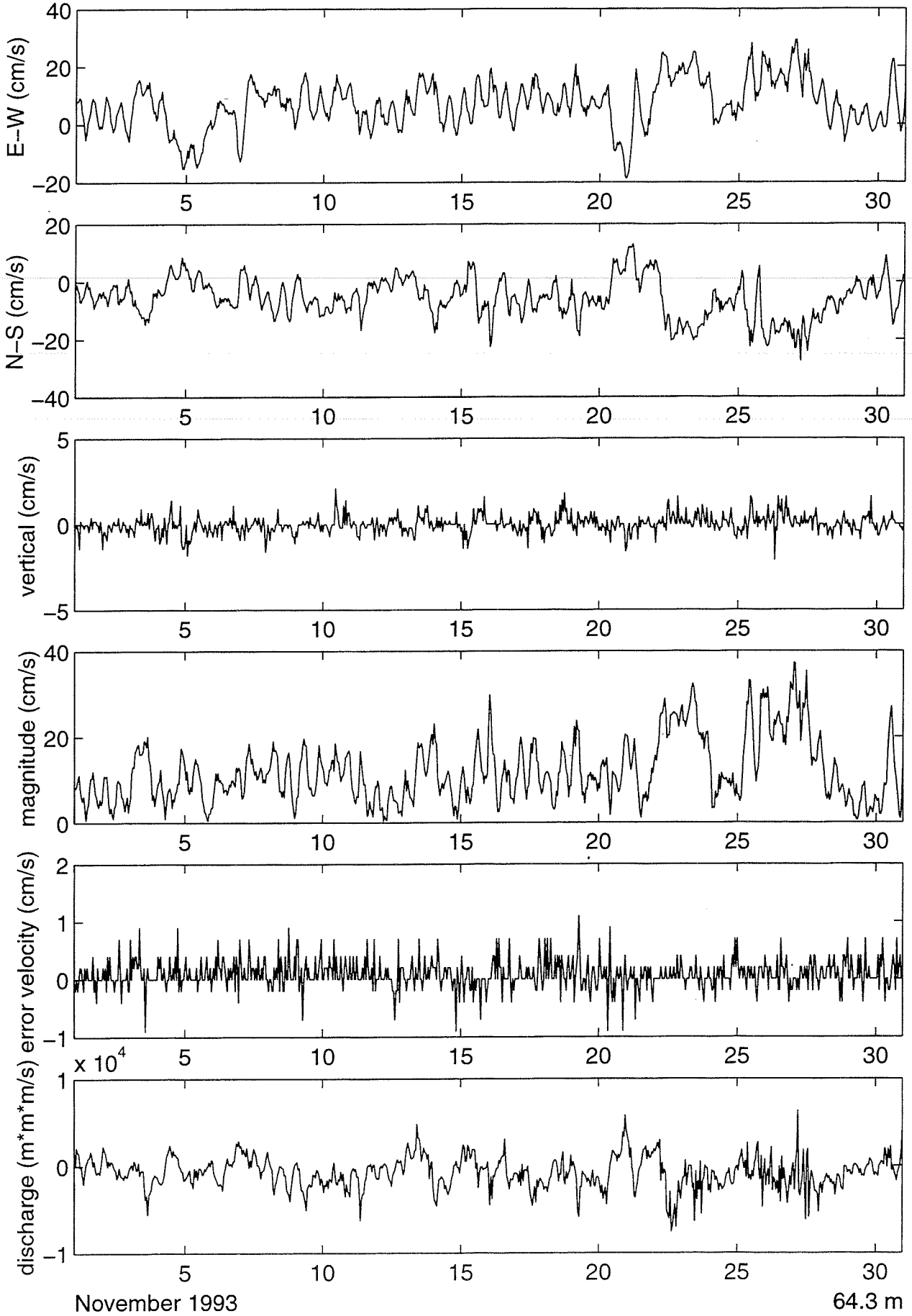
E–W (cm/s)
N–S (cm/s)
vertical (cm/s)
magnitude (cm/s)
error velocity (cm/s)
discharge (m*m*m/s)
x 10^4
November 1993
64.3 m

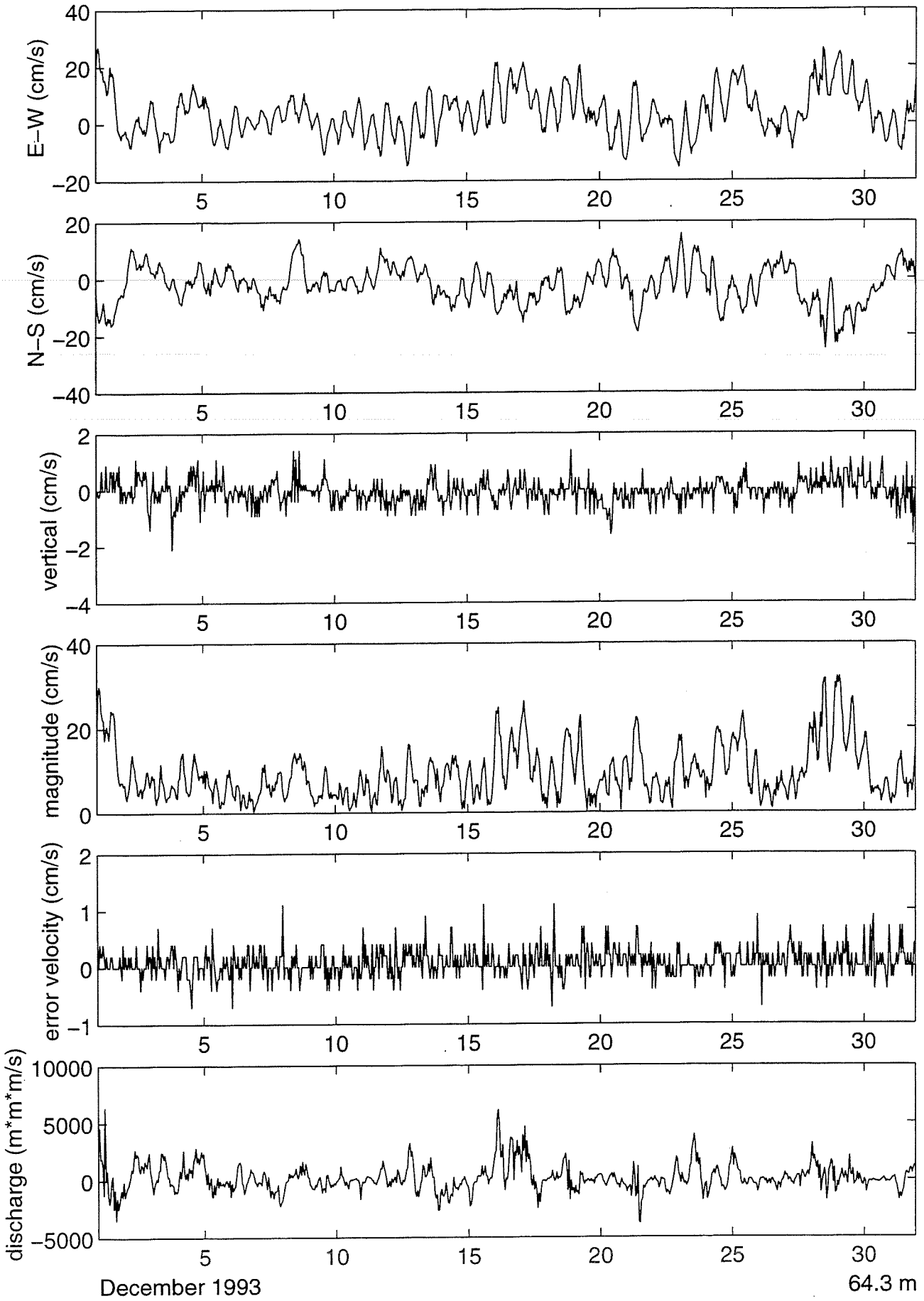
E–W (cm/s)
N–S (cm/s)
vertical (cm/s)
magnitude (cm/s)
error velocity (cm/s)
discharge (m*m*m/s)
December 1993
64.3 m

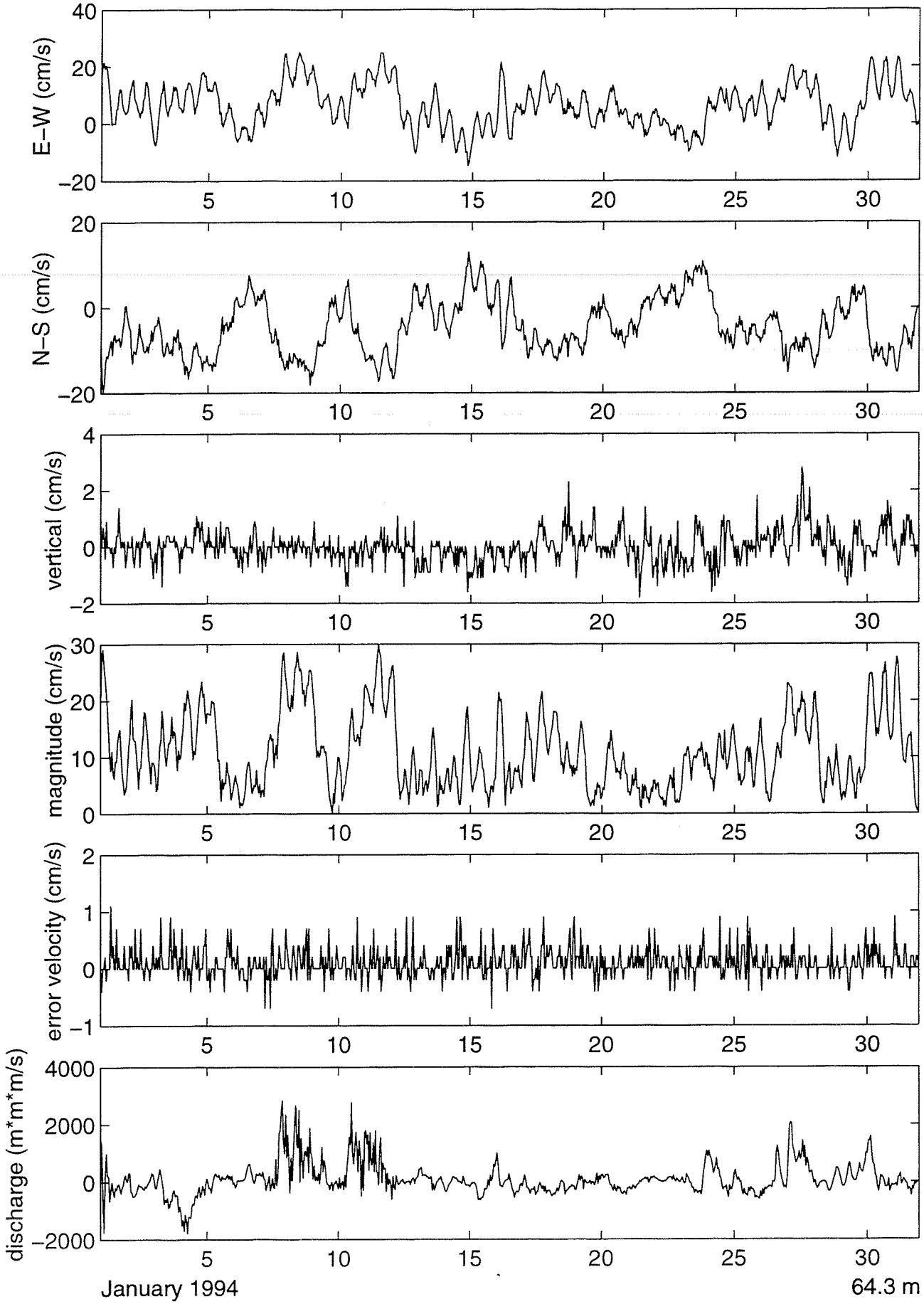
E–W (cm/s)
N–S (cm/s)
vertical (cm/s)
magnitude (cm/s)
error velocity (cm/s)
discharge (m*m*m/s)
January 1994
64.3 m

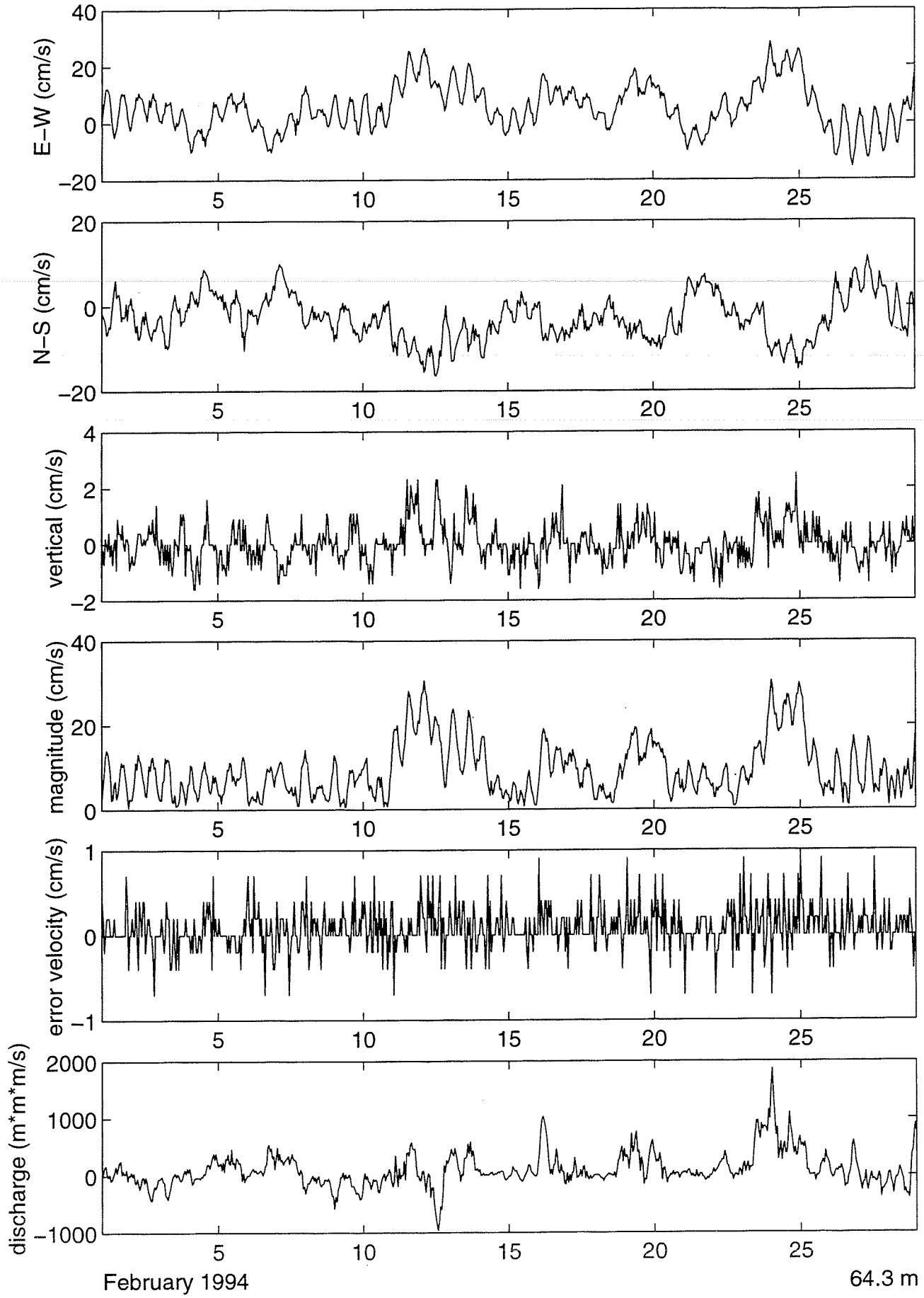
E–W (cm/s)
N–S (cm/s)
vertical (cm/s)
magnitude (cm/s)
error velocity (cm/s)
discharge (m*m*m/s)
February 1994
64.3 m

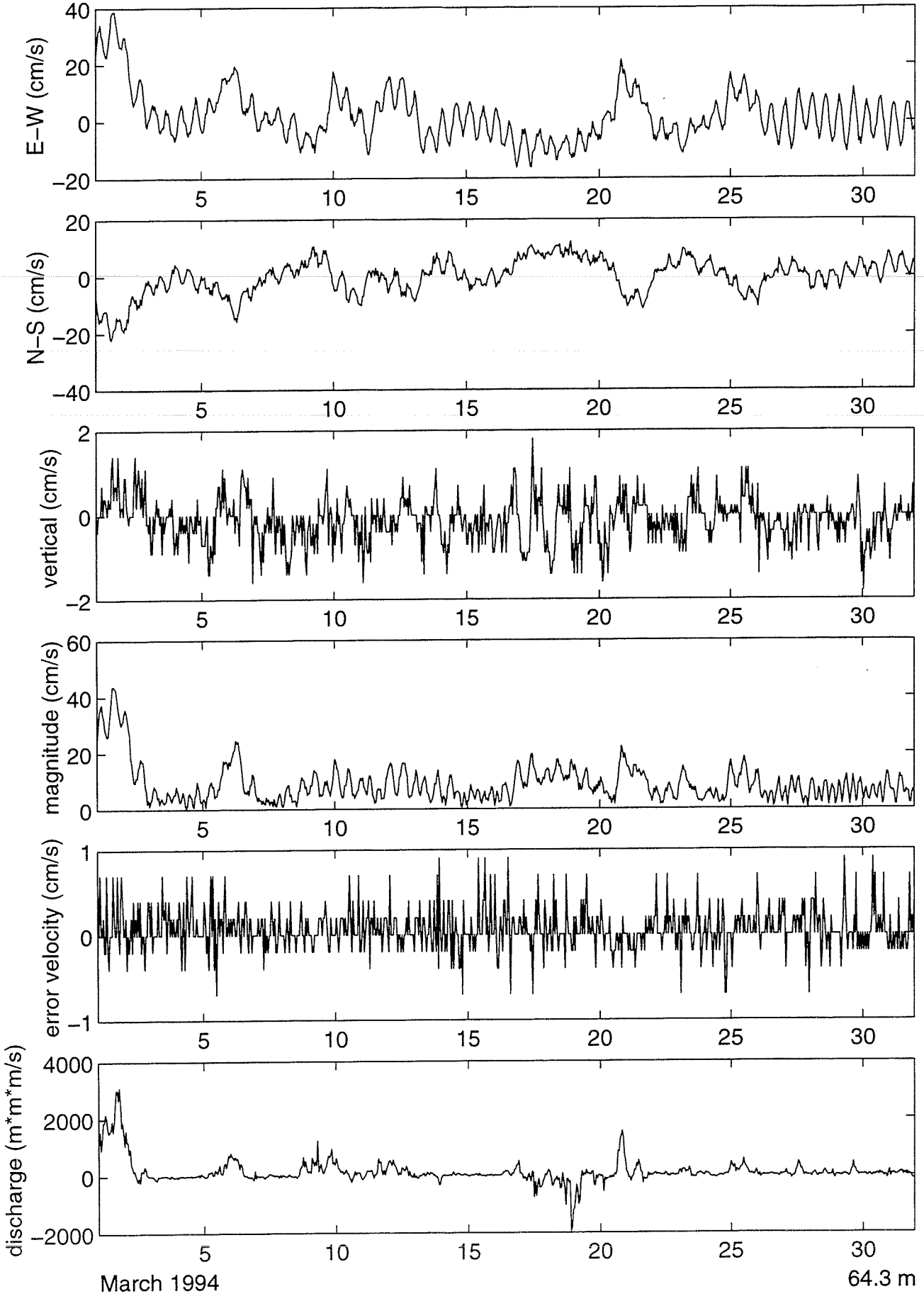
E–W (cm/s)
N–S (cm/s)
vertical (cm/s)
magnitude (cm/s)
error velocity (cm/s)
discharge (m*m*m/s)
March 1994
64.3 m

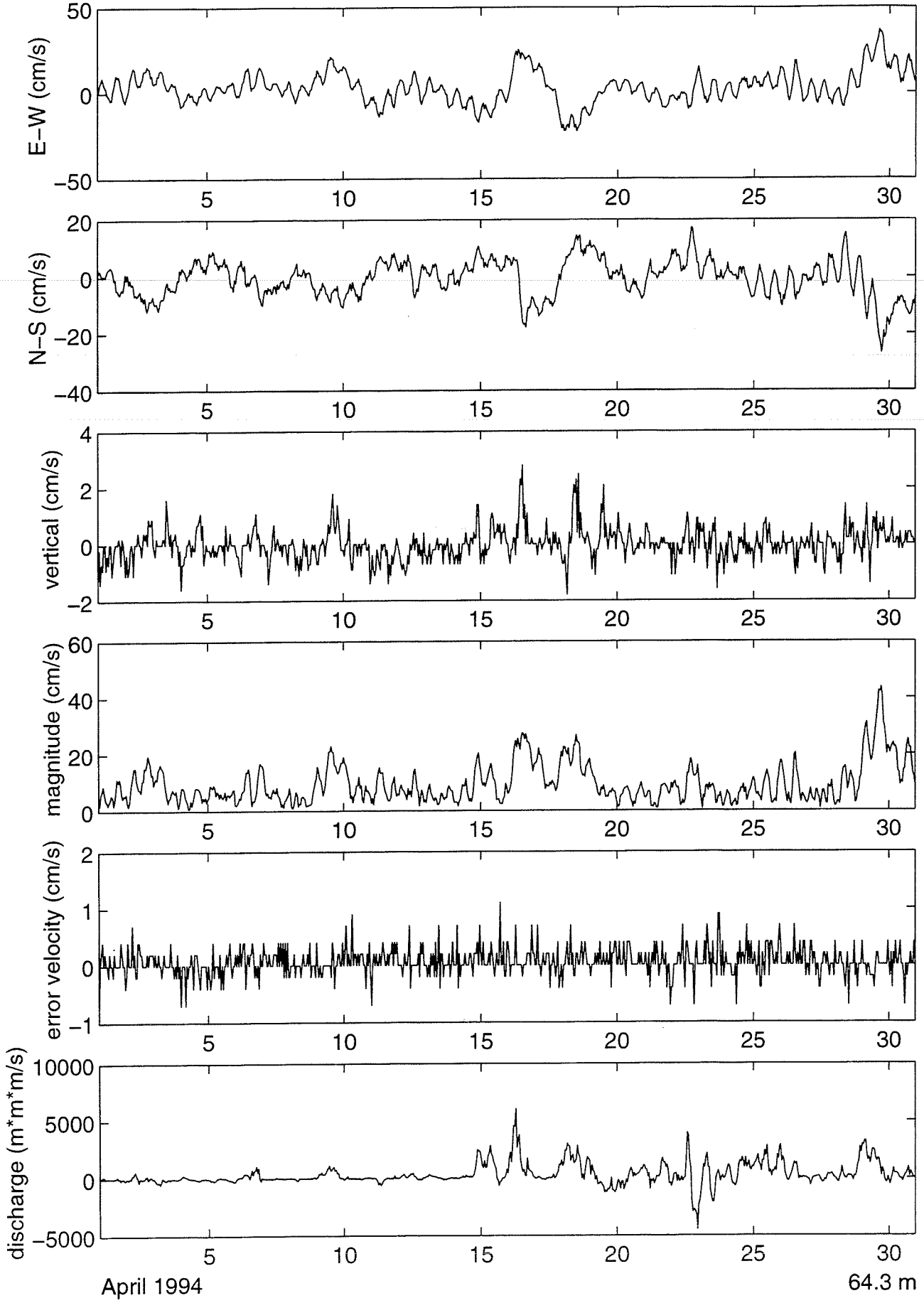
E–W (cm/s)
50
0
−50
N–S (cm/s)
20
0
−20
−40
vertical (cm/s)
4
2
0
−2
magnitude (cm/s)
60
40
20
0
error velocity (cm/s)
2
1
0
−1
discharge (m*m*m/s)
10000
5000
0
−5000
5
10
15
20
25
30
April 1994
64.3 m

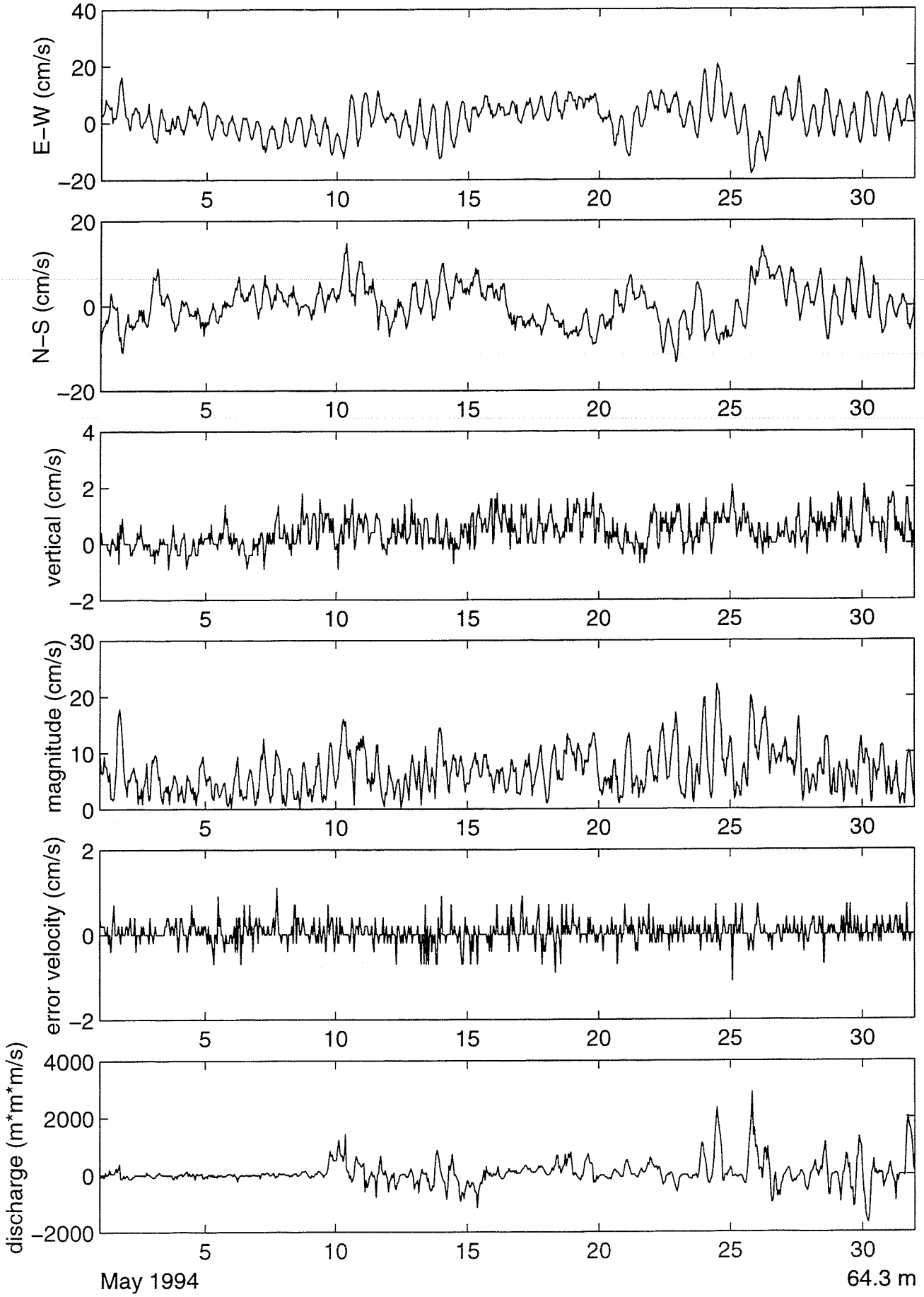
E–W (cm/s)
N–S (cm/s)
vertical (cm/s)
magnitude (cm/s)
error velocity (cm/s)
discharge (m*m*m/s)
May 1994
64.3 m

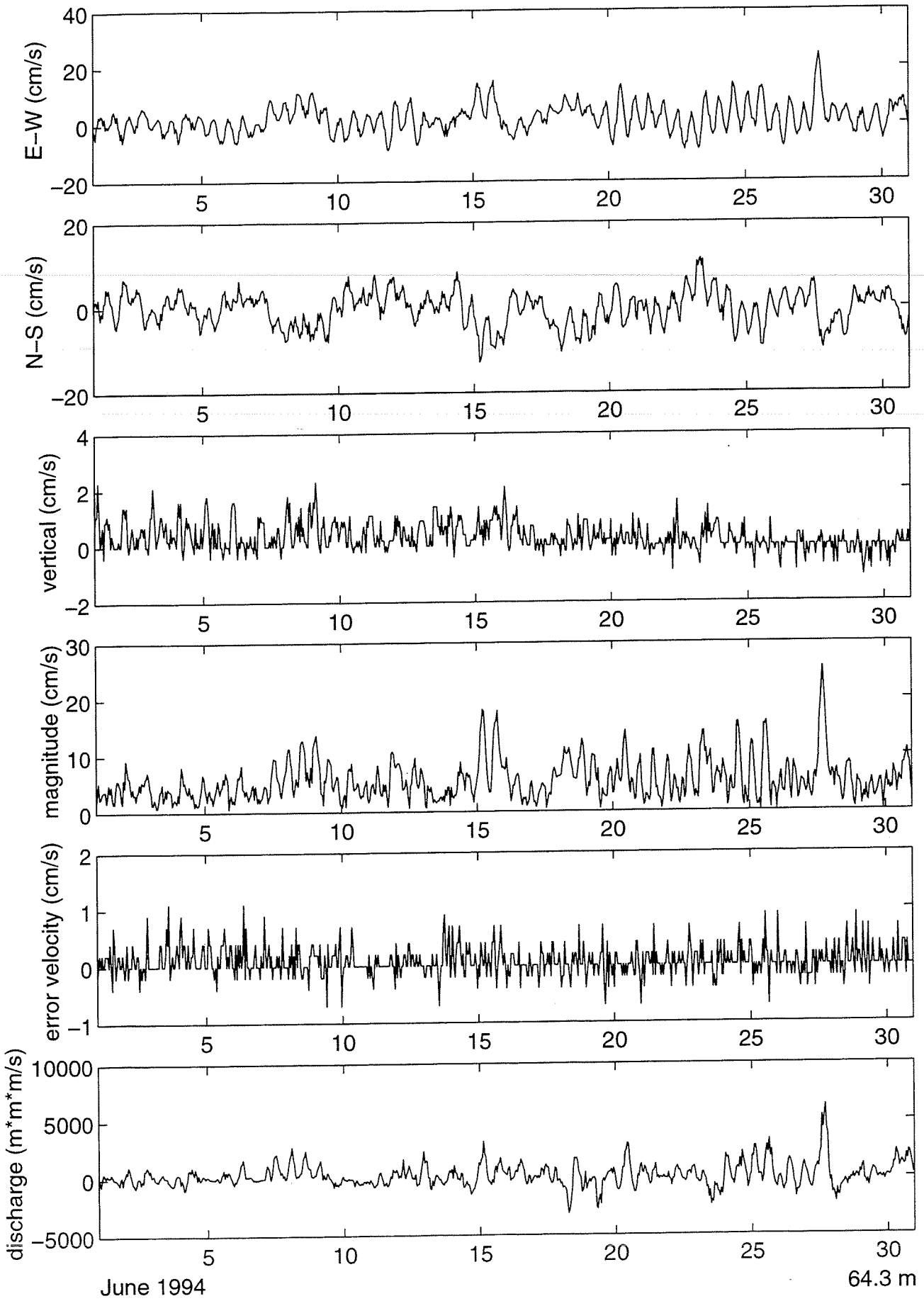
E–W (cm/s)
N–S (cm/s)
vertical (cm/s)
magnitude (cm/s)
error velocity (cm/s)
discharge (m*m*m/s)
June 1994
64.3 m

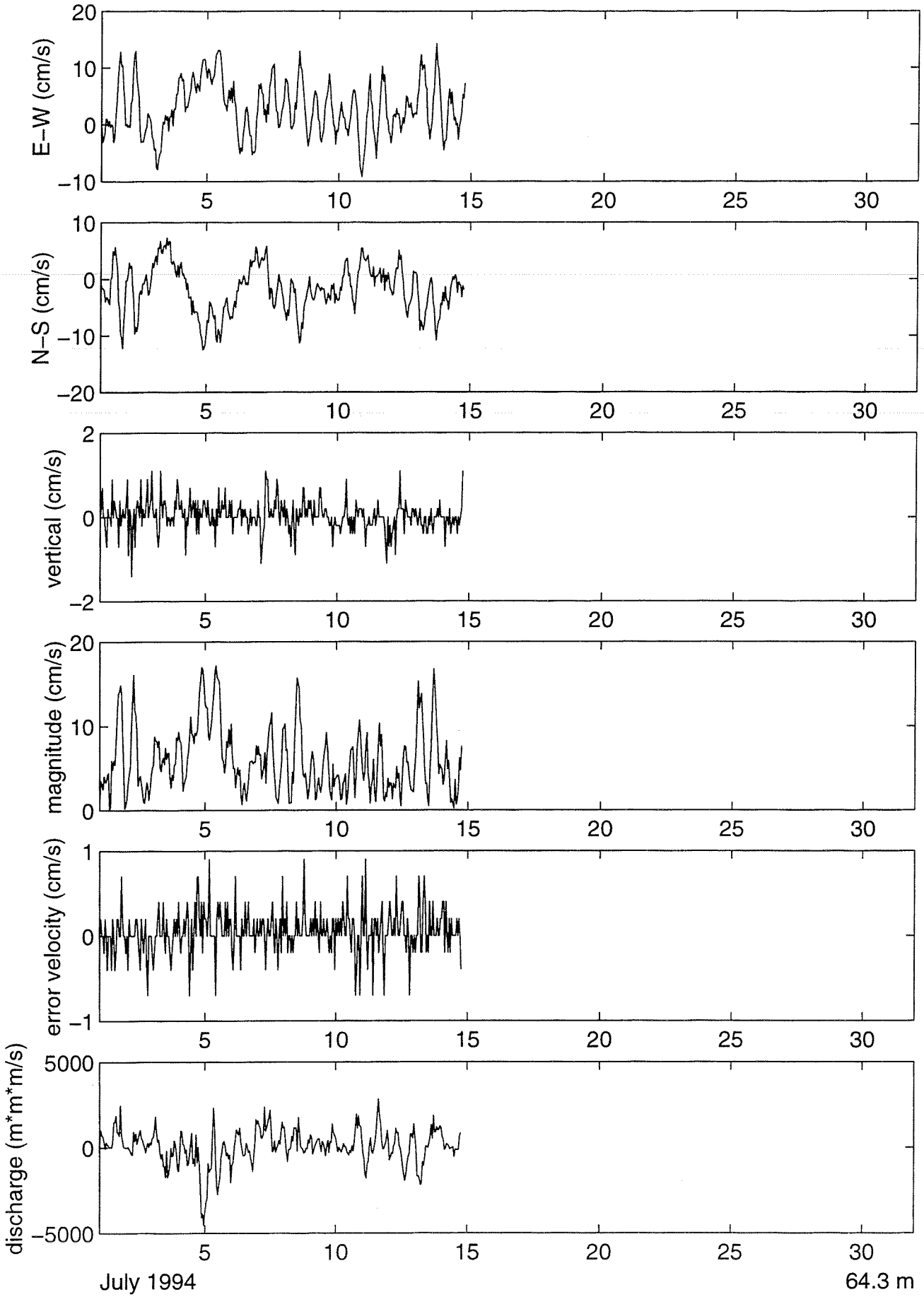
E–W (cm/s)
N–S (cm/s)
vertical (cm/s)
magnitude (cm/s)
error velocity (cm/s)
discharge (m*m*m/s)
July 1994
64.3 m

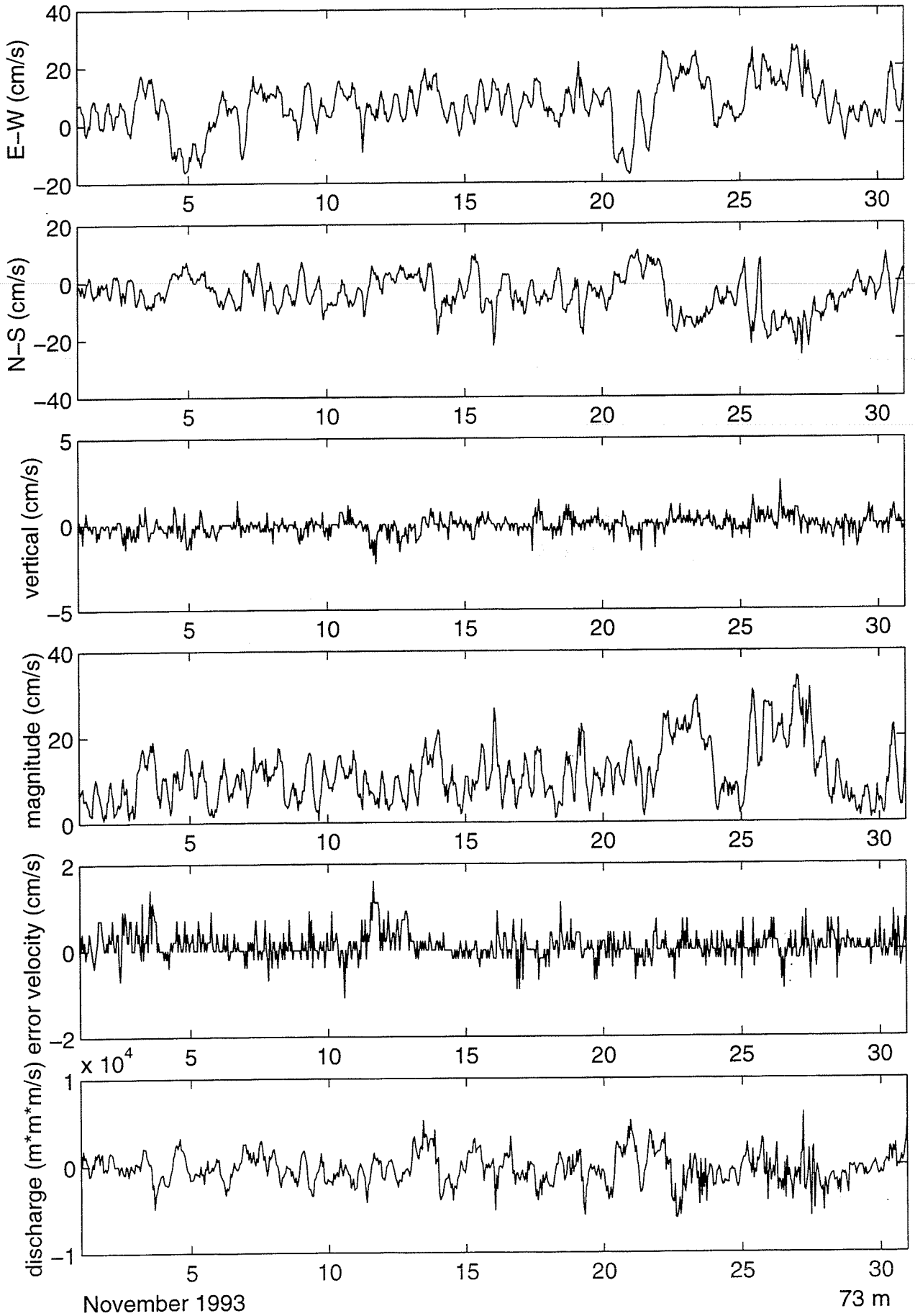
E–W (cm/s)
N–S (cm/s)
vertical (cm/s)
magnitude (cm/s)
error velocity (cm/s)
discharge (m*m*m/s)
x 10^4
November 1993
73 m

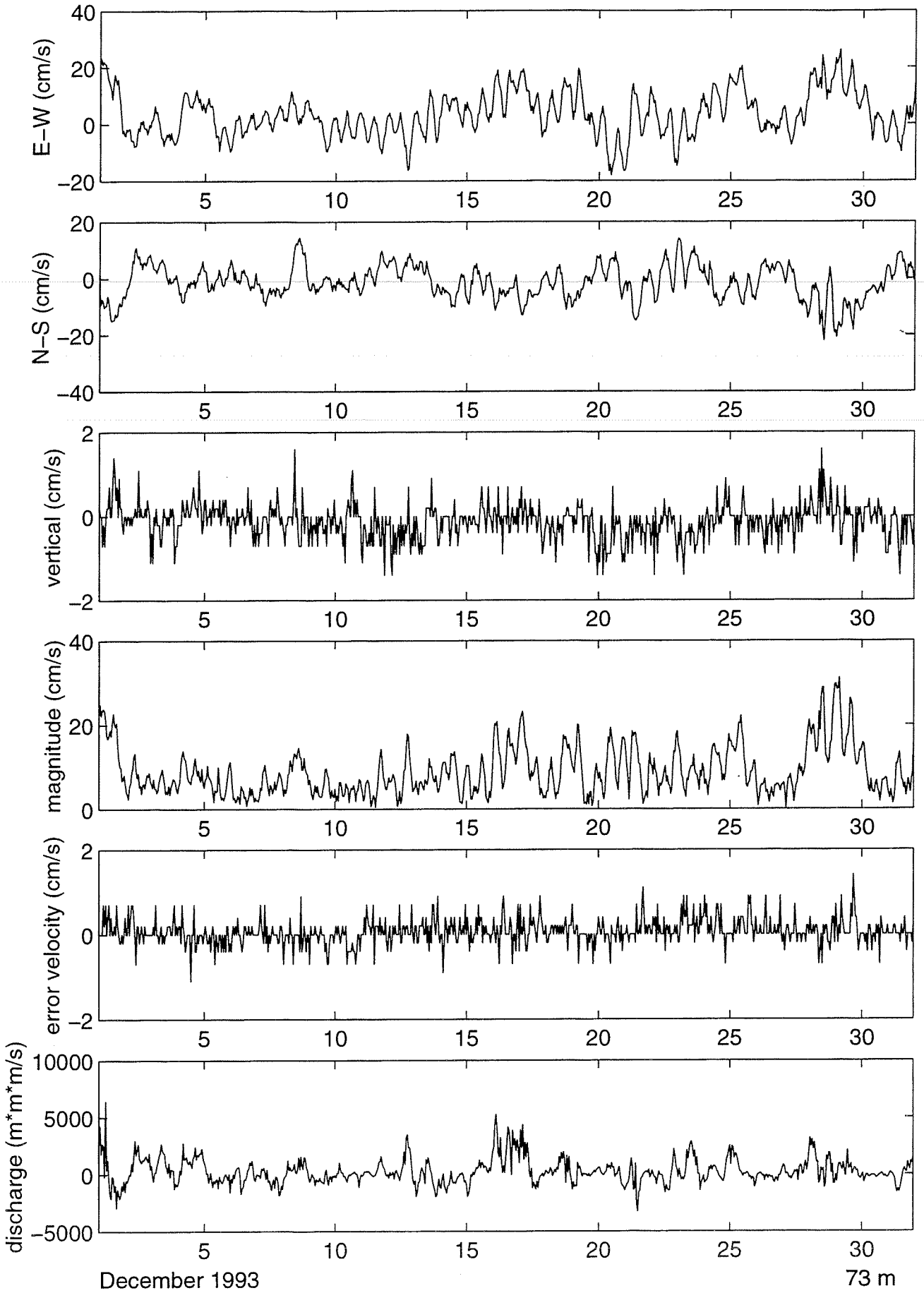
E–W (cm/s)
N–S (cm/s)
vertical (cm/s)
magnitude (cm/s)
error velocity (cm/s)
discharge (m*m*m/s)
December 1993
73 m

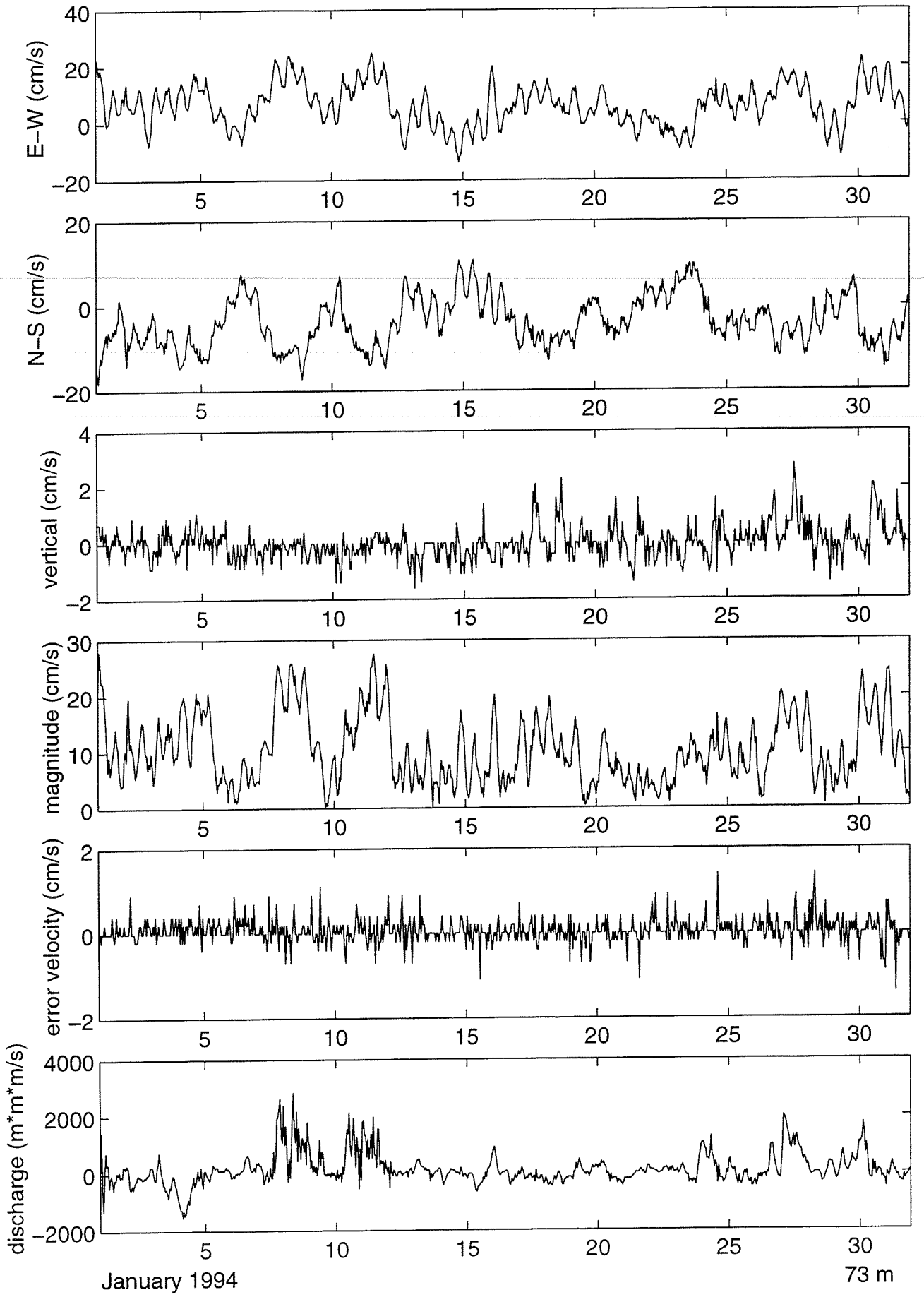
E–W (cm/s)
N–S (cm/s)
vertical (cm/s)
magnitude (cm/s)
error velocity (cm/s)
discharge (m*m*m/s)
January 1994
73 m

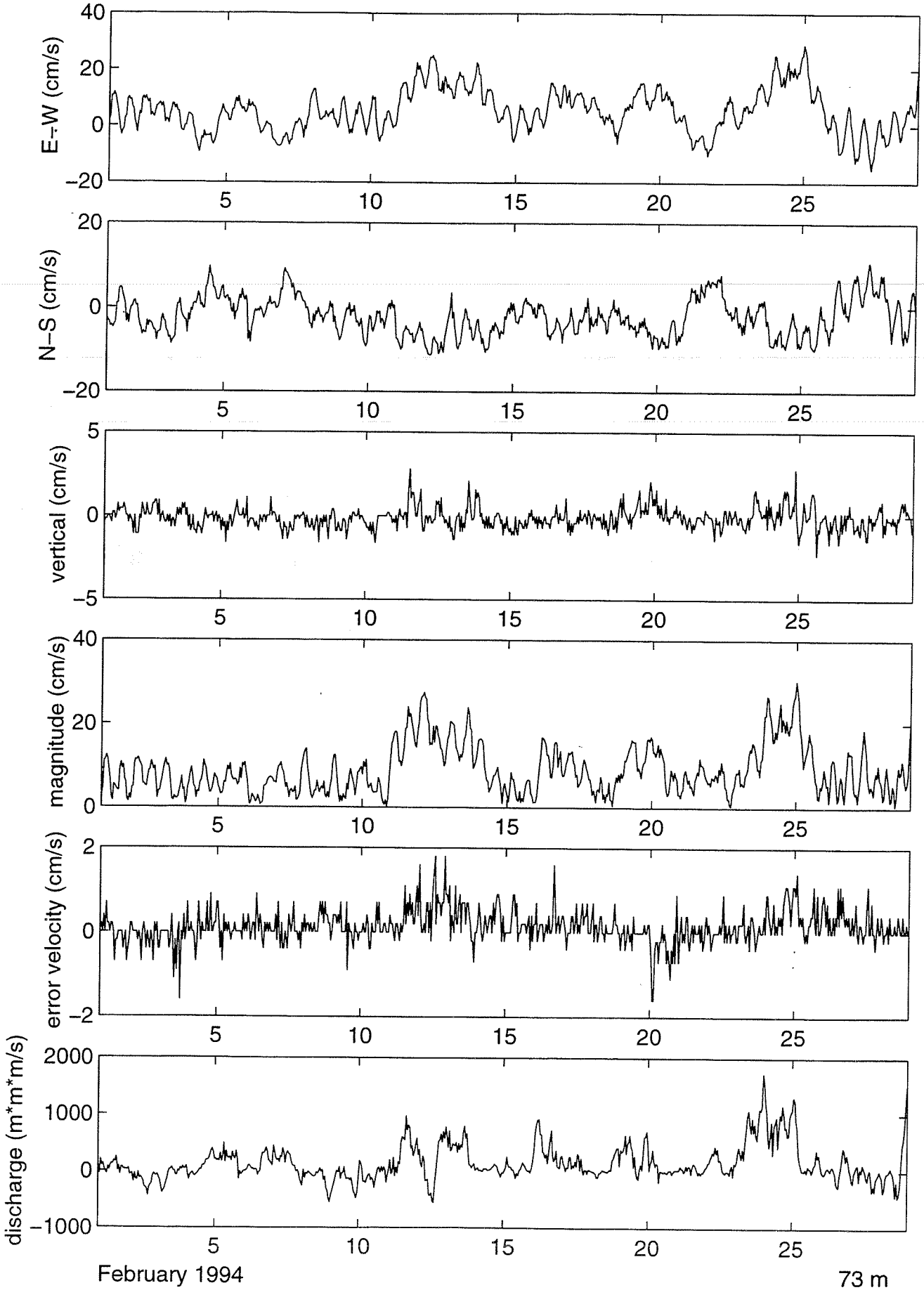
E-W (cm/s)
N-S (cm/s)
vertical (cm/s)
magnitude (cm/s)
error velocity (cm/s)
discharge (m*m*m/s)
February 1994
73 m

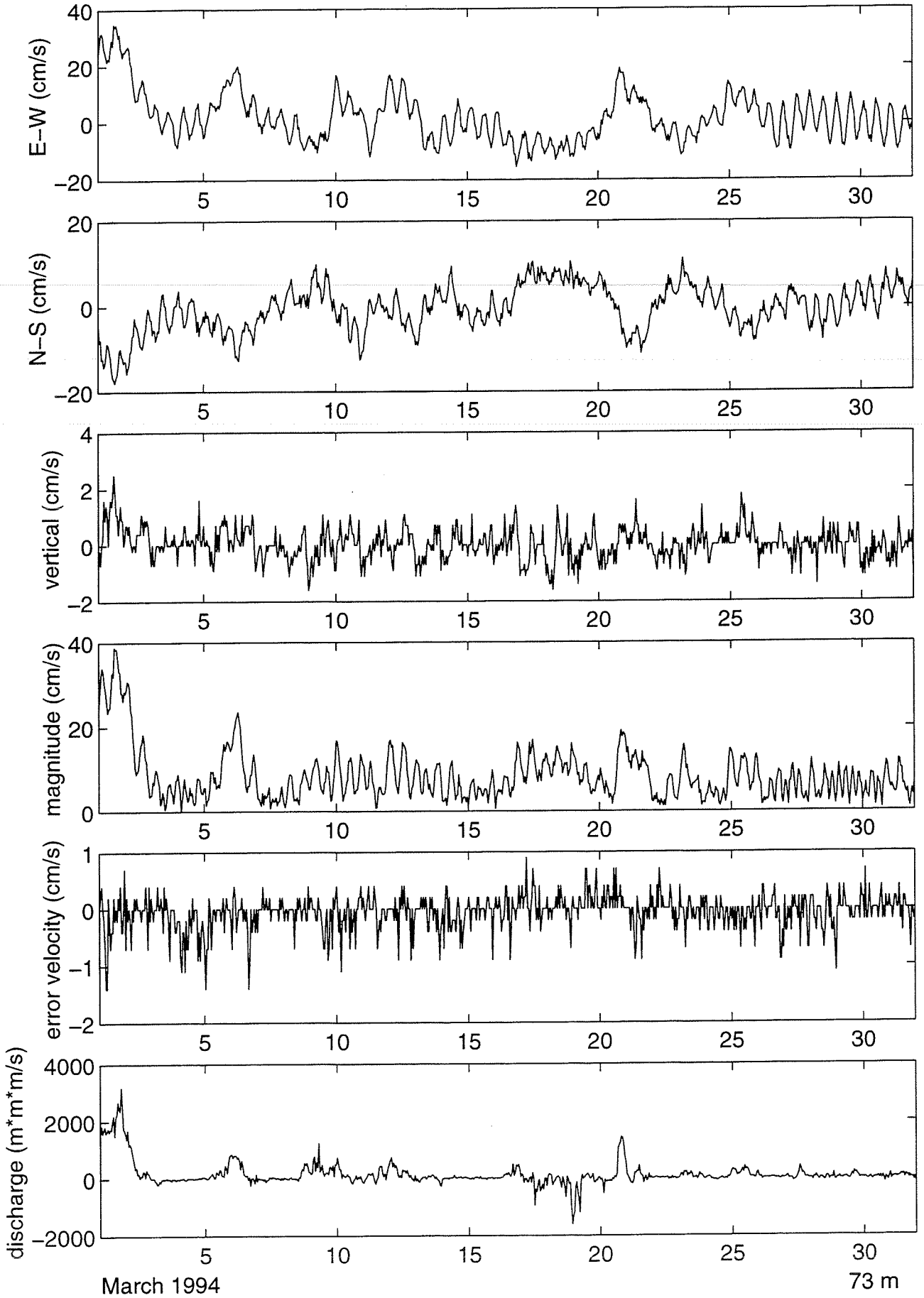
E–W (cm/s)
N–S (cm/s)
vertical (cm/s)
magnitude (cm/s)
error velocity (cm/s)
discharge (m*m*m/s)
March 1994
73 m

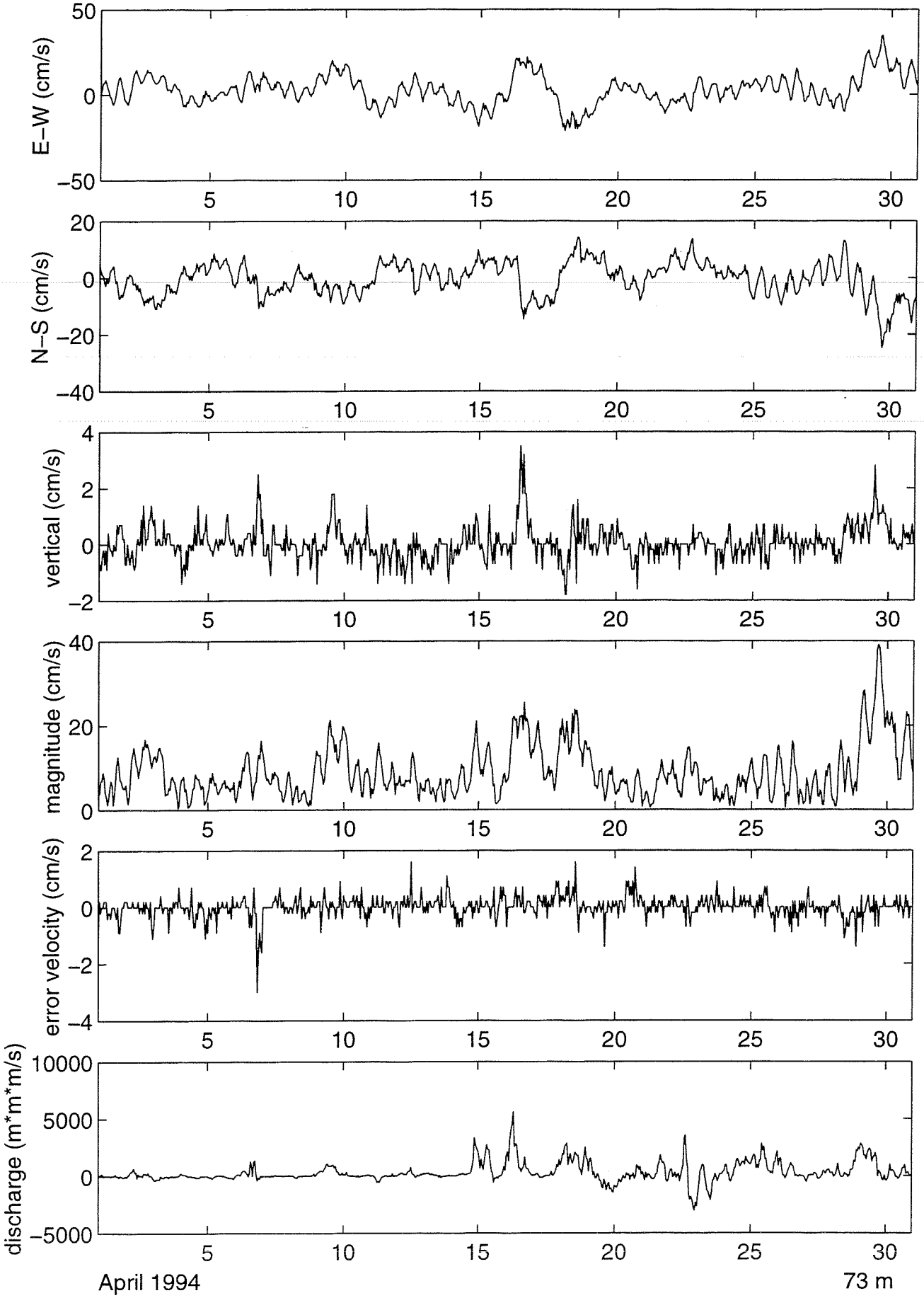
E–W (cm/s)
50
0
–50
N–S (cm/s)
20
0
–20
–40
vertical (cm/s)
4
2
0
–2
magnitude (cm/s)
40
20
0
error velocity (cm/s)
2
0
–2
–4
discharge (m*m*m/s)
10000
5000
0
–5000
5
10
15
20
25
30
April 1994
73 m

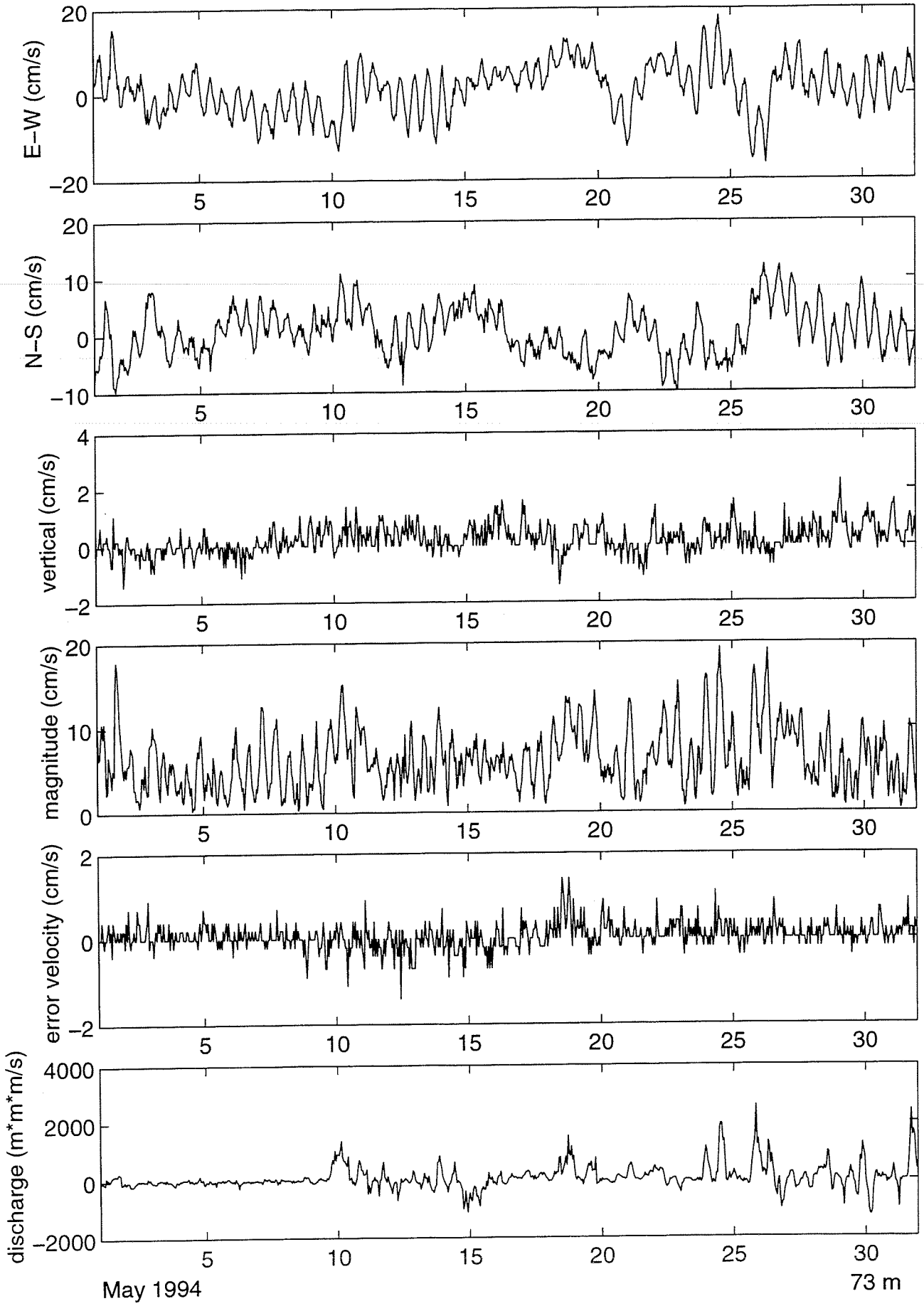
E–W (cm/s)
N–S (cm/s)
vertical (cm/s)
magnitude (cm/s)
error velocity (cm/s)
discharge (m*m*m/s)
May 1994
73 m

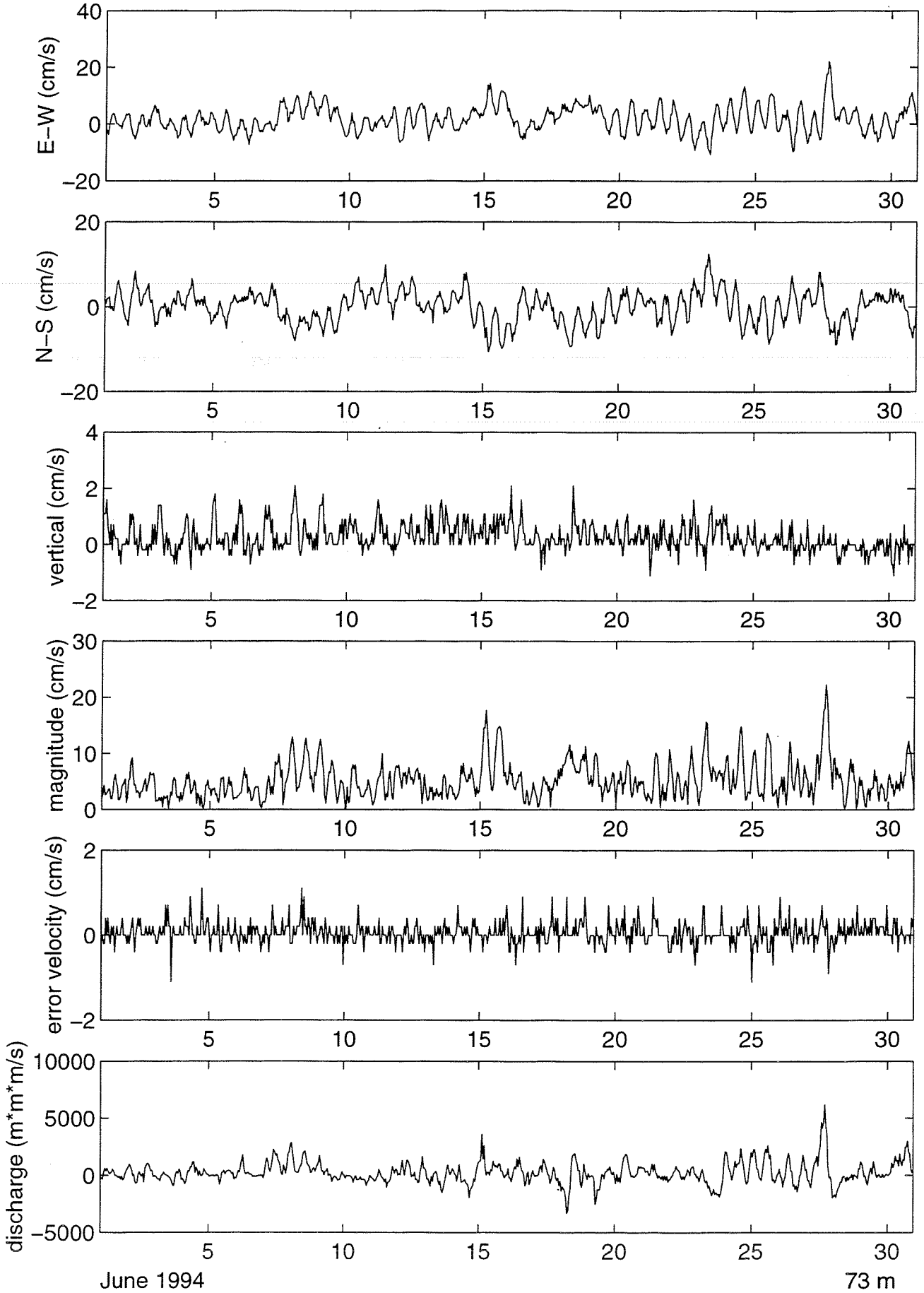
E–W (cm/s)
N–S (cm/s)
vertical (cm/s)
magnitude (cm/s)
error velocity (cm/s)
discharge (m*m*m/s)
June 1994
73 m

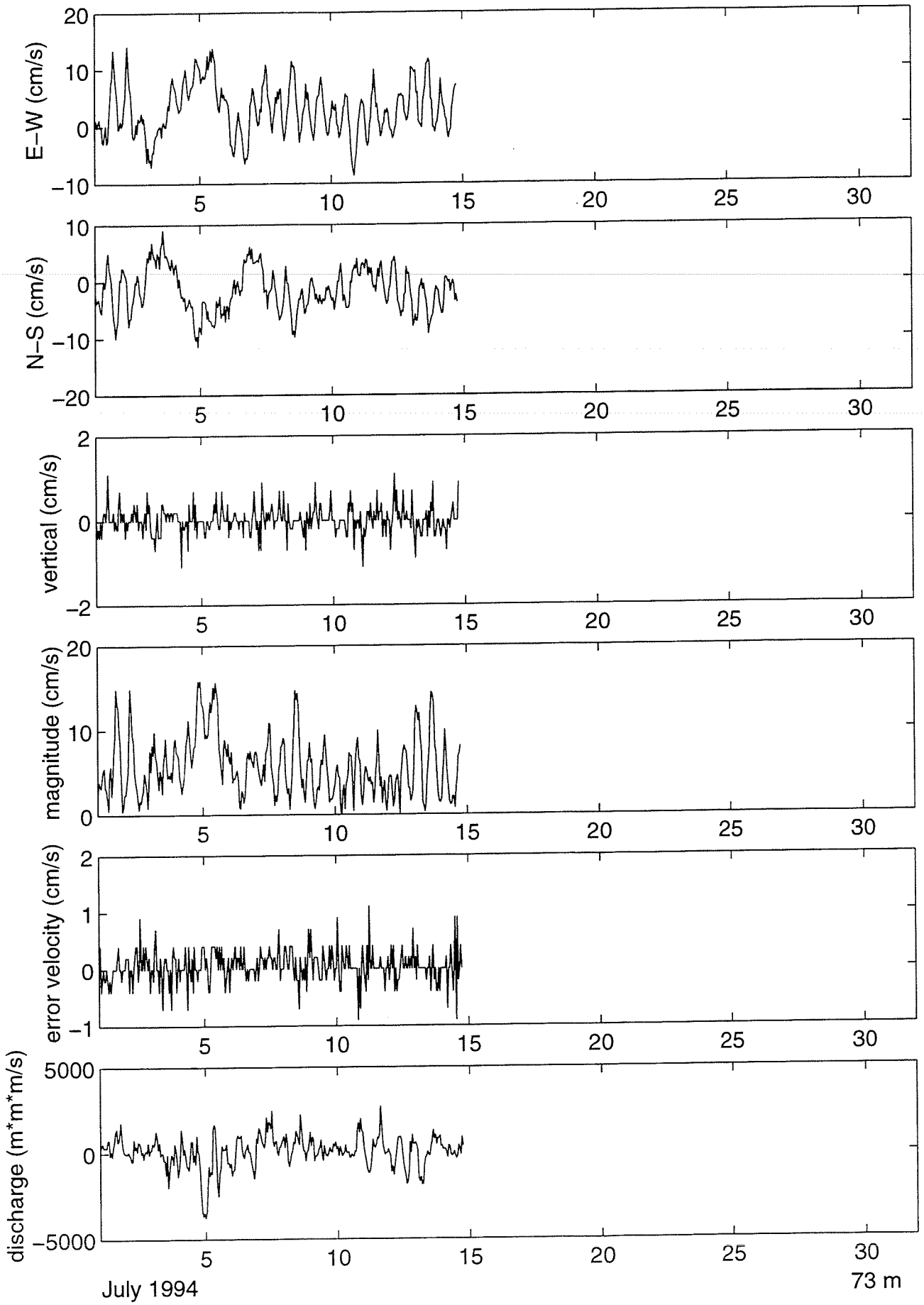
E–W (cm/s)
N–S (cm/s)
vertical (cm/s)
magnitude (cm/s)
error velocity (cm/s)
discharge (m*m*m/s)
July 1994
73 m

APPENDIX B: CORRELATION ANALYSIS OF 12-HOURLY CMC WIND AND CURRENT DATA

- stick plots of CMC 12-hourly wind data interpolated to the ADCP site and ADCP current meter data
- plots are presented for each depth bin

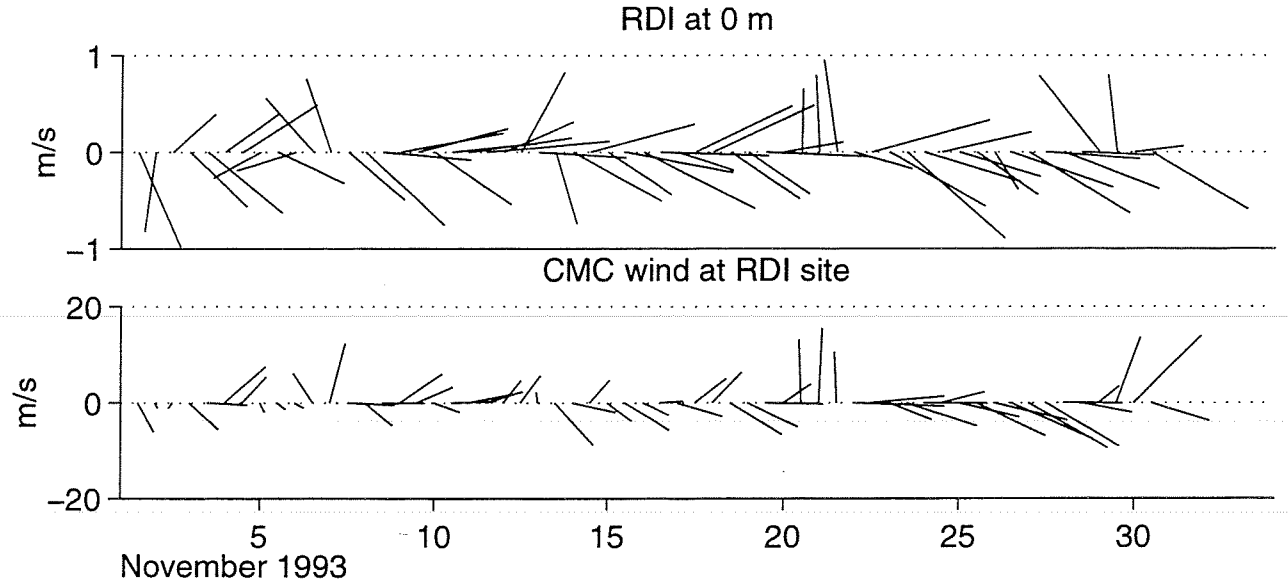
RDI at 0 m
1
0
−1
m/s
CMC wind at RDI site
20
0
−20
m/s
5
10
15
20
25
30
November 1993

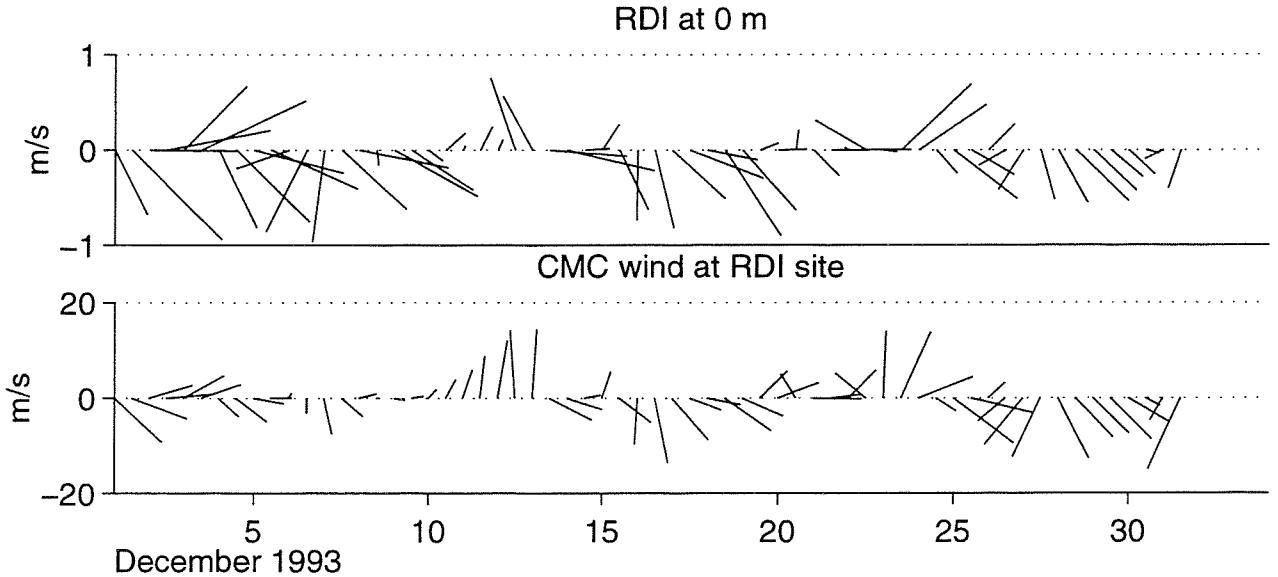
RDI at 0 m
1
0
−1
m/s
CMC wind at RDI site
20
0
−20
m/s
5
10
15
20
25
30
December 1993

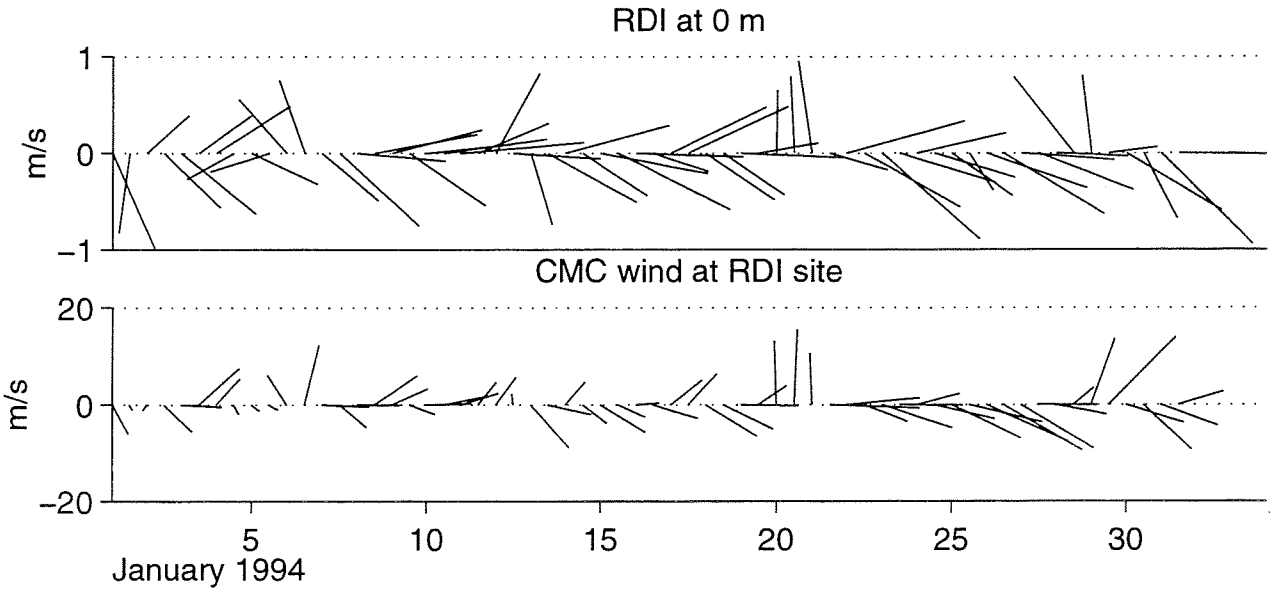
RDI at 0 m
1
0
−1
m/s
CMC wind at RDI site
20
0
−20
m/s
5
10
15
20
25
30
January 1994

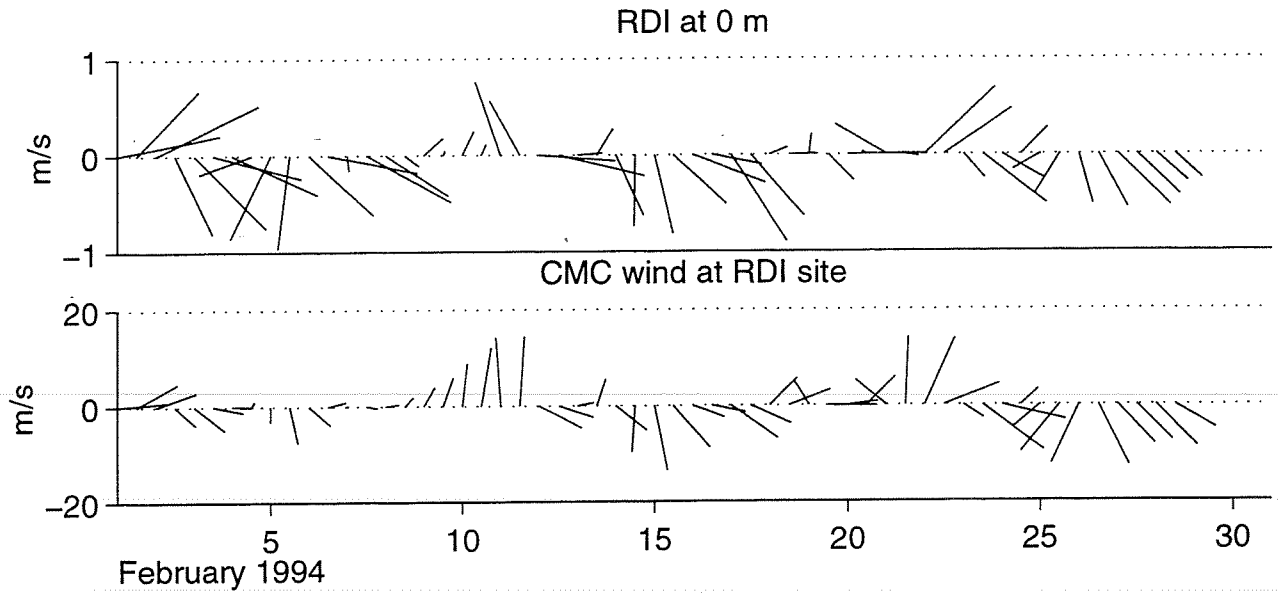
RDI at 0 m
1
0
−1
m/s
CMC wind at RDI site
20
0
−20
m/s
5
10
15
20
25
30
February 1994

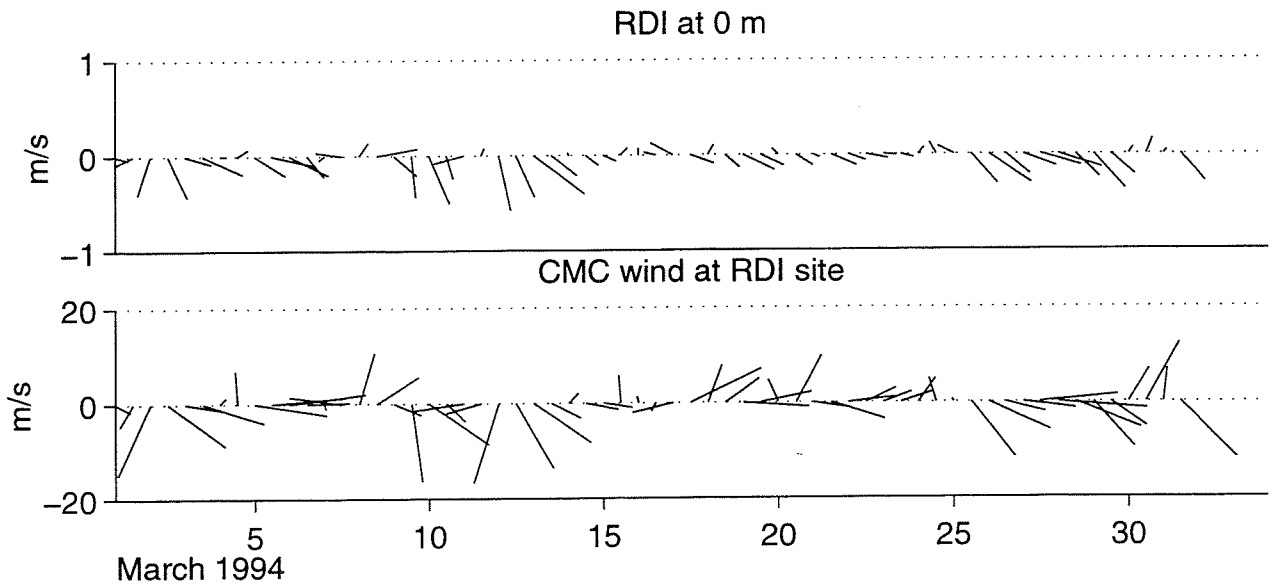
RDI at 0 m
1
0
−1
m/s
CMC wind at RDI site
20
0
−20
m/s
5
10
15
20
25
30
March 1994

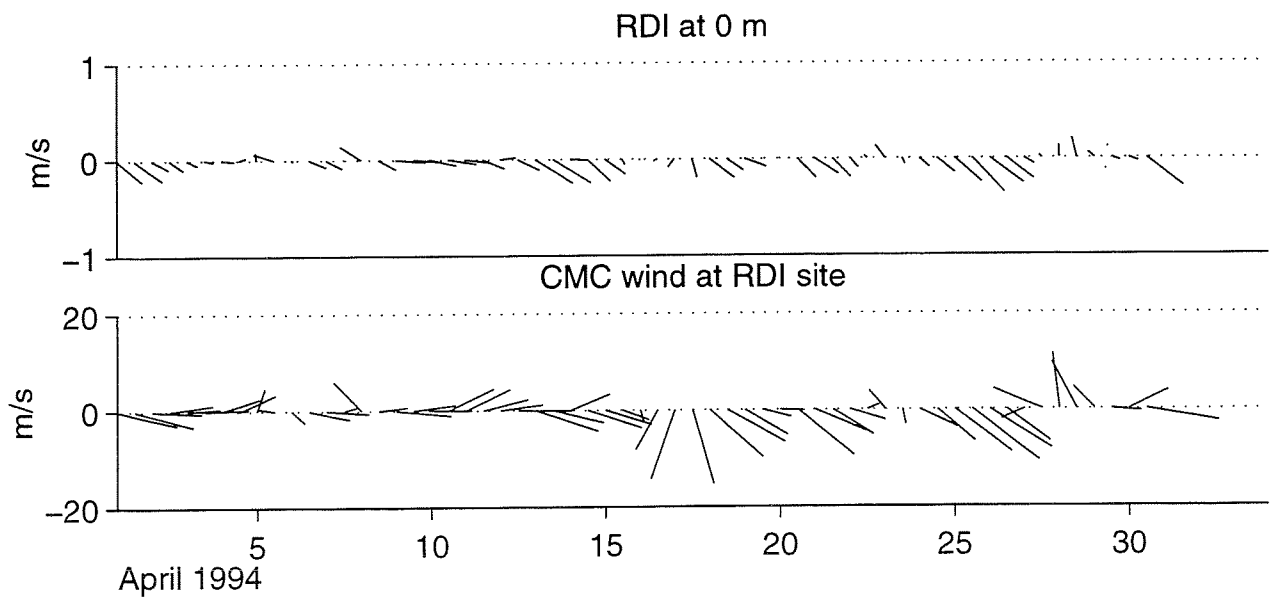
RDI at 0 m
1
0
−1
m/s
CMC wind at RDI site
20
0
−20
m/s
5
10
15
20
25
30
April 1994

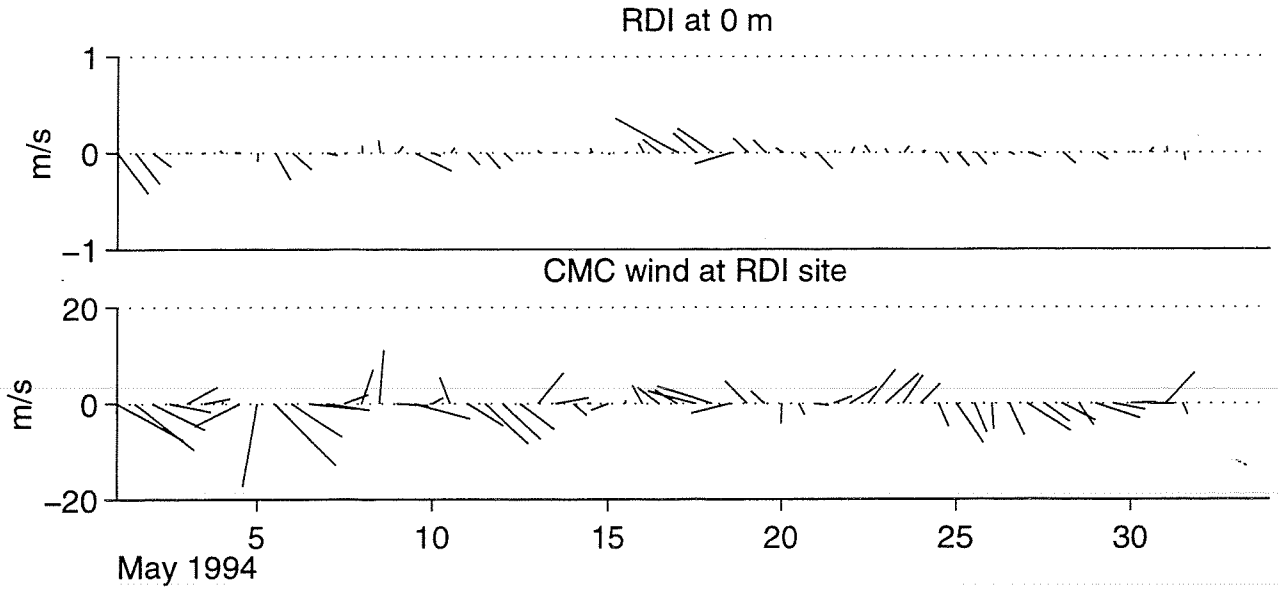
RDI at 0 m
1
0
−1
m/s
CMC wind at RDI site
20
0
−20
m/s
5
10
15
20
25
30
May 1994

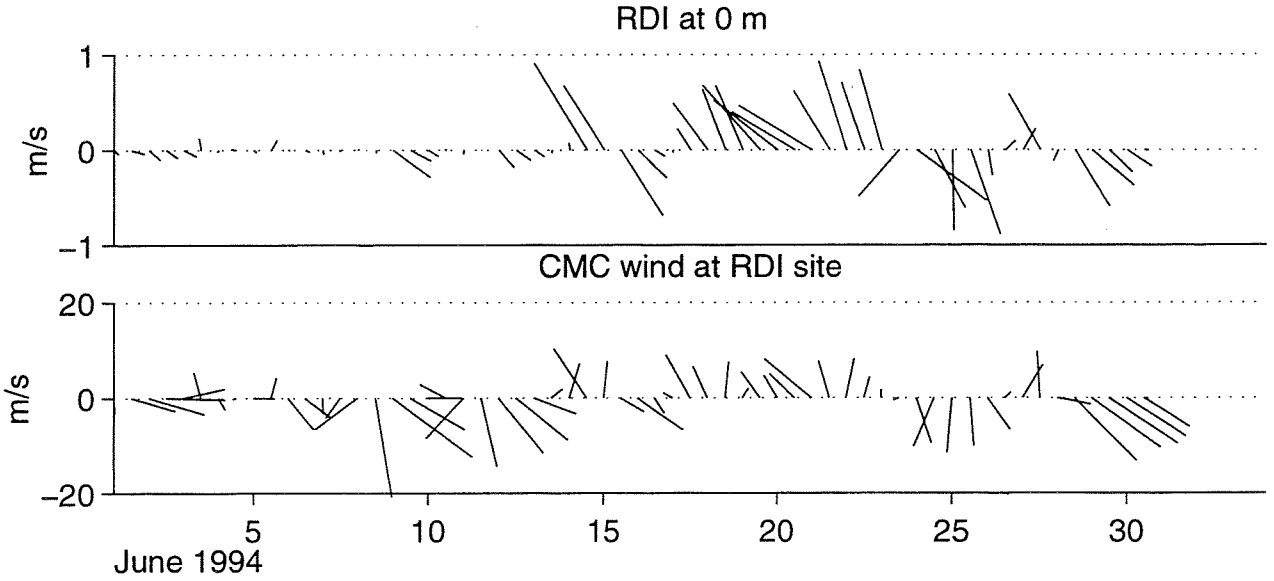
RDI at 0 m
1
0
−1
m/s
CMC wind at RDI site
20
0
−20
m/s
5
10
15
20
25
30
June 1994

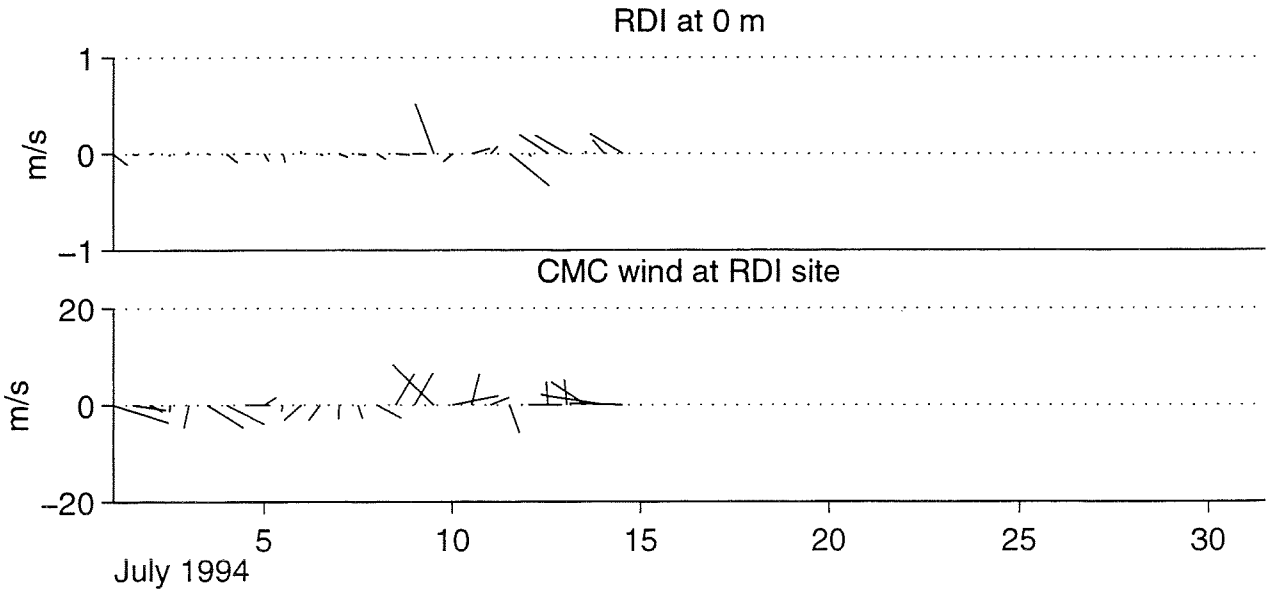
RDI at 0 m
1
0
−1
m/s
CMC wind at RDI site
20
0
−20
m/s
5
10
15
20
25
30
July 1994

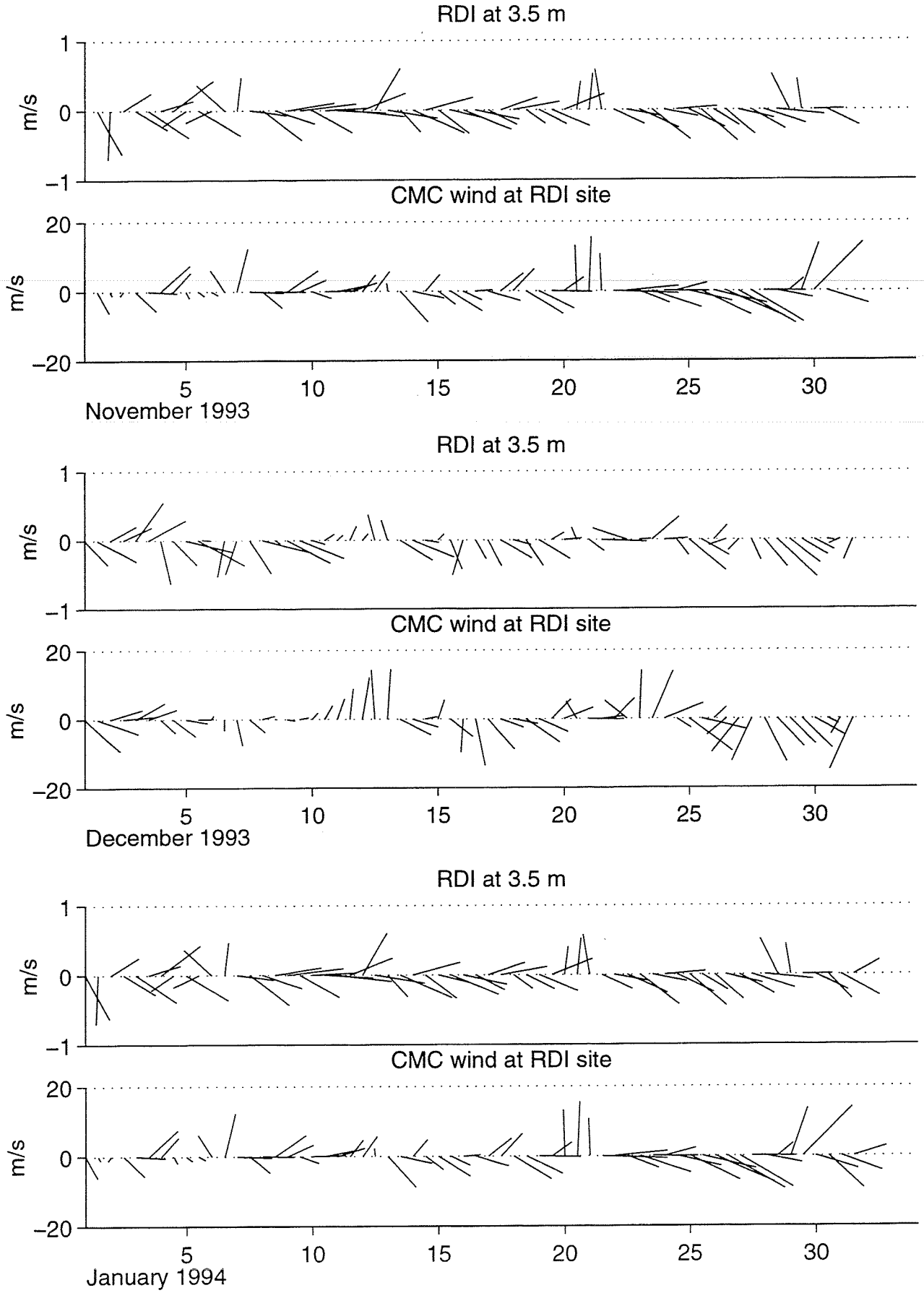
RDI at 3.5 m
m/s
1
0
−1
CMC wind at RDI site
m/s
20
0
−20
5
10
15
20
25
30
November 1993
RDI at 3.5 m
m/s
1
0
−1
CMC wind at RDI site
m/s
20
0
−20
5
10
15
20
25
30
December 1993
RDI at 3.5 m
m/s
1
0
−1
CMC wind at RDI site
m/s
20
0
−20
5
10
15
20
25
30
January 1994

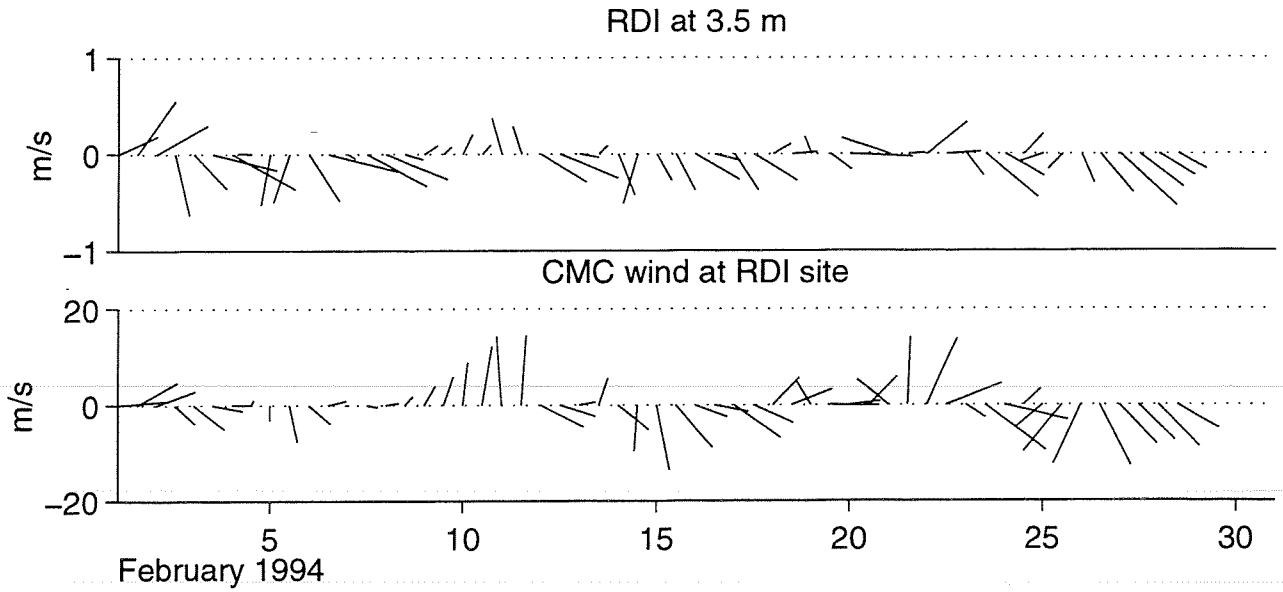
RDI at 3.5 m
1
0
−1
m/s
CMC wind at RDI site
20
0
−20
m/s
5
10
15
20
25
30
February 1994

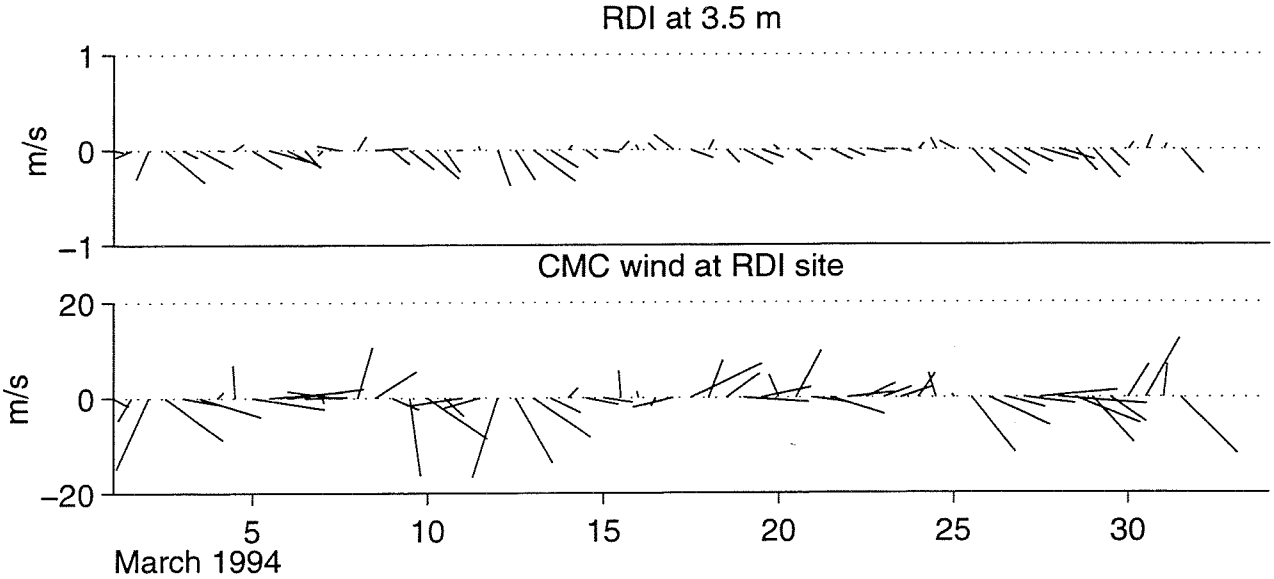
RDI at 3.5 m
1
0
−1
m/s
CMC wind at RDI site
20
0
−20
m/s
5
10
15
20
25
30
March 1994

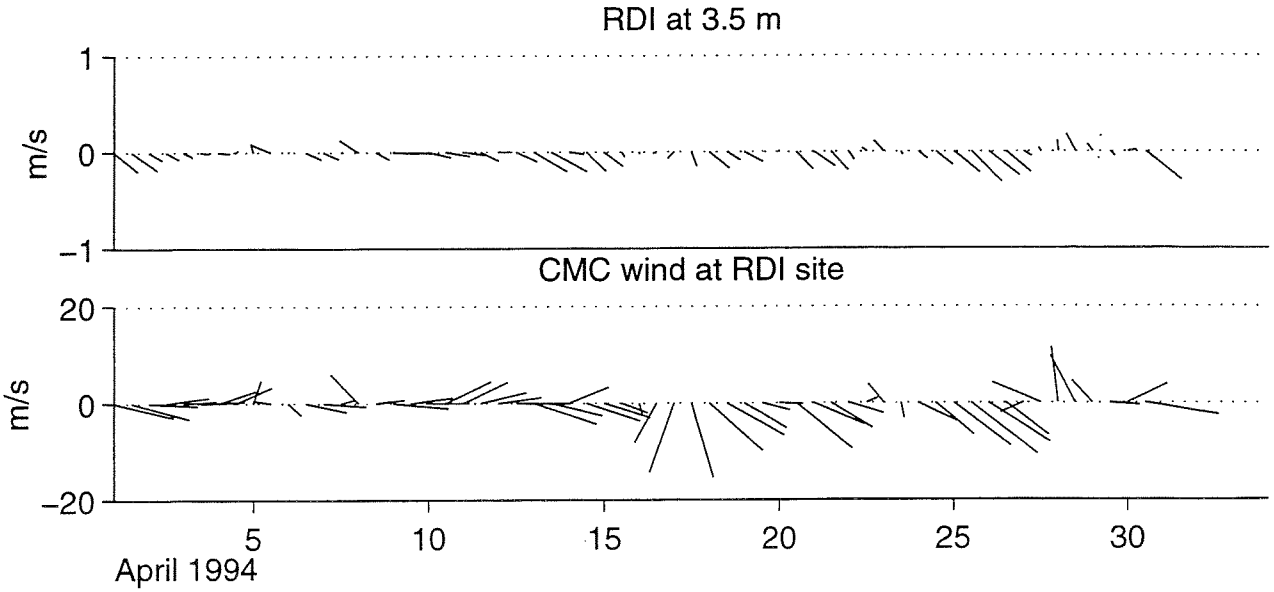
RDI at 3.5 m
1
0
−1
m/s
CMC wind at RDI site
20
0
−20
m/s
5
10
15
20
25
30
April 1994

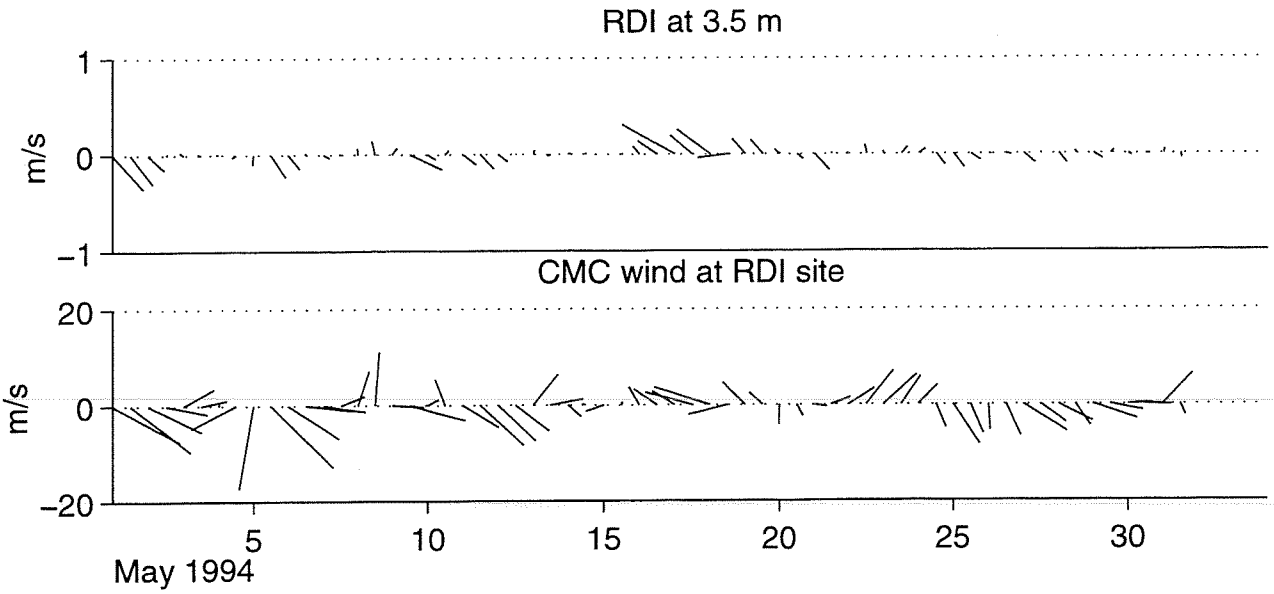
RDI at 3.5 m
1
0
−1
m/s
CMC wind at RDI site
20
0
−20
m/s
5
10
15
20
25
30
May 1994

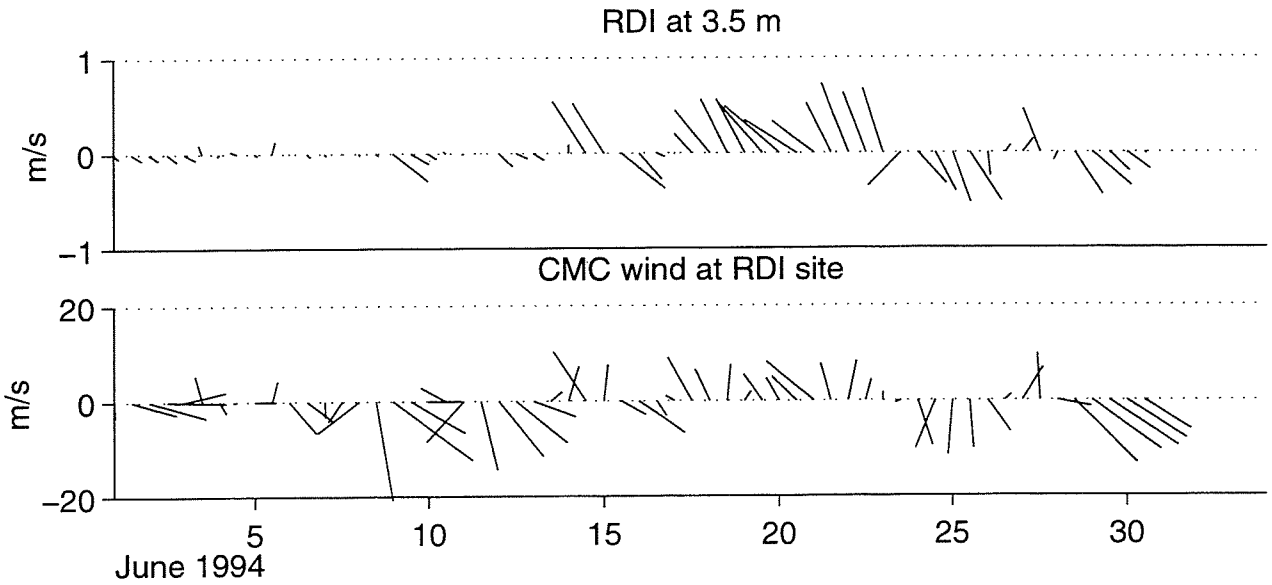
RDI at 3.5 m
1
0
−1
m/s
CMC wind at RDI site
20
0
−20
m/s
5
10
15
20
25
30
June 1994

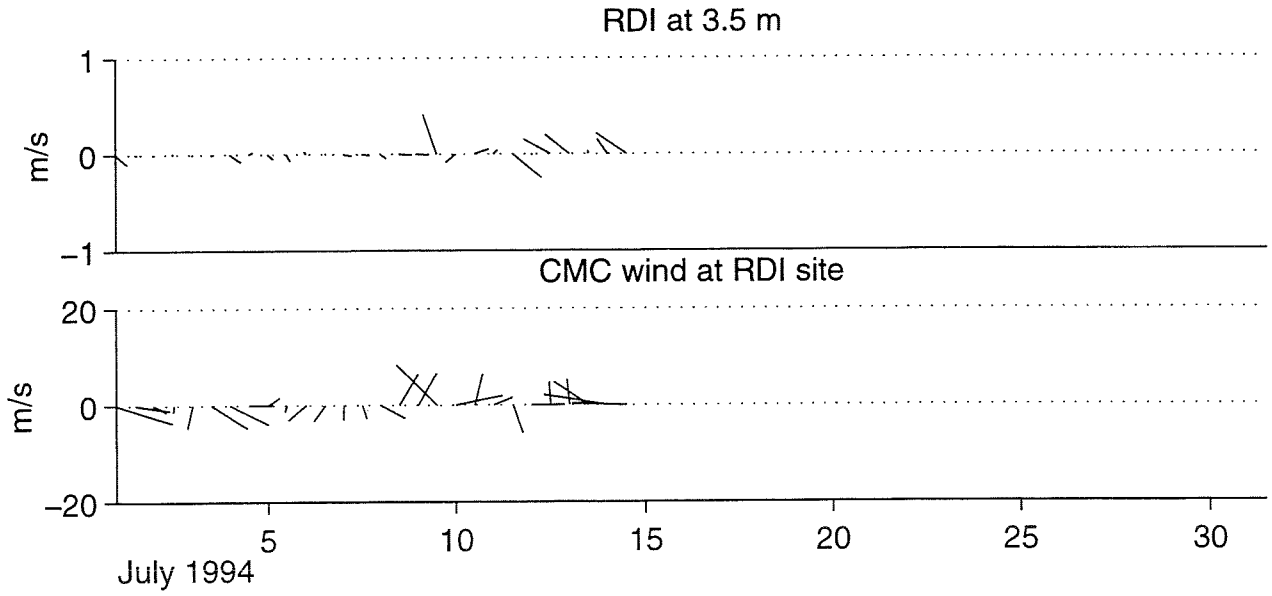
RDI at 3.5 m
1
0
−1
m/s
CMC wind at RDI site
20
0
−20
m/s
5
10
15
20
25
30
July 1994

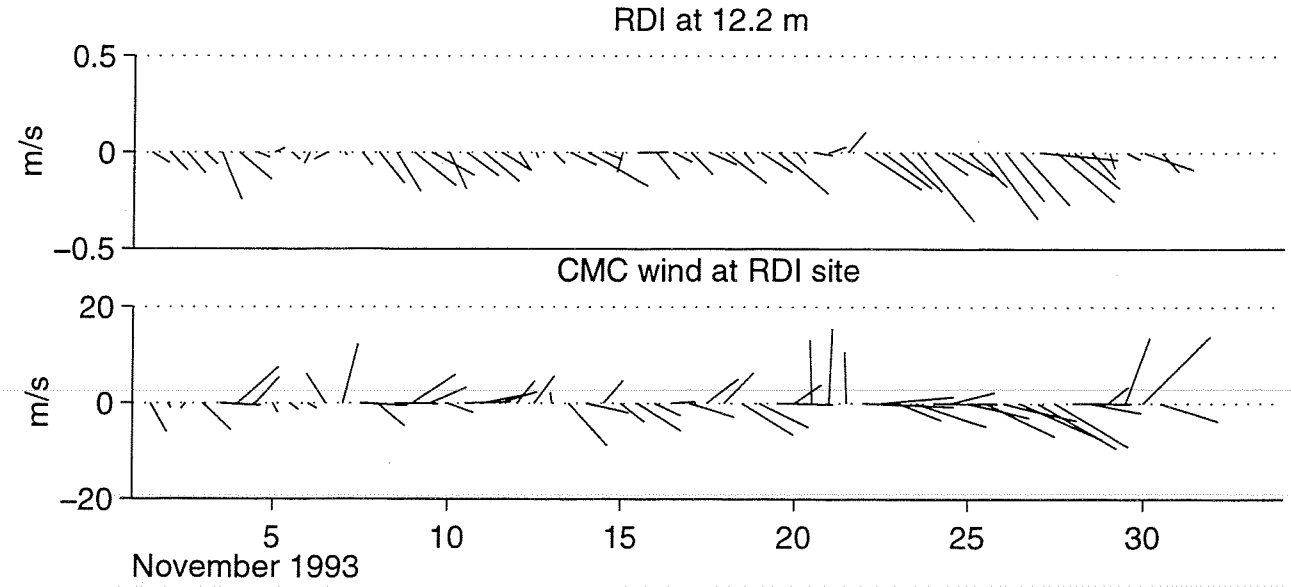
RDI at 12.2 m
0.5
0
−0.5
m/s
CMC wind at RDI site
20
0
−20
m/s
5
10
15
20
25
30
November 1993

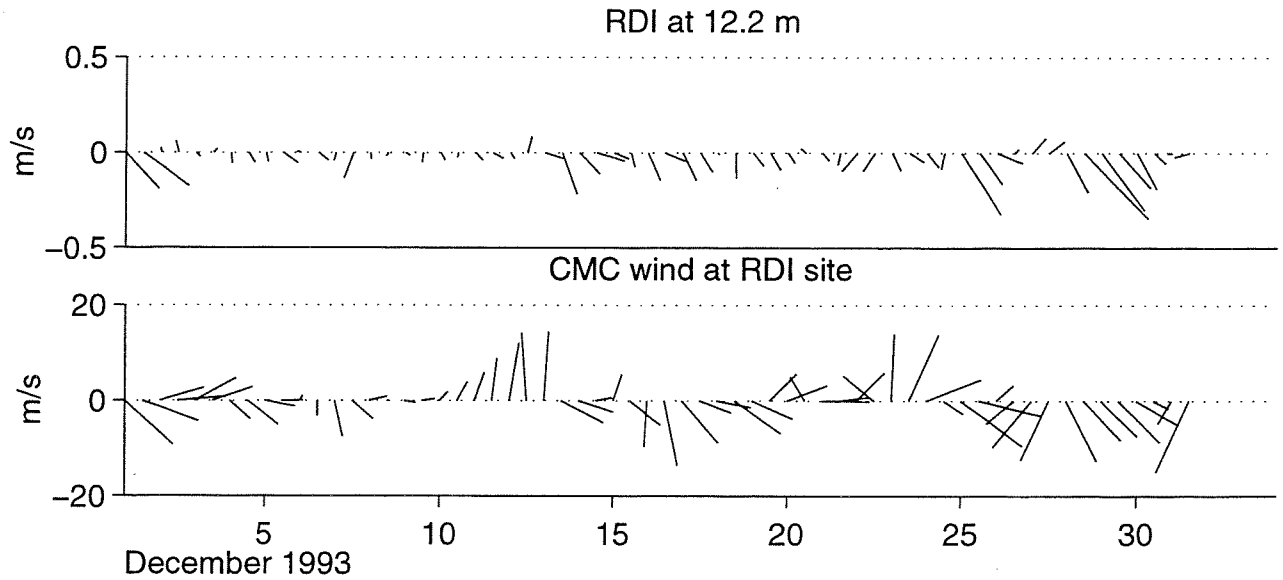
RDI at 12.2 m
0.5
0
−0.5
m/s
CMC wind at RDI site
20
0
−20
m/s
5
10
15
20
25
30
December 1993

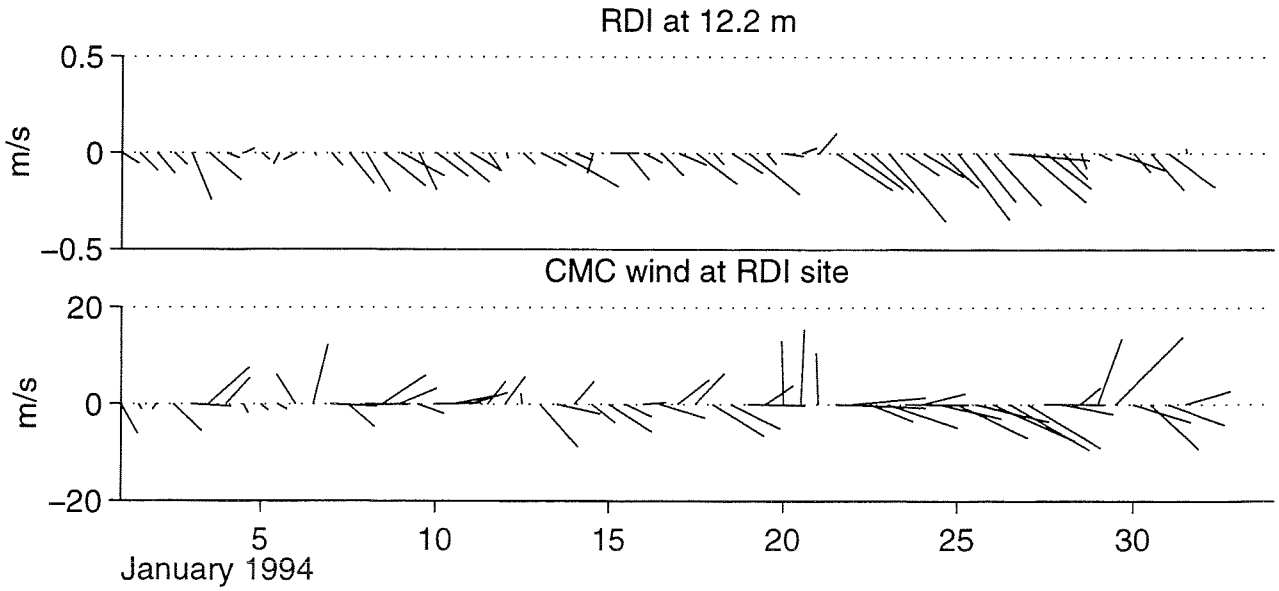
RDI at 12.2 m
0.5
0
−0.5
m/s
CMC wind at RDI site
20
0
−20
m/s
5
10
15
20
25
30
January 1994

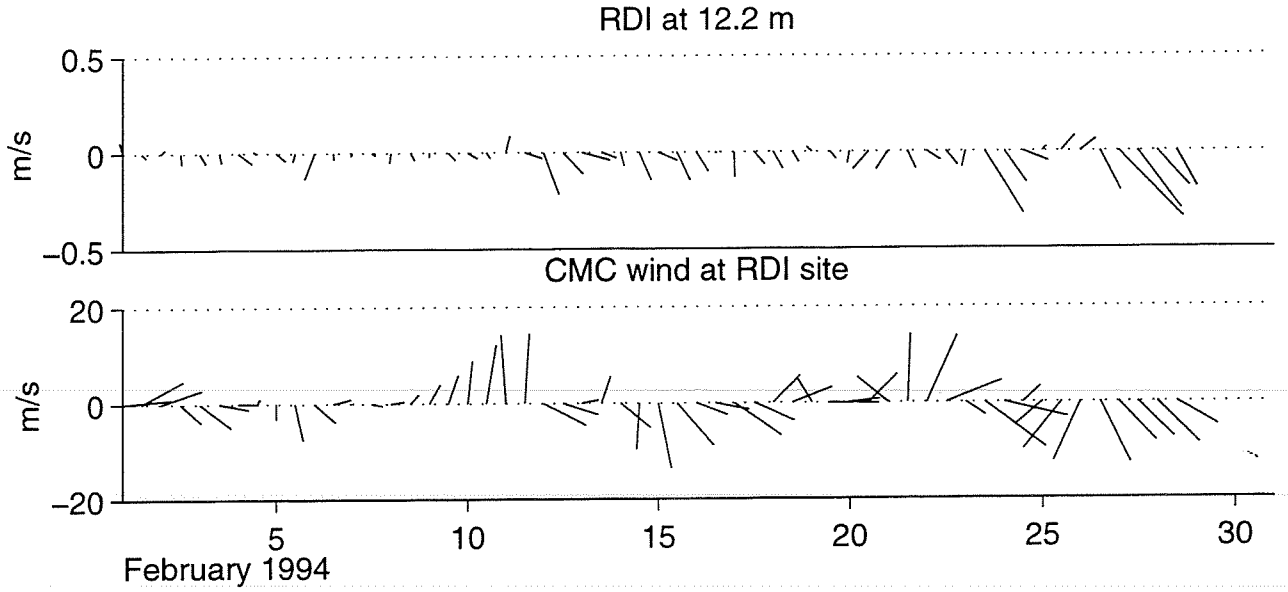
RDI at 12.2 m
0.5
0
−0.5
m/s
CMC wind at RDI site
20
0
−20
m/s
5
10
15
20
25
30
February 1994

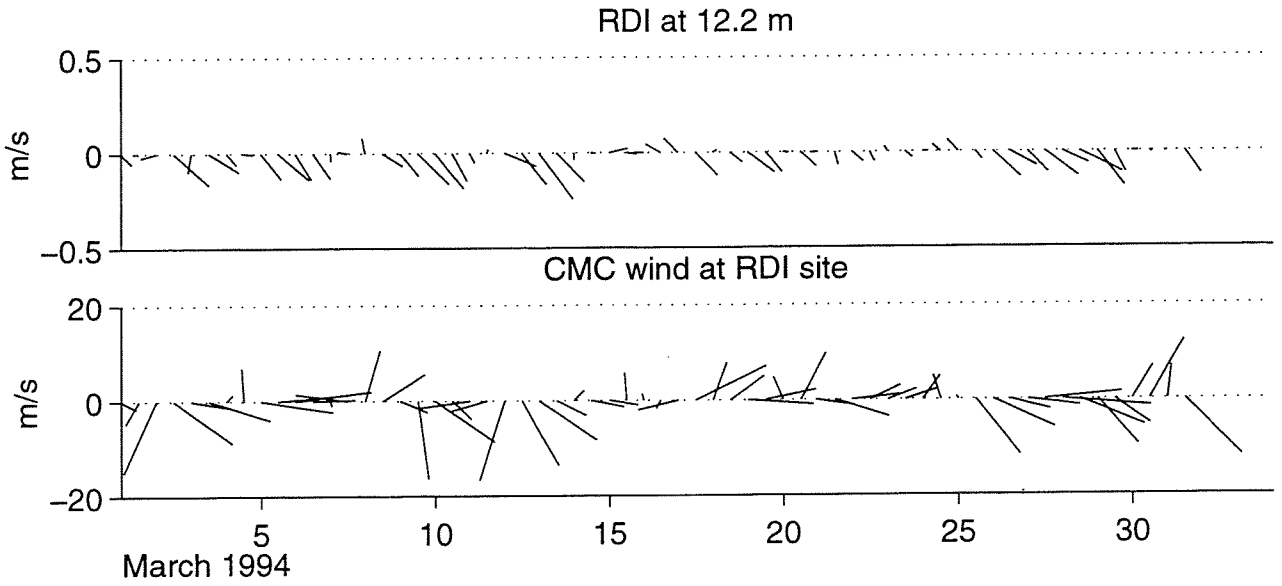
RDI at 12.2 m
0.5
0
−0.5
m/s
CMC wind at RDI site
20
0
−20
m/s
5
10
15
20
25
30
March 1994

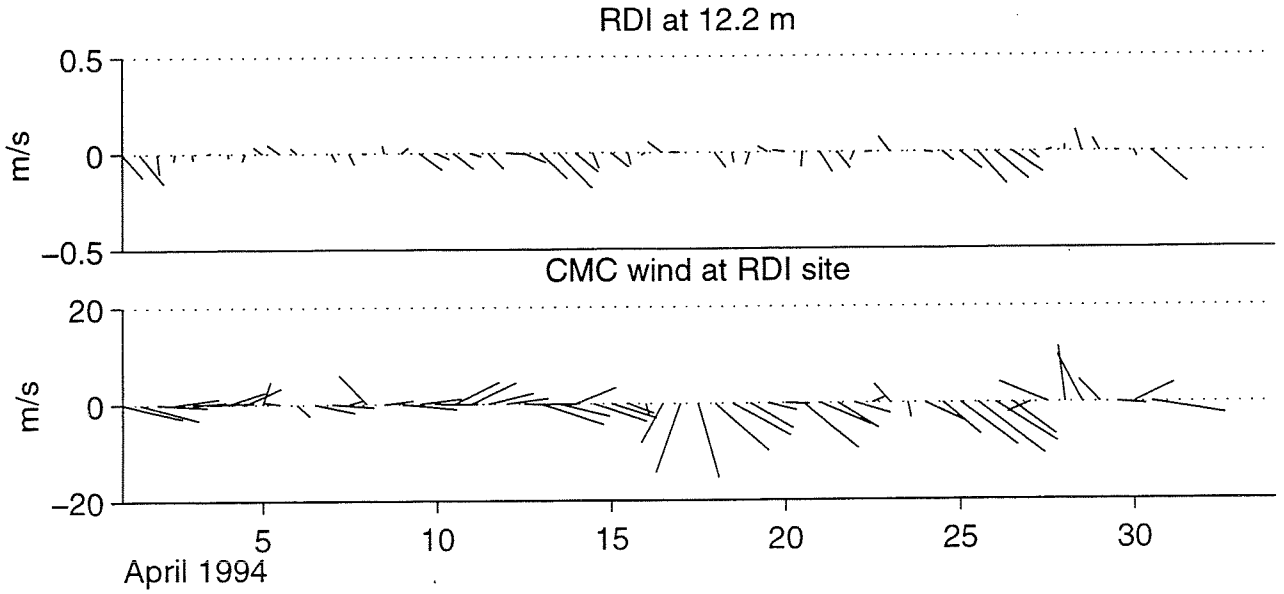
RDI at 12.2 m
0.5
0
−0.5
m/s
CMC wind at RDI site
20
0
−20
m/s
5
10
15
20
25
30
April 1994

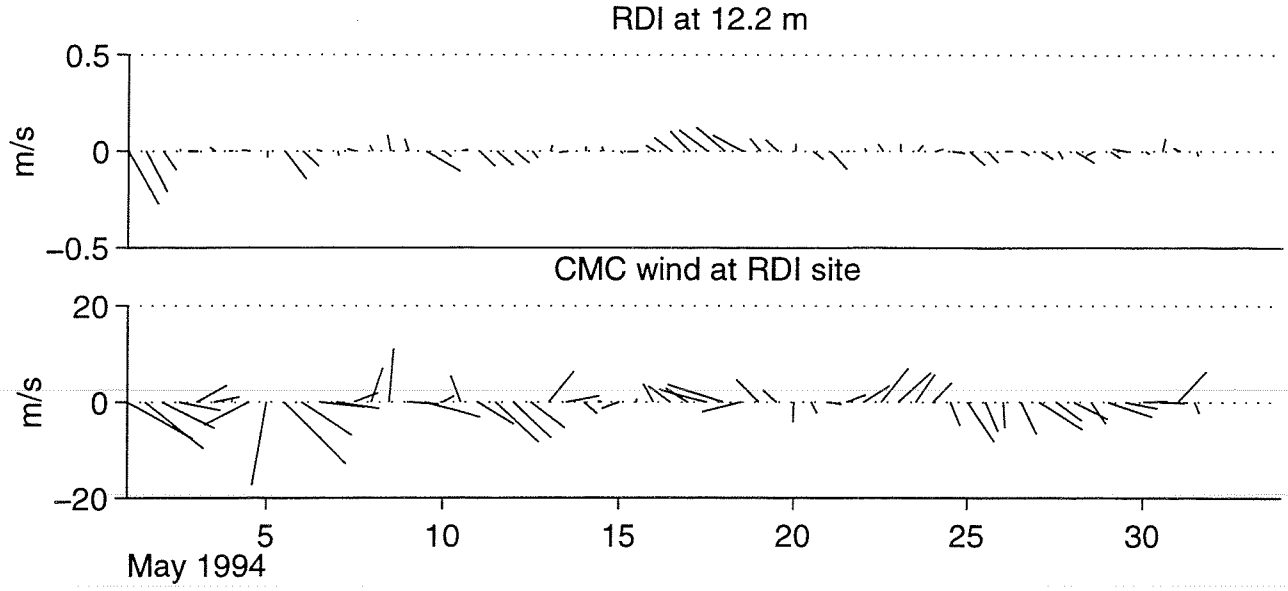
RDI at 12.2 m
0.5
0
−0.5
m/s
CMC wind at RDI site
20
0
−20
m/s
5
10
15
20
25
30
May 1994

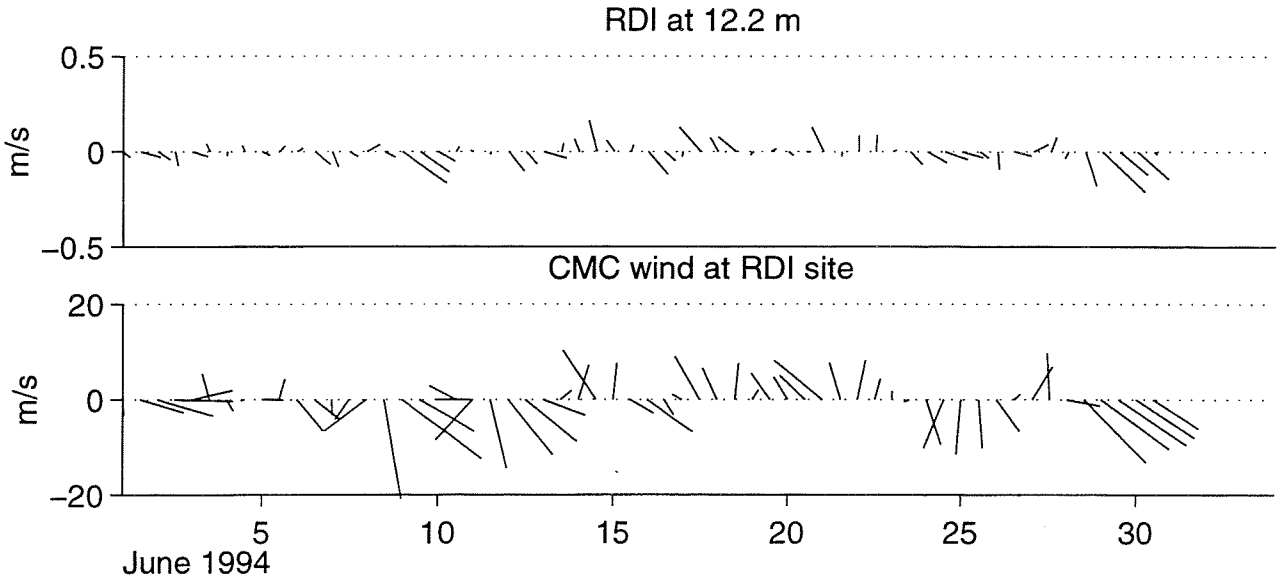
RDI at 12.2 m
0.5
0
−0.5
m/s
CMC wind at RDI site
20
0
−20
m/s
5
10
15
20
25
30
June 1994

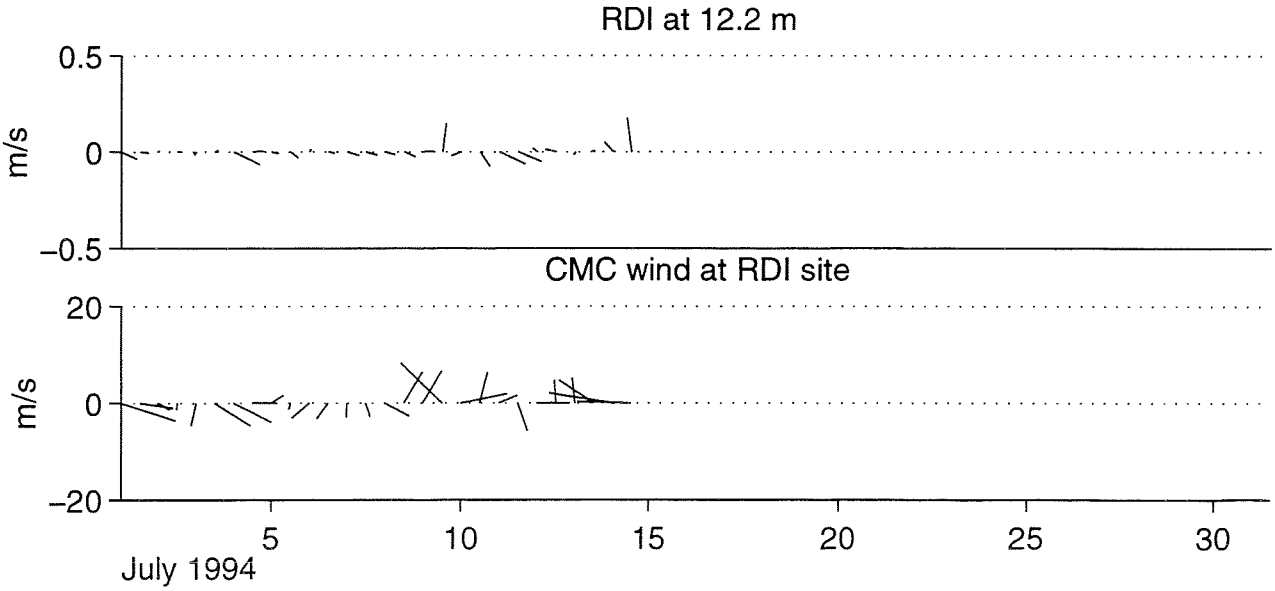
RDI at 12.2 m
0.5
0
−0.5
m/s
CMC wind at RDI site
20
0
−20
m/s
5
10
15
20
25
30
July 1994

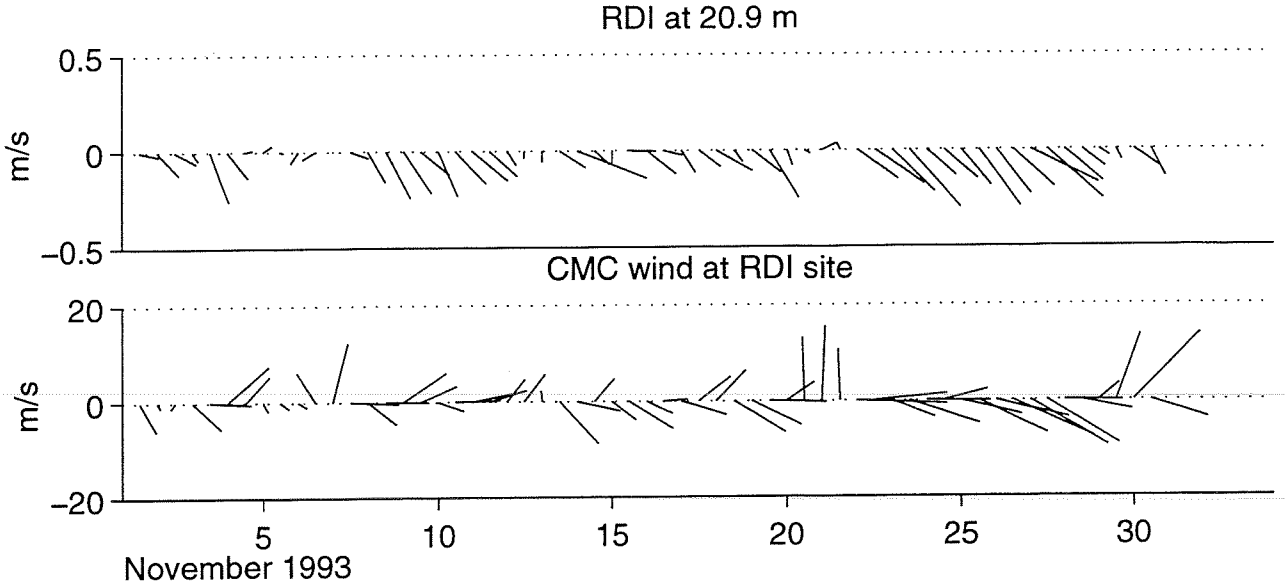
RDI at 20.9 m
0.5
0
−0.5
m/s
CMC wind at RDI site
20
0
−20
m/s
5
10
15
20
25
30
November 1993

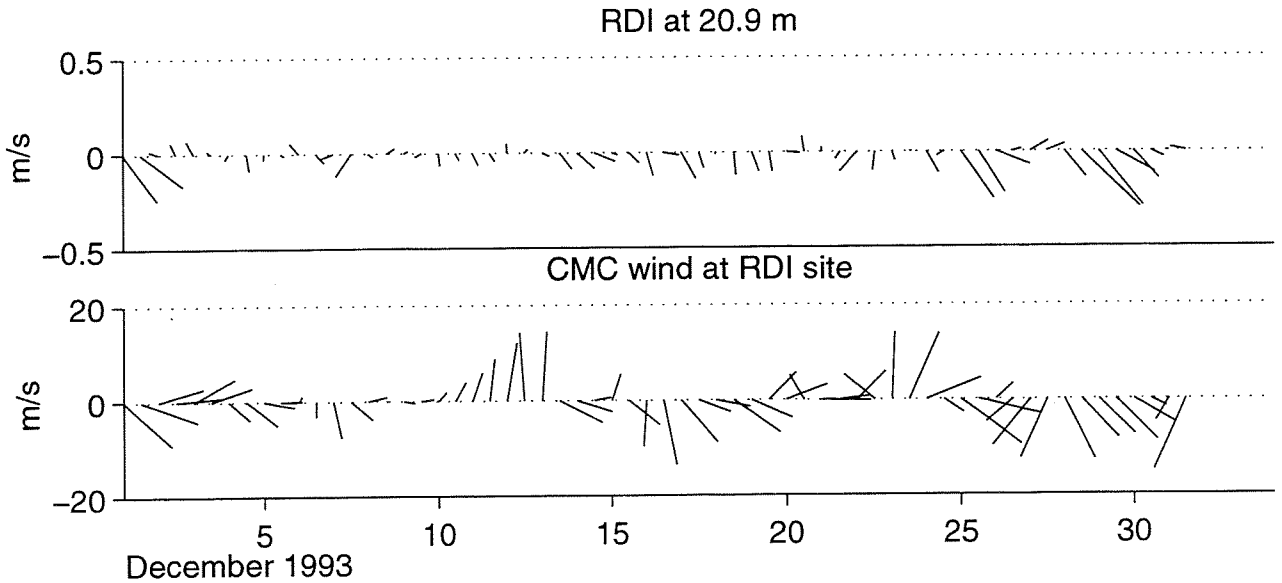
RDI at 20.9 m
0.5
0
−0.5
m/s
CMC wind at RDI site
20
0
−20
m/s
5
10
15
20
25
30
December 1993

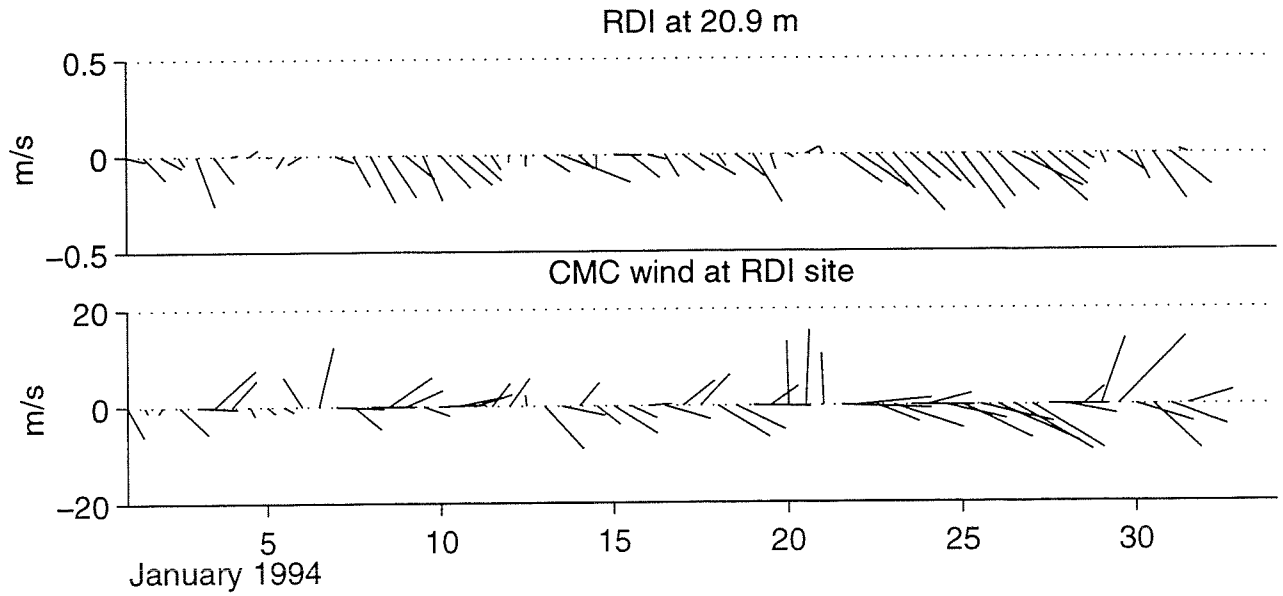
RDI at 20.9 m
0.5
0
−0.5
m/s
CMC wind at RDI site
20
0
−20
m/s
5
10
15
20
25
30
January 1994

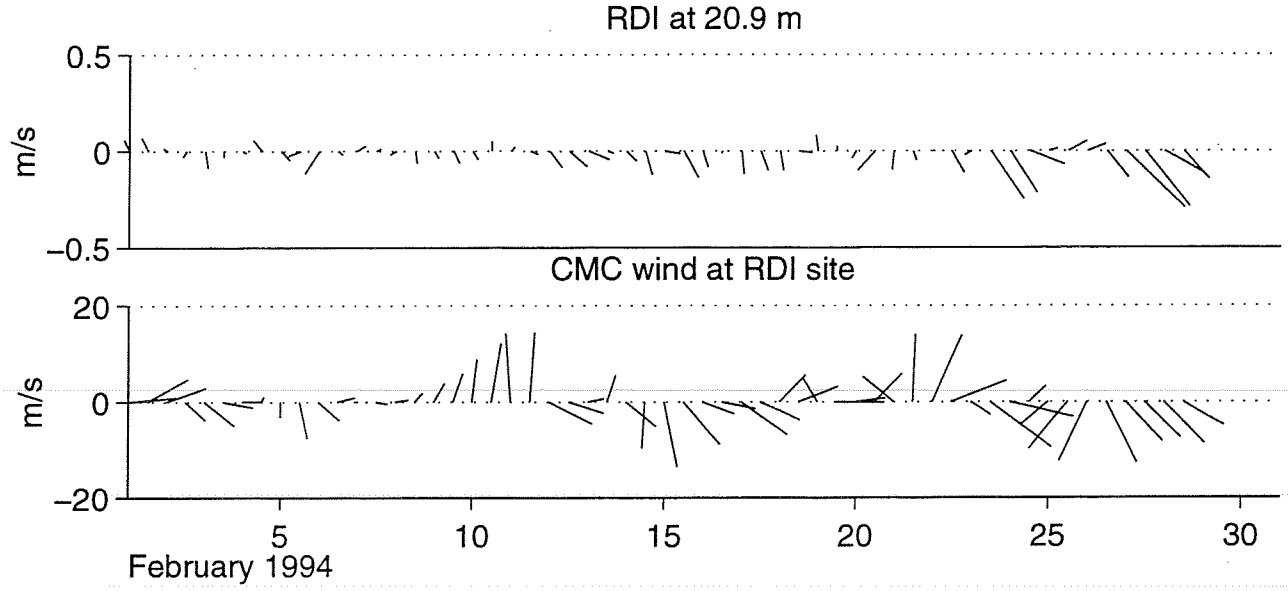
RDI at 20.9 m
0.5
0
−0.5
m/s
CMC wind at RDI site
20
0
−20
m/s
5
10
15
20
25
30
February 1994

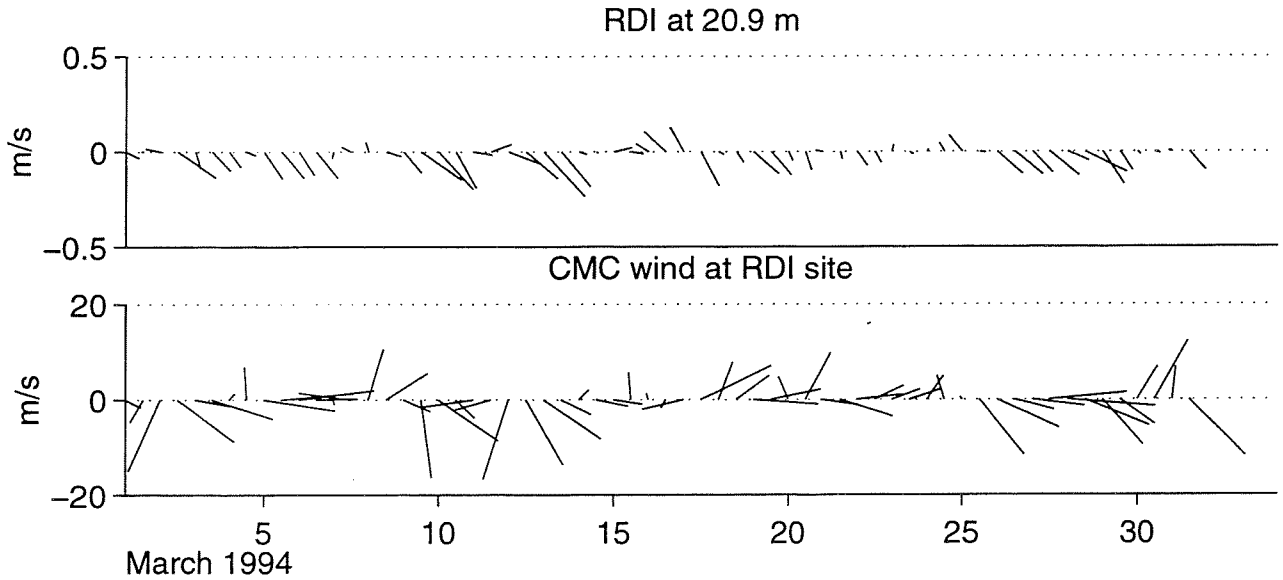
RDI at 20.9 m
0.5
0
−0.5
m/s
CMC wind at RDI site
20
0
−20
m/s
5
10
15
20
25
30
March 1994

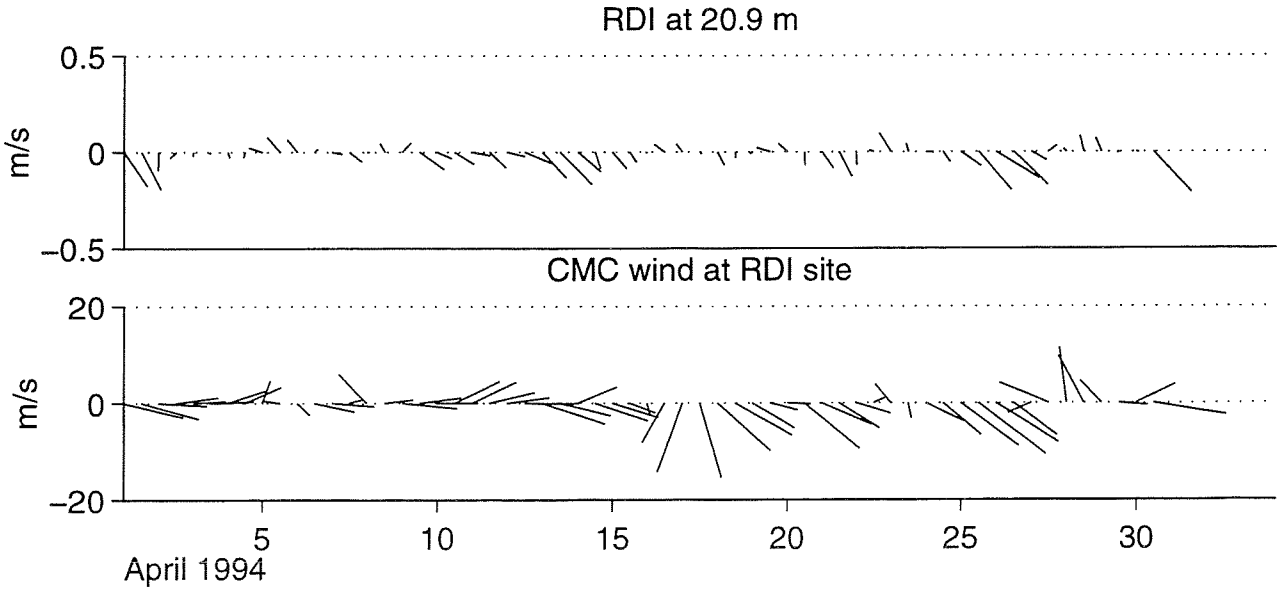
RDI at 20.9 m
0.5
0
−0.5
m/s
CMC wind at RDI site
20
0
−20
m/s
5
10
15
20
25
30
April 1994

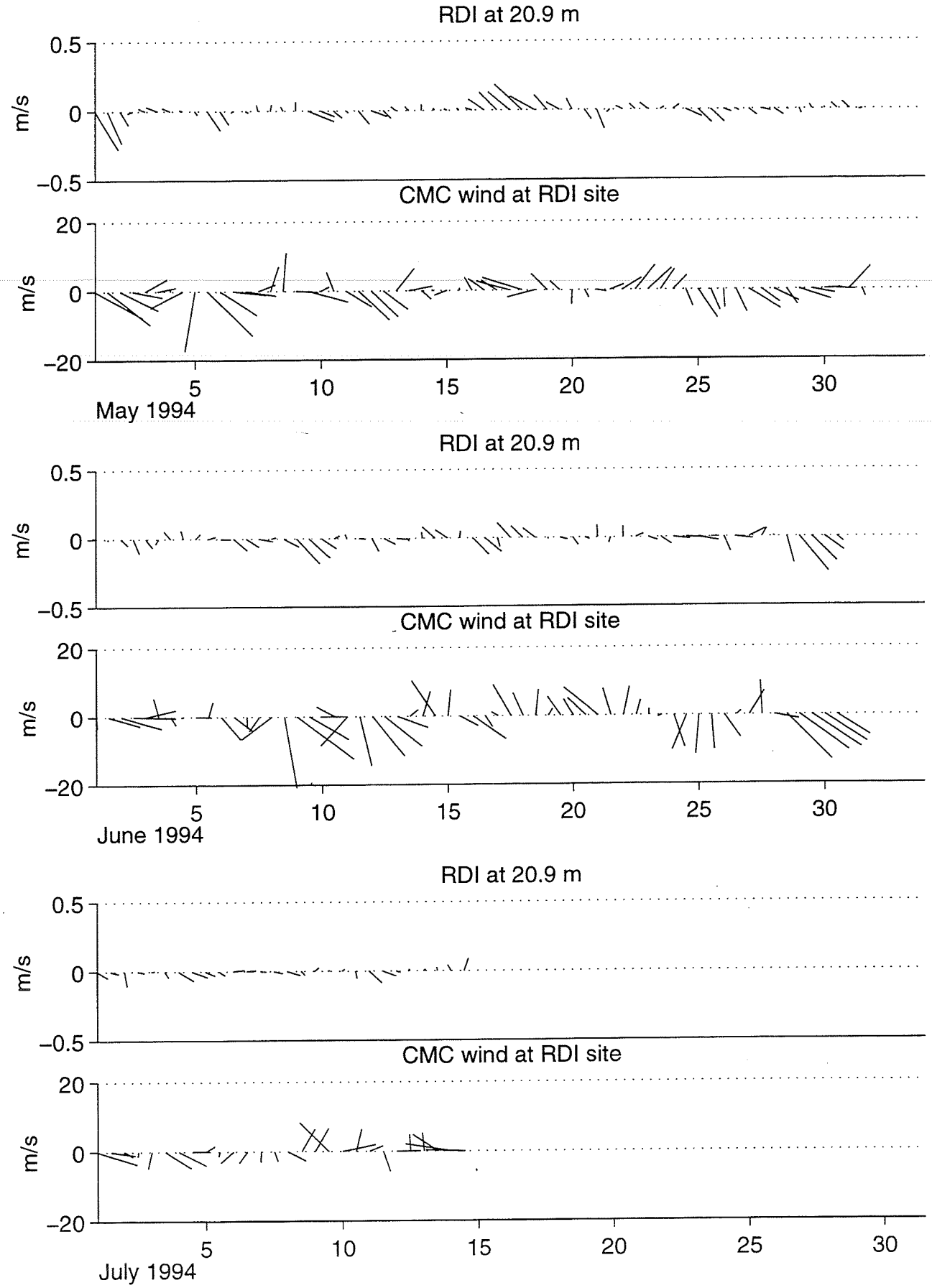
RDI at 20.9 m
0.5
0
−0.5
m/s
CMC wind at RDI site
20
0
−20
m/s
5
10
15
20
25
30
May 1994
RDI at 20.9 m
0.5
0
−0.5
m/s
CMC wind at RDI site
20
0
−20
m/s
5
10
15
20
25
30
June 1994
RDI at 20.9 m
0.5
0
−0.5
m/s
CMC wind at RDI site
20
0
−20
m/s
5
10
15
20
25
30
July 1994

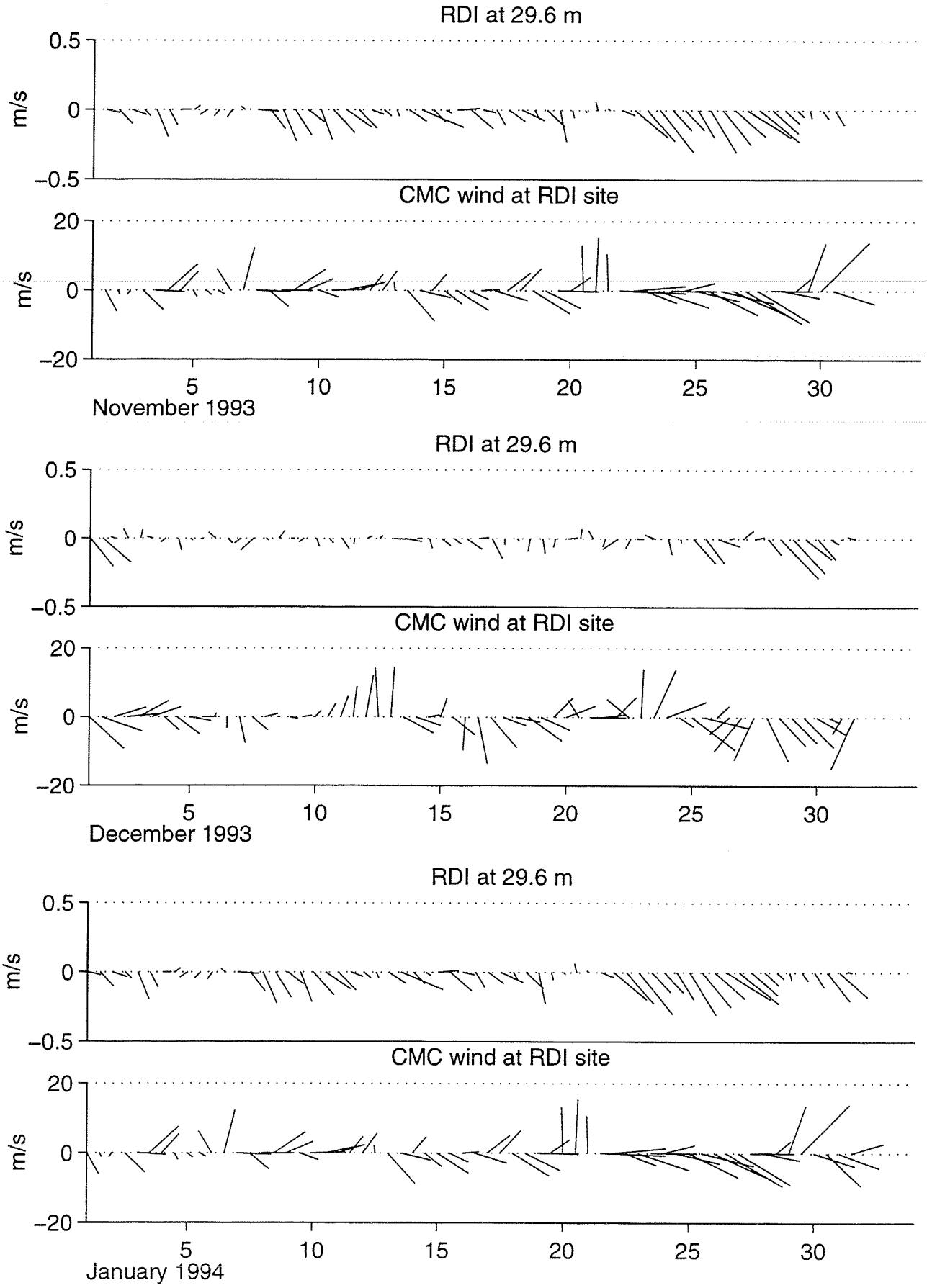
RDI at 29.6 m
0.5
0
−0.5
m/s
CMC wind at RDI site
20
0
−20
m/s
5
10
15
20
25
30
November 1993
RDI at 29.6 m
0.5
0
−0.5
m/s
CMC wind at RDI site
20
0
−20
m/s
5
10
15
20
25
30
December 1993
RDI at 29.6 m
0.5
0
−0.5
m/s
CMC wind at RDI site
20
0
−20
m/s
5
10
15
20
25
30
January 1994

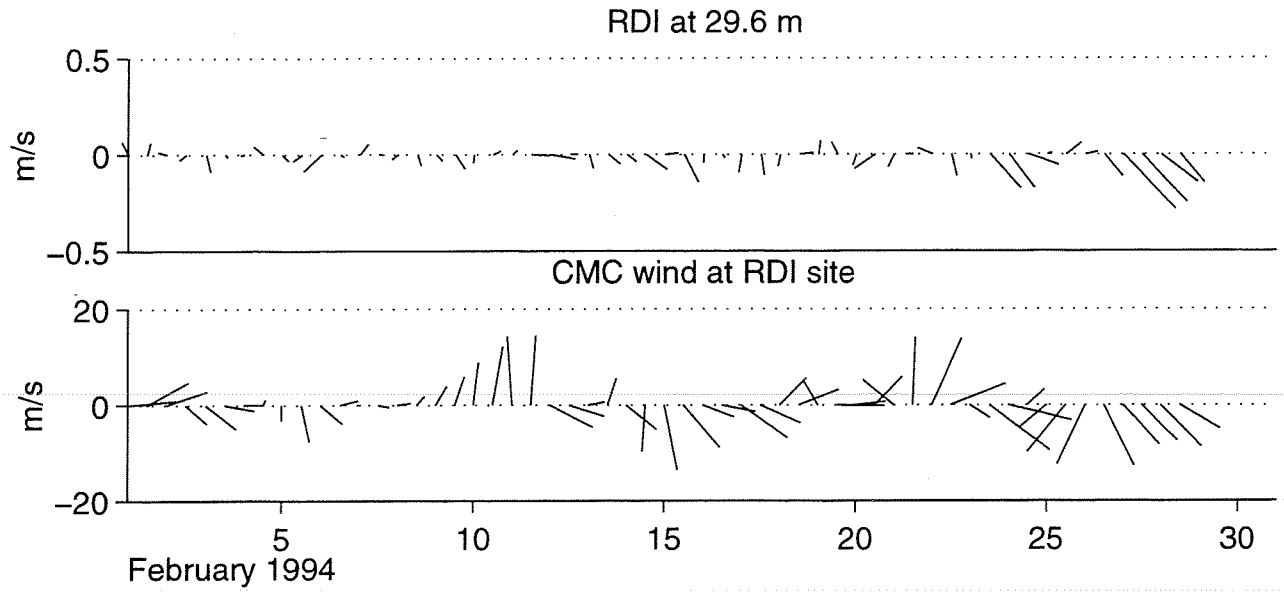
RDI at 29.6 m
0.5
0
−0.5
m/s
CMC wind at RDI site
20
0
−20
m/s
5
10
15
20
25
30
February 1994

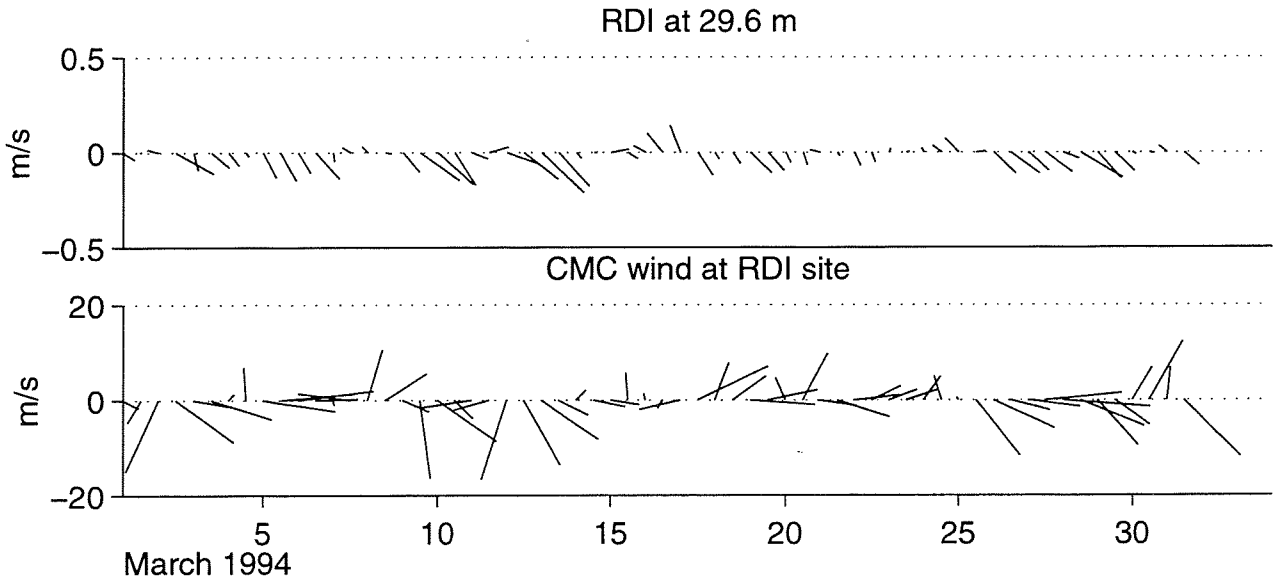
RDI at 29.6 m
0.5
0
−0.5
m/s
CMC wind at RDI site
20
0
−20
m/s
5
10
15
20
25
30
March 1994

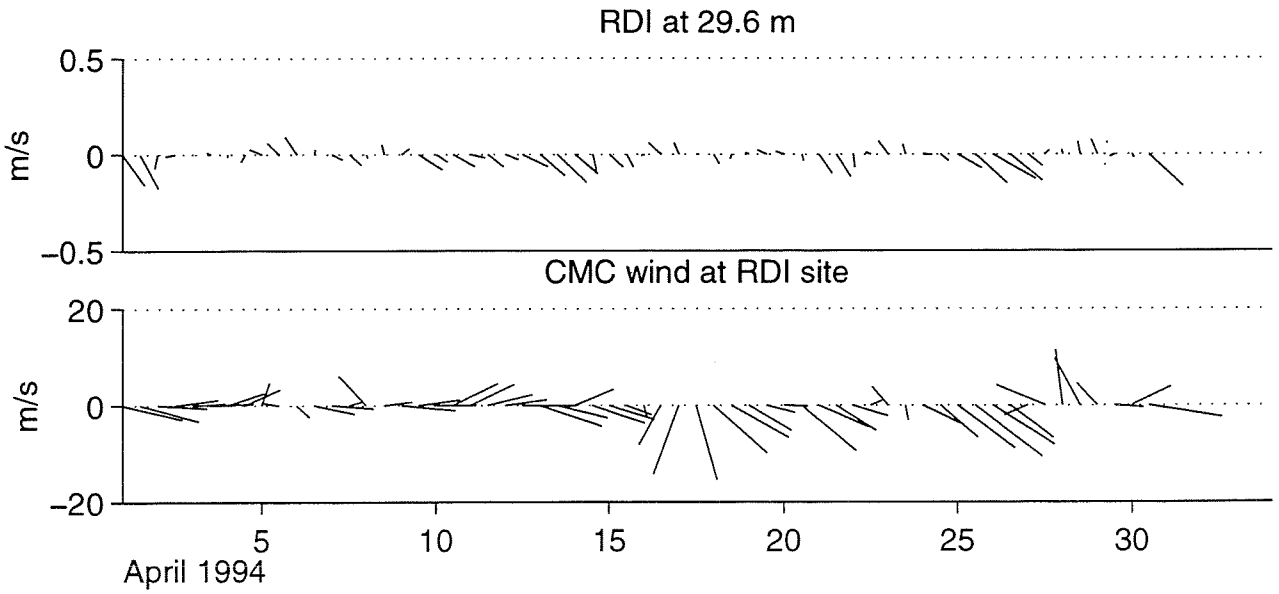
RDI at 29.6 m
0.5
0
−0.5
m/s
CMC wind at RDI site
20
0
−20
m/s
5
10
15
20
25
30
April 1994

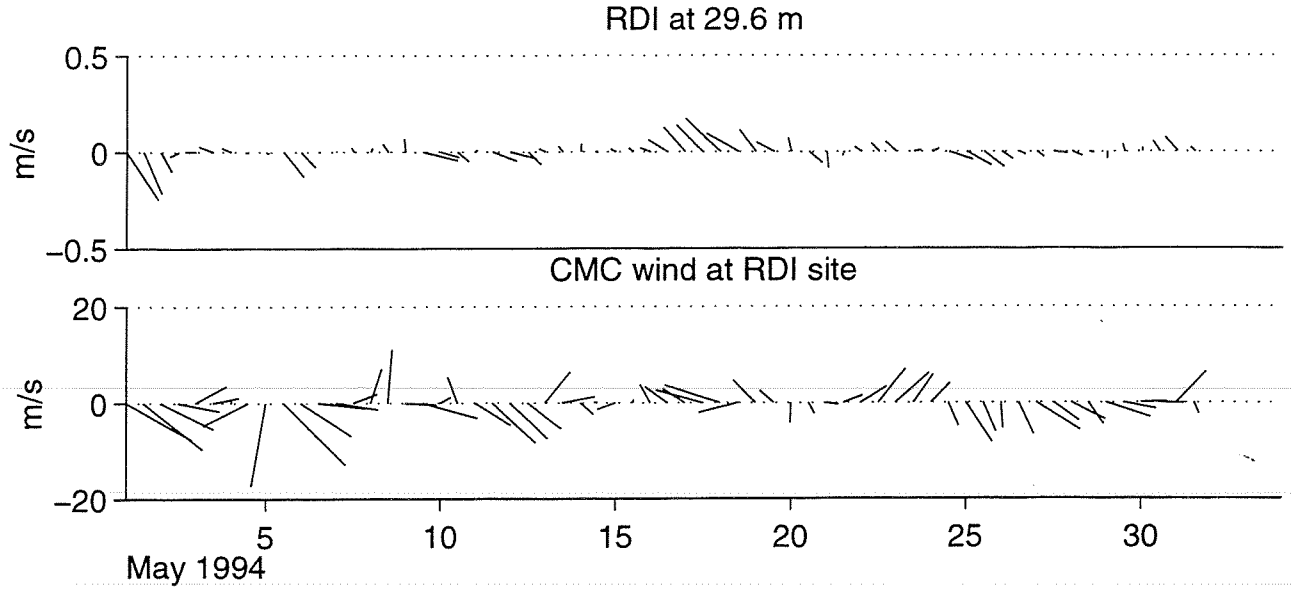
RDI at 29.6 m
0.5
0
−0.5
m/s
CMC wind at RDI site
20
0
−20
m/s
5
10
15
20
25
30
May 1994

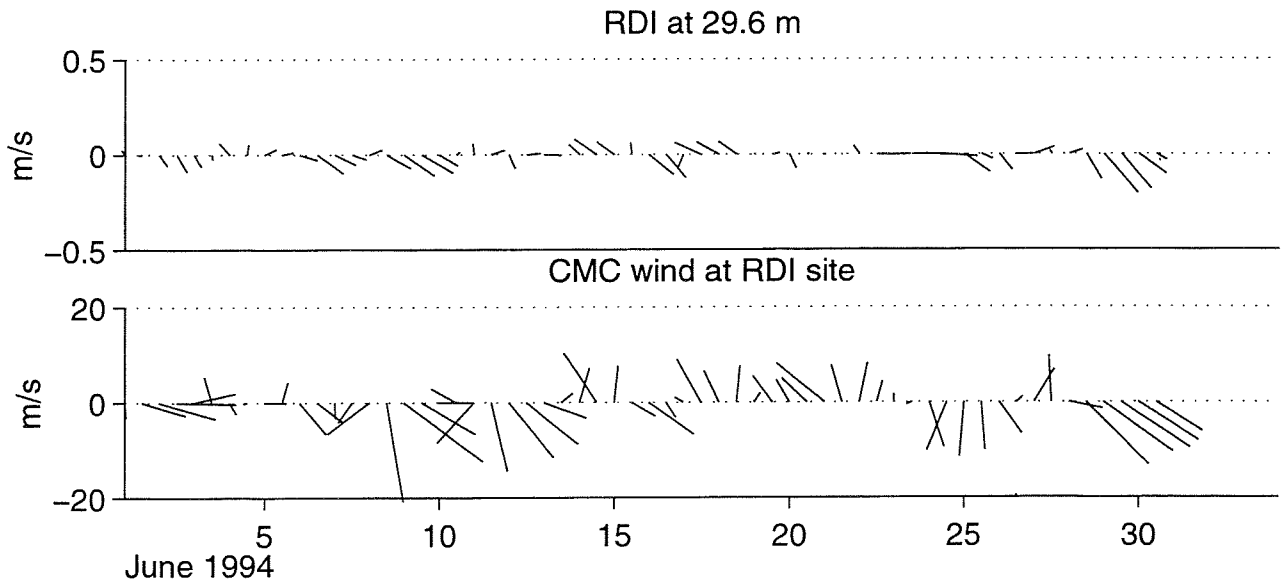
RDI at 29.6 m
0.5
0
−0.5
m/s
CMC wind at RDI site
20
0
−20
m/s
5
10
15
20
25
30
June 1994

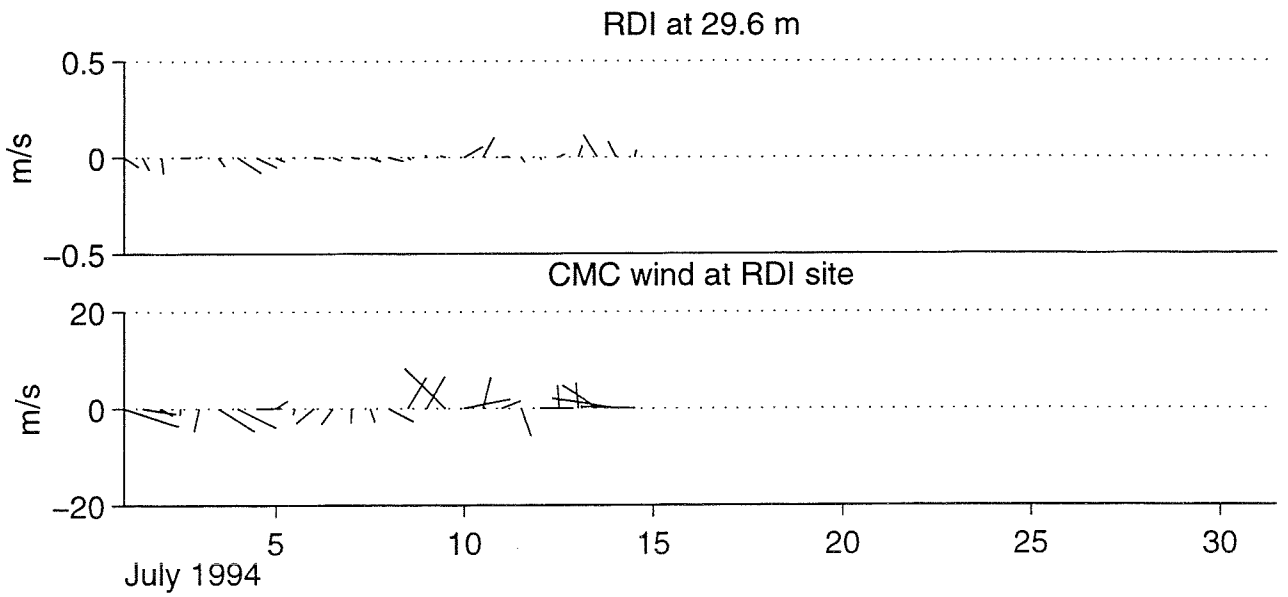
RDI at 29.6 m
0.5
0
−0.5
m/s
CMC wind at RDI site
20
0
−20
m/s
5
10
15
20
25
30
July 1994

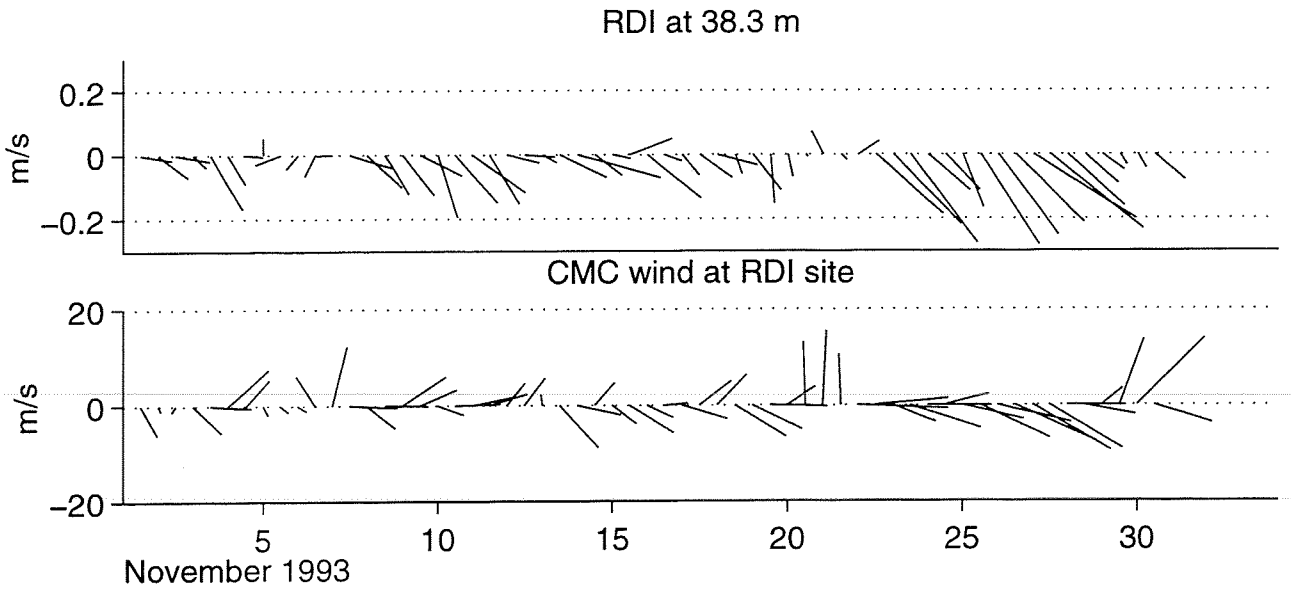
RDI at 38.3 m
0.2
0
−0.2
m/s
CMC wind at RDI site
20
0
−20
m/s
5
10
15
20
25
30
November 1993

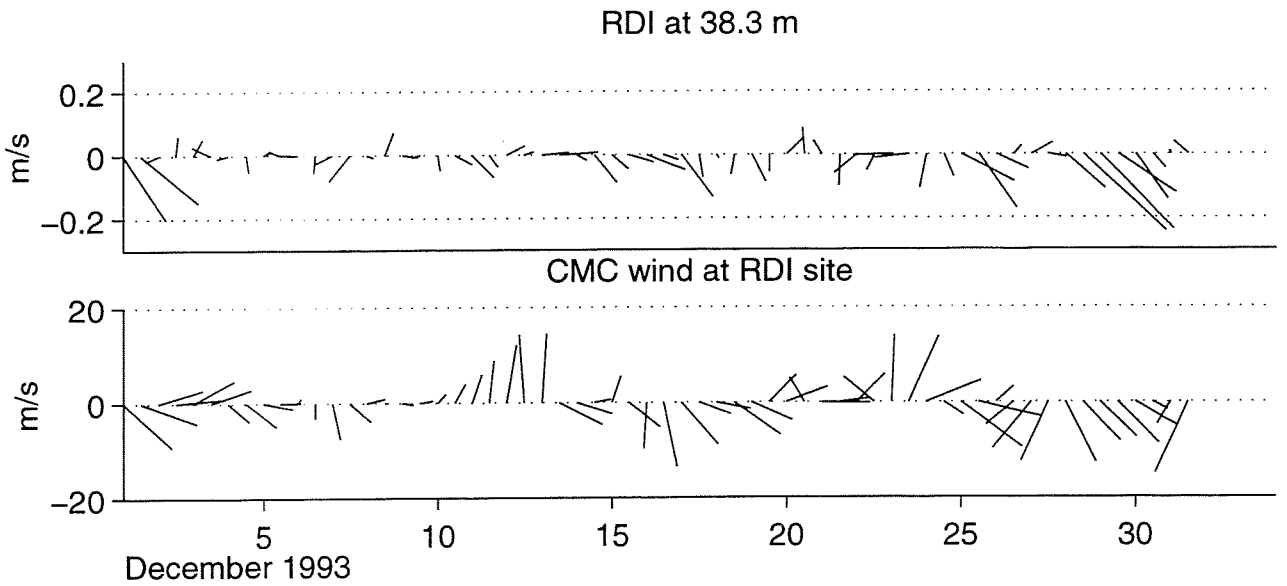
RDI at 38.3 m
0.2
0
−0.2
m/s
CMC wind at RDI site
20
0
−20
m/s
5
10
15
20
25
30
December 1993

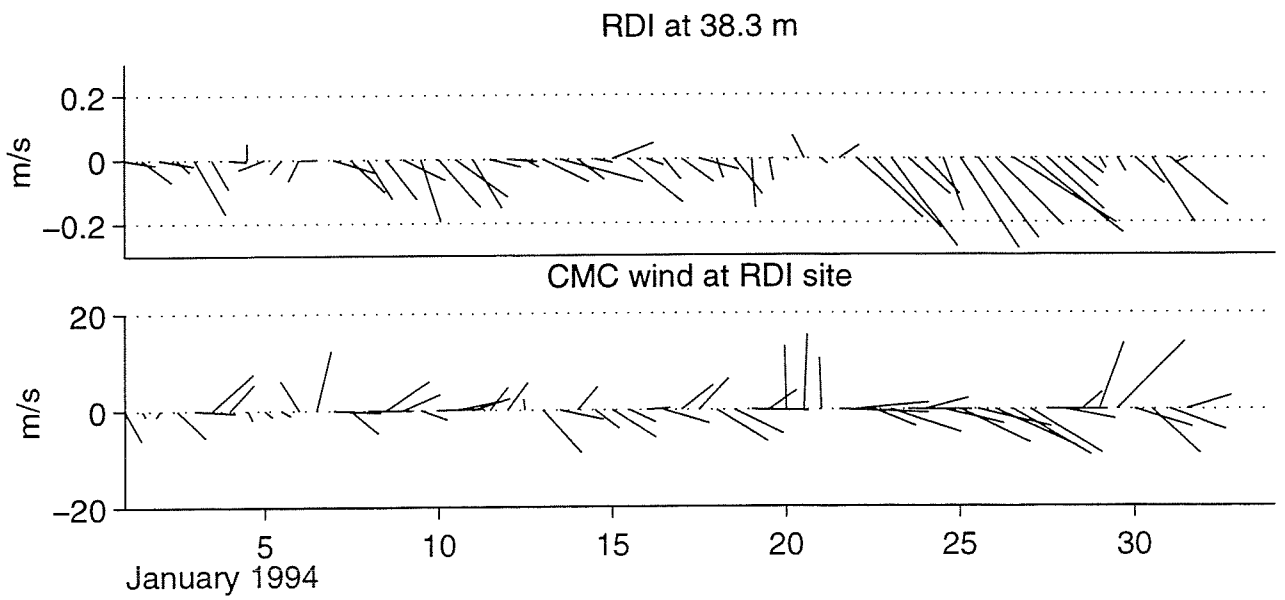
RDI at 38.3 m
0.2
0
−0.2
m/s
CMC wind at RDI site
20
0
−20
m/s
5
10
15
20
25
30
January 1994

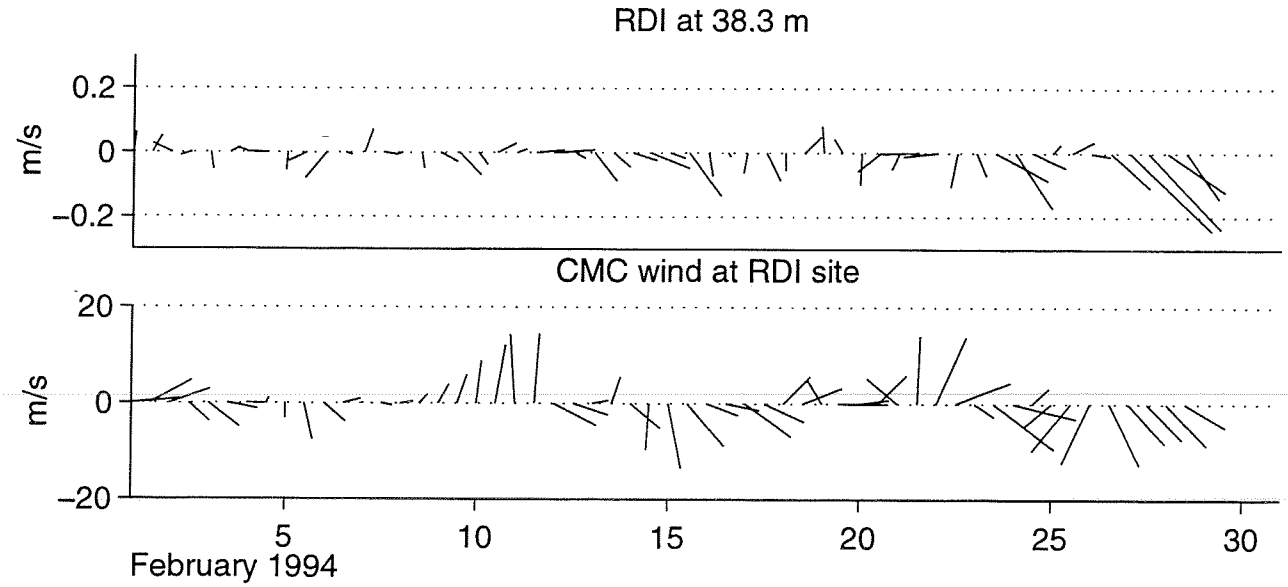
RDI at 38.3 m
0.2
0
−0.2
m/s
CMC wind at RDI site
20
0
−20
m/s
5
10
15
20
25
30
February 1994

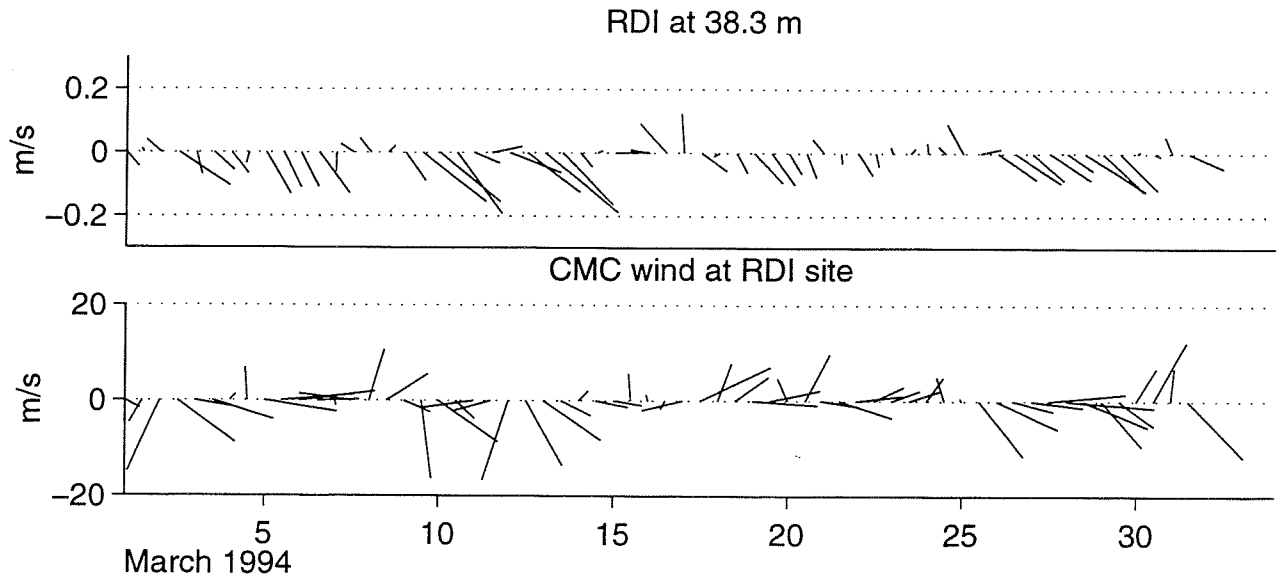
RDI at 38.3 m
0.2
0
−0.2
m/s
CMC wind at RDI site
20
0
−20
m/s
5
10
15
20
25
30
March 1994

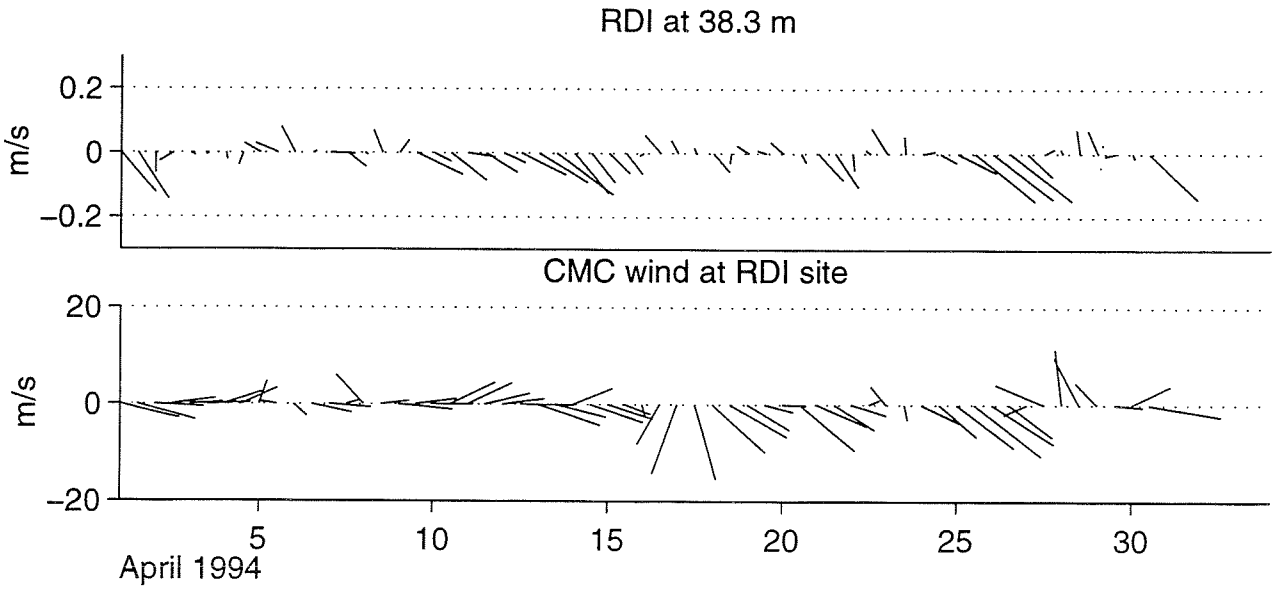
RDI at 38.3 m
0.2
0
−0.2
m/s
CMC wind at RDI site
20
0
−20
m/s
5
10
15
20
25
30
April 1994

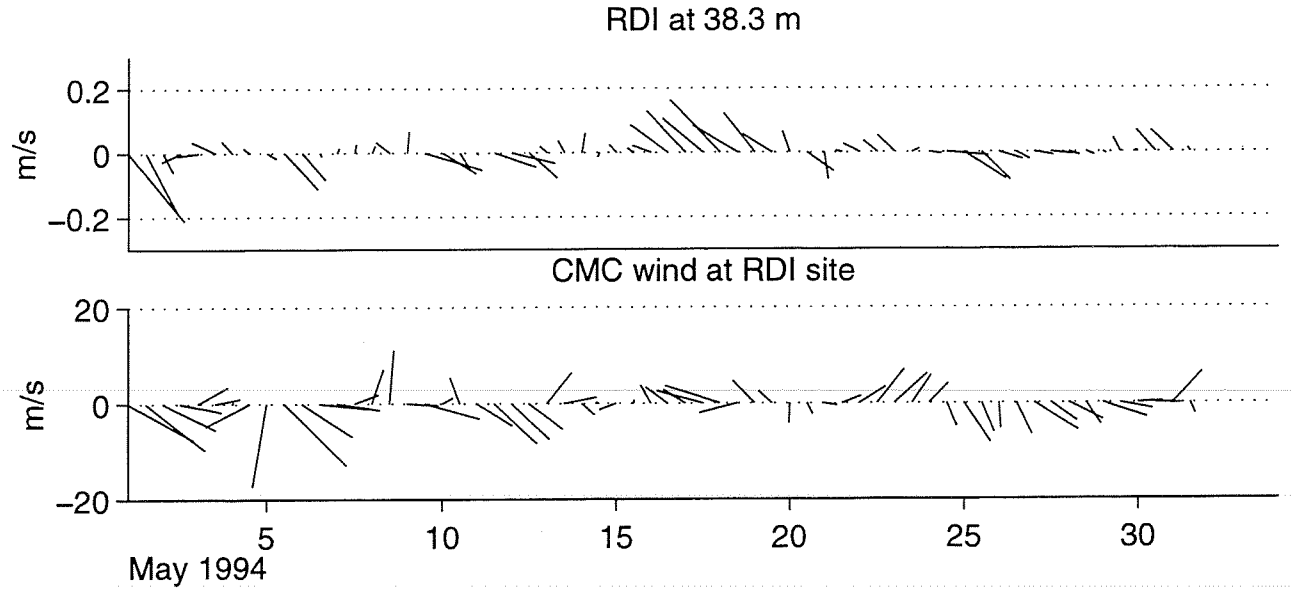
RDI at 38.3 m
0.2
0
−0.2
m/s
CMC wind at RDI site
20
0
−20
m/s
5
10
15
20
25
30
May 1994

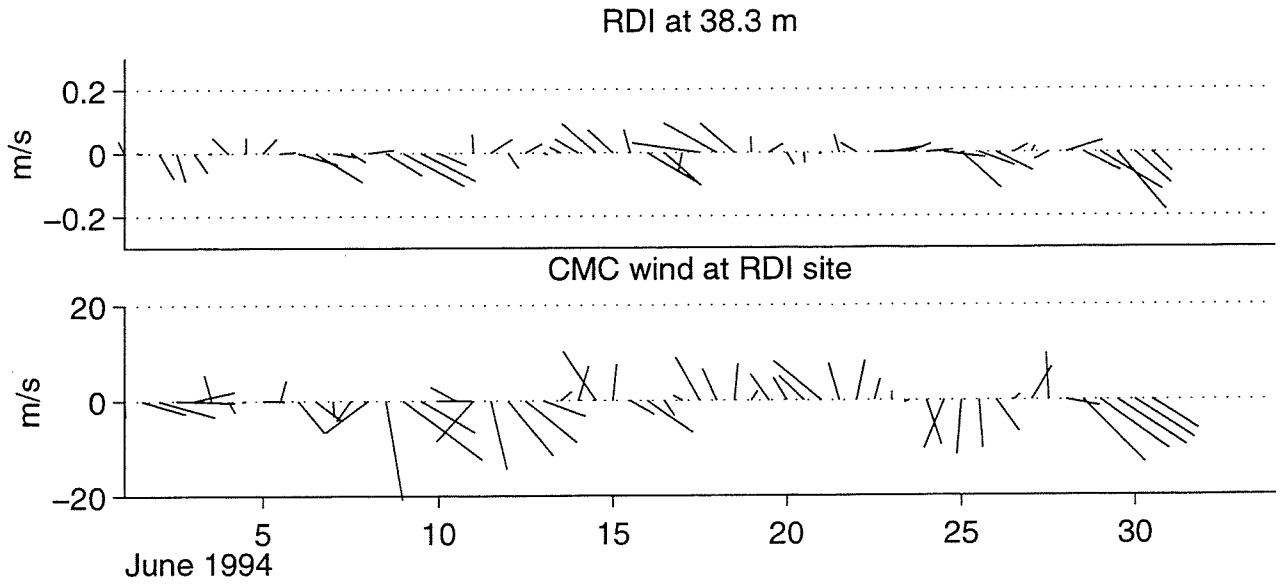
RDI at 38.3 m
0.2
0
−0.2
m/s
CMC wind at RDI site
20
0
−20
m/s
5
10
15
20
25
30
June 1994

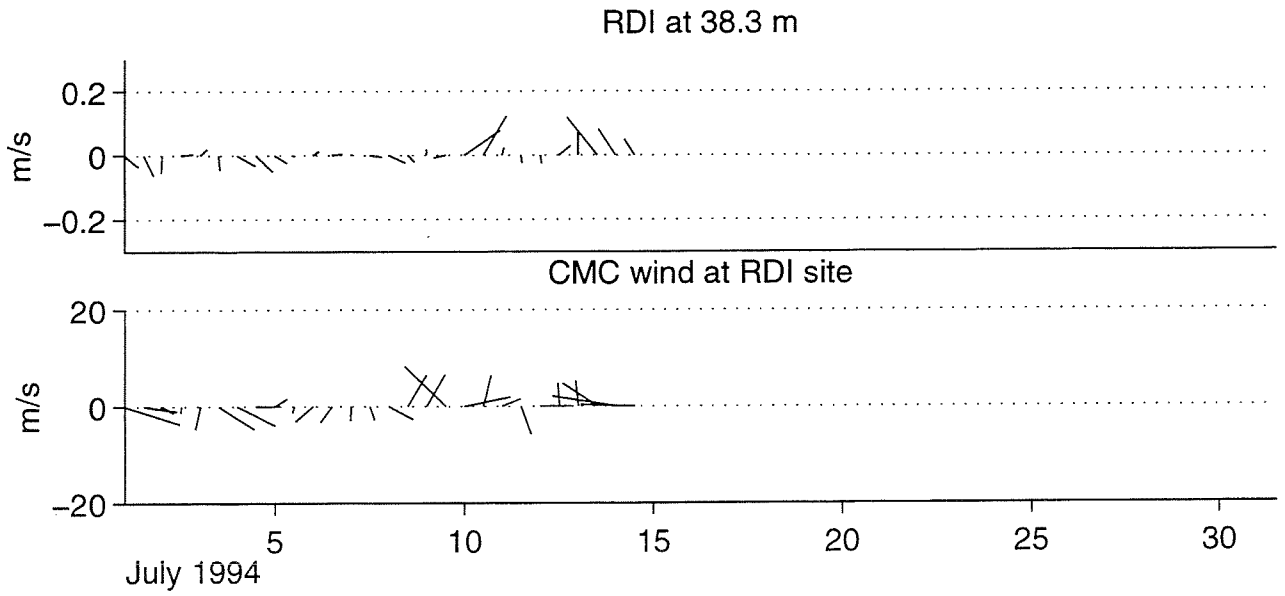
RDI at 38.3 m
0.2
0
−0.2
m/s
CMC wind at RDI site
20
0
−20
m/s
5
10
15
20
25
30
July 1994

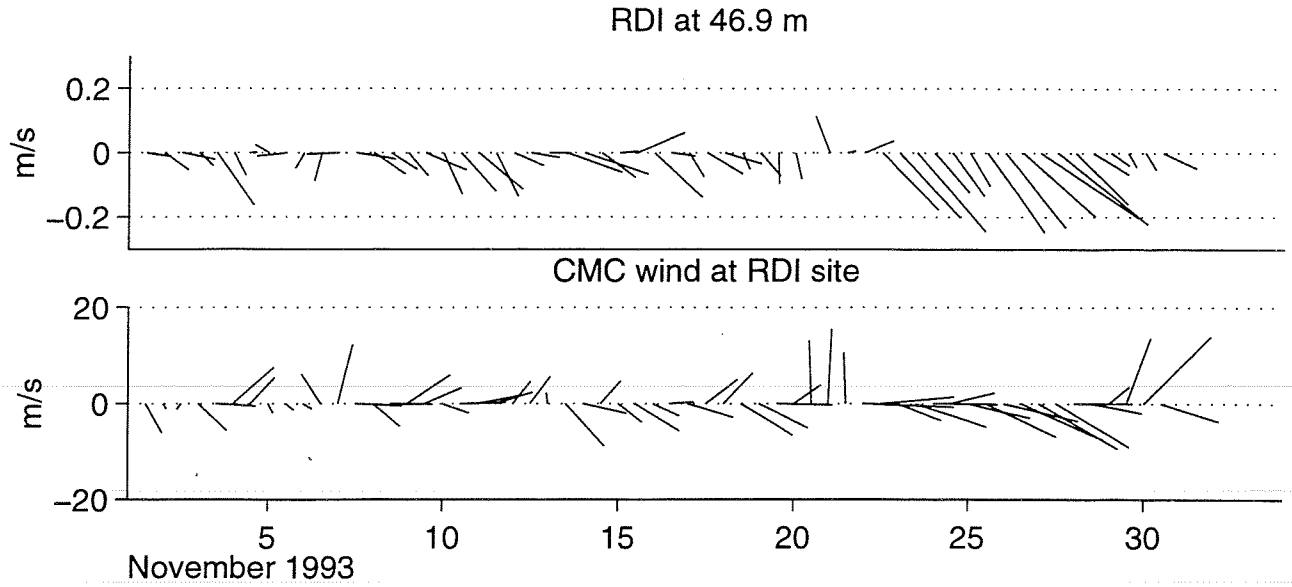
RDI at 46.9 m
0.2
0
−0.2
m/s
CMC wind at RDI site
20
0
−20
m/s
5
10
15
20
25
30
November 1993

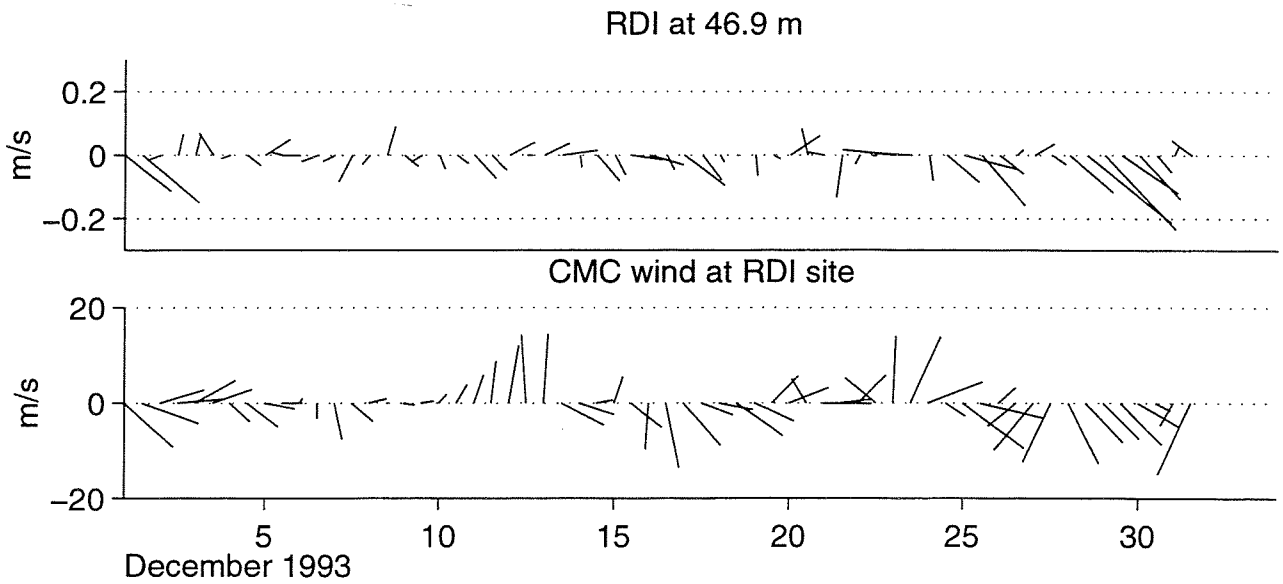
RDI at 46.9 m
0.2
0
−0.2
m/s
CMC wind at RDI site
20
0
−20
m/s
5
10
15
20
25
30
December 1993

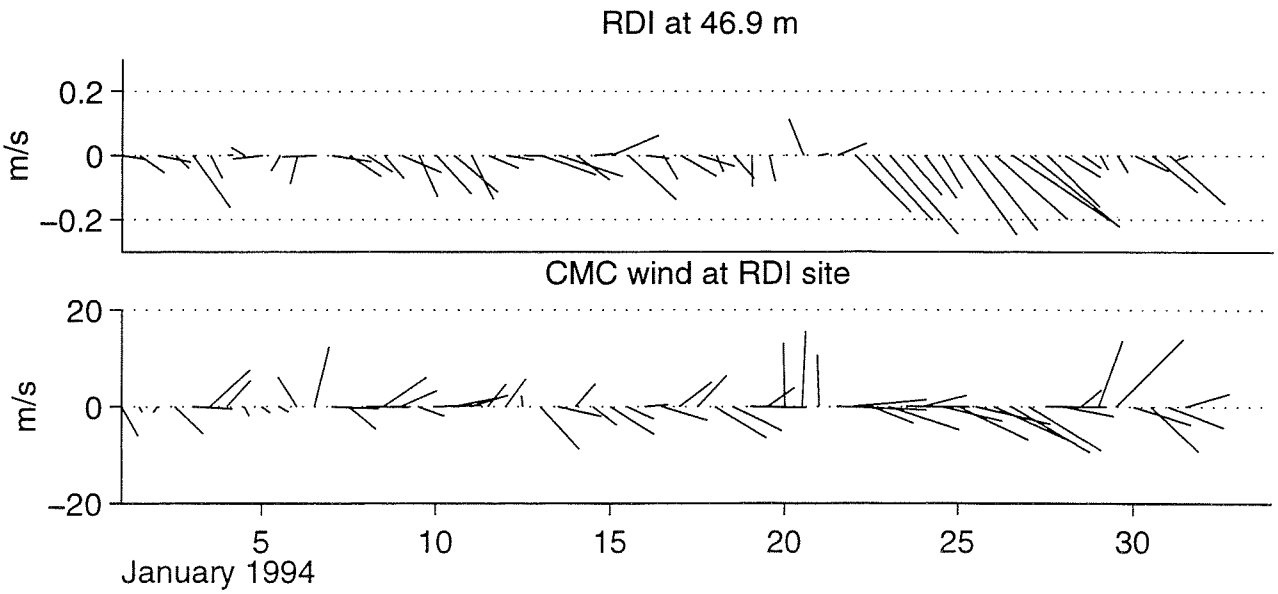
RDI at 46.9 m
0.2
0
−0.2
m/s
CMC wind at RDI site
20
0
−20
m/s
5
10
15
20
25
30
January 1994

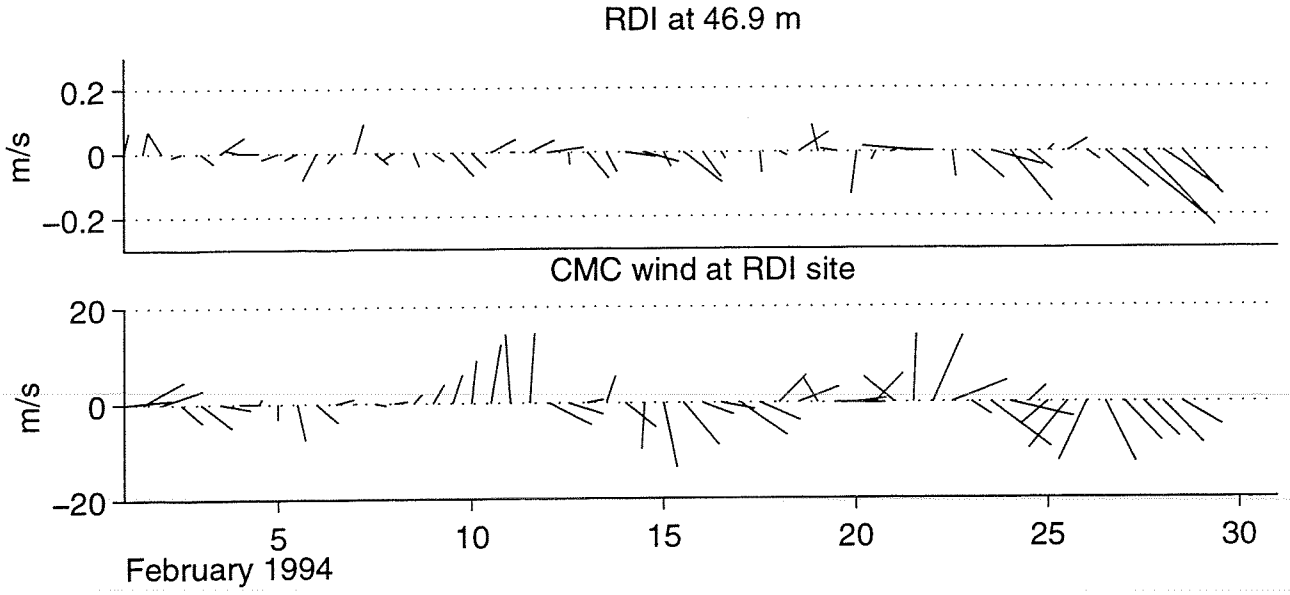
RDI at 46.9 m
0.2
0
−0.2
m/s
CMC wind at RDI site
20
0
−20
m/s
5
10
15
20
25
30
February 1994

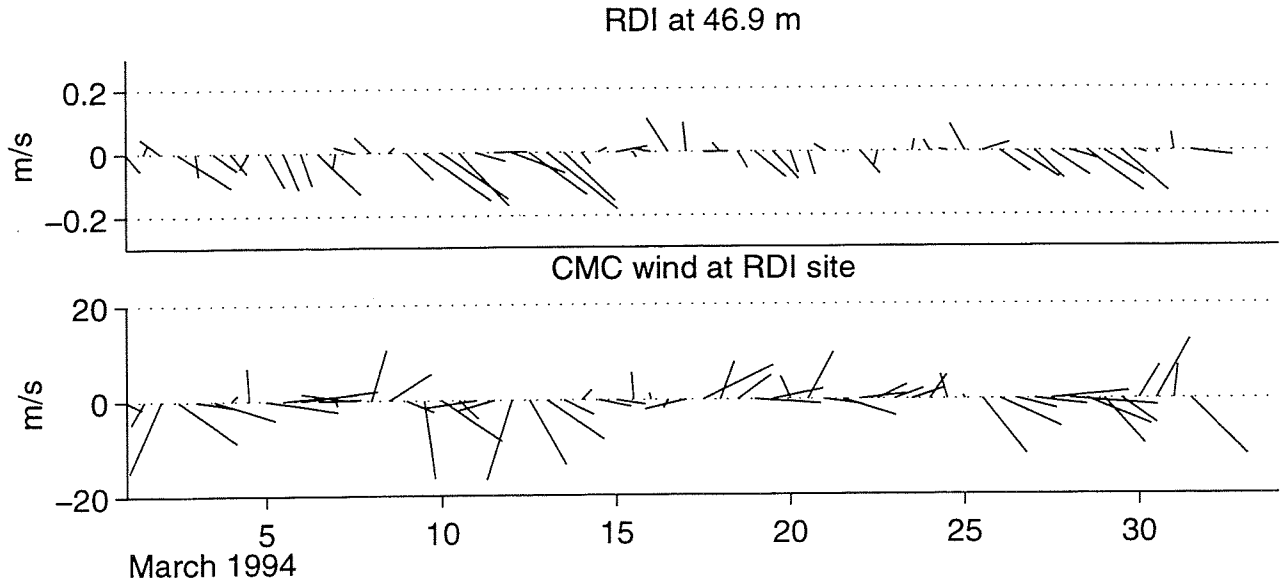
RDI at 46.9 m
0.2
0
−0.2
m/s
CMC wind at RDI site
20
0
−20
m/s
5
10
15
20
25
30
March 1994

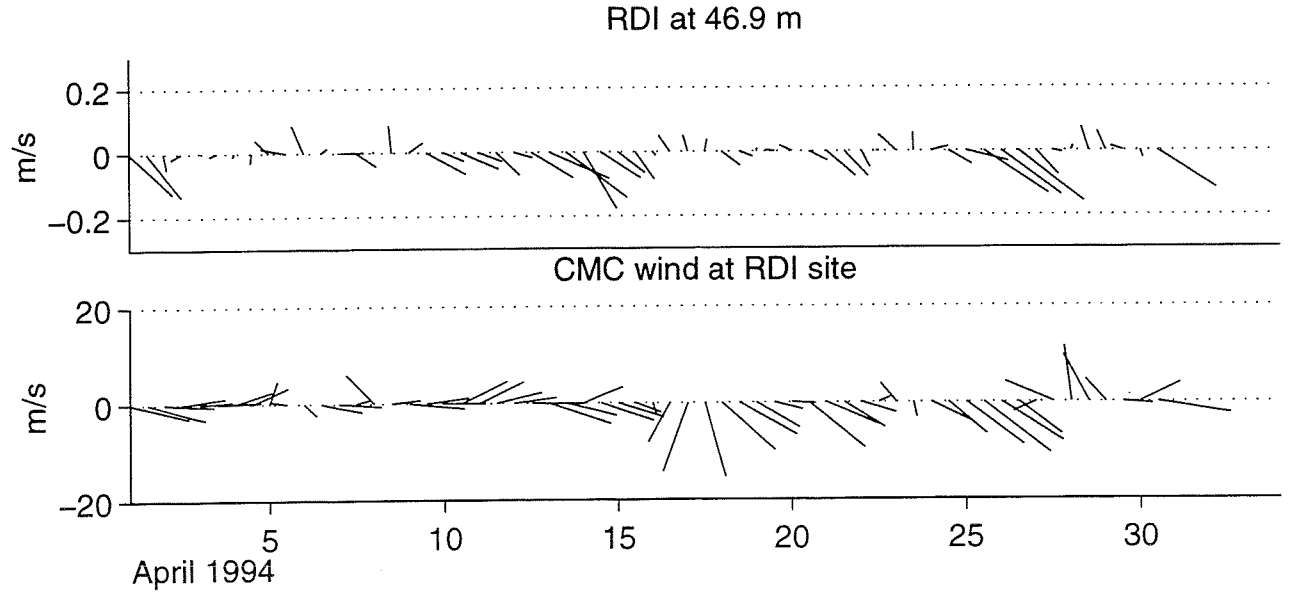
RDI at 46.9 m
0.2
0
−0.2
m/s
CMC wind at RDI site
20
0
−20
m/s
5
10
15
20
25
30
April 1994

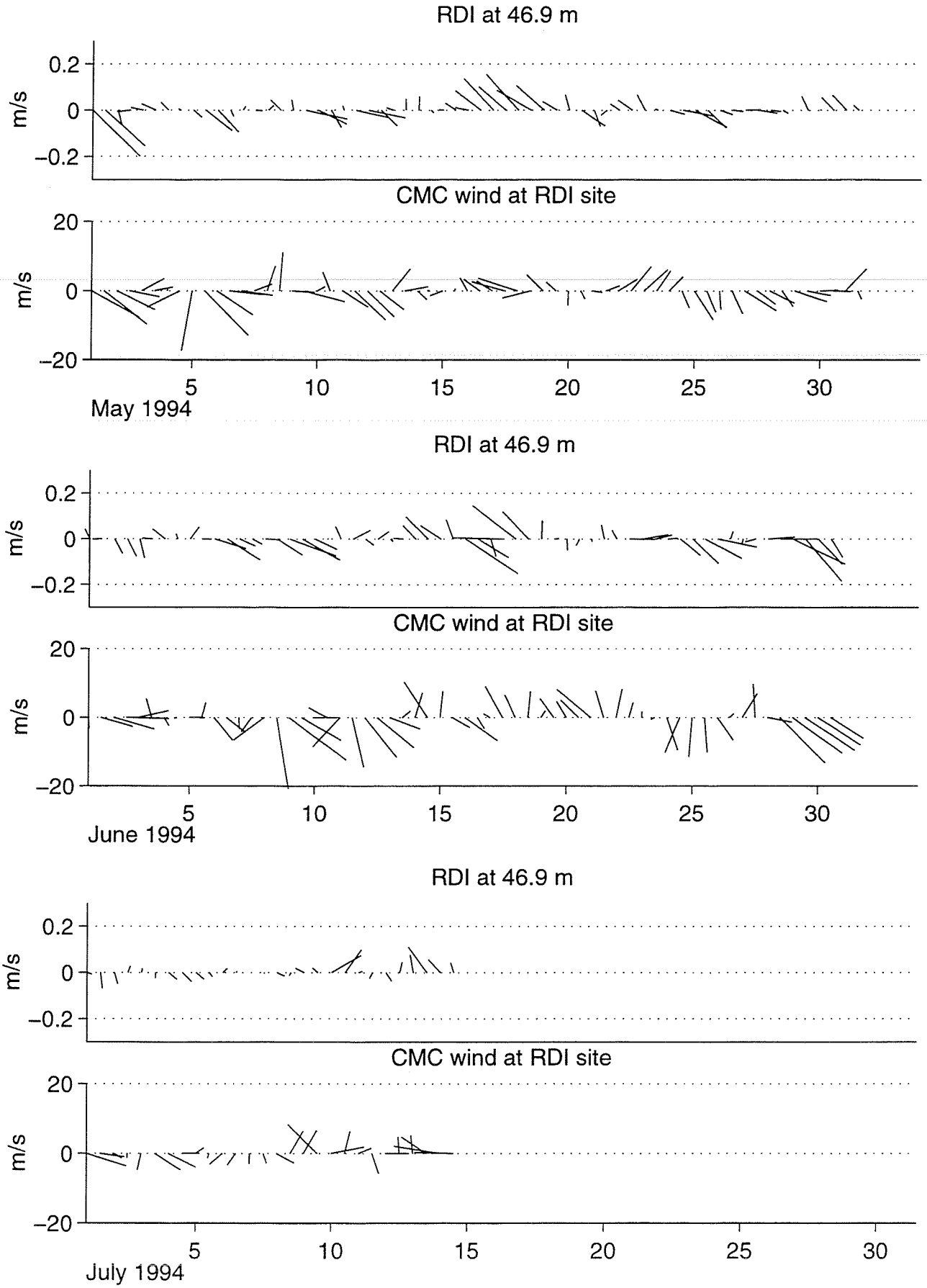
RDI at 46.9 m
0.2
0
−0.2
m/s
CMC wind at RDI site
20
0
−20
m/s
5
10
15
20
25
30
May 1994
RDI at 46.9 m
0.2
0
−0.2
m/s
CMC wind at RDI site
20
0
−20
m/s
5
10
15
20
25
30
June 1994
RDI at 46.9 m
0.2
0
−0.2
m/s
CMC wind at RDI site
20
0
−20
m/s
5
10
15
20
25
30
July 1994

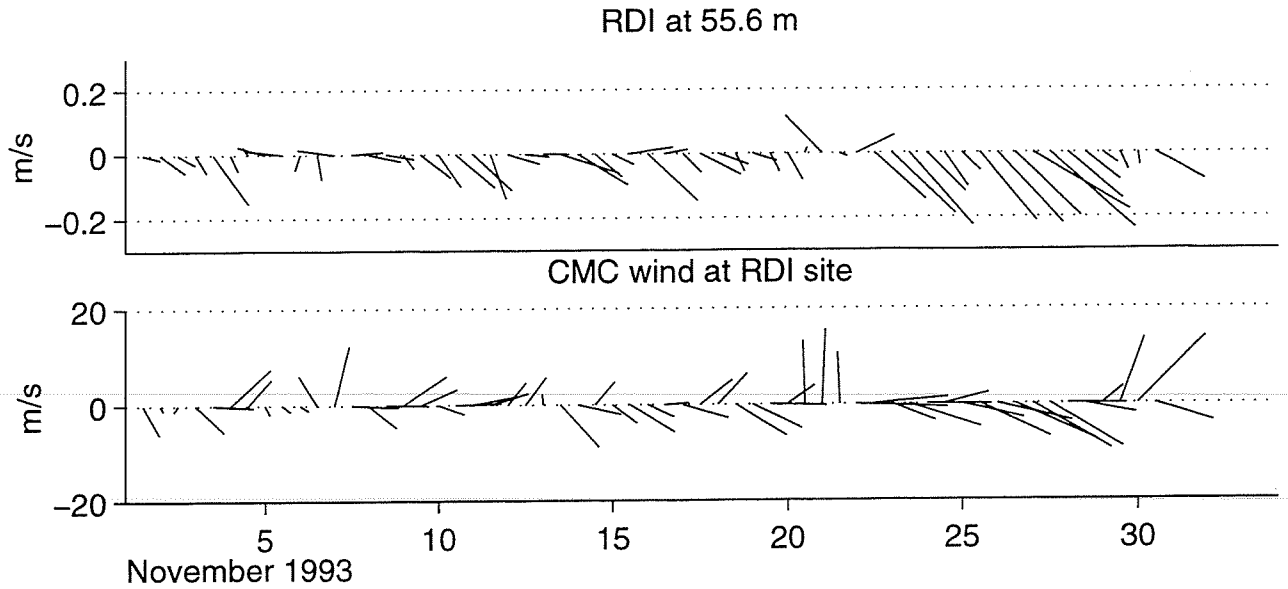
RDI at 55.6 m
0.2
0
−0.2
m/s
CMC wind at RDI site
20
0
−20
m/s
5
10
15
20
25
30
November 1993

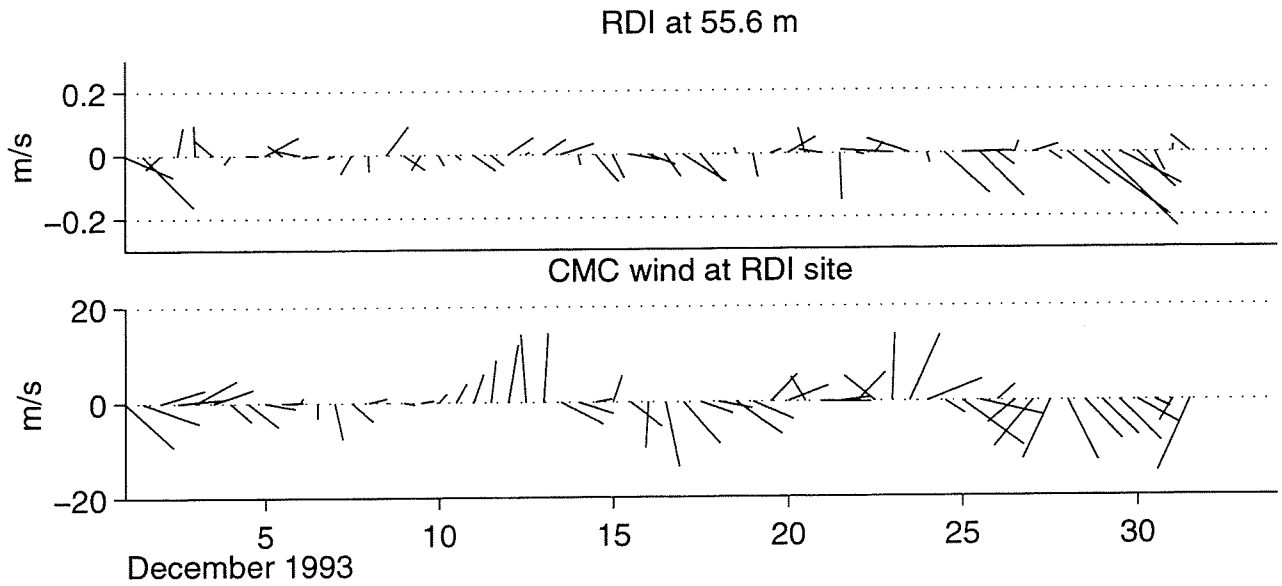
RDI at 55.6 m
0.2
0
−0.2
m/s
CMC wind at RDI site
20
0
−20
m/s
5
10
15
20
25
30
December 1993

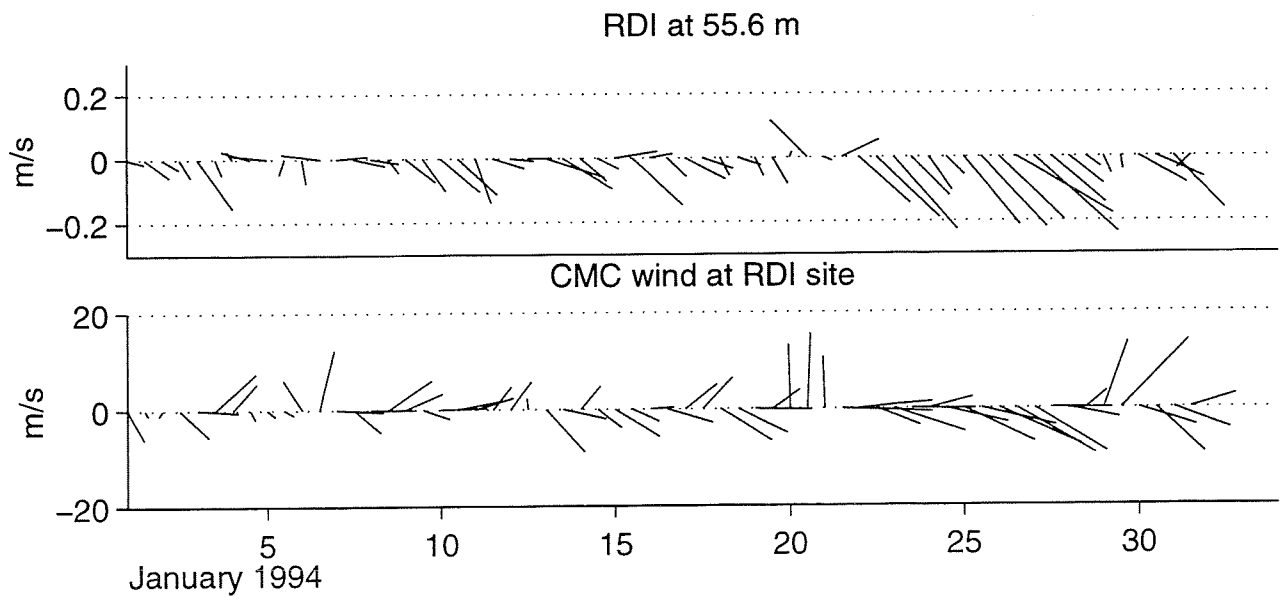
RDI at 55.6 m
0.2
0
−0.2
m/s
CMC wind at RDI site
20
0
−20
m/s
5
10
15
20
25
30
January 1994

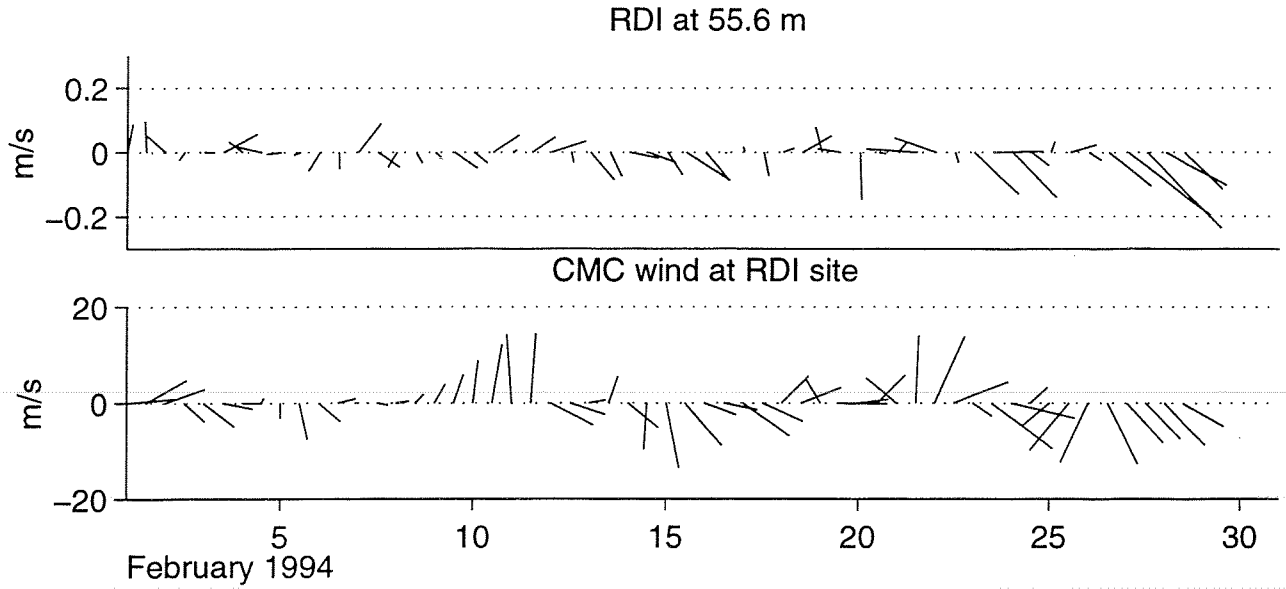
RDI at 55.6 m
0.2
0
−0.2
m/s
CMC wind at RDI site
20
0
−20
m/s
5
10
15
20
25
30
February 1994

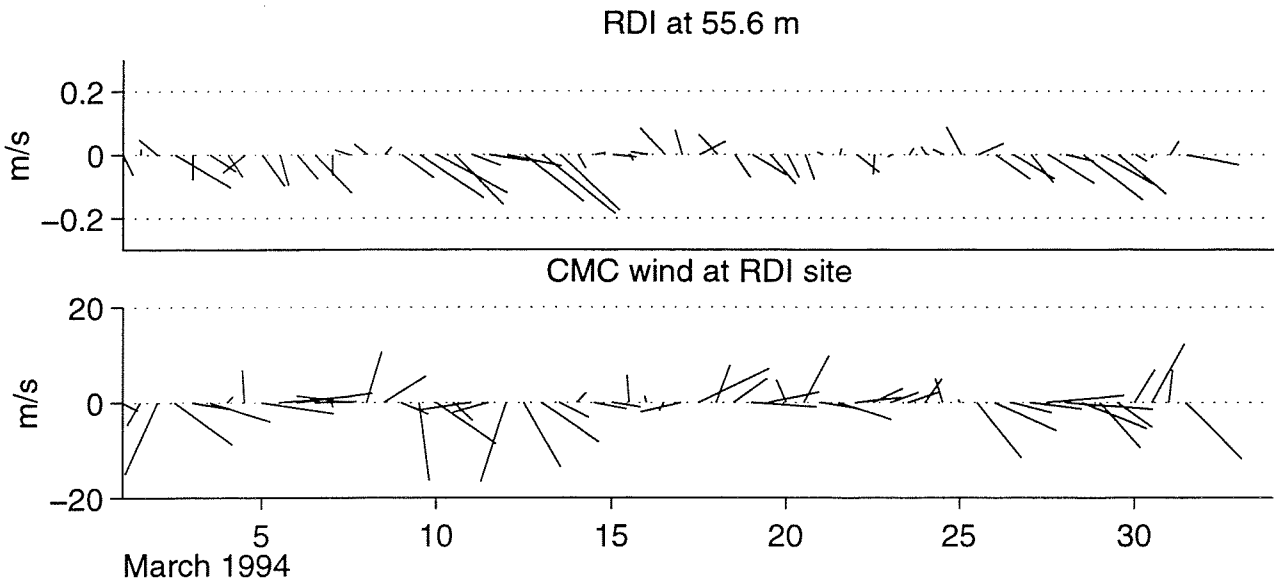
RDI at 55.6 m
0.2
0
−0.2
m/s
CMC wind at RDI site
20
0
−20
m/s
5
10
15
20
25
30
March 1994

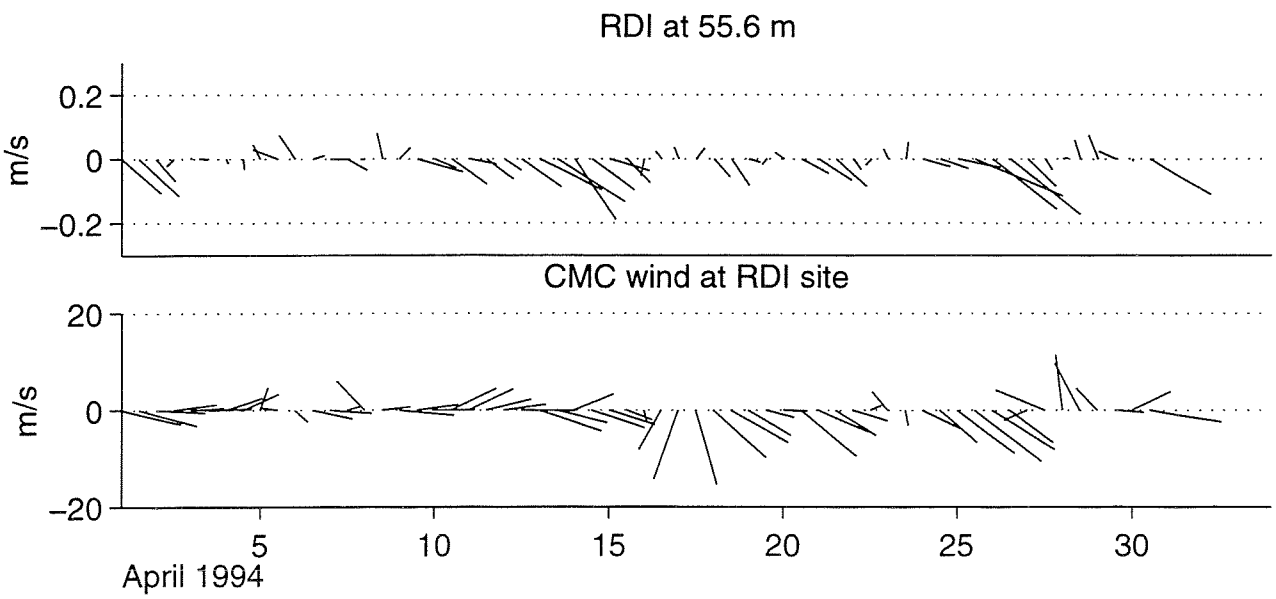
RDI at 55.6 m
0.2
0
−0.2
m/s
CMC wind at RDI site
20
0
−20
m/s
5
10
15
20
25
30
April 1994

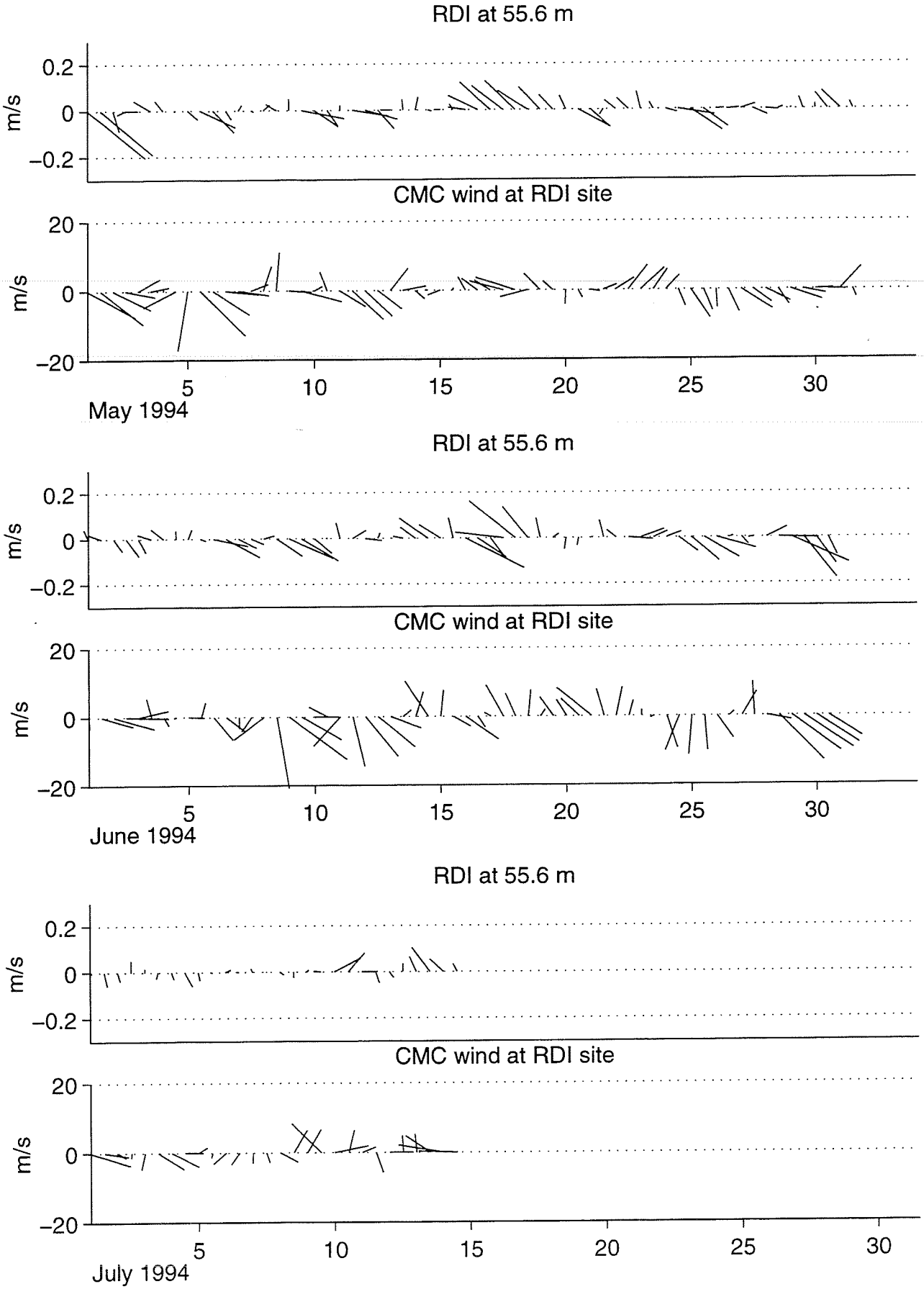
RDI at 55.6 m
0.2
0
−0.2
m/s
CMC wind at RDI site
20
0
−20
m/s
5
10
15
20
25
30
May 1994
RDI at 55.6 m
0.2
0
−0.2
m/s
CMC wind at RDI site
20
0
−20
m/s
5
10
15
20
25
30
June 1994
RDI at 55.6 m
0.2
0
−0.2
m/s
CMC wind at RDI site
20
0
−20
m/s
5
10
15
20
25
30
July 1994

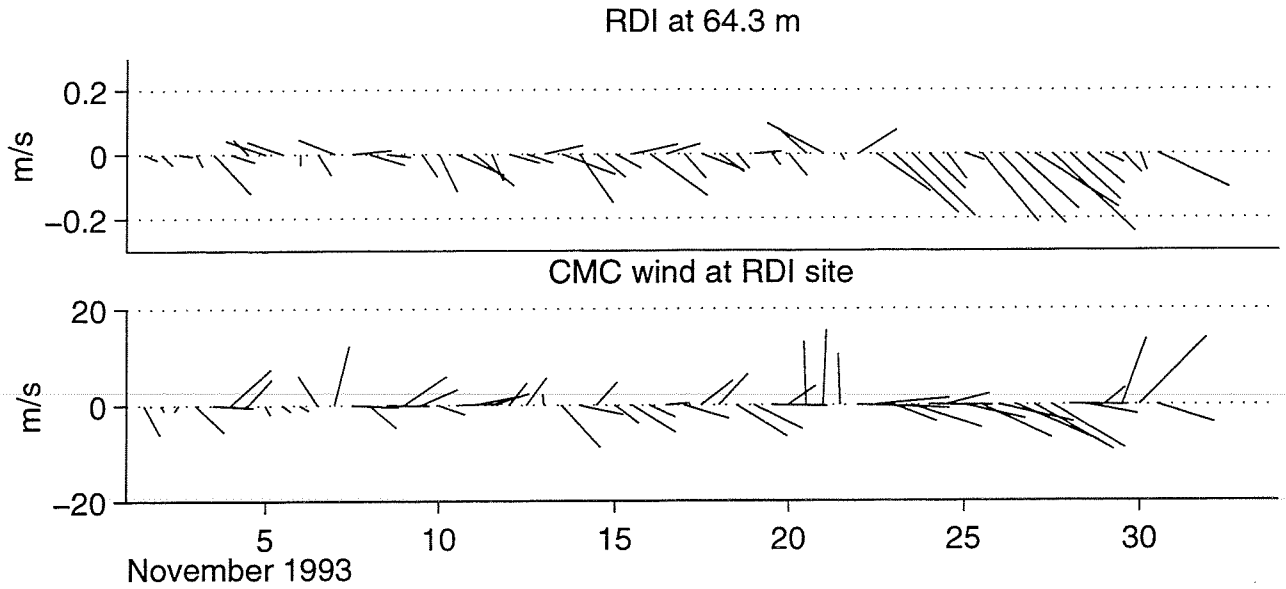
RDI at 64.3 m
0.2
0
−0.2
m/s
CMC wind at RDI site
20
0
−20
m/s
5
10
15
20
25
30
November 1993

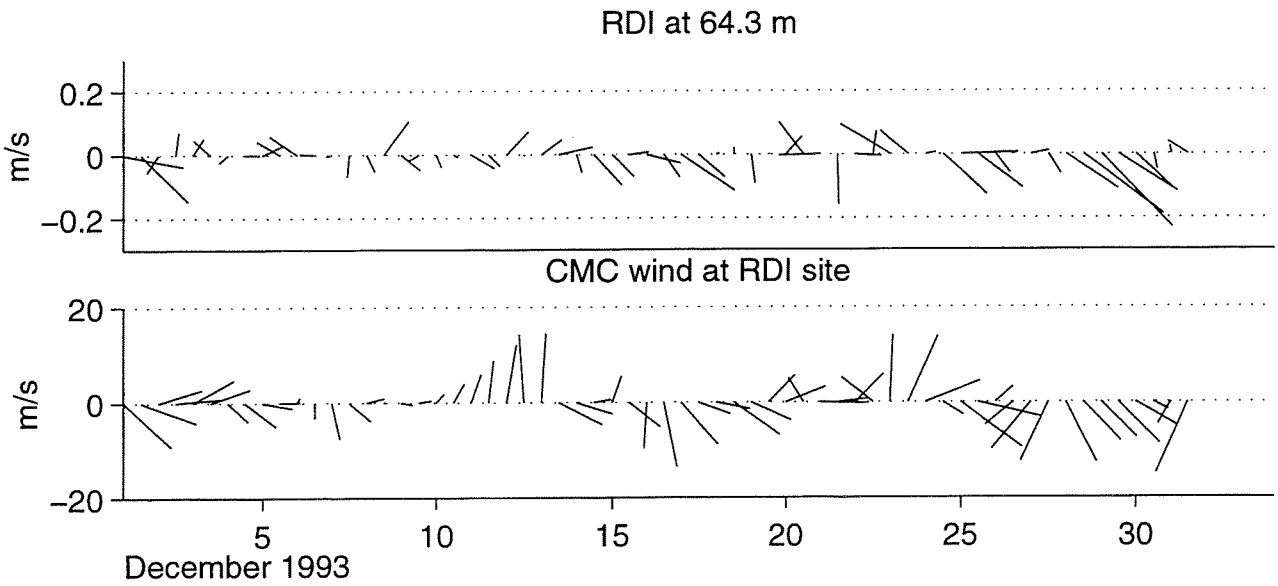
RDI at 64.3 m
0.2
0
−0.2
m/s
CMC wind at RDI site
20
0
−20
m/s
5
10
15
20
25
30
December 1993

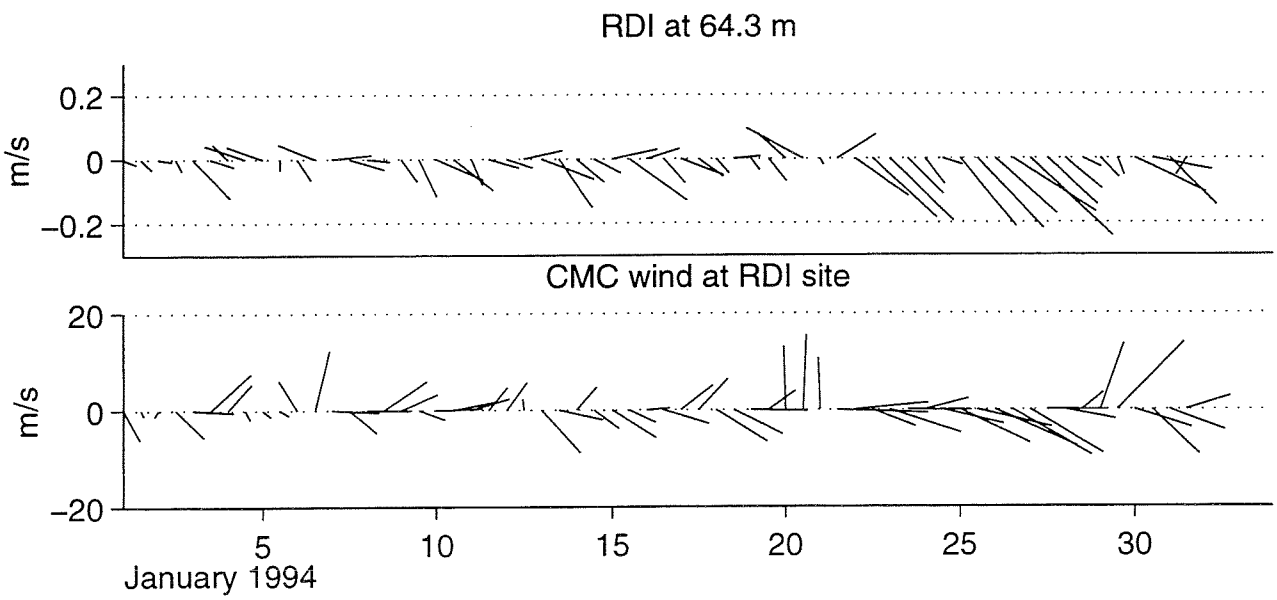
RDI at 64.3 m
0.2
0
−0.2
m/s
CMC wind at RDI site
20
0
−20
m/s
5
10
15
20
25
30
January 1994

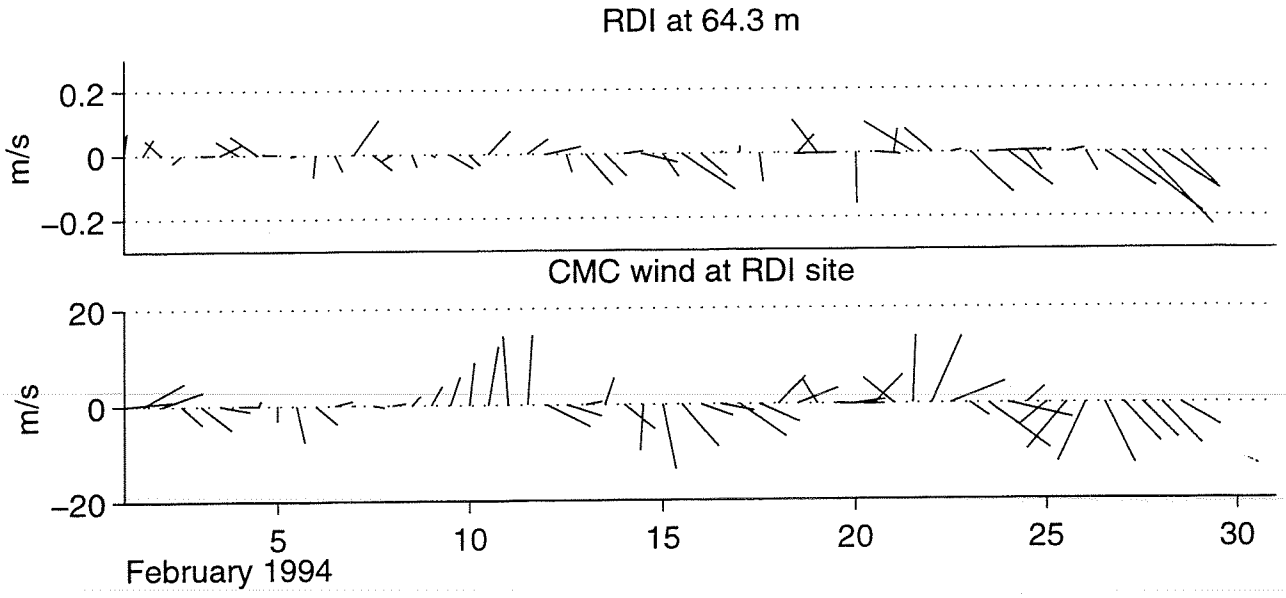
RDI at 64.3 m
0.2
0
−0.2
m/s
CMC wind at RDI site
20
0
−20
m/s
5
10
15
20
25
30
February 1994

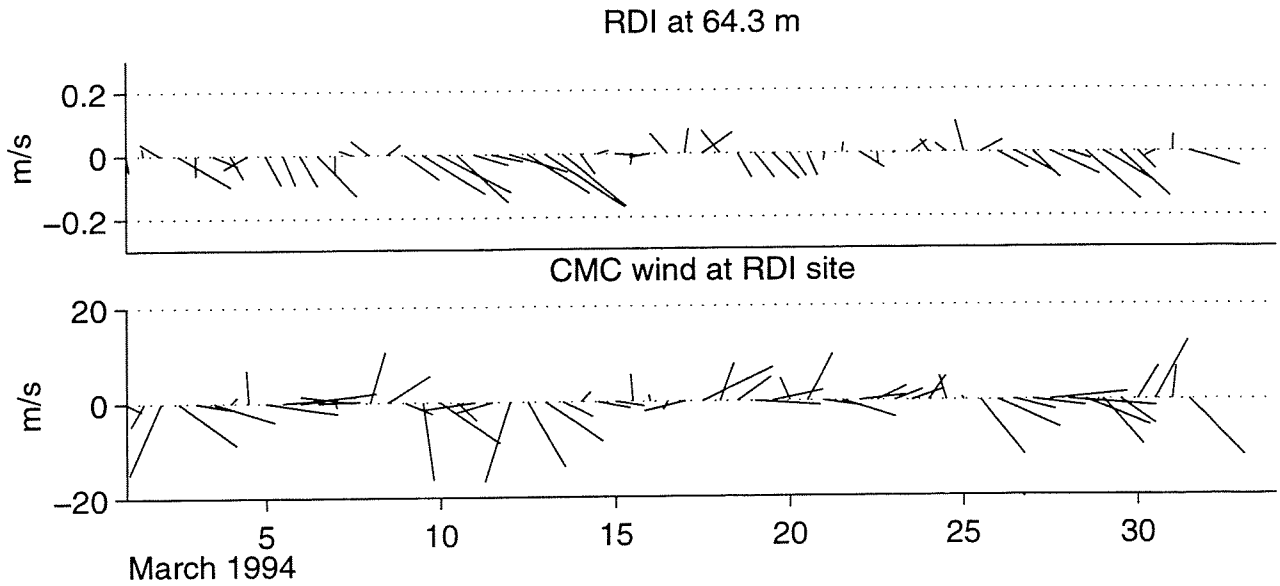
RDI at 64.3 m
0.2
0
−0.2
m/s
CMC wind at RDI site
20
0
−20
m/s
5
10
15
20
25
30
March 1994

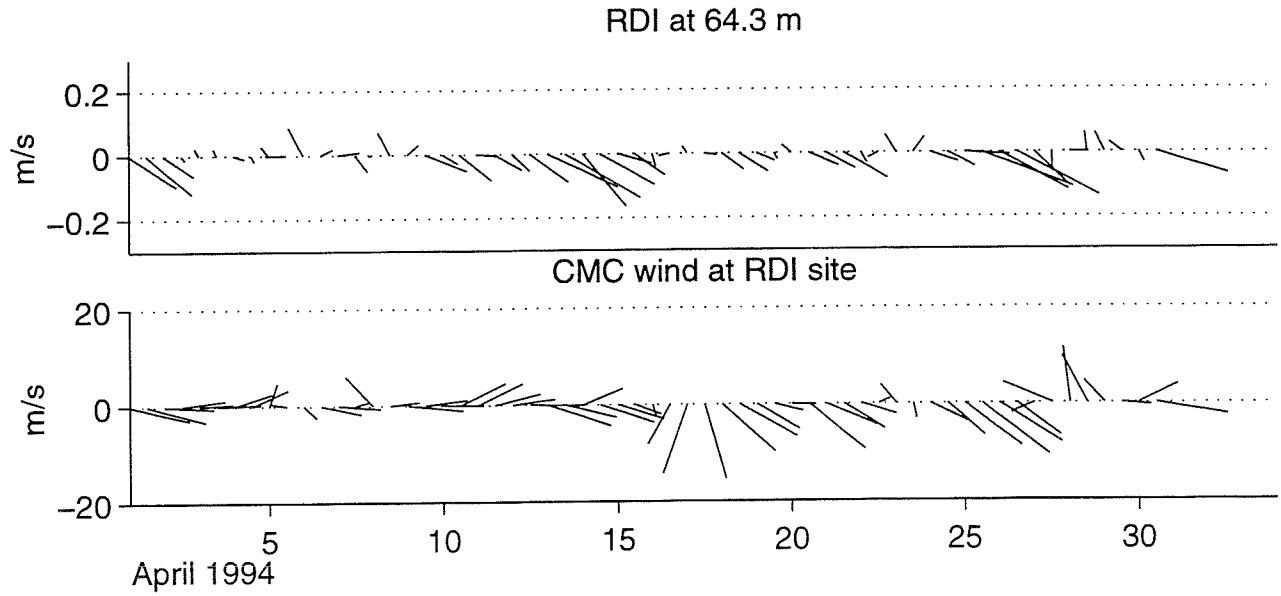
RDI at 64.3 m
0.2
0
−0.2
m/s
CMC wind at RDI site
20
0
−20
m/s
5
10
15
20
25
30
April 1994

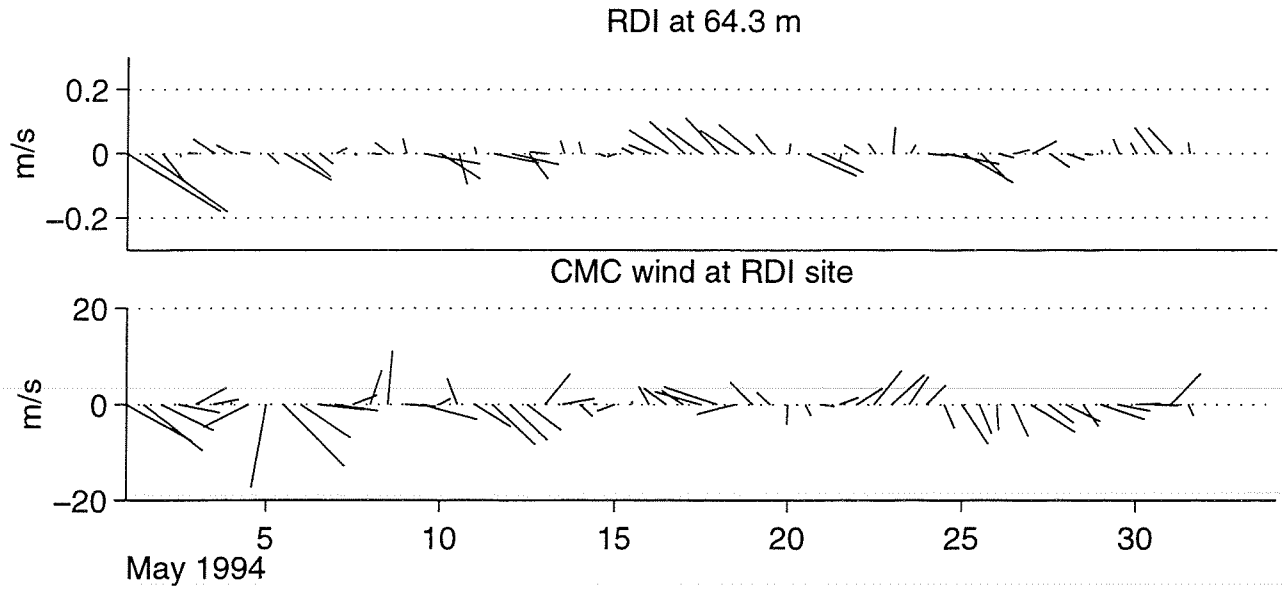
RDI at 64.3 m
0.2
0
−0.2
m/s
CMC wind at RDI site
20
0
−20
m/s
5
10
15
20
25
30
May 1994

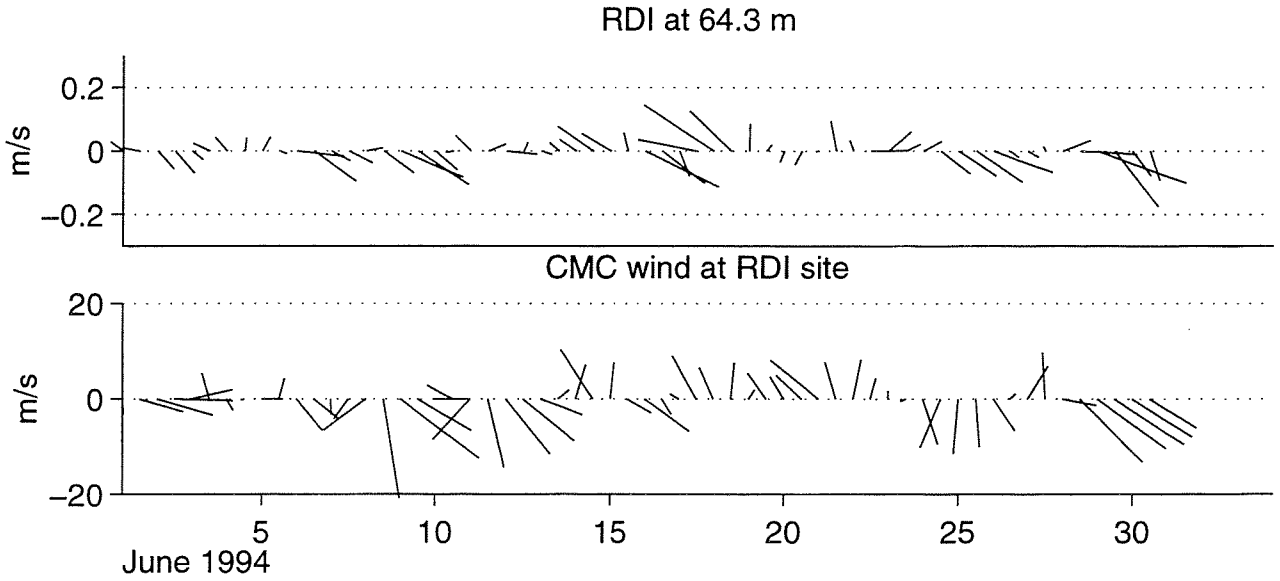
RDI at 64.3 m
0.2
0
−0.2
m/s
CMC wind at RDI site
20
0
−20
m/s
5
10
15
20
25
30
June 1994

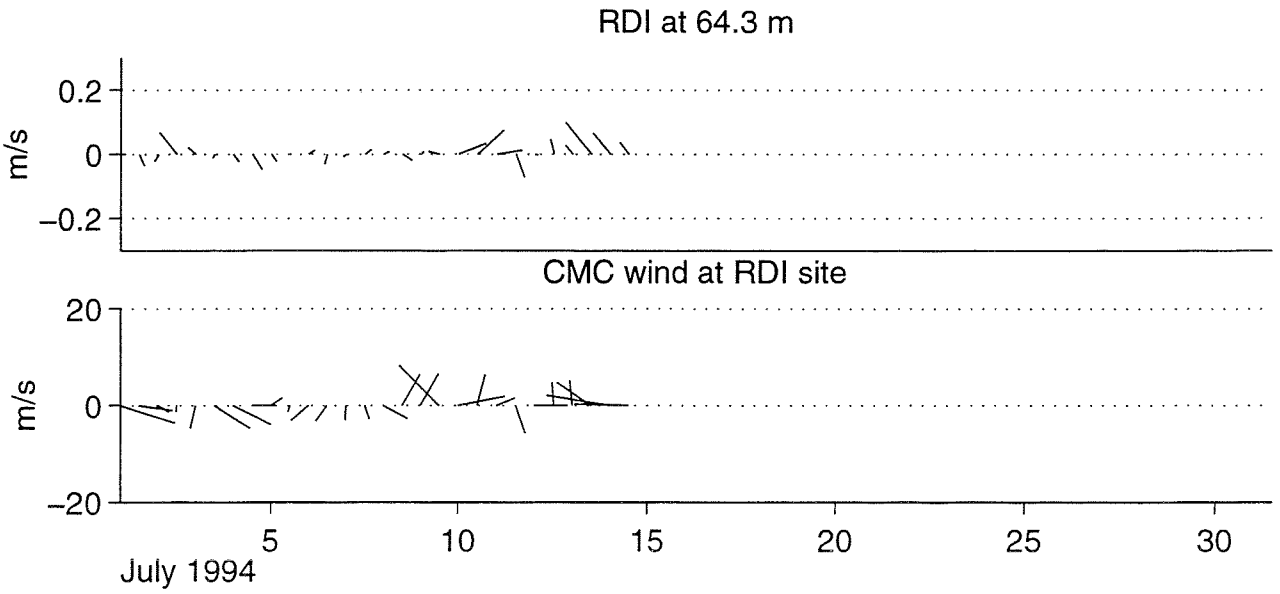
RDI at 64.3 m
0.2
0
−0.2
m/s
CMC wind at RDI site
20
0
−20
m/s
5
10
15
20
25
30
July 1994

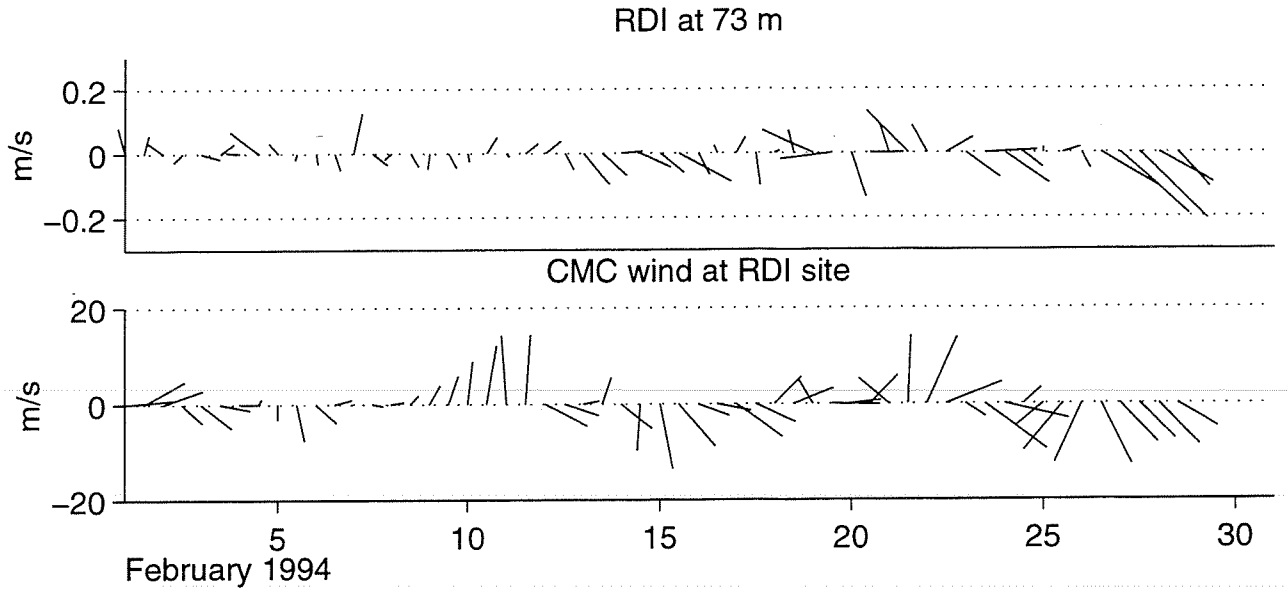
RDI at 73 m
0.2
0
−0.2
m/s
CMC wind at RDI site
20
0
−20
m/s
5
10
15
20
25
30
February 1994

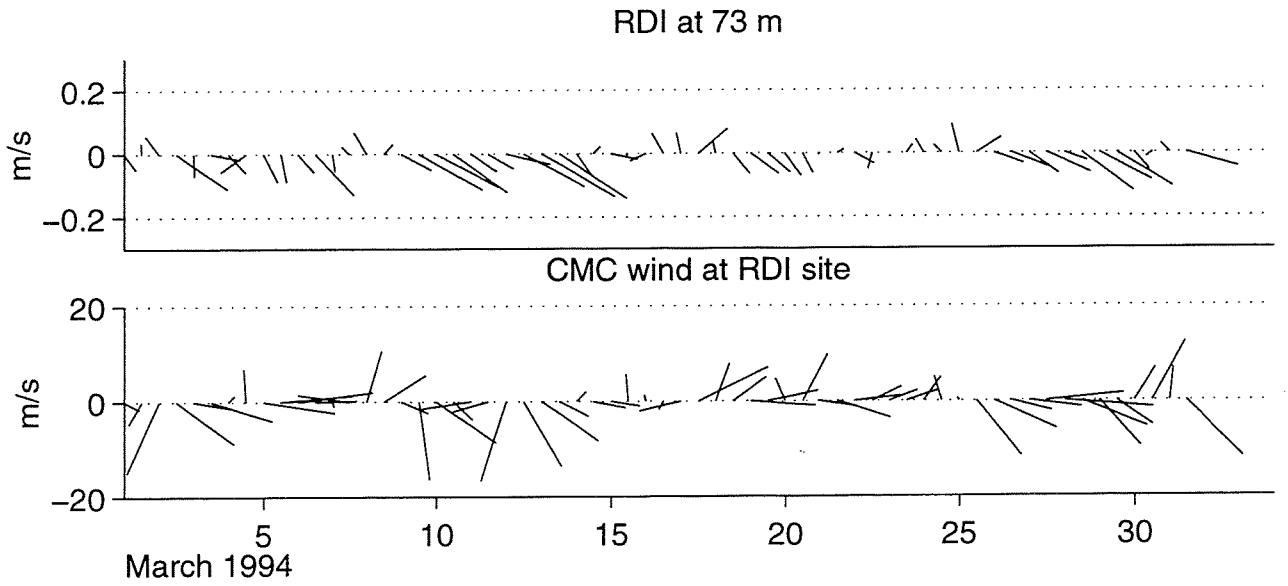
RDI at 73 m
0.2
0
−0.2
m/s
CMC wind at RDI site
20
0
−20
m/s
5
10
15
20
25
30
March 1994

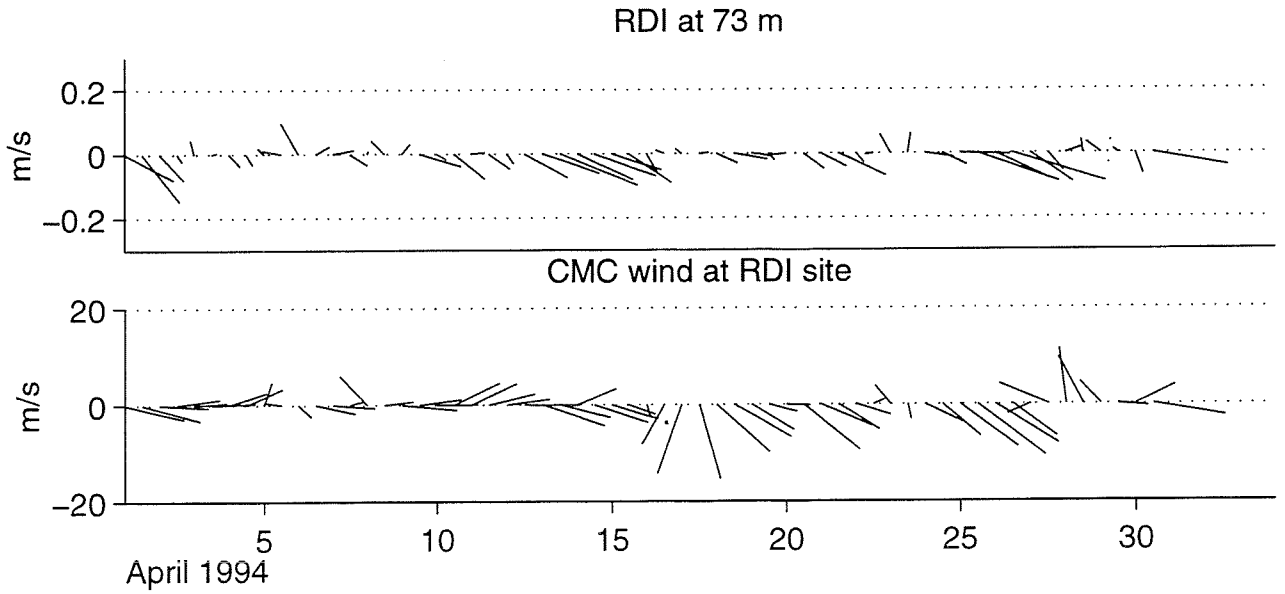
RDI at 73 m
0.2
0
−0.2
m/s
CMC wind at RDI site
20
0
−20
m/s
5
10
15
20
25
30
April 1994

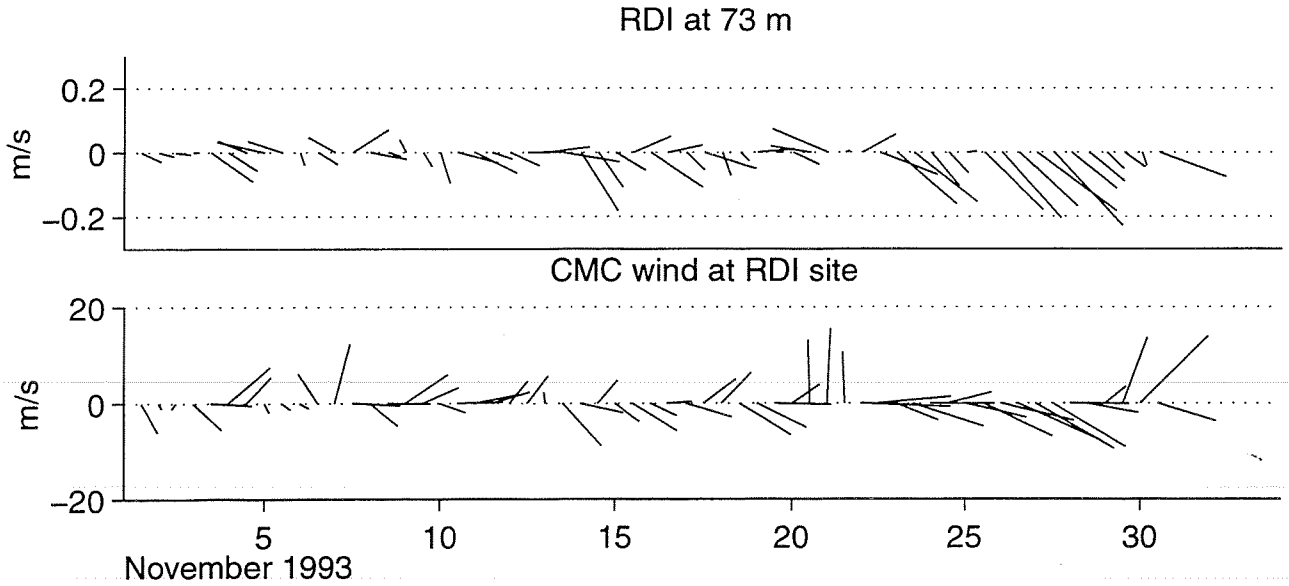
RDI at 73 m
0.2
0
−0.2
m/s
CMC wind at RDI site
20
0
−20
m/s
5
10
15
20
25
30
November 1993

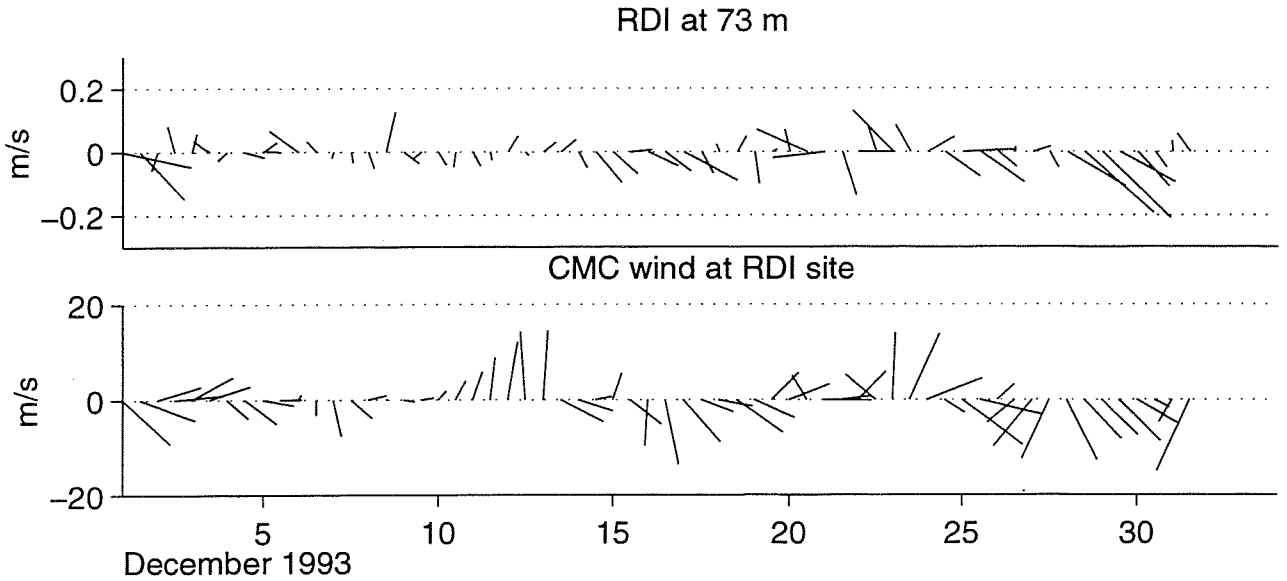
RDI at 73 m
0.2
0
−0.2
m/s
CMC wind at RDI site
20
0
−20
m/s
5
10
15
20
25
30
December 1993

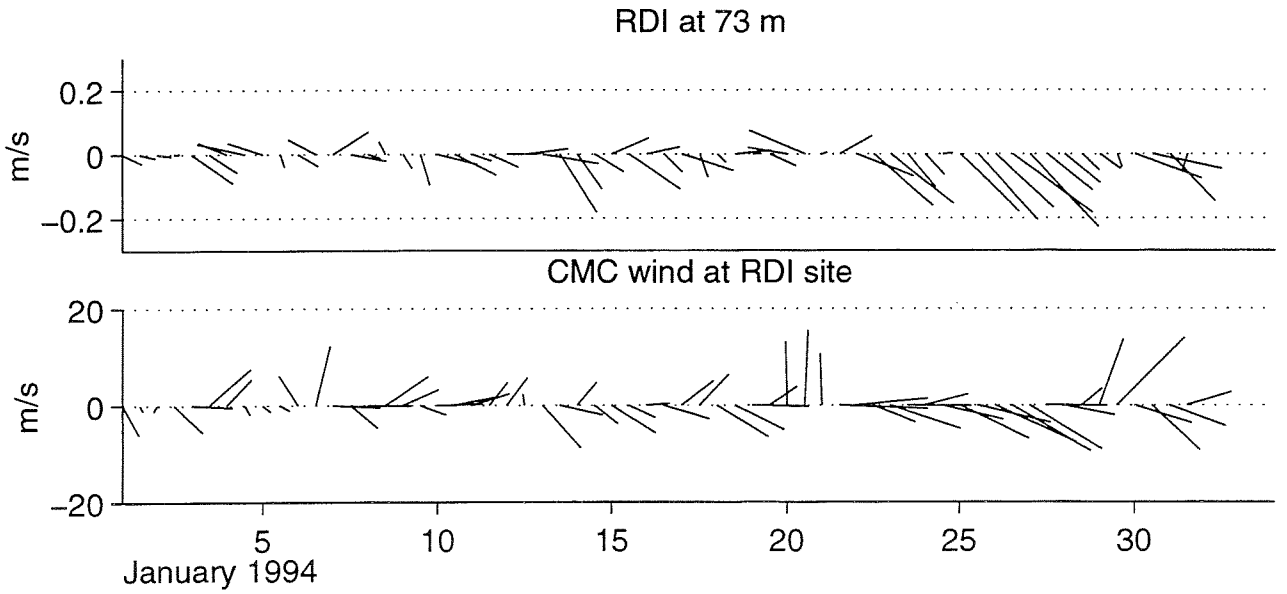
RDI at 73 m
0.2
0
−0.2
m/s
CMC wind at RDI site
20
0
−20
m/s
5
10
15
20
25
30
January 1994

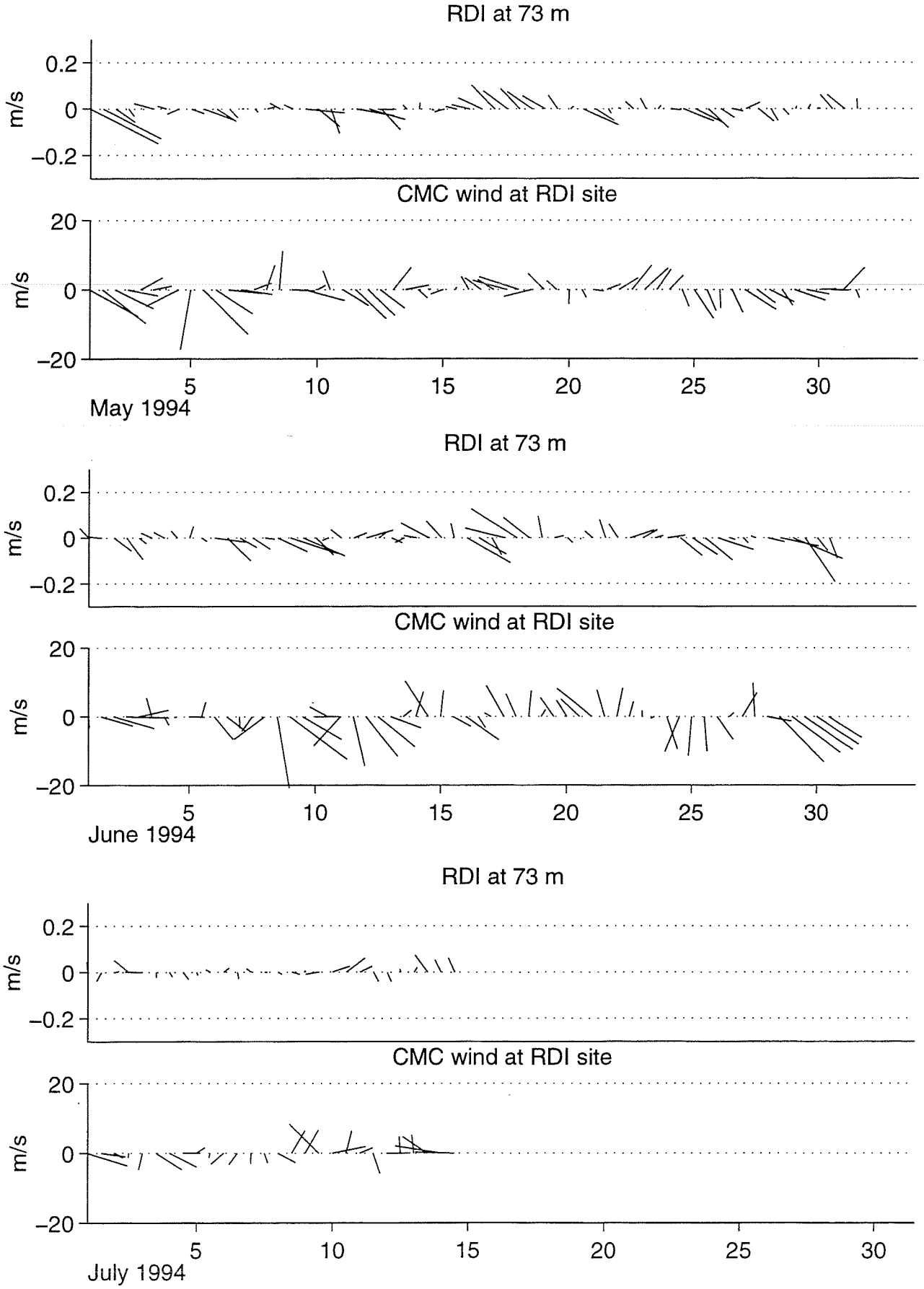
RDI at 73 m
0.2
0
−0.2
m/s
CMC wind at RDI site
20
0
−20
m/s
5
10
15
20
25
30
May 1994
RDI at 73 m
0.2
0
−0.2
m/s
CMC wind at RDI site
20
0
−20
m/s
5
10
15
20
25
30
June 1994
RDI at 73 m
0.2
0
−0.2
m/s
CMC wind at RDI site
20
0
−20
m/s
5
10
15
20
25
30
July 1994